Liquid-Solid Contact Phenomenon in Film Boiling of Leidenfrost Drops

A Dissertation Presented for the Doctor of Philosophy Degree to the University of Tennessee, Knoxville

Dudley James Benton

Accepted August 1982
Updated June 2016

Preface

It has been thirty-four years since I submitted this work to the graduate school. Someone had asked me for a copy and that became an occasion to look it over. The analysis, derivations, equations, and data are still relevant and useful, but so much has happened since the invention of microcomputers. The areas of this study most greatly impacted are the graphics, data reductions, and document formatting, especially the equations. It is for these reasons that I have updated this document in hopes that the information contained herein may be more useful to future researchers.

Acknowledgements

First, I acknowledge Jesus as my God, the creator of the phenomenon that I study, my sustainer, and the author of whatever ability I might have. I express appreciation to Dr. Edward G. Keshock for his patience and guidance throughout my studies. I also express appreciation to the Department of Mechanical and Aerospace Engineering, University of Tennessee, Knoxville for the machining and laboratory equipment used in this investigation. Recognition is given to William D. Barton, III who made the seven technical drawings of the heating surfaces and thermocouple/pin assemblies. To my wife, Patty, who has encouraged and supported me (and also reduced a substantial portion of the data) I express special appreciation and gratitude.

Abstract

The purpose of this study was to determine the effect of surface macro-roughness elements on the film boiling of discrete stationary liquid drops. The possible enhancement of boiling heat transfer rates due to the presence of these roughness elements as well as the conditions under which such enhancement might be expected was also to be determined. Film boiling of stationary discrete drops was selected as the focus of this study rather than flow boiling since flow boiling introduces additional experimental complexities normally associated with two-phase flow phenomena which might obscure the effect on heat transfer due to the macro-roughness elements alone.

Instantaneous heat transfer coefficients were obtained from photographic measurements of drop vaporization. Experiments were conducted at atmospheric pressure with four liquids on five heating surfaces at temperatures of up to 620°C. The drop sizes investigated ranged from 0.01 cc to 10 cc The liquids investigated were water, denatured ethanol, isopropanol, and ethylene-chloride. The heating surfaces which were investigated consisted of one smooth surface (for baseline comparison data), two surfaces having con centric grooves, one surface having 492 embedded cylindrical pins arranged in an evenly spaced square matrix, and one having evenly spaced hexagonal pins which were fabricated by excavating diagonal slots in the heating surface. One of the cylindrical pins and one of the hexagonal pins in each of the surfaces so fitted was fabricated with a flush-mount micro-thermocouple at the protruding surface, having a measured in-place response rate of at least 12,000°C/sec.

Increases in heat transfer rates of up to 500% were measured on the macro-roughened surfaces (compared to that which was measured on the smooth surface with the same fluid and bulk surface temperature). Also, substantial increases (up to 450°C in the case of water)·in the minimum bulk surface temperature required to maintain stable film boiling on the macro-roughened surfaces was measured (as compared to that required on the smooth surface).

Since the height of the macro-roughness elements was of the same order of magnitude as the thickness of the vapor layer which characteristically separates the heating surface from a liquid undergoing film boiling, it was postulated that the macro-roughness elements penetrating this vapor layer between the liquid and the heating surface intermittently come into direct contact with the liquid, thus providing a possible means of enhancing the heat transfer in film boiling.

Transient surface temperature measurements obtained from the flush-mounted micro-thermocouples demonstrated that direct contact between the elements and the boiling liquid does in fact occur in film boiling and that at such times substantial heat flow through the elements takes place. Thermal gradients within the elements indicated that the heat that is transferred through the macro-roughness elements as a result of direct contact with the liquid is the primary mechanism responsible for the increase in heat transfer rates observed for the surfaces having the macro-roughness elements.

A model for intermittent liquid-solid contact in film boiling on a macro-roughened surface was developed as well as a two-dimensional finite difference computer program for cylindrical macro-roughness geometry. This model in conjunction with the computer program was used to calculate heat transfer coefficients from measured contact duration and period for two of the macro-roughened surfaces. These calculated heat transfer coefficients were in reasonable agreement with measured heat transfer coefficients.

Table of Contents

List of Tables

List of Figures

List of Symbols

Ap	vertically projected drop area [cm²]
A*	dimensionless drop area (Equation 3-2)
B	dimensionless enthalpy flux parameter (Equation 3-19)
Bic	contact Biot number or modulus (Equation 6-9)
C_L	specific heat of the liquid [J/gm-°C] specific
C_S	heat of the solid [J/gm-°C]
Cpg	constant pressure specific heat of the vapor [J/gm-°C]
Eu	modified Euler number (Equation 3-18)
F	temperature distribution integral (Equation 3-41)
F_{D-S}	radiation view factor (Equation 3-45)
g	acceleration of gravity [cm/sec²]
g_c	Newton's constant [gm-cm/dyne-sec²]
G	mass flux [gm/cm²-sec]
h_c	contact heat transfer coefficient [W/cm²-°C]
h_D	total (or drop) heat transfer coefficient [W/cm²-°C]
h_F	convective (or flow) heat transfer coefficient [W/cm²-°C]
h_{FB}	film boiling heat transfer coefficient (Equation 5-4) [W/cm²-°C]
h_{fg}	latent heat of vaporization [J/gm]
h^s_{fg}	modified latent heat of vaporization (Equation 5-1) [J/gm]
h^m_{fg}	modified latent heat of vaporization (Equation 5-2) [J/gm]
h^*_{fg}	modified latent heat of vaporization (Equation 5-3) [J/gm]
h_R	radiative heat transfer coefficient [W/cm²-°C]
h^*	modified heat transfer coefficient (Equation 5-5) [W/cm²-°C]
H	dimensionless heat flux (Equation 6-3)
k_g	thermal conductivity of the vapor [W/cm-°C]
k_L	thermal conductivity of the liquid [W/cm-°C]
k_S	thermal conductivity of the solid [W/cm-°C]
l	average drop thickness (Figure 12) [cm]
L	dimensionless parameter (Equation 3-20)
Nu_C	contact Nusselt number (Equation 6-6)
Nu_D	drop Nusselt number (Equation 6-4)
Nu_F	convective (or flow) Nusselt number (Equation 6-5)
Nu_R	radiative Nusselt number (Equation 6-7)

Nu_V	volumetric drop Nusselt number (Equation 6-1)
P	pressure [bar]
P_0	ambient pressure [bar]
P^*	dimensionless pressure (Equation 3-17)
q_C	contact heat flux [W/cm²]
q_{CHF}	critical heat flux [W/cm²]
q_D	total (or drop) heat flux [W/cm²]
q_F	convective (or flow) heat flux [W/cm²]
q_{FB}	film boiling heat flux (Equation 5-7) [W/cm²]
q_{MFB}	minimum film boiling heat flux [W/cm²]
q_R	radiative heat flux [W/cm²]
Q_D	total heat transfer rate to drop [W]
r	radial distance from center of drop (Figures 12 and 81) [cm]
r^*	dimensionless "r" (Equations 3-13 and C-6)
R	drop radius (Figure 12) [cm]
Re	vapor flow Reynolds number (Equation 3-4)
t	time [sec]
T_C	contact temperature [°C]
T_L	temperature of the liquid [°C]
T_P	temperature of the thermocouple/pin junction [°C]
T_Q	quench temperature [°C]
T_R	recovery temperature [°C]
T_S	local temperature of the solid (heating surface) [°C]
T_W	bulk surface temperature [°C]
u	radial vapor velocity (Figure 12) [cm/sec]
u^*	dimensionless "u" (Equation 3-15) [cm/sec]
V_D	drop volume [cm³]
V^*	dimensionless drop volume (Equation 3-3)
w	vertical vapor velocity (Figure 12) [cm/sec]
w^*	dimensionless "w" (Equation 3-16)
z	vertical dimension (Figures 12 and 81) [cm]
z^*	dimensionless "z" (Equations 3-14 and C-7)

Greek

α_L	thermal diffusivity of the liquid [cm²/sec]

α_S thermal diffusivity of the solid [cm2/sec]

γ contact parameter (Equation 3-50)

δ vapor layer thickness (Figure 12) [cm]

$\underline{\delta}$ computed vapor layer thickness (Equation 3-30) [cm]

δ_{TH} thickness of thermal boundary layer (Equation 5-13) [cm]

Δ_{TC} (T_R -T_Q)temperature drop during contact [°C]

Δ_{TCHF} temperature difference at the critical heat flux [°C]

Δ_{Tp} (Tw-Tp) temperature difference across the pin [°C]

Δ_{TMFB} temperature difference at the minimum film boiling point [°C]

ε height of macro-roughness element [cm]

ε_L emissivity of the liquid

ε_S emissivity of the heating surface

θ (τ_C/τ) contact duration period ratio

λ liquid/vapor interface parameter (Equation 1-1) [cm]

λ_C Taylor critical wavelength (Equation 1-2) [cm]

λ_{MD} Taylor most dangerous wavelength (Equation 1-3) [cm]

Λ dimensionless superheat (Equation 6-2)

μ_g dynamic viscosity of the vapor [poise]

ν_g kinematic viscosity of the vapor [cm/sec]

ρ_f density of t liquid [gm/cm3]

ρ_g density of t vapor [gm/cm3]

ρ_s density of t solid [gm/cm3]

σ surface tension [dyne/cm]

σ_R Stephan-Boltzmann constant [W/cm²_°K^4]

τ contact period [sec]

τ_C contact duration [sec]

Ω conduction parameter (Equation 6-8)

Chapter 1. Introduction

Film boiling is usually defined as the mode of boiling that occurs when an essentially continuous layer of vapor separates the heating surface from the boiling liquid (e.g., [1][1]). Since the thermal conductivity of a vapor is typically much less than the thermal conductivity of the liquid phase, the presence of a vapor layer between the heating surface and the boiling liquid generally results in heat transfer rates which are much lower than those associated with nucleate boiling phenomena where the liquid is in direct contact with the heating surface. This characteristic of film boiling can occur when the liquid is in a pool, flowing in a channel, or in discrete drops. This last configuration of a liquid undergoing film boiling (viz. discrete drops) and more particularly stationary discrete drops is usually termed Leidenfrost boiling after Johann Gottlob Leidenfrost [2].

One of the factors which determines the mode of boiling as well as the heat flux from a particular surface to a boiling liquid is the difference in temperature between the surface and the liquid. This dependence of heat flux and mode of boiling on temperature difference is shown by the typical boiling curve Figure 1.[2] This boiling curve illustrates the four basic modes of vaporization: 1) the non-boiling region, where natural convection is the mechanism responsible for heat transfer, and vaporization takes place at the liquid/vapor interface, 2) the nucleate boiling region where vapor bubbles are generated at preferred sites (such as cavities and crevices) on the heating surface, 3) the transition boiling region where the vapor bubbles which are formed at the heating surface (in a similar manner to that which takes place with nucleate boiling) begin to coalesce at the surface and limit the area of the surface which is directly exposed to the liquid, and 4) the film boiling region where the vapor that is generated forms an essentially continuous layer between the heating surface and the boiling liquid.

Frequently associated with the study of Leidenfrost drops is a vaporization curve as shown in Figure 2. The vaporization curve is a plot of the time required to completely vaporize a drop of a given initial size vs. the temperature difference between the heating surface and the boiling liquid. This vaporization curve can be seen as similar to the inverse of the typical boiling curve. The point where the boiling curve exhibits a minimum is analogous to the point where the vaporization curve exhibits a maximum. This point is usually referred to as the Leidenfrost point (the point of minimum heat flux or the point of maximum vaporization time) although research indicates that this point is not unique to a given system (e.g., [3]). Conversely, the point where the boiling curve exhibits a maximum is analogous to the point where the vaporization curve exhibits a minimum and is usually referred to as the point of peak heat flux.

In many industrial applications (such as quenching and power production processes) boiling heat transfer necessarily takes place with large temperature differences between the heating surface and the boiling liquid. If film boiling accompanies this large temperature difference the heat flux may be substantially less than that which could be expected with nucleate boiling. This relative reduction in boiling heat flux which is observed to occur with film boiling is perhaps best illustrated by the specific (or unit) thermal resistance or the inverse of the specific thermal conductance. The specific thermal conductance is referred to as the heat transfer coefficient and is defined as the heat flux divided by the temperature difference. Figure 3 is a typical linear plot

[1] Numbers between square parentheses indicate References.
[2] All figures are in Appendix B.

of specific thermal resistance vs. temperature difference. This figure illustrates the relatively large specific thermal resistance associated with film boiling which occurs over a large range of temperature differences as compared to the relatively smaller specific thermal resistance associated with the nucleate boiling process which only occurs over a small range of temperature differences.

The four dominant parameters that effect boiling heat flux are the fluid, the system pressure, the temperature difference, and the heating surface. Frequently the first three are fixed for a particular application leaving only the fourth, the heating surface, as the dominant parameter that may be controlled to produce a desired effect such as increased boiling heat flux. Since the increase in specific thermal resistance associated with film boiling as compared to nucleate boiling is due to the presence of a layer of vapor separating the heating surface from the boiling liquid this increase in specific thermal resistance could be lessened by somehow reducing the thickness of the vapor layer or by providing an alternate path for heat flow from the heating surface to the boiling liquid. One method of providing an alternate path for heat flow, the introduction of surface macro-roughness elements, is the substance of this study.

An increase in film boiling heat transfer should result if direct contact between the heating surface and the boiling liquid were to be, if not to the degree associated with nucleate boiling, at least partially restored. It has been demonstrated experimentally (e.g., [4], [5], [6]) that direct contact between the heating surface and the boiling liquid can occur in stable film boiling even on a smooth heating surface. With Leidenfrost drops in a gravitational field, the vapor, although less dense, is below the liquid, which gives rise to Taylor instabilities that can "support" wave-like disturbances at the liquid/vapor interface. Any disturbance of this liquid/vapor interface that might result from the introduction of the drop onto the heating surface or from ambient vibrations which are generally present will result in a finite displacement of the interface and a wave propagating across the interface from the point of disturbance. Such a wave may also be reflected when it reaches the sides of the drop.

Taylor [7] demonstrated how small disturbances at such a liquid/vapor interface would either grow or decay depending on the wavelength of the disturbance. Taylor's analysis indicated that there exists a critical wavelength, Ac, below which small disturbances will tend to decay and above which these will tend to grow. The characteristic length parameter, A, for liquid/vapor interfaces is defined by Equation 1-1.

$$\lambda^2 = \frac{\sigma \cdot g_c}{\rho_f - \rho_g} \tag{1-1}$$

The Taylor critical wavelength is related to the characteristic length parameter, A, by Equation 1-2.

$$\lambda_C = 2\pi \cdot \lambda \tag{1-2}$$

Taylor also demonstrated that there exists a wavelength for which small disturbances at the liquid/vapor interface having this wavelength will tend to grow more rapidly than disturbances having any other wavelength. This wavelength corresponding to the tendency for maximum growth rate is termed the most dangerous wavelength, λ_D, and is related to the characteristic length parameter by Equation 1-3.

$$\lambda_D = 2\pi\sqrt{3} \cdot \lambda \tag{1-3}$$

Because of the Taylor instability phenomenon and the fact that small disturbances of certain wavelengths may grow rapidly resulting in wave crests large enough to span the vapor layer separating the heating surface from the boiling liquid, direct contact between the heating surface and the boiling liquid may thus occur in stable film boiling even on relatively smooth surfaces (e.g., [4]).

In the study of Tevepaugh and Keshock [8] this liquid-solid contact resulting from Taylor instabilities at the liquid/vapor interface beneath Leidenfrost drops was found to occur on a smooth surface (2 to 4 microns roughness) only at the initial moment when each drop was placed on the surface. The introduction of macro-roughness elements to the heating surface with roughness height of the same order of magnitude as the thickness of the vapor layer provides one means of increasing the probability that direct contact between the heating surface and the boiling liquid will occur during film boiling. The presence of macro-roughness elements on the heating surface has a two-fold effect on film boiling:

1. Liquid-solid contact is more likely to occur at the peaks on a roughened surface since the distance between a peak and the liquid/vapor interface beneath the drop is less and thus a smaller disturbance of the interface is required for liquid-solid contact to occur than would be required on a surface without such peaks (see Figure 4).
2. When liquid-solid contact does occur the local heat flux and resulting vaporization of the liquid in the vicinity of contact is increased due to the relatively higher thermal conductivity of the solid material of the macro-roughness element as compared to that of the vapor. This increase in local vaporization tends to agitate the liquid/vapor interface causing more and larger disturbances, which subsequently increases the probability of liquid-solid contact at other locations between the drop and the heating surface. It is, of course, also possible to fabricate a heating surface with macro-roughness elements whose height is larger than the vapor layer thickness between the heating surface and the boiling liquid.

This, in fact, was the case with at least two of the four macro-roughened surfaces that were investigated in this study. Even though macro-roughness elements may protrude above the heating surface a distance that is larger than the vapor layer thickness, this may not necessarily result in the liquid wetting the protruding tip of the macro-roughness element and a continuous direct contact between the element and the boiling liquid.

A number of studies (e.g., [4], [5], [6], [8]), indicate that most frequently in film boiling liquid-solid contact is of an intermittent rather than a continuous nature. Nishio and Harata [5] (who dealt with impinging drops rather than stationary drops) obtained photographic evidence that under certain circumstances, when the liquid comes into direct contact with the heating surface and the temperature of the surface at the point of contact is above some minimum value, rapid local vaporization will occur, causing the liquid to be lifted away from the surface at the point of contact, thus reestablishing the vapor layer separating the heating surface from the boiling liquid. This local minimum temperature that must be maintained in order to subsequently maintain the vapor layer (which is characteristic of the film boiling phenomenon) is herein termed the "local minimum film boiling temperature" abbreviated LMFBT. The bulk surface temperature required to maintain the LMFBT at every point on the heating surface where liquid-solid contact occurs is herein termed the "bulk minimum film boiling temperature" abbreviated

BMFBT. Many investigators do not make a distinction between the bulk and local minimum film boiling temperatures, in which case the abbreviation is simply be MFBT.

A few investigators (e.g., [8], [9]) have measured the BMFBT for various liquids on macro-roughened surfaces. Several investigators (e.g., [5], [6], [8], [10]) have detected liquid-solid contact in film boiling through the use of an electrical conductance probe This experimental technique takes advantage of the fact that the electrical conductance of liquids is typically orders of magnitude greater than that of their respective vapors. Thus, a measurement of the transient electrical conductance between the boiling liquid and the heating surface can be used to indicate whether or not the liquid is in direct contact with the heating surface at any point. Seki et al. [11] (dealing with impinging drops on a smooth surface) employed a thin-film thermistor to determine not only the occurrence of liquid-solid contact but also to measure the LMFBT. Two advantages of measuring local temperature fluctuations in the vicinity of liquid-solid contact (as in the study of Seki et al.) are the determination of the LMFBT rather than the BMFBT and the determination of liquid-solid contact occurrence at a point on the heating surface rather than measuring multiple, possibly simultaneous and thus indistinguishable contacts, as is the case with the conductance probe method.

The four objectives of the present study were: 1) to investigate the possible enhancement of film boiling heat flux and the possible increase in MFBT due to the presence of surface macro roughness elements, 2) to determine the possible occurrence of liquid-solid contact in film boiling and the possible effects of this contact on film boiling of liquid drops on macro-roughened surfaces, 3) to measure the LMFBT on a macro-roughened surface, and 4) to develop a model for the liquid-solid contact phenomenon in film boiling of Leidenfrost drops.

Chapter 2. Literature Survey

The two general categories of phenomena covered in this study are the Leidenfrost phenomenon and the phenomenon of liquid-solid contact in film boiling. The phenomenon of liquid-solid contact and its relationship to film boiling is the primary interest of the study, whereas the Leidenfrost phenomenon is the vehicle for the investigation. Inherent to the study of the Leidenfrost phenomenon and closely related to the phenomenon of liquid-solid contact in film boiling is the concept of the minimum film boiling temperature.

The Leidenfrost Phenomenon

"Dancing with the excitement of the intense heat," was the description given by an early observer to the phenomenon of film boiling of a liquid droplet on a heated surface. Eller first noted this phenomenon in 1746 (as reported by Gorton [12]). However, it was a German physician-scientist Johann Gottlob Leidenfrost who first objectively studied the phenomenon in 1756 and in the honor of whom the phenomenon is named. An English translation of the Latin in which Leidenfrost's work originally appeared was published in 1966[2]. In this article entitled, "On the Fixation of Water in Diverse Fire," Leidenfrost explained the characteristics of the phenomenon and drew several conclusions, as far from film boiling as the forces which bind matter together and "a new method by which the most perfect goodness of alcoholic wine can be determined" to a more practical application of the phenomenon as a possible means of measuring high temperatures. These conclusions drawn by Leidenfrost resulted in controversies that lasted for decades. It was perhaps these controversies that helped stimulate the early interest in the phenomenon. Detailed discussions of the early studies of the phenomenon as well as extensive bibliographies can be found in References 12, 13, and 14. In Reference 13, Wachters relates that Boutigny in some five articles published between 1843 and 1850 claimed the phenomenon to be a fourth state of matter to which he gave the name "spheroidal state" (the term spheroidal arising from the fact that small Leidenfrost drops appear to be spherical). Boutigny also reportedly cited the phenomenon as the cause of steam boiler explosions, said to have resulted in the death of about one thousand persons in the United States alone in the year 1840. These articles by Boutigny also reportedly resulted in "very heated" discussions and continued interest in the phenomenon [13].

Leidenfrost and Boutigny raised two questions that are still relevant today and, in fact, are two of the questions to which this study was directed. First, Leidenfrost noted that the coarser the metal surface the faster the evaporation of the drops. Leidenfrost also noted that if much rust were present on the heating surface the phenomenon would not occur. This is thought to be the earliest reference to surface roughness affecting the phenomenon. Second, Boutigny is thought to be the earliest investigator to raise the question of what is the minimum temperature of a surface necessary to permit the deposition of a drop onto the surface without the liquid wetting the surface. Thus the effects of surface roughness and the concept of a minimum film boiling temperature have been the subject of discussion for at least one hundred and forty years.

Wachters [13] reported that Pearson as early as 1842 developed the theory that the liquid was separated from the heating surface by a layer of vapor and that this theory was widely accepted by 1870. Wachters also reported that Kristensen in 1888 stated that conduction through the vapor rather than radiation was the primary transport mechanism by which heat is transferred from the heating surface to the liquid. According to Gottfried et al. [15] it was not until 1946 that the first

empirical solution to the Leidenfrost phenomenon was made. This first empirical solution is attributed to Pleteneva and Rebinder.

The first true analysis of the Leidenfrost phenomenon based on first principles is attributed to Gorton [12] in 1953.Gorton based his analysis on a potential flow of the vapor surrounding the drop. Gorton also unsuccessfully attempted to photographically measure the thickness of the vapor layer between the drops and the heating surface. Gorton concluded that the variation in heat flux measured on different surfaces was only a result of variations in the radiative properties of the surfaces.

Gottfried [16] in 1962 developed an analysis of the phenomenon that included mass transfer, radiation, viscous effects in the vapor flow, and superheating of the vapor making it the most complete analysis at that time. Lee [17] in 1965 extended and improved upon Gottfried's analysis and also obtained an empirical correlation for droplet vaporization time through dimensional analysis and least-squares regression on 72 data points. The analyses of Gottfried and Lee dealt specifically with very small drops that are essentially spherical.

In 1965 Wachters [13] developed a detailed analysis that included the fact that Leidenfrost drops are not actually spherical. Wachters obtained a numerical solution to the Laplace capillary equation (which will be given in more detail in Chapter 3) for the shape and size of a liquid drop at rest on a horizontal surface that it does not wet. Wachters also addressed the problem of small drops impinging on a hot surface. Further details of this analysis may be found in References 18 and 19.

Baumeister [20] in 1964 developed an analytical model of the Leidenfrost phenomenon for a large range of drop sizes including those that do not appear to be spherical. This model included viscous effects in the vapor flow, convection, and radiation heat transfer and permitted the most extensive correlation of experimental data at that time. Further details of this model may be found in References 21, 22, and 23.

Since the contribution of Baumeister [20] in 1964 the analysis of Leidenfrost drops has been extended in many areas such as the application to very large liquid masses by Patel [24] and Patel and Bell [25], to cryogenics by Keshock [26] and Keshock and Bell [27], to liquid-liquid systems by Hendrix and Baumeister [28], to liquid 14 metals by Baumeister and Simon [29], and to moving surfaces by Schoessow, Jones, and Baumeister [30]. The accuracy of the theory has been improved by accounting for vapor bubble breakthrough in very large drops by Keshock [26] and Baumeister, Keshock, and Pucci [31] and for significant superheating of the vapor by Baumeister, Keshock, and Pucci [31].

The Minimum Film Boiling Temperature

As mentioned previously the concept of an MFBT that is applicable to the Leidenfrost phenomenon most likely originated with Boutigny as early as 1843. The MFBT as it applies to the Leidenfrost phenomenon is frequently termed the "Leidenfrost Point" and has been defined in at least five different ways:

1. The surface temperature at which it is just possible to deposit a drop onto a surface without wetting it (Boutigny).
2. The minimum surface temperature at which there is no direct contact between the liquid and the heating surface (see Reference 14).

3. The surface temperature corresponding to the minimum heat flux or maximum vaporization time (e.g., [8], [9], [14], and [17] through [31] inclusive).
4. The surface temperature above which if a drop falls on the surface a vapor layer immediately forms beneath the drop (e.g., [11]).
5. The surface temperature corresponding to "the onset of stable spheroidal state or the upper limit of liquid-solid-contact" [5].

According to Wachters [13] no such "point" can be defined other than the saturation temperature of the liquid and that no true spheroidal state exists. Despite the differences in the definition of the MFBT or Leidenfrost Point, scores of investigators since 1843 have performed various experiments to determine this value for various liquids, surfaces, etc. and many articles have been published which present theoretical predictions and empirical correlations. It has been pointed out that significant variation can be found between experimental values of the MFBT– variations that are much larger than the typical uncertainty associated with experimental heat transfer data (e.g., [3], [10], [13], [14], [29], and [32] through [35] inclusive).

Wachters [13] and Baumeister and Simon [29] stress the importance of the manner in which the drops are introduced onto the heating surface, the roughness of the surface, and the effect of ambient vibrations on the experimentally measured MFBT. Baumeister et al. [36] demonstrated that vibrations of a Leidenfrost drop might be thermally driven even if ambient vibrations are not present. Wachters [13] postulated that once a drop is supported by a vapor layer above an ideally smooth surface the temperature of the surface could be slowly reduced with a limiting value of the saturation temperature of the liquid and the Leidenfrost phenomenon be maintained provided all vibrations are isolated from the system. Baumeister et al. [3] supported this postulate with experimental data and offered an explanation for this anomaly in terms of liquid-solid contact.

Baumeister and Simon [29] developed a theoretical model for the MFBT on a smooth surface based on the assumption that direct contact between the heating surface and the boiling liquid would occur at temperatures near the MFBT and that the thermal response of the heating surface at the point of contact would determine whether or not film boiling will continue. Baumeister and Simon postulated that the MFBT measured on a smooth surface having infinite thermal capacity is determined by liquid properties alone. Baumeister and Simon also postulated that the MFBT measured on a surface of finite thermal capacity is elevated above the value which would be measured on surface having infinite thermal capacity by an amount that is determined by the transient conduction which would occur in the event of contact between the liquid and the surface. This model for the MFBT thus included both liquid and heating surface thermophysical properties and indicates that a relationship exists between liquid-solid contact, the MFBT, and film boiling.

Liquid-Solid Contact in Film Boiling

Bradfield [4] experimentally measured liquid-solid contact in film boiling of Leidenfrost drops and pool-type quenching. Bradfield stated that this liquid-solid contact could be "periodic or quasi-continuous depending on the surface roughness, (liquid) subcooling, and heating surface thermal conductivity." Bradfield also stated that, "liquid-solid contact can be achieved at stable film boiling temperatures by any means which will induce surface roughness elements to tickle the liquid-vapor interface." Bradfield obtained evidence of this liquid-solid contact by means of electrical conductance and by photographs. Bradfield postulated that there were four parameters

which determine the occurrence of liquid-solid contact and its effect on film boiling: 1) the ratio of the vapor and liquid Prandtl numbers, 2) the ratio of the thermal capacities of the vapor and liquid, 3) the Biot number based on the maximum roughness height, and 4) the ratio of the maximum roughness height to the vapor layer thickness. Bradfield also speculated that, "it may become desirable to control heat flow by controlling liquid-solid contact in the stable film boiling regime."

The only reference to theoretical modeling of this liquid-solid contact that Bradfield [4] made was to that of Bankoff and Mehra [37]. Bankoff and Mehra dealt with liquid-solid contact in transition rather than film boiling. Bankoff and Mehra modeled the liquid-solid contact occurrences as being pulse-like periodic and the thermal exchange which takes place during contact as that which theoretically occurs between two semi-infinite static media. Bankoff and Mehra at the time of publication had made no measurements of liquid-solid contact or transition boiling heat flux.

Baumeister and Simon [29] employed a model for liquid-solid contact that is essentially the same as that of Bankoff and Mehra [37] except that the model of Baumeister and Simon permitted radial temperature variations. Baumeister and Simon applied this model directly to the Leidenfrost phenomenon and the MFBT. Henry [32] used the same modeling approach to liquid-solid contact as did Bankoff and Mehra [37] (that of the contact between two semi-infinite static media). Henry used the ratio of the thermal capacities of the liquid and the heating surface material from the analysis of the transient conduction between two semi-infinite static media and the film boiling theory of Berenson [38], together with regression analysis, to determine an empirical relationship for the MFBT that included the effects of liquid-solid contact.

Yao and Henry [6] conducted experiments to determine the effect of pressure on the MFBT for a thin liquid layer on a smooth surface. The definition of MFBT implied by Yao and Henry is the surface temperature above which liquid-solid contact either does not occur or at least does not occur in a "stable" manner. Yao and Henry offered portions of a theoretical model for liquid-solid contact using the same model for the heat flux during contact as did Bankoff and Mehra [37] (that of the contact of two semi-infinite static media). Yao and Henry also concluded that the mechanism by which vaporization of the liquid takes place in the vicinity of liquid-solid contact is that of preferred site nucleation similar to that which occurs in nucleate boiling (Excellent discussions of preferred site nucleation, which is not the focus of this study, may be found in References 39, 40, 41, 42, and 43.). Yao and Henry employed the nucleation theory of Hsu [40] in their analysis of vapor production resulting from liquid-solid contact. Yao and Henry did not offer experimental data in verification of their theoretical concepts nor did they demonstrate any correlation between their model and their experimental data for MFBT. Further details of their theoretical concepts and experimental data can be found in Reference 10.

Nishio and Hirata [5] measured the MFBT and the occurrence of liquid-solid contact for small drops of water and ethanol impinging on a smooth surface at atmospheric pressure. Nishio and Hirata also developed a theoretical model for the MFBT based on the bubble nucleation theory of Han and Griffith [43] and the nucleate boiling theory of Kutateladze [44]. This model of Nishio and Hirata employed the same transient conduction formulation during contact as that of Baumeister and Simon [29] but differed from the model of Baumeister and Simon in the concept of bubble nucleation. Nishio and Hirata presented a comparison of their theoretical model for MFBT and experimental data. Although Nishio and Hirata cited the work of Baumeister and Simon they made no comparison of their respective predictions of MFBT.

Objectives of the Present Study

Most of the investigations reviewed which studied the Leidenfrost phenomenon and liquid-solid contact (with the exception of Knobel and Yeh [9] and Tevepaugh and Keshock [8]) only dealt with small drops that are essentially spherical in shape. One of the objectives of the present study was to investigate this phenomenon with large drops and extended liquid masses. Only one of the investigations reviewed (that of Seki et al. [11]) offered experimental data for the LMFBT (and that investigation dealt only with small drops impinging on a smooth surface). Another objective of the present study was to measure both the BMFBT and the LMFBT on macro-roughened surfaces. A third objective of the present study was to measure the frequency at which liquid-solid contact occurs at a point on the surface as well as the duration of the contact and to use these data to develop a model for liquid-solid contact which would include the difference between the bulk surface temperature and the temperature of the surface in the vicinity of contact. Finally, it was also an objective of the present study to determine the possible relationship between liquid-solid contact in film boiling on macro-roughened surfaces, the local transient temperature response of the macro-roughness elements to this contact, and the increase in heat flux as compared to a smooth surface that may accompany this contact.

Chapter 3. Modeling Large Drops on Roughened Surfaces

Modeling the Leidenfrost phenomenon for large drops and extended liquid masses on macro-roughened surfaces is divided into five major parts: modeling the drop geometry, modeling the vapor flow, modeling the mass transfer process, modeling the heat transfer processes, and modeling intermittent liquid-solid contact.

Modeling the Drop Geometry

Leidenfrost drops may assume a wide range of shapes depending on their volume. Very small drops (less than 0.001 cc for most liquids) appear to be essentially spherical, whereas very large drops (greater than 1.0 cc for most liquids) have been described as being shaped similar to a pancake (e.g., [24], [26]). An additional modeling complication arises with large drops in that relatively large vapor bubbles can be observed to form within the liquid and periodically break away through the upper surface of the drop. These vapor bubbles are typically an order of magnitude larger than those that are observed in nucleate pool boiling. This vapor bubble formation and breakaway phenomenon is usually termed "vapor bubble breakthrough." This range of drop geometries was illustrated schematically by Baumeister et al. [21]. Figure 5 is a reproduction of this illustration of Baumeister et al. Oscillations of the drops 21 22 (as mentioned previously in conjunction with Reference 36) results in yet another modeling complication. Each of these aspects of the phenomenon will be considered separately.

The necessity for modeling drop geometry arises from both theoretical and experimental considerations. In order to develop a theoretical model for the overall phenomenon it is necessary to first model the drop geometry since this is perhaps the most basic modeling requirement. Modeling the drop geometry is also necessary for the experimental determination of heat flux since the relationship between drop projected area and volume is needed to determine drop volume from photographs showing projected area (This aspect of the experimental investigation will be developed in detail in Chapter 5). It is for these reasons (i.e., for the theoretical and experimental requirements) that two distinct models for drop geometry were developed. These models for drop geometry are referred to as the disk model (after Baumeister et al. [21]) and the capillary model (after Wachters [13] and Hartland and Hartley [45]). Since the disk model is a simplification of the capillary model, the capillary model will be presented first.

Wachters [13] assumed that, "a drop resting on a horizontal surface is radially symmetric around a vertical axis. Hence, the question about the shape of the drop can be reduced to the question of the form of a meridian." Wachters then assumed that the Laplace capillary equation (Equation 3-1) was the governing relationship for the liquid interface of the drop.

$$\Delta p = \frac{\sigma}{\frac{1}{R_1} + \frac{1}{R_2}} \tag{3-1}$$

Where Δp is the pressure difference across the liquid/vapor interface, σ is the surface tension, and R_1 and R_2 are the major radii of curvature. The Leidenfrost phenomenon actually violates two basic assumptions of the Laplace capillary equation: no acceleration of the interface (which is violated by oscillations) and no mass or heat transfer through the interface (which is violated by the vaporization process). In their investigation of drop oscillations, Baumeister et al. [36] postulated that Leidenfrost drops oscillate about their equilibrium shape (this equilibrium shape being defined by the Laplace capillary equation). The postulate that Leidenfrost drops do, in fact,

oscillate about the equilibrium shape predicted by the Laplace capillary equation and that the average area/volume relationship as determined from experimental measurements is well approximated by the equilibrium relationship is supported by the area/volume data of Baumeister [20] and Keshock [26] as well as data taken in the present study.

The effect of interfacial mass and heat transfer on the size and shape of Leidenfrost drops was assumed to be negligible in the analyses of References 3, 12, 13, 15, 16, 17, 20, 22, 23, 24, 26, and 30. Experimental area/volume data taken in the present study (which will be presented subsequently) demonstrated that a 200% increase in vaporization rate did not result in any distinguishable pattern of variation in the size or shape of the drops, thus indicating that the effect of interfacial mass and heat transfer on the size and shape of Leidenfrost drops is significantly less than the effect of drop oscillations. It is therefore assumed that the equilibrium (or at least time average) size and shape of Leidenfrost drops may be described by the Laplace capillary equation.

Wachters [13] obtained a numerical solution to the Laplace capillary equation using a digital computer. A more detailed analysis and discussion of this solution as well as a more stable numerical formulation may be found in chapters 2, 7, 9, and 10 of Reference45. If the characteristic length parameter for liquid/vapor interfaces, λ, as defined by Equation 1-1 is used to non-dimensionalize the drop area and volume as in Equations 3-2 and 3-3 respectively, the solution of the Laplace capillary equation provides a single-valued relationship between dimensionless drop area and dimensionless drop volume.

$$A^* = \frac{A_P}{\lambda^2} \tag{3-2}$$

$$V^* = \frac{V_D}{\lambda^3} \tag{3-3}$$

This relationship is shown in Figure 6. The computed drop cross-section for several values of dimensionless drop volume is shown in Figure 7. (A description of the computer program used to solve the Laplace capillary equation may be found in the Appendix under the name "VOLUME").

The relationship between drop area and volume thus derived from the Laplace capillary equation is a function of only one parameter, A. If the surface tension, liquid density, and vapor density are known then A may be calculated directly. To further improve the accuracy of this area/volume relationship, experimental data for area and volume were obtained as described in Reference 26 and in Chapter 4. A computer program (a description of which may be found in the Appendix under the name "LAMBDA") was then used to determine the value of λ that provided a best correlation between the experimental area/volume data and the solution to the Laplace capillary equation. The area/volume data and the correlation based on the solution to the Laplace capillary equation for the four liquids investigated in the present study are shown in Figures 8 through 11. (The references in these Figures to SMTH, CG01, and CG02 indicate heating surfaces investigated in the present study as detailed in the second section of Chapter 4. Basically, SMTH refers to the smooth surface and CG refers to macro-roughened surfaces having concentric grooves.) This area/volume data (which is only of peripheral interest in the present study) are presented here to bring out a second important modeling aspect of the size and shape of Leidenfrost drops on macro-roughened surfaces, that of the possible effect of the

macro-roughness elements on drop geometry. As can be seen from Figures 8 and 9, there is no distinguishable difference in the area/volume relationship as measured on the smooth surface and the macro-roughened surfaces for the range of drop sizes investigated. It is 26 therefore assumed that the effect of macro-roughness elements on the drop area/volume relationship is significantly less than the effect of drop oscillations.

As pointed out by Keshock [26] the effect of vapor bubble breakthrough on the drop area/volume relationship may be quite significant. The possible effect of vapor bubble breakthrough on the drop area/volume relationship was included in the present study by measuring the area of the vapor bubbles and consistently subtracting this from the total drop area. This correction for vapor bubble breakthrough is precisely that proposed by Keshock, Equation 70, page 125, Reference 26. Since the area/volume data from which the value of A for each liquid were determined included drops where vapor bubble breakthrough was present, the resulting area/volume correlation included this effect.

The present study primarily focused on large drops and extended liquid masses where one or occasionally two vapor bubble breakthroughs were present. No data were taken where more than three vapor bubble breakthroughs were present. Drop sizes investigated ranged from 0.01 cc to 10 cc that corresponds to a range of dimensionless drop volumes of approximately 10 to 10,000. Baumeister et al. [23] gave an upper limit on the dimensionless drop volume of 0.8 corresponding to small drops that are essentially spherical. Thus the drops investigated in the present study may be schematically illustrated by (b), (c), and (d) in Figure 5. This range of drop sizes is also illustrated in Figure 7. A disk may approximate the shape of these drops.

Baumeister [20] first proposed this disk-shaped model for Leidenfrost drops and applied this model to the entire range of drop sizes from small to extended liquid masses. The disk model has also been successfully employed in a number of other analyses (e.g., [21], [22], [23], [26], [30], and [31]). Figure 12 is a reproduction of Baumeister's illustration of the disk model for Leidenfrost drops. The most important aspect of the disk model that was employed in the present analysis is the uniform vapor layer thickness beneath the drop as shown in the figure. Wachters et al. [18] performed an analysis of the phenomenon that included a non-constant vapor layer thickness (due to the radial pressure gradient in the vapor) and compared the results with their analysis that assumed a constant vapor layer thickness and with experimental data. Wachters et al. concluded from this comparison that their analysis that assumed a constant vapor layer thickness was in better agreement with experimental data than their analysis that assumed a non-constant vapor layer thickness. Thus the assumption of a constant vapor layer thickness seems to be justified from experimental data.

Modeling the Vapor Flow

The evaporation which occurs at the under side of the drop results in vapor flowing down toward the heating surface and thus "feeding" the vapor gap which supports the drop above the heating surface. This vapor must flow out between the under side of the drop and heating surface until it escapes at the periphery except in the occurrence of vapor bubble breakthrough when some of the vapor escapes through the top of the drop.

Wachters [13] assumed that the vertical velocity of the vapor could be neglected, that the flow was laminar, that the inertia forces could be neglected, that the thermophysical properties were constant (equal to the mean value), and that the liquid/vapor interface was not "pulled along" with the vapor flow thus providing two stationary boundaries (i.e., the under side of the

drop and the heating surface). Leidenfrost [2] as well as several other investigators (e.g., [12], [13], [16], [18], and [20]) noted that the liquid surface does move. However, Wachters et al. [18] stated that this motion of the liquid surface was primarily due to surface tension gradients (resulting from temperature gradients on the surface of the drop) and not predominantly a result of the vapor flow. Wachters et al. also stated that the vapor velocity was much larger than the liquid surface velocity (as measured photographically by tracking particles of dust or soot on the surface of the liquid) and thus concluded that the motion of the liquid could be neglected in modeling the vapor flow. In addition to these assumptions of Wachters and Wachters et al., Baumeister and Hamill [22] assumed the vapor flow to be incompressible having negligible energy dissipation, that the gravitational body force on the flow was negligible, that the flow although transient was quasi-steady, that the vapor flux from the under side of the drop was uniform, and that the flow was axisymmetric. Baumeister and Hamill did, however, include the vertical velocity of the vapor in contrast to the analysis of Wachters.

Baumeister [20] solved the complete Navier-Stokes equations for the vapor flow and concluded that the Reynolds number was small enough to neglect the inertia forces in modeling the flow. Keshock [26] stated that the results of Lee [17] indicated that the Reynolds number never exceeded 16 for all of the liquids and conditions in his investigation. The Reynolds number, defined by Equation 3-4, is directly proportional to the product of the drop radius, R, and the average vapor mass flux from the under side of the drop, $\underline{G}$.

$$\mathrm{Re} = \frac{R\overline{G}}{2\mu_g} \tag{3-4}$$

Based on the analysis of Baumeister et al. [22] and experimental data taken in the present study, the Reynolds number for a 1.25 cc drop of ethylene-chloride on a smooth surface at 490°C is 100. Since vapor mass flux increases with· increasing heat flux, as has been observed to occur on macro-roughened surfaces, the Reynolds number may be even larger in some cases. Thus the inertia effects on the vapor flow are not necessarily negligible with the fluids and surfaces investigated in the present study. (Numerical flow computations demonstrated that the inclusion of inertia effects does not alter the final results more than 15%, nevertheless, the inertia effects were retained for completeness.)

The model used for the vapor flow in the present study may be summarized as follows: laminar, incompressible, axisymmetric, non-dissipating, quasi-steady flow of a constant property fluid between two co-axial disks with uniform blowing from the upper disk. The two-dimensional continuity equation (Equation 3-5), Navier-Stokes (or momentum) equations (Equations 3-6 and 3-7), and the energy equation (Equation 3-8) were employed in cylindrical coordinate form.

$$\frac{1}{r}\frac{\partial}{\partial r}(ru) + \frac{\partial w}{\partial z} = 0 \tag{3-5}$$

$$u\frac{\partial u}{\partial r} + w\frac{\partial u}{\partial z} = -\frac{g_c}{p_g}\frac{\partial p}{\partial r} + \nu_g\left[\frac{1}{r}\frac{\partial}{\partial r}\left(r\frac{\partial u}{\partial r}\right) + \frac{\partial^2 u}{\partial z^2} - \frac{u}{r^2}\right] \tag{3-6}$$

$$u\frac{\partial w}{\partial r} + w\frac{\partial w}{\partial z} = -\frac{g_c}{p_g}\frac{\partial p}{\partial z} - g + \nu_g\left[\frac{1}{r}\frac{\partial}{\partial r}\left(r\frac{\partial w}{\partial r}\right) + \frac{\partial^2 w}{\partial z^2}\right] \tag{3-7}$$

$$p_g Cp_g \left(u\frac{\partial T}{\partial r} + v\frac{\partial T}{\partial z} \right) = k_g \left[\frac{1}{r}\frac{\partial}{\partial r}\left(r\frac{\partial T}{\partial r} \right) + \frac{\partial^2 T}{\partial z^2} \right] + dissipation \tag{3-8}$$

The following non-dimensionalization of variables was performed to determine the order of magnitude of the various terms in the equations.

$$\frac{1}{r^*}\frac{\partial}{\partial r_*}\left(r^* u^* \right) + \frac{\partial w^*}{\partial z^*} = 0 \tag{3-9}$$

$$\begin{aligned} &\mathrm{Re}\left(\frac{\delta}{R} \right)\left(u^* \frac{\partial u^*}{\partial r^*} + w^* \frac{\partial w^*}{\partial z^*} \right) = -2Eu\frac{\partial P^*}{\partial r^*} \\ &+ \left(\frac{\delta}{R} \right)^2 \frac{1}{r^*}\frac{\partial}{\partial r^*}\left(r^* \frac{\partial u^*}{\partial r^*} \right) + \frac{\partial^2 u^*}{\partial z^{*2}} - \left(\frac{\delta}{R} \right)^2 \frac{u^*}{r^{*2}} \end{aligned} \tag{3-10}$$

$$\begin{aligned} \mathrm{Re}\left(\frac{\delta}{R} \right)^3 \left(u^* \frac{\partial w^*}{\partial r^*} + w^* \frac{\partial w^*}{\partial z_*} \right) &= -Eu\frac{\partial P^*}{\partial z^*} - \left(\frac{\delta}{R} \right)^3 L \\ &+ \left(\frac{\delta}{R} \right)^4 \frac{1}{r^*}\frac{\partial}{\partial r^*}\left(r^* \frac{\partial w^*}{\partial r^*} \right) + \left(\frac{\delta}{R} \right)^2 \frac{\partial^2 w^*}{\partial z^{*2}} \end{aligned} \tag{3-11}$$

$$B\left(u_* \frac{\partial T}{\partial r^*} + w^* \frac{\partial T}{\partial z_*} \right) = 2\left(\frac{\delta}{R} \right)^2 \frac{1}{r^*}\frac{\partial}{\partial r^*}\left(r^* \frac{\partial T}{\partial r^*} \right) + 2\frac{\partial^2 T}{\partial z^{*2}} \tag{3-12}$$

$$r^* = \frac{r}{R} \tag{3-13}$$

$$z^* = \frac{z}{\delta} \tag{3-14}$$

$$u^* = \frac{2\delta \rho_g u}{R\overline{G}} \tag{3-15}$$

$$w^* = \frac{\rho_g w}{\overline{G}} \tag{3-16}$$

$$P^* = \frac{\left(P - P_0 \right) g_c}{\left(\rho_f - \rho_g \right) g} \tag{3-17}$$

$$Eu = \frac{g\, l \delta^2 \left(\rho_f - \rho_g \right) \rho_g}{\sigma\, g R^2 \overline{G}} \tag{3-18}$$

$$B = \frac{\delta C_{pg} \overline{G}}{k_g} \tag{3-19}$$

$$L = \frac{g \delta \rho_g^2 R}{\mu_g \overline{G}} \tag{3-20}$$

Neglecting all terms which are multiplied by (δ/r), the continuity, Navier-Stokes (or momentum), and energy equation become:

$$\frac{1}{r}\frac{\partial}{\partial r}(ru) + \frac{\partial w}{\partial z} = 0 \tag{3-21}$$

$$u\frac{\partial u}{\partial r} + w\frac{\partial u}{\partial z} = -\frac{g_c}{\rho_g}\frac{\partial P}{\partial r} + \nu_g \frac{\partial^2 u}{\partial z^2} \tag{3-22}$$

$$0 = -\frac{g_c}{\rho_g}\frac{\partial P}{\partial z} \tag{3-23}$$

$$\rho_g C_{pg} w \frac{\partial T}{\partial zr} = k_g \frac{\partial^2 T}{\partial Z^2} \tag{3-24}$$

These partial differential equations may be solved numerically (or analytically if the radial velocity profile is assumed). Baumeister and Hamill [22] stated that the numerical solution to the complete Navier-Stokes equations performed by Baumeister [20] indicated that the radial velocity profile did not differ in shape significantly from a parabola. Therefore, in the present analysis the radial velocity profile was assumed to be parabolic in z. If a parabola is used for the radial vapor velocity, u, which satisfies the no-slip conditions at the heating surface (z=0) and the bottom of the drop (z=δ), the form of the vertical vapor velocity, w, can be shown to be that of a cubic in z from the continuity equation (Equation 3-21). These two vapor velocities may then be substituted into the radial momentum equation (Equation 3-22) to determine the radial pressure distribution in the vapor flow beneath the drop.

The vertical vapor velocity, w, may also be substituted into the energy equation for the vapor flow (Equation 3-24) to obtain a differential equation for the vertical temperature distribution (non-dimensionalization and order-of-magnitude analysis as detailed above indicates that the radial variation in the temperature of the vapor is insignificant as compared to the vertical variation). The differential equation for the vertical temperature distribution may be solved through the use of an integrating factor. The resulting solutions for the radial velocity, the vertical velocity, the pressure, and the temperature distributions in the vapor flow beneath the drop are given by Equations 3-25 through 3-28 respectively. These equations are identical to those of Baumeister et al. [31] with the exception of the Reynolds number correction in Equation

$$u = \left(\frac{3\overline{G}r}{\delta \rho_g}\right)\left[\left(\frac{z}{\delta}\right) - \left(\frac{z}{\delta}\right)^2\right] \tag{3-25}$$

$$w = \left(\frac{\overline{G}}{\rho_g}\right)\left[z\left(\frac{z}{\delta}\right)^3 - 3\left(\frac{z}{\delta}\right)^2\right] \tag{3-26}$$

$$P - P_0 = \left(\frac{3\overline{G}R^2\mu_g}{\delta^3 \rho_g} \right) \left\{ 1 + \frac{3}{20} \mathrm{Re} \left(\frac{\delta}{R} \right) \left[1 - \left(\frac{r}{R} \right)^2 \right] \right\} \tag{3-27}$$

$$\frac{T - T_L}{T_W - T_L} = \frac{\int_0^{\frac{z}{\delta}} e^{\left[-B\left(x^3 - \frac{x^4}{2} \right) \right]} dx}{\int_0^1 e^{\left[-B\left(x^3 - \frac{x^4}{2} \right) \right]} dx} \tag{3-28}$$

The vapor flow pattern beneath a drop on a macro-roughened surface is unknown at the present. It is doubtful that any investigation has ever been undertaken to measure this flow pattern. Such a measurement is beyond the scope of the present study. Since different macro-roughness element geometries would most likely produce different vapor flow patterns, and such flow patterns are unknown for any geometry other than a smooth surface, it was assumed that the vapor flow which occurs on a macro-roughened surface could be approximated by that which would occur beneath a similar drop on a smooth surface were it to have the same vaporization rate which occurs on the macro-roughened surface.

The modeling of the vapor flow is completed by performing a force balance on the entire drop (The weight of the drop, less the buoyancy force, must be supported by the total pressure force beneath the drop.). This force balance is given). by Equation 3-29 (which is identical to that derived by Baumeister and Hamill [22]

$$\frac{\left(\rho_f - \rho_g \right) g V_D}{g_c} = \int_0^R 2\pi r \left(P - P_0 \right) dr \tag{3-29}$$

The radial pressure distribution (Equation 3-27) may be substituted into the integral (Equation 3-29) and the resulting relationship solved for the thickness of the vapor layer, to yield:

$$\overline{\delta} = \left[\frac{3 g_c \overline{G} \mu_g A_P^2}{2\pi g \rho_g \left(\rho_f - \rho_g \right) V_D} \right] \left[1 + \frac{3}{20} \mathrm{Re} \left(\frac{\delta}{R} \right) \right] \tag{3-30}$$

This equation differs from that of Baumeister and Hamill only by the Reynolds number correction. Since G, R, and V are determined from experimental measurements, the computed vapor layer thickness,&, and the enthalpy flux parameter, B, may be computed from Equations 3-19 and 3-30 respectively.

Modeling the Mass Transfer Process

As in References 20, 21, 22, and 23, in the present study the heat and mass transfer at the sides and the top of Leidenfrost drops were assumed to be insignificant (compared to that which takes place at the bottom of the drops). Keshock [26] and Keshock and Bell [27] pointed out that heat and mass transfer at the sides and top of a drop are not negligible when dealing with cryogenic liquids. However, the four liquids investigated in the present study all have normal boiling points above the laboratory ambient temperature (but not sufficiently above the ambient that heat loss to the surroundings would be significant as the temperature difference between the

boiling liquids and the ambient was significantly less than the temperature difference between the heating surface and the boiling liquids). Using the relationships given in References 13, 26, and 49, the heat and mass transfer from the sides and top of Leidenfrost drops on a smooth surface is computed to be less than 6% and 5% respectively of that which occurs beneath the drops for the four liquids, range of drop sizes, range of bulk surface temperatures, and range of laboratory temperatures in the present study. Since heat transfer (and thus evaporation) has been shown to increase on macro-roughened surfaces over that which occurs on smooth surfaces (e.g., [8], [9]), and this increase is thought to occur predominantly beneath the drops where the liquid comes into direct contact with the heating surface, the relative effect of heat and mass transfer at the sides and top of the drops as compared to that which takes place beneath the drops should be no greater than that which occurs on a smooth surface. In fact, the relative contribution of heat and mass transfer at the sides and top of the drops when undergoing film boiling on macro-roughened surfaces should be less than that which occurs on a smooth surface.

Bell [14] addressed the subject of heat and mass transfer at the sides and top of Leidenfrost drops by contrasting the model of Baumeister et al. [20], [21], [22], and [23], which neglected the effect of heat and mass transfer at the sides and top of the drops, and the model of Gottfried et al. [15] which included this effect. Bell concluded that the differences in the apparent effect of heat and mass transfer at the sides and top of Leidenfrost drops is less than the uncertainty in the experimental data. Thus Bell suggested that the two models (which respectively neglected and included the effect of heat and mass transfer at the sides and top of Leidenfrost drops) were in agreement to within the uncertainty of the experimental data and that this agreement "may indicate that some errors tend to cancel each other out over the range tested" (Data with cryogens were not included in this comparison.). Baumeister and Schoessow [49] stated that the total contribution to vaporization resulting from diffusion for water undergoing Leidenfrost film boiling on a smooth surface in an air atmosphere was less than 10%. Since water vapor has the smallest Schmidt number of the vapors of the four liquids investigated in the present study, the corresponding contribution of diffusion for the other three vapors should also be less than 10%. It was therefore assumed in the pre sent study that the heat and mass transfer at the sides and the top of Leidenfrost drops is insignificant when compared to that which takes place at the bottom of the drops.

Modeling the Heat Transfer Processes

The first consideration in modeling any heat transfer process is the definition of a thermodynamic control surface. In the present study the thermodynamic control surface associated with the Leidenfrost phenomenon was defined by the surface of the liquid. The thermodynamic control volume enclosed by this control surface included only the liquid and the liquid/vapor interface. This control volume did not include the vapor beneath the drop, the vapor surrounding the drop, the heating surface, nor the macro-roughness elements. In defining a heat transfer coefficient it is necessary to define three basic quantities: the heat transfer, the reference area, and the reference temperature difference. The heat transfer that was considered in relationship to this control surface is that from all sources (assumed to be predominantly from the heating surface) to the drop. In the present study the reference area was defined as the vertically projected area of the drop. The reference temperature difference was defined as the difference between the bulk temperature of the heating surface and the saturation temperature of the liquid. The defined heat transfer coefficient for Leidenfrost drops (denoted by the subscript "D") follows from these three quantities is given by Equation 3-31.

$$h_D = \frac{\dot{Q}_D}{A_P(T_W - T_L)} \tag{3-31}$$

A considerable discrepancy exists in the literature concerning the definition of the heat transfer coefficient for Leidenfrost drops. This discrepancy in definition subsequently leads to discrepancies in experimental values of heat transfer coefficients as these are computed from experimental data through different relationships depending on the definition used by the investigator. The present definition was adopted because it involves quantities which are primary or direct experimental measurements (e.g., If the heat transfer coefficient were to be defined in terms of the heat transferred from the heating surface, rather than that which is transferred to the drop, the additional heat which is transferred from the heating surface to the vapor resulting in superheating would have to be determined separately, such as by measuring vapor velocity and temperature profiles. Similarly, if the heat transfer coefficient were to be defined in terms of the total drop area or some other fraction thereof this area would have to be computed from projected area or measured from stereoscopic photographs, since planar photography records only projected area. Thus heat transfer coefficients so defined would be tertiary data rather than secondary data, since these would be computed from secondary rather than primary experimental data such as temperature and projected area.).

As in References 9, 12, 13, 15, 16, 18, 19, 20, 21, 22, 23, 25, and 30, it was assumed in the present study that all of the heat transferred to the drop results in vaporization at the under surface of the drop. This follows logically from the assumption that heat transfer, and particularly mass transfer, at the sides and the top of a Leidenfrost drop is insignificant when compared to that which takes place at the bottom of a drop. The same evidence justifying the latter assumption justifies the former under the conditions of the present study. This assumption concerning vaporization at the under side of the drop gives rise to the following relationship between heat flux and average vapor mass flux, G:

$$\dot{Q}_D = h_{fg} A_P \overline{G} \tag{3-32}$$

Since the mass transfer at the sides and top of the drop is assumed to be insignificant when compared to that which occurs at the bottom of the drop, the following relationship exists between the average vapor mass flux and the drop volume (this relationship will be dealt with in greater detail in Chapter5):

$$-A_P \overline{G} = \rho_f \frac{dV_D}{dt} \tag{3-33}$$

Thus, the average vapor mass flux and the heat flux may be determined from experimental data. The actual method that was used to obtain the experimental data and to compute these quantities from that experimental data will also be given in detail in Chapter 5. These relationships are presented here as they are modeling aspects that involve engineering assumptions and approximations that are common to both the analytical and experimental investigation.

The heat transfer to the drop is assumed to be the result of three mechanisms: convection in the vapor flow beneath the drop (designated by the subscript "F" to distinguish it from contact), radiation (designated by the subscript "R"), and intermittent liquid-solid contact (designated by the subscript "C"). These three modes of heat transfer occur simultaneously and are defined

implicitly so as not to violate the additivity principle of heat transfer coefficients for parallel heat transfer mechanisms. The respective heat fluxes are additive and are related by:

$$q_D = q_F + q_R + q_C \tag{3-34}$$

The respective heat transfer coefficients are defined by dividing each heat flux by the same temperature difference (i.e., the difference between the bulk temperature of the heating surface and the saturation temperature of the liquid):

$$h_F = \frac{q_F}{(T_W - T_L)} \tag{3-35}$$

$$h_R = \frac{q_R}{(T_W - T_L)} \tag{3-36}$$

$$h_C = \frac{q_C}{(T_W - T_L)} \tag{3-37}$$

When defined in this manner, the heat transfer coefficients are additive:

$$h_D = h_F + h_R + h_C \tag{3-38}$$

The convective heat transfer contribution is determined from the vapor flow beneath the drop and is given by Equation 3-39.

$$q_F = -k_g \left.\frac{\partial T}{\partial z}\right|_{z=\delta} \tag{3-38}$$

The partial derivative of the temperature is obtained from Equation 3-28; so that convective heat transfer coefficient is given by Equation 3-40.

$$h_F = \frac{k_g}{\delta F(B)} \tag{3-40}$$

$$F(B) = \int_0^1 e^{\left[\frac{B}{2}\left(1-2x^3+x^4\right)\right]} dx \tag{3-41}$$

This expression implicitly involves convection, radiation, and intermittent liquid-solid contact, as the enthalpy flux parameter, B, is related to the average vapor mass flux, G, through Equation 3-19. The average vapor mass flux, G, is related to the respective heat transfer contributions through Equations 3-32 and 3-34. The convective Nusselt number based on the computed vapor layer thickness is given by Equation 3-42.

$$N_{uF} = \frac{1}{F(B)} \tag{3-42}$$

Since F(B) is a monotone increasing function of the enthalpy flux parameter, B, having a minimum value of unity (which occurs at B=0), the convective Nusselt number has a maximum value of unity and decreases with increasing B. (A monotone increasing function is one which has at most one minimum, a first derivative which is always greater than zero, and a second derivative which is always greater than or equal to zero.)

$$F(B) \geq 1 \tag{3-43}$$

$$N_{uF} \leq 1 \tag{3-44}$$

This behavior of the convective Nusselt number is a result of the "blowing" from the under surface of the drop which tends to decrease the vertical temperature gradient near the under surface of the drop and increase the vertical temperature gradient in the vapor near the heating surface. This reduction of the temperature gradient in the vapor at the under surface of the drop with increasing B (from the linear gradient and a Nusselt number of unity which would accompany pure conduction) is caused by two factors: l) the continuous injection of vapor at essentially the saturation temperature from the under surface of the drop into the vapor flow near the under surface, and 2) the increase in average vapor layer thickness that results from an increase in B (The increase in average vapor layer thickness results from an increase in the downward vertical momentum of the vapor flow which increases with increasing vapor mass flux.). Thus, the convective heat transfer contribution may be determined from B that may be determined from experimental data as outlined previously.

The radiation heat transfer contribution is given by Equation 3-45 (assuming gray-diffuse radiative exchange, isothermal surfaces, and no emitting, scattering, or absorbing in the vapor):

$$q_R = \frac{\sigma_R \left(T_W^4 - T_L^4\right)}{\left(\frac{A_P}{A_S}\right)\left(\frac{1-\varepsilon_S}{\varepsilon_S}\right) + \left(\frac{1}{F_{D-S}}\right) + \left(\frac{1-\varepsilon_L}{\varepsilon_L}\right)} \tag{3-45}$$

If the area of the drop is significantly less than the area of the heating surface then uncertainties in the emissivity of the heating surface do not affect the radiative heat exchange (see the first term in the denominator of Equation 3-45). The heating surfaces investigated were either nickel stainless or nickel-plated steel. The tabulated emissivity of oxidized nickel at the temperatures investigated is approximately 0.9 [66]. According to Eckert and Drake [50], the reflectivity and transmissivity of liquid layers greater than a few millimeters is essentially zero for wavelengths in the infrared range. The view factor between the bottom of the drop and the heating surface is unity (this holds by reciprocity for smooth or macro-roughened surfaces). The radiation heat transfer coefficient is then determined from Equations 3-36 and 3-45.

The heat transfer contribution due to liquid-solid contact must be determined experimentally as no general theory exists for this phenomenon at the present time. The modeling of liquid-solid contact is discussed in the next section.

Modeling Intermittent Liquid-Solid Contact

The experimental evidence of References 4, 5, 6, 10, 11, and the analyses of References 5, 6, 10, 29, 32, and 37 indicate that liquid-solid contact and the MFBT (minimum film boiling temperature) are intimately related. The definition of the MFBT employed in the present study is stated in terms of liquid-solid contact: should direct contact between the boiling liquid and the heating surface occur at any point (due to Taylor instabilities, impingement, macro-roughness elements, etc.) and sufficient vaporization in the vicinity of the liquid-solid contact result, such that the liquid is expulsed from the heating surface in the vicinity of contact, then the local temperature of the surface at the instant preceding contact is said to be greater than or equal to the LMFBT. In this context direct liquid-solid contact implies a local wetting of the surface by the liquid. The experimental data of Seki et al. [11] (as well as data taken in the present study)

indicate that the LMFBT so defined is discernable from transient temperature measurements in the vicinity of liquid-solid contact. Thus, this definition is not unfounded in experiment. In conjunction with this definition of the LMFBT is the definition of the BMFBT: the bulk surface temperature necessary to maintain the LMFBT at every point on the surface which experiences liquid-solid contact under whatever conditions are present is defined as the BMFBT.

These definitions of the LMFBT and BMFBT inherently associate a locally intermittent character with liquid-solid contact in film boiling. As referenced previously, Bradfield [4] stated that the liquid-solid contact in what he termed "stable film boiling" could be "periodic" (presumably intermittent) or "quasi-steady" (presumably not intermittent or continual but rather continuous). It should be noted that this statement is not necessarily incompatible with the present definition since Bradfield did not measure "local" liquid-solid contact. The experimental technique employed by Bradfield (electrical conductance probe as described in the third section of Chapter 2) gives only the total of all liquid-solid contact over the entire area of the heating surface that is exposed to film boiling. Thus this technique records simultaneous, overlapping in time, and therefore indistinguishable local contact occurrences making such a characterization of local liquid-solid contact impossible with his experimental technique.

For completeness it should be noted that by the present definition of the LMFBT (and thus the presence or absence of film boiling), if the local contact is not intermittent then the local boiling process is not said to be film boiling. This definition follows logically from the most primitive characterization of film boiling, the presence of a vapor layer separating the heating surface from the boiling liquid (i.e., if the contact at a point is not at least intermittent then there can be no characteristic separating vapor layer at that point). It also follows from this definition that certain areas on a heating surface could experience what is defined as film boiling while other areas on the same surface simultaneously experience what is not defined as film boiling. Therefore, the liquid-solid contact in film boiling which was modeled in the present study is by definition of an intermittent nature.

Intermittent liquid-solid (or liquid-liquid) contact was modeled as the contact of two semi-infinite static media in References 4, 5, 6, 10, 11, 32, 35, 37, 44, 51, 52, 53, 54, 55, and 56. Only one of the references cited treated intermittent liquid-solid contact in any other manner than this (viz. [29]). Baumeister and Simon [29] assumed that during liquid-solid contact the heat transfer process could be characterized by an unknown time dependant heat transfer coefficient. Baumeister and Simon obtained a correlation for this "unknown" heat transfer coefficient which is identical in behavior to that which is determined by the analysis for the contact of two semi-infinite static media, (i.e., the heat transfer coefficient is inversely proportional to the square root of time). Thus, their contact analysis does not differ significantly in final form from the others listed. Some improvements to the basic model employed by Bankoff and Mehra [37] have been made (e.g., finite speed of propagation for a thermal disturbance [57], [58], [59], and [60], and radiation [61]; but these improvements do not significantly alter the basic physics of the modeling.

The local transient temperature measurements of Seki et al. [11] for small drops impinging on a smooth surface (as well as similar data taken in the present study for macro-roughened surfaces) indicate that the intermittent liquid-solid contact phenomenon ma be modeled as the contact of two semi-infinite static media under certain conditions (which will be detailed in the last section of Chapter 5). Therefore, the formulation of the contact of two semi-infinite static media is chosen here as the basic model for intermittent liquid-solid contact as it occurs in

Leidenfrost film boiling (certain modifications to extend the generality of the basic formulation will be detailed in Chapter 5).

The transient conduction equation in cylindrical coordinates may be written as:

$$\rho C \frac{\partial T}{\partial t} = \frac{1}{r}\frac{\partial}{\partial r}\left(k\, r \frac{\partial T}{\partial r}\right) + \frac{\partial}{\partial z}\left(k \frac{\partial T}{\partial z}\right) + \frac{1}{r^2}\frac{\partial}{\partial \theta}\left(k \frac{\partial T}{\partial \theta}\right) \tag{3-46}$$

When applied to the droplet this equation neglects convective effects within the liquid. The experimental data of References 4, 5, 6, 10, and 11 (as well as data taken in the present study) indicate that the characteristic time frame of liquid-solid contact in film boiling under the conditions investigated is on the order of 0.1 second. This time frame of the liquid-solid contact phenomenon in film boiling suggests that convection within the liquid during contact is insignificant when compared to conduction, hence the liquid is modeled herein as a static media during the period of contact. Assuming a uniform temperature distribution prior to contact in both the liquid and the solid, constant properties, and semi-infinite static media, the solutions to Equation 3-46 for the temperature in the solid and liquid are given by Equations 3-47 and 3-48 respectively (details of this solution may be found in Reference 50):

$$T = T_C + (T_S - T_C)\, erf\left(\frac{z}{2\sqrt{\alpha_S t}}\right) \tag{3-47}$$

$$T = T_C + (T_L - T_C)\, erf\left(\frac{z}{2\sqrt{\alpha_S t}}\right) \tag{3-48}$$

$$T_C = \frac{T_W + \gamma T_L}{1+\gamma} \tag{3-49}$$

$$\gamma = \sqrt{\frac{(\rho C k)_L}{(\rho C k)_S}} \tag{3-50}$$

Where t is the time from the initiation of contact, z is the distance from the point of contact in either the liquid or the solid, and Tc is referred to as the "contact" temperature and is independent of time. This formulation and solution will be hereafter referred to as the "error function" formulation or solution. The error function formulation is precisely the formulation used in References 4, 5, 6, 10, 11, 32, 35, 37, 44, 51, 52, 53, 54, 55, and 56. The restrictions on this formulation are: one-dimensional temperature variation, constant properties, short duration {such that convective effects in the liquid may be neglected), semi infinite static media, negligible effects due to radiation, no vaporization of the liquid during the contact period (vaporization might reasonably be thought to occur at the end of the contact period rather than during it), and uniform temperature distributions within both the liquid and the solid prior to the contact. The instantaneous heat transfer coefficient associated with the error function solution is given by Equation 3-51 (this 49 equation is obtained by taking the derivative of Equation 3-48 with respect to time, applying the Fourier law of conduction at the point of contact (z=0), dividing by the initial temperature difference (Tw-TL)and substituting Equation 3-48 for Tc):

$$h_C = \frac{k_L}{(1+\gamma)\sqrt{\pi \alpha_L t}} \tag{3-51}$$

The instantaneous heat flux associated with the error function formulation is given by Equation 3-52:

$$q_C = \frac{k_L (T_C - T_L)}{(1+\gamma)\sqrt{\pi \alpha_L t}} \tag{3-52}$$

This formulation must be modified to permit application to finite macro-roughness elements. Two-dimensional effects, variable properties, finite media, and non-uniform initial temperature distributions (as are present under experimental conditions in macro-roughness elements which are exposed to intermittent liquid-solid contact) essentially preclude any tractable analytical solution for heat flux and temperature distribution which more closely approximates the true response of such a macro-roughness element. Accordingly a two-dimensional transient finite difference model based on modifications of the error function solution was developed as a part of this study and will be presented in Chapter 5.

Closure of the Model

At the present time no general relationship for contact heat flux on macro-roughened surfaces exists. Since contact heat flux is necessary to permit closure of any model for the Leidenfrost phenomenon on macro-roughened surfaces (as convective heat transfer implicitly depends on both contact and radiative heat transfer), a model prediction apart from specific experimental data is not possible at this time. Since the modeling of the Leidenfrost phenomenon presented thus far requires knowledge of either contact heat flux or total heat flux (which must be obtained from experimental data), the verification of this model by experimental data is necessarily inductive rather than deductive. With the present formulation the apparent heat flux contribution due to intermittent liquid-solid contact on macro-roughened surfaces may be computed from experimental data for total heat flux. This may be done by solving Equations 3-30, 32, 38, 40, and 45 simultaneously for the contact heat flux. Also the heat flux contribution due to intermittent liquid-solid contact may be computed using the finite difference model (described in the last section of Chapter 5) and experimentally measured local temperature variations, contact duration and period (the definition of contact duration and period as it pertains to the present study is also given in the fourth section of Chapter 5). These two computations of contact heat flux based on completely separate experimental data and theory may be compared to demonstrate consistency and inductive verification of the modeling of the phenomenon.

Chapter 4. Experimental Apparatus and Procedure

Liquids Investigated

Film boiling of stationary, discrete (Leidenfrost) drops on horizontal heating surfaces at atmospheric pressure was investigated using the following four liquids: water, Baker Chemicals' specially denatured Ethanol (3-9401), isopropanol, and ethylene-chloride. These four liquids were chosen to provide a range of thermodynamic property values, molecular structure (polar/non-polar), and composition (inorganic/organic). The normal boiling point of the liquids ranged from 78.4°C (ethanol) to 100°C (water). Since the experiments were conducted under atmospheric conditions, liquids were chosen which had normal boiling temperatures in this range to minimize the experimental uncertainties which might possibly result from heat transfer from the laboratory surroundings to the boiling liquids or from the boiling liquids to the laboratory surroundings (as detailed in the third section of Chapter 3). The range of drop sizes investigated was approximately 0.0l cc to 10 cc.

Heating Surfaces

Five heating surfaces were investigated: a smooth surface (for baseline comparison data), two surfaces into which were machined concentric grooves, one surface into which were embedded 492 cylindrical pins, and one surface into which were excavated diagonal slots forming right-hexagonal pins projecting from the surface.

The smooth surface, referred to as "SMTH", was fabricated from mild steel, polished to 0.13 -0.25 micron roughness, and plated with approximately 0.005 cm of nickel to inhibit corrosion. Further details of this surface are given in Figure 13.

The first grooved surface, referred to as "CGOI" (for con centric grooves, 0.01 inch depth), was fabricated from mild steel and plated with approximately 0.005 cm of nickel to inhibit corrosion. The radial spacing of the concentric grooves was 0.051 cm and the depth was 0.025 cm Further details of this surface are given in Figure 14.

The second grooved surface, referred to as "SCG02" (for stainless steel, concentric grooves, 0.02 inch depth), was fabricated from type 321 stainless steel (no plating was required). The radial spacing of the grooves was 0.071 cm and the depth was 0.051 cm Further details of this surface are given in Figure 15.

The surface having the embedded cylindrical pins, referred to as "CP54" (for cylindrical pins, 0.050 inch pin height, and pin spacing of V4 the Taylor most critical wavelength for Refrigerant-Ill), was fabricated from mild steel (The Taylor most dangerous wavelength was defined in the first section of Chapter 1.). This surface was initially fabricated in a similar manner as SMTH. Then a numerically controlled milling machine was used to drill 492 #51 holes, 0.1702 cm diameter and 0.224 cm deep, vertically down into the top of the surface. These were drilled in a 53 square array having a center-to-center in-line spacing of 0.305 cm The 492 cylindrical pins were also fabricated from mild steel, having a diameter of 0.1704 cm and a length of 0.279 cm The pins were individually pressed into the holes. The center pin was fabricated into a flush-mounted micro-thermocouple (which will be described in the next section). Finally the entire surface and pins were plated with approximately 0.005 cm of nickel to inhibit corrosion. Further details of this surface are given in Figure 16.

The surface with the hexagonal pins, referred to as "SHP2612" (for stainless steel, hexagonal pins, 0.020 inch pin height, 0.06 in width hexagons, 0.12 inch center-to-center spacing), was fabricated from type 321 stainless steel (no plating was required). The surface was fabricated by milling three sets of 0.159 cm (1/16 inch) wide by 0.051 cm deep slots having 0.305 cm center-to-center spacing. The three sets of slots were cut at 30 degree angles, forming hexagonal pins of 0.051 cm height, 0.146 cm width, and 0.305 cm center-to-center hexagonal-close-packed spacing. The center hexagonal pin was drilled-out and a thermocouple/pin was fabricated and pressed into the hole. Further details of this surface are given in Figure 17.

Thermocouple/Pins

The thermocouple/pin for surface CP54 was fabricated by drilling a #80 (0.0343 cm diameter) hole through one of the cylindrical pins followed by a concentric #68 (0.079 cm diameter) hole drilled from the bottom to within 0.008 -0.013 cm from the top of the pin. A ceramic insulator and a #30 AWG (0.0254 cm diameter) constantan wire were then inserted from the bottom. The constantan wire was brazed with 24K gold at the tip of the pin to form a thermocouple junction. The top of the pin with the exposed junction was milled flush to remove the excess brazing material. The thermocouple/pin was then pressed into the surface and nickel plated with the rest. Further details of this thermocouple/pin are given in Figure 18.

The thermocouple/pin for surface SHP2612 was fabricated in the same manner as the one for surface CP54, except that the exposed tip of the thermocouple was milled to a hexagonal shape, the protrusion height was only 0.0508 cm the overall length was 0.813 cm and the dissimilar metal wire used was Alumel rather than constantan. Further details of this thermocouple/pin are given in Figure 19.

Calibration of the Thermocouple/Pins

The differential voltage produced by the dissimilar metal junction at the top/center of the thermocouple/pins was measured against a reference junction (of the same two metals) that was maintained at 0°C in an ice bath. The reference junction for surface CP54 was iron/constantan and the reference junction for surface SHP2612 was SS-321/alumel. The differential voltage output of the junction was measured by a Doric Model DS-100 digital microvolt meter during the calibration process. The temperature of the junction corresponding to the differential voltage was determined from a Chromel-Alumel thermocouple that was affixed to the pins during the calibration process. The voltage/temperature calibration plots for the CP54 and SHP2612 thermocouple/pin junctions are shown in Figures 20 and 21 respectively. The differential voltage produced by the thermocouple/pin junctions was amplified by a Honeywell Accudata Model 122 differential amplifier, displayed on an oscilloscope, and recorded on a Brush Mark V strip chart recorder.

The amplifier gain was determined for each thermocouple/pin junction from the slope of the respective voltage/temperature calibration plots. This slope was determined by fitting a least-squares straight line through the voltage/temperature data points. The offset voltage of the differential amplifier was adjusted to appropriately locate 0°C on the strip chart recorder. The amplifier gain and offset voltage was calibrated against the digital microvolt meter before sequence of data was taken to minimize the experimental uncertainty associated with "drift" of the differential amplifier. The offset voltage and gain of the differential amplifier was thus used to provide an approximately linear voltage/temperature relationship for interfacing with the strip chart recorder.

Response Rate of the Thermocouple/Pins

The response rate of the junction in the top/center of the thermocouple pins was determined by recording the temperature excursion of the junction, initially at 500°C. This was accomplished by heating the surface to 500°C and pouring ice water directly onto the thermocouple/pin. The resulting boiling process was quite rapid 56 so that the liquid completely evaporated in a few seconds. The temperature of the junction dropped sharply when the ice water contacted the pin and slowly recovered to the initial value some time after the water evaporated. This was done several times with consistent results. A typical strip chart record of the response of the CP54 junction is shown in Figure 22. On an expanded time scale (25 cm./sec. strip chart speed), the initial time rate of change of the temperature of the junction under these conditions was found to be at least 12,000°C/sec. The response rates of the two thermocouple/pin junctions (CP54 and SHP2612) were essentially the same. The maximum response rate was not determined beyond this point as this testing procedure was far more severe than any which would actually occur in the film boiling experiments conducted.

Heating the Surfaces

The surfaces were heated from beneath by a Bunsen burner or an electric hotplate. The electric hotplate was a Chromalox Model ROPH-20L 2000 watt hotplate. The temperature of the hotplate was controlled by a Variac Model V20HM variable transformer. The maximum temperature which could be maintained by the electric hotplate was approximately 530°C. The data taken at bulk surface temperatures above 530°C were taken with the surface heated by the Bunsen burner. When heating the surfaces with the Bunsen burner, a steel heat shield of approximately 30 cm diameter was used to protect the camera and the thermocouple lead wires. The shield also 57 served to reduce the draft induced by the flame in the vicinity of the boiling drops. The Bunsen burner was only used when boiling water as the other three liquids are highly flammable. The surfaces were supported by the hotplate while being heated by the hotplate, whereas the surfaces were supported by a ring stand while being heated by the Bunsen burner.

Photography

The evaporating liquid drops were photographed from above with a Bolex Model H16RX5 16 mm single-frame/movie camera. The camera was positioned approximately 50 cm directly above the center of the heating surface (lens facing down) such that the vertically projected drop area was viewed by the camera lens. The camera was manually operated and the time between photographs was determined from a stopwatch. The evaporating liquid drops were also photographed from several perspectives with a 35 mm SLR camera. These photographs will be presented in Chapter 7.

Bulk Surface Temperature Measurements

The bulk temperature of the heating surfaces was determined from a Chromel-Alumel thermocouple that was inserted horizontally into the 0.178 cm diameter holes detailed in Figures 13 through 17. The vertical temperature gradient within the heating surfaces (under the most extreme cases, based on steady, one-dimensional conduction) was less than 120°C/cm. Since a vertical temperature gradient always exists in the heating surface by virtue of the heat being conducted from the hotplate (or Bunsen burner) through the heating surface to the boiling drops, no unique "bulk" surface temperature exists. In the present study bulk surface temperature was taken as characterized by the Chromel-Alumel thermocouple which was located approximately

in the center (vertical) of the surface. The only exception to this is the bulk surface temperature measurements made on surface SHP2612, where the Chromel-Alumel thermocouple was located directly at the base of the thermocouple/pin (see Figure 17). The temperature of the Chromel-Alumel thermocouple was determined from readings made using an Omega Model 2166A Digital Thermometer. The voltage of the Chromel-Alumel thermocouple junction was also conditioned by a Honeywell Accudata Model 106 Type K thermocouple control unit, amplified by a Honeywell Accudata Model 122 differential amplifier, and recorded on a Brush Mark V strip chart recorder. The temperature measurements and calibration of the thermocouple/pins will be presented in the eighth section of this chapter.

Preparation of Heating Surfaces

Although the heating surfaces were either nickel plated or high nickel stainless, some oxidation occurred. It was observed that the surfaces became discolored within a few minutes at high temperatures regardless of the polishing or cleaning prior to heating. After one hour above 500°C the nickel oxide which formed on the surfaces appeared to remain relatively constant with time. For this reason each surface was "seasoned" for at least one hour at 500°C before experiments were performed.

Introduction of the Liquids to the Heating Surfaces

In order to minimize the number of experimental variables, the liquids were heated to saturation prior to introduction to the heating surfaces. The liquids were introduced to the heating surfaces by gently pouring them onto the surfaces from a beaker. Since the actual volume of the vaporizing drop at any particular time was determined from the photographs (in the manner which will be given in detail in the next section the precise initial liquid volume was immaterial (and could not be determined as some vaporization inevitably occurs while heating the liquid to saturation prior to its introduction to the heating surfaces). This technique of introducing the liquid to the heating surfaces eliminates three experimental variables typically associated with Leidenfrost film boiling data: 1) initial subcooling of the liquid, 2) initial drop volume, and 3) the height from which the drops fall (for impingement studies).

Drop Area/Volume Calibration

Known volumes of liquid (necessarily subcooled because of possible evaporation) were gently poured onto the surfaces and several photographs taken at the time of deposition. The vertically projected drop area was determined from the photographs (in the 60 manner detailed in the first section of the next chapter). The vertically projected drop area was then extrapolated backward in time to the point when the drop was introduced to the surface. These area/volume data points were used in conjunction with computer program "LAMBDA" (a description of which may be found in Appendix C) to determine the optimum value of the liquid/vapor interface parameter, A (Equation 1-1), which best related the drop area/volume data to the numerical solution to the Laplace capillary equation (section 1 of Chapter 3).

The values of λ determined in this manner were 0.219 cm, 0.119 cm 0.0929 cm and 0.0889 cm for water, ethanol, isopropanol, and ethylene-chloride respectively. These data points and the numerical solution to the Laplace capillary equation are shown in Figures 8 through 11. The numerical solution to the Laplace capillary equation and the respective value of A was used to determine the drop volume from the vertically projected drop area for each of the subsequent data points. As mentioned in section 1 of Chapter 3, no distinguishable difference in the drop

area/volume relationship was noted on the macro-roughened surfaces as compared to the smooth surface (see Figures 8 and 9).

Chapter 5. Data Reduction and Computational Procedure

Determination of Contact Period and Duration from Thermocouple/Pin Data

The duration of intermittent liquid-solid contact was taken as the time during which the temperature of the micro-thermocouple junction in the top/center of the instrumental pin was falling. The contact period was taken as the time between successive maxima in the temperature of the junction. The maxima and minima were determined from the strip chart records of junction temperature vs. time. Each liquid-solid contact occurrence evidenced a maximum and a minimum temperature. The maximum temperature during the contact period (which occurred just prior to contact) is referred to as the recovery temperature, T_R, and the minimum temperature during the contact period (which occurred at the end of contact) is referred to as the quench temperature, T_Q (for illustration of the quantities T, Tc, T_R, and T_Q see Figure 26). Further details of this data will be given in Chapters 6 and 7.

Computed Heat Transfer Coefficients from Contact Period and Duration

The average contact period and duration as determined from the thermocouple/pin data were used to compute a theoretical value of heat transfer coefficient based on the modeling of the intermittent liquid-solid contact phenomenon presented in the last section of Chapter 3. The heat transfer due to convection in the vapor flow beneath the drops and radiation was computed from Equations 3-36, 3-40, and 3-45. The heat flux due to intermittent liquid-solid contact was computed from the contact period/duration data by the two dimensional, transient finite difference model detailed in the next section. The enthalpy flux parameter, B (Equation 3-40), was not computed from experimental vaporization data. Instead, the value of B was computed by solving Equations 3-36, 3-40, and 3-45 simultaneously with Equations 3-19 and 3-32. Thus the computed heat transfer coefficients for the macro-roughened surfaces required only bulk surface temperature, contact period, and contact duration (as well as macro-roughness element geometry and thermophysical properties). The heat transfer coefficients computed in this manner will be compared to the experimental heat transfer coefficients (computed from drop vaporization) in Chapter 6.

2D Pin Subjected to Pulse-Like Periodic Liquid-Solid Contact

A two-dimensional, transient finite difference computer program was developed to model the liquid-solid contact phenomenon and the thermal response of a cylindrical pin to that contact. This program is named "2-D PINT" (a description may be found in Appendix C). The following assumptions were made in developing the two-dimensional, transient finite difference model:

1) circumferential symmetry
2) the pin is embedded in an isothermal substrata
3) the liquid-solid contact is pulse-like periodic (ON-OFF-ON-OFF-ON••••) with period T and duration Tc
4) when and where liquid-solid contact is assumed to occur a contact-type heat flux (detailed subsequently) is imposed
5) when and where contact is assumed not to occur a pool-type boiling heat flux is imposed
6) when and where contact is assumed not to occur the entire

1. pool boiling curve is used to determine the local heat flux based on the local surface temperature

7) the imposed heat flux varies with time, location, and local surface temperature

8) the thermophysical properties of the solid material are allowed to vary with temperature (and therefore also with time)

9) the presence of the ceramic insulator (see Figures 18 and 19) is included as illustrated in Figure 29

The location of the nodal points as well as further information about the finite difference modeling is given in Figure 29. Liquid-solid contact is assumed to occur only during the "ON" periods and only when the local surface temperature is above the MFBT (minimum film boiling temperature). At all other times (at external locations on the pin) a pool boiling heat flux is imposed. The pool boiling curve (see Figure 1) is determined in the following manner: for temperatures above the MFBT the boiling mechanism is assumed to be film boiling and the heat flux is computed by the relationships of Baumeister, Keshock, and Pucci [31]. These relationships are given in Equations 5-1 through 5-7. The minimum and critical heat fluxes are computed by the relationships of Zuber, Tribus, and Westwater [65], the MFBT is computed by the relationship of Berenson [38], and the critical temperature (viz., the temperature corresponding to the critical heat flux) is computed as suggested by Bankoff and Mehra[37]. These relationships are given in Equations 5-8 through 5-11. Equation 5-8 also contains Kutateladze's improvement [44].

$$h_{fg}^{S} = \frac{h_{fg}}{\left(1+\frac{7}{20}\Lambda\right)^{3}} \tag{5-1}$$

$$h_{fg}^{m} = h_{fg}\left[\frac{2\ln\left(1+\frac{\Lambda}{2}\right)}{\Lambda}\right]^{3} \tag{5-2}$$

$$h_{fg}^{*} = \frac{h_{fg}^{S} + h_{fg}^{m}}{2} \tag{5-3}$$

$$h_{fB} = 0.41\left[\frac{k_g^3 \rho_g \left(\rho_f - \rho_g\right) g h_{fg}^{*}}{\mu_g \left(T_S - T_L\right)\lambda}\right]^{\frac{1}{4}} \tag{5-4}$$

$$h_R = \frac{\sigma_R \left(T_S^4 - T_L^4\right)}{\left(T_S - T_L\right)} \tag{5-5}$$

$$h^{*} = h_{FB}\left(\frac{h_{FB}}{h^{*}}\right)^{\frac{1}{3}} + h_R \tag{5-6}$$

$$q_{FB} = h^{*}\left(T_S - T_L\right) \tag{5-7}$$

$$q_{CHF} = 0.18\, h_{fg}\left[\frac{g\lambda\rho_f\rho_g\left(\rho_f-\rho_g\right)}{\left(\rho_f+\rho_g\right)}\right]^{\frac{1}{2}} \tag{5-8}$$

$$\Delta T_{CHF} = 0.26\frac{h_{fg}}{\sqrt{\left(\rho C k\right)_L}}\left[\frac{g\lambda^3\rho_f^2\rho_g^3\left(\rho_f-\rho_g\right)}{\left(\rho_f+\rho_g\right)^2}\right]^{\frac{1}{4}} \tag{5-9}$$

$$q_{MFB} = q_{CHF}\left(\frac{\rho_g}{\rho_f+\rho_g}\right)^{\frac{1}{2}} \tag{5-10}$$

$$\Delta T_{MFB} = 3.13\left(\frac{\lambda q_{MFB}}{k_g}\right)\left[\frac{\mu_g\, q_{MFB}}{g h_{fg}\rho_g\left(\rho_f-\rho_g\right)}\right]^{\frac{1}{3}} \tag{5-11}$$

The entire boiling curve is pieced together by assuming a straight line on a log-log plot of heat flux vs. temperature difference between the points of critical and minimum heat flux (Similar to Figure 1). During the "ON" period (where intermittent liquid-solid contact is assumed to occur and when the local surface temperature is above the MFBT) the heat flux from the pin to the liquid is assumed to be given by Equation 5-12 (Reference 37).

$$q_C = \sqrt{\frac{\left(\rho C k\right)_L}{\pi t}}\left(T_S - T_L\right) \tag{5-12}$$

where t is the time since contact was initiated and Ts is the instantaneous local surface temperature. Equation 5-12 is a modification of the standard error function formulation for the contact of two semi-infinite static media as presented in the last section of Chapter 3 (Equation 3-52). The modification applied to Equation 3-52 which results in Equation 5-12 consists of two changes: 1) the contact temperature in Equation 3-52 (which is theoretically constant with respect to time according to the error function formulation) has been replaced with the instantaneous local surface temperature (which in general is not constant with respect to time) and 2) only the heat flux and not the temperature is computed using this modification of the error function formulation and that only involves liquid thermophysical properties and local surface temperature. The temperature of the solid (pin) is determined by solving the transient heat conduction equation (3-46) using finite differences. These finite difference equations are standard and may be found in most conduction textbooks (e.g., [62]).

Equation 5-12 assumes that the liquid (and not the solid) is a semi-infinite static medium. This assumption that the liquid is a semi-infinite static medium during intermittent liquid-solid contact is justified by the following reasoning: The contact recovery ("OFF") time is on the order of 0.1 second (as stated in the last section of Chapter 3). The time required for a liquid to re-establish equilibrium is on the order of the molecular collision period which is orders of magnitude less than 0.1 second [39]. This indicates that the liquid will essentially "recover" from the intermittent liquid-solid contact very rapidly, thus re-establishing an essentially uniform medium before the initiation of the next contact.

The penetration depth of the thermal boundary layer into the liquid from the point of contact, δ_{TH}, based on the error function solution is given by Equation 5-13

$$\delta_{TH} = \sqrt{7.28\,\alpha_L\,\tau_C} \tag{5-13}$$

where τ_c is the contact period and α_L is the thermal diffusivity of the liquid. Equation 5-13 is obtained by solving Equation 3-48 for the location where the temperature is 99% of the far field value. For the contact periods measured in the present study this penetration depth is less than 0.003 cm. This penetration depth is much less than the thickness of the drops investigated (e.g., 0.2 cm for a 0.03 cc water droplet). It is therefore assumed that the liquid is essentially semi-infinite during the intermittent liquid-solid contact process.

Equation 5-13 is more general than the error function formulation (Equation 3-52) in that it only assumes that the liquid is semi-infinite and uniform prior to contact. In the error function formulation, the transient conduction equation (Equation 3-46) is solved in the media on both sides of the point of contact. In the error function formulation uniform initial conditions are assumed to exist in both media. Closure of the error function formulation is obtained by setting the temperatures and heat fluxes equal in both media at the point of contact. In the present formulation the temperature distribution within the pin is determined by finite differences whereas the temperature distribution within the liquid is determined from the analytical solution (Equation 3-48). Closure of the present model is also obtained by setting the temperatures and heat fluxes equal at the nodal point on the surface of the pin.

Measurement of Drop Vertically Projected Area

The vertically projected area of the drops was photographed during vaporization at equally spaced intervals of from 1 to 10 seconds (as detailed in section 5 of Chapter 4). The photographs were projected one frame at a time onto a drafting table with an1-W International Model 224A Mark V 16mm projector and the outlines of the drops sketched on paper. The scaling factor of the projected photographs was determined from the diameter of the disk-shaped heating surfaces (the outline of which was also shown in the photographs). The area of the drop in each sketch was determined with a K&E Model 620015 polar planimeter. The actual drop area was determined from the area of the sketched drop outline by dividing by the scaling factor squared. The scaling factor used was approximately 4. This value was selected so that the range of drop area investigated (0.04 to 40 sq. cm) would be within the design range of the polar planimeter.

Uncertainty of the Area/Time Data

As mentioned in Chapter 1 and section 1 of Chapter 3, a hydrodynamic instability is present in Leidenfrost drops. This hydrodynamic instability may support the presence of thermally driven drop oscillations (e.g., [36]). This hydrodynamic instability may also support drop oscillations which result from rapid local vaporization accompanying intermittent liquid-solid contact (e.g., [2], [4]. Some degree of drop oscillation was noted in every experimental sequence in the present study. As stated in section 1 of Chapter 3, the drop is assumed to oscillate about its equilibrium shape. Photographs, however, show only instantaneous drop area rather than time averaged area that is thought to be the equilibrium area. The time frame of the drop oscillations is approximately two orders of magnitude less than the vaporization time for the size drops investigated in the present study. However, the time frame of the oscillations is also approximately an order of magnitude smaller than the time interval between the photographs taken in the present study. The drop oscillations, vaporization, and photographic sampling may

be illustrated by the solid curve, dashed curve, and triangles respectively in Figure 23. To reduce the area/time data to heat transfer coefficients, all of the quantities in Equation 5-14 must be determined.

$$h_D = -\frac{\rho_f h_{fg} \frac{dV_D}{dt}}{A_P\left(T_W - T_L\right)} \tag{5-14}$$

(Equation 5-14 is obtained by solving Equations 3-31, 3-32, and 3-33 simultaneously.) Therefore, it is necessary to determine the dashed line in Figure 23 (which represents the vaporization curve) from the triangles alone (which represents the photographic area/time data). As illustrated in Figure 24 there are many curves which might be drawn through any particular set of area/time data. The particular relationship defining the vaporization curve selected in the present study was determined from the analysis detailed in the next section.

Knobel and Yeh [9] stated that, "The major deviations in the experimental heat transfer coefficients arise from small errors in the area measurement (1 percent error in area can lead to 20-40 percent error in the incremental change in volume). Drop oscillations which result in deviations from the equilibrium drop shape can produce significant error in the determination of drop volume from instantaneous drop area. If the instantaneous drop area is used to determine drop volume and subsequently computed heat transfer as described by Knobel and Yeh, the errors associated with this data reduction process are an order of magnitude greater than the experimental uncertainties (such as initial drop volume, temperatures, etc.) and the other stages of the data reduction (such as a polar planimeter or camera parallax). For this reason the drop oscillations represent the largest obstacle in the path toward increasing the accuracy of Leidenfrost heat transfer measurements. Merely taking photographs at smaller time intervals will not resolve this inherent uncertainty in the data. It is therefore necessary to develop an algorithm for data reduction that will not amplify further the experimental uncertainty in the area data and will average out the effect of the drop oscillations. Such an algorithm was developed in the present study and is detailed in the next section.

Determination of Heat Transfer Coefficients from Drop Area/Time Data

The drop heat transfer coefficient as defined in the present study is given by Equation 5-14. Thus the determination of heat transfer coefficients necessitates the determination of the derivative of drop volume with respect to time from area/time data. Mathematically the differentiation process is an expansion [67]. One characteristic of a mathematical expansion is that uncertainties in the original quantity will result in relatively larger uncertainties in the derivative of that quantity [68]. An example of an expansion would be exponentiation (i.e., $10^{(5\pm1\%)} = 105\pm23\%$). An engineering example of the expansion property of differentiation would be that changes in an object's position indicate larger relative changes in the object's velocity that, in turn, indicate still larger relative changes in the object's acceleration. As a result of this mathematical property of the differentiation process when applied to experimental data, even if the uncertainty in the experimental quantity is known, the uncertainty in the derivative of that quantity cannot be determined precisely. The uncertainty in the derivative of an experimental quantity can only be estimated based on certain assumptions about the mathematical behavior of the experimental quantity (viz., the number of continuous derivatives, the magnitude of the next highest derivative to the desired derivative, the truncation error in the differentiation algorithm, etc.).

The typical value of uncertainty associated with heat transfer coefficients for Leidenfrost drops in the literature is 27% (e.g., [9], [14]). This quantity is rather arbitrary and is more reflective of the inconsistency between one investigator and another or between two data points taken by the same investigator than the uncertainty of the data itself, however, it can neither be confirmed nor refuted through rigorous analysis. Such a figure as 27% associated with heat transfer coefficients for Leidenfrost drops in the literature should more accurately be referred to as the degree of inconsistency rather than uncertainty, since technically the uncertainty is unknown.

The transformation of area/time data to volume/time data (through the numerical solution to the Laplace Capillary equation) is an expansion (e.g., a 15% uncertainty in the area of a 0.1 cc drop of water leads to a 20% uncertainty in its volume). Therefore, in the "straightforward" determination of heat transfer coefficients from area/time data by solving Equation 5-14 directly, there are at least three compounded uncertainties: 1) the uncertainty in the area/time data itself, 2) the uncertainty in the area-volume transformation, and 3) the uncertainty of the differentiation process. This procedure for determining heat transfer coefficients for Leidenfrost drops compounds the uncertainty of the data and thus the inconsistency between one set of data and another or between the data of one investigator and another. This compounding of uncertainties can be greatly reduced by transforming Equation 5-14 and incorporating the definitions of dimensionless drop area and volume (Equations 3-2 and 3-3) to obtain Equation 5-15.

$$h_D = -\frac{\rho_f h_{fg} \lambda}{A_P \left(T_W - T_L\right)} \frac{dV^*}{dA^*} \frac{d\left[\ln\left(A^*\right)\right]}{dt} \tag{5-15}$$

Mathematically, Equation 5-15 is equivalent to Equation 5-14. However, Equation 5-15 does not compound any of the uncertainties associated with the area/time data. Equation 5-15, except for the differentiation process, actually decreases the uncertainty of the experimental area/time data. This reduction in uncertainty is not a violation of any mathematical principle (e.g., the integration process always reduces the uncertainty in an experimental quantity and in no way violates mathematical principles). The transformation of A to A* does not increase the uncertainty since this amounts to multiplying by a constant. The transformation from A to ln(A*) is a contraction (i.e., any uncertainty in the area will result in a smaller uncertainty in the natural log of the area). Notice also that the time derivative eliminates the A to A* transformation in the natural logarithm since the derivative of the logarithm of a constant times a variable is equal to the derivative of the logarithm of the variable. The contraction property of the logarithm may be illustrated by the following example: a 15% uncertainty in an A* of 100 will result in only a 6.6% uncertainty in the logarithm of A* (i.e., ln(100±15%)= 4.6±6.6%). The dimensionless volume/area derivative (dV*/dA*) is also a contraction and only a "weak" function of the dimensionless drop area (e.g., a 15% uncertainty in an A* of 10 will result in only a 6% uncertainty in the dimensionless volume/area derivative). The dimensionless volume/area derivative is also computed from the Laplace Capillary equation and is shown in Figure 25. Thus Equation 5-15 is an optimum computational form through which to determine heat transfer coefficients from area/time data since all of the transformations are contractions (except for the differentiation process–which cannot be eliminated).

Further improvement in the data reduction algorithm is obtained by eliminating the numerical or graphical differentiation process (most investigators either use finite differences to compute the time derivatives–which greatly increases the uncertainty–or graphical differentiation–which

adds the uncertainties of deter mining tangents). This is accomplished by obtaining a best-fit approximating function to the data points and performing analytical differentiation on the approximating function. The type of best-fit necessary to produce the most accurate representation of the data is not least-squares [61] (since 10 ± 1 is treated the same as 0.1± 1 by a least-squares algorithm, which is certainly not an acceptable tolerance in an area). A least-squares relative fit to the data is also inappropriate since it tends to weight most heavily those data points having the greatest scatter [61]. The minimum-maximum (or Chebyshev) fit is likewise inappropriate since it produces a fit which weights only the data point having the greatest scatter [61]. The only "best-fit" which is appropriate is the least absolute relative fit (which weights all the data points equally) [61]. The LAR (least absolute relative) fit is that which satisfies Equation 5-16.

$$\min\left[\sum_{i=1}^{N}\left|\frac{A(i)-A_i}{A_i}\right|\right] \tag{5-16}$$

Where A_I represents the I'th data point and A(I) represents the corresponding I'th value of the approximating function. This type of best fit cannot be determined in a finite number of computations nor through any linear optimization algorithm [61, 63]. A computer program was developed to solve the minimization problem associated with the LAR fit of the area/time data. This program is called "DATABASE" (a description may be found in Appendix C). The approximating function that was to be fit to the area/time data (in the LAR sense) was determined from observing the nature of the experimental data. One hundred and twenty-five semi-log plots were made from the data taken in the present study (semi-log plots were selected because this is the form of Equation 5-15).

The approximating function selected for the data reduction algorithm was constrained by the nature of Leidenfrost film boiling to have the following four properties: 1) the function must have no more than one real zero (which occurs when the log of the area becomes zero–one square centimeter), 2) the function must have no real zeroes of the first time derivative (otherwise the drop would cease to evaporate), 3) the function must have a second time derivative which is always less than or equal to zero (otherwise the drop could increase in size with time), and 4) the function must have one and 76 only one real singularity (at the vaporization time the area is zero and the log becomes negative infinity). The simplest function which was found to have all these properties and which was similar in form to the semi-log plots of the experimental data was a single branch of a hyperbola. There are five constants in general which determine a hyperbola. Only four of these constants are arbitrary (since property 4 above requires that one be zero). Thus four constants must be determined which will result in the LAR fit (or the minimum average absolute relative discrepancy with the experimental area/time data.

The approximating hyperbola may be written in the form of Equation 5-17.

$$\ln(A)=\frac{C_1(C_2-t)(C_3-t)}{(C_4-t)} \tag{5-17}$$

Clearly C4 is the vaporization time and C2 and C3 are the points where the two branches of the hyperbola pass through zero. Only the lower branch is used (in order to satisfy property 1 stated previously). To meet all four properties the following four constraints are placed on the solution:

$$0 < C_1 < C_2 < C_4 < C_3 \tag{5-18}$$

The minimization algorithm developed in the present study for data reduction assures that these four constraints (Equation 5-18) are always met. It should also be noted that standard smoothening, approximating, and differentiating algorithms based on polynomials and least-squares relationships (e.g., Reference 61) are completely inappropriate and quite unsuccessful at approximating the present data as can be noted from property 4 (no polynomial can provide an infinite value for a finite argument). Several polynomial based algorithms were investigated in the present study before developing the present algorithm–all those investigated proved most unacceptable.

The various quantities such as Nusselt numbers, convective, radiative, and contact heat transfer coefficients, etc. which are given in the discussion on modeling the phenomenon in Chapter 3 were computed by solving the respective equations in Chapter 3. This was accomplished by either program "SMOOTH" for the smooth surface or "ROUGH" for the macro-roughened surfaces. Descriptions of these programs (as well as examples of the computed quantities may be found in Appendix C. The output of the programs will be presented and discussed in Chapters 6 and 7 respectively.

Chapter 6. Results

Data Taken in the Present Study

The temperature response of the thermocouple/pin junction in surface CP54 throughout 45 discrete drop lifetimes was recorded as detailed in section 8 of Chapter 4 and section 1 of Chapter 5 (17 of water, 8 of ethanol, 9 of isopropanol, and 11 of ethylene-chloride). This data consisted of 45 separate strip chart records of thermocouple junction temperature vs. time. A total of 746 discrete contact occurrences were selected from these 45 data sequences. The temperature response of the thermocouple/pin junction in surface SHP2612 throughout 30 discrete drop lifetimes was also recorded (5 of water, 8 of ethanol, 9 of isopropanol, and 8 of ethylene-chloride). This data consisted of 30 separate strip chart records of thermocouple junction temperature vs. time. A total of 1684 discrete contact occurrences were selected from these 30 data sequences. There were a total of 75 strip chart records taken and a total of 2430 discrete contact occurrences selected from these.

Since only one of the pins in surfaces CP54 and SHP2612 were instrumented, as the size of the drops decreased with vaporization, periods may occur during a drop lifetime when the drop is not resting on the surface in the vicinity of the instrumented pin. Liquid/solid contact data could only be collected while the drop was 79 resting on the surface over the instrumented pin. The previous con tact data sequences are the selection of those periods where the drop was in the vicinity of the instrumented pin. The contact period, duration, recovery temperature, and quench temperature for each of these contact occurrences was individually determined from the strip chart records as detailed in section 1 of Chapter 5. These data sequences are summarized in Tables 1 and 2.[3]

The vaporization of 29 discrete drops was photographed on surface SMTH (7 of water, 8 of ethanol, 7 of isopropanol, and 7 of ethylene-chloride). This data consisted of 714 photographs. The bulk surface temperatures ranged from 190°C to 535°C. The vaporization of 27 discrete drops was photographed on surface CG01 (4 of water, 7 of ethanol, 8 of isopropanol, and 8 of ethylene-chloride). This data consisted of 463 photographs. The bulk surface temperature ranged from 190°C to 500°C. The vaporization of 24 discrete drops was photographed on surface SCG02 (3 of water, 7 of ethanol, 7 of isopropanol, and 7 of ethylene-chloride). This data consisted of 966 photographs. The bulk surface temperature ranged from 210°C to 525°C. The vaporization of 21 discrete drops was photographed on surface CP54 (2 of water, 6 of ethanol, 6 of isopropanol, and 7 of ethylene-chloride). This data consisted of 674 photographs. The bulk surface temperature ranged from 220°C to 620°C. The vaporization of 24 discrete drops was photographed on surface SHP2612 (3 of water, 7 of ethanol, 7 of isopropanol, and 7 of ethylene-chloride). This data consisted of 779 photographs. The bulk surface temperature ranged from 200°C to 550°C. There were a total of 125 discrete drop vaporizations photographed (a total of 3596 photographs). These were individually projected, sketched, and measured as detailed in section 4 of Chapter 5. These data sequences are summarized in Tables 3 through 7. Other data taken in the present study included 347 photographs of vertically projected drop area which were used to determine the area/volume calibration curves for the four liquids investigated (as detailed in the last section of Chapter 4), and 67 voltage/temperature measurements for the calibration of the thermocouple/pins (21 for CP54 and 46 for SHP2612) these appear in Figures 20 and 21.

[3] All tables are in Appendix A.

Strip Chart Records of Thermocouple/Pin Junction Temperature vs. Time

The response of the thermocouple/pin junction temperature with time as recorded on the 75 strip charts could be classified into three categories. These three categories are illustrated by the four segments of actual strip chart records which are included as Figures 22, 26, 27, and 28.

Figure 26 shows the response of the CP54 thermocouple/pin initially at 420°C to a 5 cc drop of saturated isopropanol. In Figure 26 the liquid first contacts the pin at the 6th time division from the left. This event corresponds to drop deposition. Drop vaporization occurred approximately 230 time divisions beyond the right side of the figure. Since most of the 75 strip charts were 81 recorded at 5 times the chart speed illustrated in Figure 26, it is not feasible to include more than a few representative segments of these strip chart records.

In Figure 26 the temperature of the junction can be seen to vary somewhat periodically about a mean value that asymptotically approaches 360°C. This first category of temperature response to liquid-solid contact is termed "stable" because film boiling and intermittent liquid-solid contact persists throughout the entire drop lifetime.

Figure 27 shows the response of the CP54 thermocouple/pin initially at 330°C to a 10 cc drop of saturated water. The temperature of the junction varies much more irregularly than in Figure 26 (note also that the temperature scale in Figure 27 is 5 times that in Figure 26). After about 15 contacts (the 36th division from the left) the temperature reaches a point after which it falls off rapidly and never recovers until after the drop vaporizes. This point (280°C in Figure 27) is defined as the LMFBT (local minimum film boiling temperature).

At this point (the LMFBT) the boiling process was observed to change dramatically: the drop would suddenly collapse onto the heating surface so that the liquid no longer appeared like a drop but rather like a frothy bubbling sheet. Since the temperature of the junction (approximately 180°C at the right edge of Figure 27) was significantly above the maximum surface temperature typically associated with nucleate boiling (124°C [50])yet the frothy bubbling appearance of the boiling process was similar to nucleate 82 boiling, this boiling process is termed "quasi-nucleate". This phenomenon of drop collapse and subsequent quasi-nucleate boiling has been described by many investigators including Leidenfrost in 1756 [2] (see for instance Reference 3). The liquid-solid contact process illustrated in Figure 27 is termed "metastable" since intermittent liquid-solid contact and film boiling only occur for part of the drop lifetime.

The third category of liquid-solid contact that was observed in the present study is illustrated in Figures 22 and 28. Figure 22 shows the response of the CP54 thermocouple/pin initially at 440°C to 5 cc of subcooled water at 0°C. The temperature of the junction can be seen to drop from 440°C to 115°C in 0.14 sec. and then recover to 150°C in another 0.37 sec. This liquid-solid contact process is termed "unstable" since the first contact is sustained from deposition to vaporization and only quasi-nucleate boiling is present during the drop lifetime.

Figure 28 shows the response of the CP54 thermocouple/pin initially at 280°C to 10 cc of saturated water. Four liquid-solid contacts may be seen (the first at the 7th time division from the left of the figure and the fourth at the 22nd division). After the fourth contact the temperature drops to and remains constant at 130°C until vaporization. This liquid-solid contact process is also termed "unstable" as in the case of Figure 22. The slight recovery in Figure 22 (which is not evidenced in Figure 28) is thought to be a result of the initial subcooling of the liquid as this

slight recovery phenomenon after unstable liquid-solid contact was only evidenced in the cases where subcooled liquid was used.

These three categories of liquid-solid contact together with Figures 26, 27, and 28 illustrate the present definitions of local and bulk minimum film boiling temperatures (LMFBT and BMFBT respectively). The definition point of the LMFBT is shown in Figure 27. The initial junction temperature in Figure 27 is said to be above the LMFBT, whereas after the 36th time division it is said to be below the LMFBT. The junction temperature throughout the entire drop lifetime for the case shown in Figure 26 is said to be above the LMFBT. The junction temperature throughout the entire drop lifetime for the case shown in Figure 28 is said to be near or below the LMFBT. Therefore, by the present definitions both stable and metastable liquid-solid contact can occur if the surface temperature is above the LMFBT; and only unstable liquid-solid contact can occur if the surface temperature is below the LMFBT.

By the present definition of BMFBT (the bulk surface temperature necessary to sustain the LMFBT at every point where liquid-solid contact occurs throughout the boiling process), only stable liquid-solid contact can occur if the bulk surface temperature is above the BMFBT; and both metastable and unstable liquid-solid contact occur if the bulk surface temperature is below the BMFBT. Therefore, the initial surface temperature in Figure 26 is said to be above both the BMFBT and the LMFBT, in Figure 27 it is said to be below the BMFBT but above the LMFBT, and in Figure 28 it is said to be below the BMFBT and near or below the LMFBT.

Contact Data

The thermocouple/pin data for the two instrumented surfaces (CP54 and SHP2612) was reduced as detailed in section 8 of Chapter 4 and section 1 of Chapter 5. This data includes contact period, τ, contact duration, τ_C, bulk surface temperature, T_W, recovery temperature, T_R, quench temperature, T_Q, average pin tip temperature, Tp, temperature depression across the pin, $\Delta T_C=T_W-T_P$, and the temperature change during contact, $\Delta T_C=T_R-T_P$ (these quantities are illustrated in Figure 26). This data is summarized in Tables 10 and 11 for surfaces CP54 and SHP2612 respectively. The average quantities are listed in the tables with the standard deviation (where applicable) listed beside these in parentheses.

The contact period, T, and its standard deviation are listed in column 4 of Tables 10 and 11. The first entry in Table 10 indicates that water on surface CP54 at a bulk temperature of 495°C (column 6) experienced 16 contacts (column 3) that had an average period of 0.15 sec. The shortest average contact duration listed in Table 10 is 0.080 sec. (strip #17, segment d) and in Table 11 is 0.058 sec. (strip #46, segment d). The longest average contact duration listed in Table 10 is 0.43 sec. (strip #38, segment a) and in Table 11 is 0.31 sec. (strip #46, segment a).

The contact duration, Tc, for convenience is presented in the form of the duration to period ratio, e. This is the ratio of the "ON" time to the "ON" plus the "OFF" time of contact. The duration/period ratio is presented rather than the contact duration 85 itself (which is the product of 6 and T) because the persistence of liquid-solid contact is more clearly seen in this ratio. The absence of contact corresponds to 6=0 and continuous contact corresponds to 6=1. Theta and its standard deviation are listed in column 5 of Tables 10 and 11. The first entry in Table 10 indicates that the liquid-solid contact persisted for an average of 44% of the contact period (6=0.44). The second entry in Table 10 indicates that liquid-solid contact persisted for an average of 36% of the contact period, the third entry 31%, etc. The maximum value of con tact duration/period ratio listed is 84% in Table 10 (strip #24, segment a) and 77% in Table 11 (strip

#46, segment c). The minimum value of contact duration/period ratio listed is 26% in Table 10 (strip #14, segment b) and 28% in Table 11 (strip #49, segment a).

The standard deviation in the contact period, T, and duration/period ratio, 6, are also listed in Tables 10 and 11 (in parentheses beside the respective quantities). These standard deviations are listed as they indicate the periodicity and regularity of the liquid-solid contact. Specifically, if the liquid-solid contact were truly periodic the standard deviation in the period would be zero. Conversely, if the standard deviation of the contact period is large compared to the period, the process is not periodic. Since all of the standard deviations of contact period and duration/period ratio listed in Tables 10 and 11 are of the same order of magnitude as (although smaller than) the respective average quantities, the liquid-solid contact phenomenon as measured in the present study can only be considered marginally periodic or regular. 86

The temperature depression across the pin (i.e., the bulk surface temperature minus the temperature of the junction on the exposed tip of the instrumented pin), Tp, is listed in the 10th column of Tables 10 and 11. This temperature depression is roughly proportional to the heat flux through the pin. It should be noted that the vertical distance between the center of the two thermocouples used to measure temperature depression across the instrumented pin on surface CP54 was 0.305 cm (Figure 16) and on surface SHP2612 was 0.178 cm (Figure 17). The maximum temperature depression listed in Table 10 is 147°C (strip #47, segment d) and in Table 11 is 20l°C (strip #47, segment b).

The temperature change of the thermocouple/pin junction during contact, Tc, is listed on column 11 of Tables 10 and 11. This temperature change represents the average rise and fall of the junction temperature during the "OFF" and "ON" portions of the contact period respectively. The largest value of Tc listed on Table 10 is 2l°C (strip #21, segment a) and in Table 11 is 70°C (strip #46, segment d). It should also be noted that these largest values of both Tp and Tc occur with water.

Experimental Heat Transfer Coefficients

The area/time data was reduced to heat transfer coefficients by program "DATABASE" as detailed in section 6 of Chapter 5. The output of program "DATABASE" for a smooth surface and a macro-roughened surface is illustrated in Tables 8 and 9, respectively. In these tables the experimental area/time data is listed in the first two 87 columns and the time-smoothened area ("ASMTH") is listed in the third column. The experimental area data (column 2) and the time smoothened area (column 3) represent the triangles and the dashed curve respectively in Figure 23. A comparison of the second and third columns in Tables 8 and 9 and Figure 30 illustrates the function of program "DATABASE" to remove the effect of drop oscillations from the data (section 6 of Chapter 5). Figure 30 is a plot of the data in Table 9.

The experimental heat transfer coefficients (viz. those computed from the experimental area/time data) are given in column 9 of Tables 8 and 9 for the respective data sequences. The ratio of the experimental heat transfer coefficients to the theoretical heat transfer coefficient which would occur on a smooth surface at the same bulk surface temperature for the same liquid and the same drop size is listed in column 10 C'HE/HB") of Tables 8 and 9. In this case the experimental heat transfer coefficient is that which is computed from the experimental area/time data through Equation 5-15 and the theoretical heat transfer coefficient is that which is computed by solving simultaneously Equations 3-38, 3-39, 3-40, and 3-45. The average discrepancy between the smooth surface heat transfer data and theory (Equations 3-38, 3-39, 3-40, and 3-45)

for the 714 data points taken on the surface SMTH was 0.7% with a standard deviation of 12%. This small discrepancy between the smooth surface data and theory is thought to be evidence of the overall consistency of the theory and data reduction (at least when applied to smooth surface data).

The primary non-dimensionalization of the heat transfer coefficients was based on the drop volume rather than the vapor layer thickness, as is typically the case for Leidenfrost drop heat transfer coefficients, since vapor layer thickness was not an experimentally measured quantity in the present study. The cubed root of drop volume was selected for the non-dimensionalization as it was thought to be the most convenient readily available length parameter. The volume Nusselt number, Nuv, for Leidenfrost drops is defined by Equation 6-1.

$$Nu_V = \frac{h_D V_D^{\frac{1}{3}}}{k_g} \tag{6-1}$$

The bulk surface temperature is represented in non-dimensional form by the dimensionless superheat, A , defined by Equation 6-2.

$$\Lambda = \frac{Cp_g \left(T_W - T_L\right)}{h_{fg}} \tag{6-2}$$

The dimensionless heat flux, H, is defined as the product of the volume Nusselt number, Nuv, and the dimensionless superheat, A , Equation 6-3.

$$H = \Lambda \, Nu_V \tag{6-3}$$

The volume Nusselt number, Nuv, and the dimensionless heat flux, H, are listed for each data point in columns 11 and 12 respectively of Tables 8 and 9. The dimensionless heat flux, H, is plotted vs. the dimensionless drop volume, v* (Equation 3-3), for the range of dimensionless superheat, A , for each of the 3596 data points (for each of the 4 liquids on each of the 5 surfaces) in the present study in Figures 31 through 50. These figures were plotted by program "PLOT:HV" (a description of which may be found in Appendix C).

The data in Figures 31 through 50 are plotted using numerals (0, 1, 2, 3, ...). The dimensionless superheat corresponding to each data sequence is located along the top of each figure. The numerals (0, 1, 2, 3, ...) are arranged in order of increasing superheat (or increasing bulk surface temperature). Namely, the data sequence represented by "1" corresponds to a bulk surface temperature which is hotter than the sequence represented by "0" etc. In a particular Figure "6" or "7" corresponds to the hottest bulk surface temperature and "0" corresponds to the least hot. Although the temperatures corresponding to each numeral are not evenly spaced, the variation in dimensionless heat flux with surface temperature can be seen by noting that the surface temperature corresponding to the data is roughly proportional to the numerals which are used to plot the data. The data summaries in Tables 3 through 7 are also arranged in the same order as the numerals in the figures (viz. the "0" through "6" in Figure 31 correspond to the first 7 entries in Table 3).

The increase in heat flux for each data point with each of the 4 liquids on each of the 4 macro-roughened surfaces, over that which would theoretically occur on a smooth surface at the same bulk surface temperature for the same liquid and the same drop size, is plotted vs.

dimensionless drop volume, V*, for the range of dimensionless superheat, A, in Figures 51 through 66. These figures were 90 plotted by program "PLOT:HT%" (a description of which may be found in Appendix C). Note that the increase in heat flux on the macro-roughened surfaces is equivalent to the increase in heat transfer coefficient (since the temperature difference in each case is the same). The numerals used to plot the data in Figures 51 through 66 are identical to those used in Figures 35 through 50. The variation in increased heat flux with surface temperature may be deduced from the figures in a similar manner as is the variation in dimensionless heat flux.

As can be seen from Figures 51 to 66, one effect of surface macro-roughness on Leidenfrost film boiling is an increase in heat flux. This increase is predominantly between 50% and 150% for the 4 liquids on the 4 macro-roughened surfaces, although several cases are shown where the increase is at least 500% (viz. "0" in Figure 55, "0" and "1" in Figure 59, "0" in Figure 61' "0" in Figure 62, "0: in Figure 63, "0" and "1" in Figure 64, "0" in Figure 65, and "0" in Figure 66). It should be noted that the critical heat flux (Equation 5-11) would amount to between 2000% and 4000% increase over the smooth surface film boiling heat flux. In Figures 51 to 66 the increase on the heat flux was truncated at 500% so that the other data points would not be obscured by an unnecessarily large vertical scale. There was no case in the present study in which a decrease on heat flux was observed on a macro-roughened surface (over that on a smooth surface). It should also be noted that throughout the present study the definition of heat flux is that to the drop (based on the vertically projected area of the drop) and not the heat flux from the heating surface (nor that based on the total area of the heating surface including the macro-roughness elements).

Recalling that the numeral "0" in Figures 51 through 66 corresponds to a lower bulk surface temperature than does the numeral "1" and "2" etc., it can be seen from Figures 55 and 60 through 66 that the largest increases in heat flux occur at the lowest bulk surface temperatures (ie. as indicated by the O's and occasionally l's appearing above the 5's and 6's in the figures).

Computed Heat Transfer Coefficients

Heat transfer coefficients on the macro-roughened surfaces which were instrumented with the thermocouple/pins (viz. CP54 and SHP2612) were computed using the two-dimensional transient finite difference model as detailed in section 3 of Chapter 5 from the thermocouple/pin data which is summarized in Tables 10 and 11. These computed heat transfer coefficients for each of the 4 liquids on each of the 2 instrumented macro-roughened surfaces (CP54 and SHP2612) are plotted together with experimental heat transfer coefficients on the same surfaces vs. bulk surface temperature in Figures 78 through 74. The experimental heat transfer coefficients represent the range of values measured for large drops and extended liquid masses (which is the focus of the present study).

Baumeister et al. [31] define the demarcations for extended liquid masses, large drops, and small drops by dimensionless drop volumes above 155, between 155 and 0.8, and less than 0.8 92 respectively. The drop aspect ratio (diameter divided by average thickness–see Figures 5, 7, and 12) is perhaps more illustrative at this point. Using the numerical solution to the Laplace capillary equation (Chapter 3, section 1) to determine drop diameter, 2R, and average drop thickness, 1, the aspect ratio, 2R/l, is found to be greater than 5 for drops of dimensionless volume, v*, greater than 75. For V*=0.8 (the lower limit for large drops given by Baumeister et al.) The aspect ratio is computed to be 1.5 via. the numerical solution to the Laplace capillary equation. The lower limit for large drops used in the present study is: aspect ratio greater than 5

(or v* greater than 75). Drops having dimensionless volumes between 0.8 and 75 are termed "medium" sized. The appearance of vapor bubble breakthrough might be thought of as the demarcation between large drops and extended liquid masses. Vapor bubble breakthrough typically occurs in drops having dimensionless volume above 155 (e.g., [24], [26], [27], and [30]).

Experimental Determination of Contact Temperature

One further test of the applicability of the modified error function formulation for the contact of two semi-infinite static media to the present case of intermittent liquid-solid contact (as presented in section 3 of Chapter 5) was made in addition to the comparison of calculated and measured heat transfer coefficients (Figures 67 through 74). This further test was the comparison of experimental and calculated contact temperatures (Equation 3-49). 93 Before the liquid is introduced onto the heating surface the instrumented pin is essentially at uniform temperature (as determined from the 2 thermocouples in each of the instrumented surfaces as detailed in sections 3 and 6 of Chapter 4 and shown in Figures 16 through 19).

Uniform temperature prior to contact with the liquid is one of the major criteria for the applicability of the error function formulation for contact temperature (section 5 of Chapter 3). If the error function formulation is to be applied to the intermittent liquid-solid contact phenomenon under any circumstances it should be in agreement with this most basic application. Since the temperature depression (initial temperature minus contact temperature) due to contact is most pronounced in the case of water (water has the largest value of Y, Equation 3-50, of the four liquids investigated), the comparison is made for water on the two instrumented surfaces (CP54 and SHP2612). This comparison of experiment and theory is given in Table 13. The average discrepancy between calculated and experimental contact temperature for the data in Table 13 is 7% of the temperature depression due to contact (with a standard deviation of 21%). As detailed in the section 3 of Chapter 5, the error function formulation for the contact of two semi infinite static media was modified for use in the two-dimensional finite difference model to account for the finiteness of the pin and non-uniform initial temperature distribution. 94

Minimum Film Boiling Temperature

The BMFBT's on surface CP54 for water, ethanol, isopropanol, and ethylene-chloride were determined to be approximately 600°C, 255°C, 240°C, and 235°C respectively. The BMFBT's on surface SHP2612 for water, ethanol, isopropanol, and ethylene-chloride were determined to be approximately 540°C, 260°C, 230°C, and 230°C respectively. These values are illustrated in Figures 67 through 74 by the solid vertical line (except for water on surface CP54 which is listed as "uncertain" due to a scarcity of data). These values of BMFBT are referred to as "approximate" quantities for the reasons detailed in the section on minimum film boiling temperature in Chapter 2.As mentioned in Chapter 2, Wachters [13] proposed that no minimum film boiling temperature exists and many investigators have reported significant variation in experimental values of MFBT even on smooth surfaces (e.g., [3], [10], [13], [14], [29], and [32] through [35] inclusive).

The LMFBT's on surface CP54 for water, ethanol, isopropanol, and ethylene-chloride was determined to be approximately 265°C, 220°C, 220°C and 225°C respectively. The LMFBT's on surface SHP2612 for water, ethanol, isopropanol, and ethylene-chloride was determined to be approximately 265°C, 190°C, 170°C, and 170°C respectively. These values of LMFBT are also referred to as "approximate" quantities for the same reasons. These values of BMFBT and

LMFBT may be compared to the smooth surface minimum film boiling temperatures calculated using only liquid properties, 95 Equation 5-11 (after Berenson [38]). These smooth surface MFBT's for water, ethanol, isopropanol, and ethylene-chloride are 288°C, 160°C, 130°C, and 200°C respectively.

Other Computed Quantities

In addition to the computed heat transfer coefficients, volume Nusselt number, and dimensionless heat flux, the following quantities were computed for each data point (where applicable): convective (flow) heat transfer coefficient ("HF"), contact heat transfer coefficient ("HC"), radiation heat transfer coefficient ("HR"), computed vapor layer thickness ("DELTA"), dimensionless enthalpy flux ("B"), drop (or total) Nusselt number based on computed vapor layer thickness ("NUD"), convective (flow) Nusselt number based on computed vapor layer thickness ("NUF"), contact Nusselt number based on computed vapor layer thickness ("NUC"), radiation Nusselt number based on computed vapor layer thickness ("NUR"), conduction parameter, n , ("OMEGA"), and contact Biot number or modulus ("BlOT#"). The convective heat transfer coefficient is defined by Equations 3-40 and 3-41. The radiation heat transfer coefficient is defined by Equations 3-36 and 3-45. The computed vapor layer thickness is defined by Equation 3-30. The dimensionless enthalpy flux parameter is defined by Equation 3-19. The drop (or total) Nusselt number, the convective (flow) Nusselt number, the contact Nusselt number, and the radiation Nusselt number based on the computed vapor layer thickness are defined by Equations 6-4 through 6-7 respectively. 96 Nun = kg

$$Nu_D = \frac{h_D \overline{\delta}}{k_g} \tag{6-4}$$

$$Nu_F = \frac{h_F \overline{\delta}}{k_g} \tag{6-5}$$

$$Nu_C = \frac{h_C \overline{\delta}}{k_g} \tag{6-6}$$

$$Nu_R = \frac{h_R \overline{\delta}}{k_g} \tag{6-7}$$

The conduction parameter, Ω, and the contact Biot number or modulus are defined by Equations 6-8 and 6-9 respectively. (6-8), where:

$$\Omega = \frac{\delta k_S}{\varepsilon k_g} \tag{6-8}$$

$$Bic = \frac{h_C \varepsilon}{k_S} \tag{6-9}$$

The conduction parameter, n, is the ratio of the unit thermal conductance of the macro-roughness elements, ks/ε, to the unit thermal conductance of the vapor layer between the liquid drop and the heating surface, kg/δ. The contact Biot number, Bic, is the ratio of the contact heat

transfer coefficient, he, to the unit thermal conductance of the macro-roughness elements, ks/ε. The significance of these quantities will be discussed in Chapter 7.

These 11 quantities (viz. h_F, h_C, h_R, δ, B, Nu_D, Nu_F, Nu_C, Nu_R, Ω, and Bic) were calculated either by program "SMOOTH" for the smooth surface data or "ROUGH" for the macro-roughened surface data. The quantities dealing with contact were, of course, omitted from the reduction of the smooth surface data as liquid-solid contact was not thought to be significant on the smooth surface (e.g., [8]). Samples of the output of programs "SMOOTH" and "ROUGH" are given in Tables 14 and 15 respectively. The 11 quantities defined above are listed in Tables 14 and 15 for each data point in the sequence and may be found under the columns in the tables having the headings given previously in quotes. Descriptions of programs "SMOOTH" and "ROUGH" may be found in Appendix C. These calculated quantities will be referenced in Chapter 7.

The apparent relative contribution to the total heat transfer of convection (flow), contact (on the macro-roughened surfaces), and radiation were computed and plotted for each sequence of data (a total of 125 plots). Two samples of these plots of relative contribution of the 2 (or 3) modes of heat transfer (one plot for the smooth surface and one plot for a macro-roughened surface) are given in Figures 75 and 76 respectively. These figures were plotted by program "PLOT:FRC" (a description of which may be found in Appendix C). These plots will be referenced in Chapter 7. Note that the information in Tables 8 and 14 and Figure 75 all refer to the same sequence of data as does that in Tables 9 and 15 and Figures 30 and 76.

Chapter 7 Analysis And Discussion

Intermittent Liquid-Solid Contact on Macro-Roughened Surfaces

The contact periods, τ, listed in Tables 10 and 11 (column 4) are on the order of 0.1 sec which is the same order of magnitude as the period associated with the Taylor most dangerous instability (Chapter 1). The most dangerous Taylor instability periods are 0.17, 0.13, 0.15, and 0.12 sec. for water, ethanol, isopropanol, and ethylene-chloride respectively. The present data, however, are not conclusive evidence that the contact period is approximately the same as the Taylor most dangerous period since all the liquids investigated have Taylor most dangerous periods which are of the same order of magnitude and thus do not represent a wide enough range to permit making such a deduction.

Significant variation in contact period was seen even during a single drop lifetime (e.g., strip #1, Table 10: τ = 0.15, 0.12, 0.096, 0.10, 0.087, 0.086 sec). The standard deviation in the con tact period (which is a statistical measure of its regularity) was also seen to vary significantly during a single drop lifetime (e.g., strip #1, Table 10: τ = 0.054, 0.054, 0.072, 0.033, 0.036, 0.028). These variations in contact period indicate that intermittent liquid-solid contact on the macro-roughened is somewhat irregular rather than strictly pulse-like periodic.

As mentioned in Chapter 6, the contact duration/period ratios, $\theta = \tau_c/\tau$, listed in Tables 10 and 11 range from 26% to 84%. Variation is also seen in e throughout a single drop lifetime (e.g., strip #1, Table 10: e 44%, 36%, 31%, 42%, 41%, 36%). The standard deviations in θ are typically significant compared to the mean (e.g., strip #1, segment a, the first entry in Table 10 θ = 0.44 and $\sigma\theta$ = 0.22). This variation in e is further indication of the irregularity of the liquid-solid contact phenomenon.

If the contact duration, τ_c, or the "ON" time of contact is assumed to be the length of time required to produce sufficient vaporization in the vicinity of contact to "push" the liquid away from the heating surface at the point of contact, the contact duration is then analogous to a nucleation "waiting time" as in nucleate boiling (i.e., the time required for a bubble to form). This is precisely the assumption made by Nishio and Hirata [5] in their analysis of liquid-solid contact for impinging Leidenfrost drops. In fact, Nishio and Hirata directly employed the theoretical waiting time for nucleate boiling developed by Han and Griffith [43]. The theoretical waiting time of Han and Griffith is based on the presence of small vapor filled cavities in the heating surface and is therefore not necessarily applicable to liquid-solid contact in film boiling since liquid-solid contact in film boiling, especially on a macro-roughened surface, is most likely to occur at protrusions from the surface rather than cavities in the surface. The waiting times calculated by Nishio and Hirata (using the theory of Han and Griffith) for water were less than 0.01 sec. The contact duration for water listed in Table 10 ($\tau_c = \theta\tau$, the product of columns 4 and 5) range from 0.030 sec. (strip #1, segment c) to 0.066 sec. (strip #1, segment a) and in Table 11 from 0.039 sec. (strip #49), segment a) to 0.127 sec. (strip #46, segment a). Thus the waiting time of Han and Griffith does not appear to be applicable to Leidenfrost film boiling on macro-roughened surfaces.

The data in Tables 10 and 11 indicate that the temperature depression across the instrumented pin in surface CP54 and SHP26I2 respectively, Tp (column 10 in the tables), was greatest for water (viz. the first 10 entries in Table 10 and the first 9 entries in Table 11 are for water, column 2) and least for ethylene chloride (viz., the last 9 entries in Table 10 and the last 17 entries in Table II are for ethylene-chloride, column 2). This data (Tables 10 and 11) also indicate that the

temperature change during contact, Tc (column 11 in the tables), is greatest for water and least for ethylene-chloride (note the same sequences of data given to illustrate the temperature depression). According to the error function formulation for the contact of two semi-infinite static media (section 5 of Chapter 3, Equations 3-47 through 3-50), given the same initial temperatures of the liquid and solid, the change in temperature due to contact is determined by the single thermophysical property group γ (Equation 3-50). Of the four liquids investigated water has the largest value of γ and ethylene-chloride has the smallest, indicating at least a qualitative agreement between experiment and theory.

Local Wetting of the Heating Surface

Wetting of a surface by a liquid is defined in terms of the contact angle as shown in Figure 77 (e.g., [69], p.33). Figure 77 shows the three classifications of liquid/surface interaction related to the present study. The drop shown at the top of Figure 77 does not contact the surface, the center drop contacts the surface but does not "wet" the surface, and the lower drop contacts and "wets" the surface as indicated. Liquid/surface interaction in all three classifications are observed during film boiling of liquid drops on macro-roughened surfaces, as illustrated in Figures 78 through 80.

Figure 78 shows a 1.5 cc drop of water undergoing film boiling on surface SMTH (Figure 13). Right cylindrical ALNICO magnetic pins have been arranged on the surface in a square array having a center-to-center spacing of 0.38 cm. The diameter and height of the cylindrical pins is 0.127 cm. The photograph was taken at an angle of approximately 30 degrees from the horizontal plane. The reflection of the drop can be seen in the polished nickel-plated surface. The division between the drop itself and its reflection is indicated by the white arrow at the right of the figure. At the point indicated by this white arrow the liquid surface can be seen to curve under and disappear beneath the drop (similar to the upper drop in Figure 77). Since there was a vapor layer present between the drop and the surface (otherwise the drop would have collapsed and the film boiling would have changed to quasi-nucleate boiling), the underside of the drop could not be as is illustrated in the center of Figure 77. (Here it is assumed to be common knowledge that a large drop of water will not "bead-up" on even a polished hot nickel surface unless that surface is above the minimum film boiling temperature, and that a drop "beads-up" during film boiling because of the presence of a vapor layer between the liquid and the surface.) However, the undersurface of the drop could not be exactly as is illustrated at the top of Figure 77 since there are 18 cylindrical pins beneath the drop.

In Figure 78 the liquid does not wet the heating surface (i.e., the angle between the surface of the drop and the heating surface near the white arrow at the right of the figure is less than 90°). The liquid does, however, wet the pins (the contact angle indicated by the white arrow at the bottom of the figure is approximately 135°). It is therefore possible for a film boiling drop to contact and/or wet a macro-roughened heating surface in one location and not in another simultaneously.

Figure 79 shows a 0.5 cc drop of ethanol resting on surface CP54 (Figure 16). This photograph was taken at an angle of approximately 45 degrees from the horizontal plane. In the locations indicated by the white arrows in Figure 79, the surface of the liquid can be seen to "bulge" between the pins rather than "engulf" the pins as in Figure 78. The angle between the liquid and the pin at the tip of the left white arrow in Figure 79 is approximately 60° indicating that the liquid does not wet the pin in this instance.

As in Figure 78, in Figure 79 the liquid does not appear to wet the subsurface in which the pins are embedded (this can be seen by observing the gap between the drop and the smooth subsurface beneath the white arrows in the figure). Some of the ALNICO magnets (from Figure 78) can be seen around the periphery of Figure 79. These were used as a "fence" to confine the drop for the purposes of photography only and were not present when the data were taken. The surface was also cleaned, polished, and re-plated before any data were taken.

Figure 80 shows the edge of a 2 cc drop of ethanol resting on a surface that is identical to CP54 (Figures 16 and 79) except for the pin height (0.0508 cm in this case instead of 0.127 cm in the case of CP54). This photograph was taken at an angle of approximately 45 degrees from the horizontal plane. The edge of the drop appears to be relatively undisturbed by the presence of the pins (i.e., the liquid does not "bulge" between the pins as in Figure 79 nor "engulf" the pins as in Figure 78). The surface of the liquid appears to roll under and disappear beneath the drop as indicated by the curved white arrow in the figure. The liquid does not appear to wet the pins in the areas indicated by the straight white arrows. Due to the extreme heat (necessitating the use of a telephoto lens), rapid shutter speed (to stop drop motion), desired magnification (note that the pin diameter is only 0.165 cm.), and problems developing the film (which was originally a color slide), the contrast in Figure 80 is not as sharp as in Figure 79. The "halo" about the pins and the dark appearance of the heating surface is a 104 result of the intense directional lighting used when taking the photograph and are not indications of any difference between this surface and the one in Figure 79 (except for the pin height). The same contrast and shadowing effects can be seen in Figure 79 to a lesser degree.

Although the pin diameter in Figure 79 is 0.165 cm., as compared to 0.127 cm in Figure 78, the pin heights are identical (0.127 cm.). In both cases the pins are right cylinders. It was also noted that both water and ethanol readily wet both nickel plate and ALNICO at room temperature. The bulk surface temperature in both cases (Figure 78 and 79) is above the smooth surface minimum film boiling temperature. The typical pin tip temperature depressions, Tp (bulk surface temperature minus pin tip temperature), measured in the present study on surface CP54 (see column 10 of Table 10) for water are significantly larger than those measured for ethanol (e.g., entry 1 in Table 10 lists 70° for water and entry 11 in Table 10 lists 48° for ethanol). Since the pin tip temperature depressions for water are typically larger than for ethanol, the temperature at the pin tip would typically be lower for water than for ethanol even at the same bulk surface temperature. It should also be noted that there is a non-zero solid-solid contact resistance between the ALNICO magnetic pins and the surface (Figure 78) that is not present with the embedded pins in surface CP54 (Figure 79). Thus, the Tp in Figure 78 should be even larger than would be expected under the same conditions on surface CP54 due to this solid-solid contact resistance. As the Tp increases the likelihood of the pin tip temperature falling below the LMFBT increases even if the bulk surface temperature is above the BMFBT.

These observations concerning the similarities and differences between Figures 27 and 28 (i.e., pin geometry, wettability at room temperature, and increased Tp) indicate that the local wetting on a macro-roughened surface (all other variables held constant) depends on the local temperature. More specifically, if the local temperature is above the LMFBT the liquid may contact the surface but it will not wet the surface. This deduced relationship between wetting/non-wetting and the LMFBT is consistent with the present definition of the LMFBT as given in Chapter 1. That is, the LMFBT marks the division between continuous and continual liquid-solid contact (by definition "continuous" means "ON" all the time, whereas "continual"

means "ON" and "OFF" all the time). This relationship between wetting, contact, and the LMFBT follows logically: If the liquid truly wets the surface at a point then the contact at that point would presumably be continuous. If the contact is continuous at a point then there can be no separating vapor layer at that point. If there is no separating vapor layer (which is the basic characteristic of film boiling) at that point then the boiling process at that point is not film boiling. Therefore, the local temperature must be below the LMFBT. This deduced relationship does not indicate whether or not contact will occur at a given location, only whether or not wetting will occur (assuming that the liquid could wet the surface under non-boiling conditions).

The Effect of Surface Macro-Roughness on Film Boiling Heat Flux

As stated in Chapter 6, there was no case in the present study where a decrease in heat flux was measured on a macro-roughened surface (over that which was measured on a smooth surface for the same liquid, drop size, and bulk surface temperature). It was also stated in Chapter 6 that the increase in heat flux on the macro-roughened surfaces was typically between 50% and 150%. However, several cases were given where the increase in heat flux was 300% to 500%.

As stated in Chapter 6, the largest increases in heat flux on the macro-roughened surfaces were seen at low bulk surface temperatures. One illustration of this is Figure 60 (ethanol on surface CP54). The data in Figure 60 indicated by "0" corresponds to a dimensionless superheat of 0.328 (listed at the top of the figure) that is equivalent to a bulk surface temperature of 220°C (the third entry in Table 7). The data in Figure 60 indicated by "1" and "5" correspond to dimensionless superheats of 0.421 and 0.954 and bulk surface temperatures of 260°C and 490°C respectively. The data in Figure 60 indicate approximately 300% increase in heat flux at 220°C and only about 100% increase for bulk surface temperatures between 260°C and 490°C. This same phenomenon of larger increases in heat flux at lower bulk surface temperatures and relatively smaller increases in heat flux at higher bulk surface temperatures with little variation as bulk surface temperature continues to increase (i.e., "0" and perhaps "1" may be substantially 107 above "2", "3", "4", etc and there is little difference between "2", "3", "4", etc.) is evidenced in Figures 55, 61, 62, 63, 64, 65, and 66.

The dimensionless superheat ranges corresponding to the shift between relatively larger and smaller increases in heat flux as described in the previous paragraph for the data in Figures 55, 60, 61, 62, 63, 64, 65 and 66 are 0.270-0.315, 0.328-0.421, 0.478-0.652, 0.388-0.531, 0.278-0.405, 0.398-0.513, 0.444-0.618, and 0.374-0.517 respectively. The average of these ranges is 0.37-0.50. The mini mum dimensionless superheat covered by the data in Figures 51 to 66 is 0.225 (water on CG0l at 350°C) and the maximum is 1.627 (isopropanol on SHP2612 at 550°C). The maximum dimensionless superheat obtained in the present study with water was 0.468 (Figure 59, CP54 at 620°C). While the dimensionless superheat does not account for the macro-roughness and does not include any thermophysical properties of the surface it is thought to give some indication as to why the relatively smaller increases in heat flux (50% to 150%)are not evidenced with water on surfaces SCG02, CP54, and SHP2612 (Figures 55, 59, and 63) as is the case with the other three liquids on the same surfaces. Presumably if a dimensionless superheat of 1.0 (which would correspond to a surface temperature of 1200°C) were achieved for water on these surfaces the same sort of diminished improvement in heat transfer would be seen.

In contrast to the lack of relatively smaller increases in heat flux (50% to 150%)noted with water on surfaces SCG02, CP54, and SHP2612, all four liquids lack the relatively larger increases in heat flux (300% to 500%) on surface CG01 (Figures 51 through 54). Since the

increases in heat flux are significantly larger on surfaces SCG02 (£=0.0508 cm.), CP54 (£=0.127 cm.), and SHP2612 (€=0.0508 cm.), Figures 55 through 66, than on surface CG01 (€=0.0254 cm.), Figures 51 through 54, and the increases in heat flux are not significantly larger on surface CP54 (Figures 59 through 62) than on surfaces SCG02 and SHP2612 (Figures 55 through 58 and 63 through 66), there appears to be an effective threshold macro-roughness height necessary to obtain significant increases in film boiling heat flux (in these cases this threshold is between 0.0254 cm and 0.0508 cm.). It also appears that once this threshold is reached a further increase in macro-roughness height (even by a factor of 2.5 as is the case of CP54 as compared to SCG02 and SHP2612) does not produce a proportionate increase in heat flux. This concept of a macro-roughness threshold height is consistent with the observations of Knobel and Yeh [9].

As noted previously, the water drop in Figure 78 appears to "engulf" and "wet" the 0.127 cm magnetic pins while the ethanol drop in Figure 79 appears to "bulge" out between but not significantly "wet" the 0.127 cm pins and the ethanol drop in Figure 80 appears to "rest" upon the 0.0508 cm pins relatively undisturbed (compared to Figures 78 and 79). These observations, together with the evidence for a macro-roughness threshold height indicate that the increase in heat flux on the macro-roughened surfaces is directly related to the macro-roughness height, the vapor layer 109 thickness, and the dimensionless superheat and that the increase in heat flux is primarily a result of increased liquid-solid contact. This deduced relationship between increased liquid-solid contact, vapor layer thickness and dimensionless superheat is consistent with Leidenfrost boiling theory in that the analysis of Baumeister and Hamill (Reference 22, Equation 49) as well as the present analysis predicts that vapor layer thickness increases with increasing dimensionless superheat. An increase in film boiling heat flux with increasing liquid-solid contact is also consistent with the analyses and observations of References 4, 5, 8, 9, and 51 (e.g., recall the statement made in 1966 by Bradfield [4] previously quoted in Chapter 2, "liquid-solid contact can be achieved at stable film boiling temperatures by any means which will induce surface roughness elements to tickle the liquid-vapor interface it may become desirable to control heat flow by controlling liquid-solid contact in the stable film boiling regime.").

Local vs. Overall Film Boiling Heat Flux on the Macro Roughened Surfaces

The bulk surface temperature was measured at a location only 0.178 cm. and 0.127 cm. below the smooth subsurface from which the macro-roughness elements protruded in the case of surface CP54 and SHP2612 respectively (see Figures 16 and 17). Throughout a single drop lifetime the bulk surface temperature, Tw (column 6 in Tables 10 and 11), dropped only slightly when compared to the average temperature at the tip of the instrumented pin, Tp (column 9 in Tables 110 10 and 11). An example of this is illustrated in strip #1 (the first 6 entries in Table 10): Tw drops from 495°C to 425°C while Tp drops from 495°C to 286°C. By virtue of the Fourier law of conduction which states that the local heat flux within a static media is proportional to the product of the thermal conductivity and the temperature gradient (e.g., [50]), these relatively larger drops in temperature at the pin tip when compared to a location just below the surface indicate that the local heat flux through the pins was significantly larger than the heat flux through the smooth surface surrounding the pins.

If the heat flux through the pin is roughly estimated by one-dimensional steady conduction (viz. $q=k\Delta T/\varepsilon$) the data for strip #1 (the first 6 entries in Table 10) indicate heat fluxes through the pin of 76, 101, 105, 115, 127, and 150 W/cm respectively. The critical heat flux for water as computed from Equation 5-8 (after Zuber et al. [65] and Kutateladze [44] is 142 W/cm. Thus the local heat flux during liquid-solid contact appears to be of comparable magnitude to the critical

heat flux. The smooth surface heat flux under the same conditions as in strip #1 is only about 8W/cm2 (this heat flux depends on drop volume, 8 W/cm is characteristic of that measured for large drops and extended liquid masses, column 9 of Table 8 times 500-100°C). The overall heat flux on CP54 under the same conditions as strip #1 is only about 48W/cm2 a 500% increase). The top of the cylindrical pins in surface CP54 only accounts for 25% of the total area of the heating surface. Assuming that 150W/cm flows through the top of the pins while 8 W/cm flows Ill through the rest of the surface the average heat flux would be approximately 0.25xl50+0.75x8 44 W/cm. These rough heat flux calculations substantiate the postulate that the increase in heat flux that was measured on the macro-roughened surfaces is primarily due to liquid-solid contact and that this contact occurs primarily at the top of the pins.

Modeling the Leidenfrost Phenomenon on Macro-Roughened Surfaces

The presence of macro-roughness on the heating surface and the accompanying increase in the probability of liquid-solid contact add significantly to the complexity of modeling the Leidenfrost phenomenon (as compared to the smooth surface case). Some of these complexities are: the effect of macro-roughness on 1) vapor flow beneath the drop, 2) drop shape and the possible alteration of the vapor bubble breakthrough process and interfacial instability phenomenon, and 3) the effect of liquid-solid contact on local heat transfer. As mentioned in Chapter 3, very little is known about the vapor flow beneath Leidenfrost drops on macro-roughened surfaces and no experimental studies have been undertaken (to the knowledge of the author at the present time) to shed any light on the matter. In the present analysis the effect of macro-roughness on vapor flow beneath the drop is not addressed.

There are two aspects of drop shape which are integral parts of the present study: I) the relationship between vertically projected drop area and drop volume and 2) the disk shape approximation for large drops and extended liquid masses. The relationship between vertically projected drop area and drop volume was used throughout the data reduction process (with the exception of the thermocouple data) to deduce drop volume from photographs showing only vertically projected area. Thus, none of the data illustrated in Figures 31 through 66 can be separated from this assumed relationship. The basis for this relationship (as detailed in section 1 of Chapter 3) is the Laplace capillary equation that applies to sessile drops at rest and in mechanical and thermal equilibrium. It was also assumed that the drops oscillate about their equilibrium shape and that the vapor bubble breakthrough could be accounted for by subtracting the area of the vapor bubbles from the total area.

The observed drop shapes varied significantly from the equilibrium shape (e.g., Figure 7). This variation was most pronounced for large drops and least pronounced for small drops. This difference between small drops and large drops is thought to be due to an effective rigidity of small drops (i.e., surface tension forces are relatively small in large drops because the radii of curvature are large, whereas surface tension forces are relatively large in small drops because the radii of curvature are small–e.g. Equation 3-1). The vertically projected equilibrium shape of a drop would be a circle. However, the observed drops ranged from circular for small drops to "ameba-shaped" and even "dumbbell-shaped" for large drops. As detailed in section 4 of Chapter 5 the vertically projected area was measured using a polar planimeter regardless of the shape of the drops. As mentioned in the last section of Chapter 11 the liquid/vapor interface parameter, A, was selected to provide a best-fit of the Laplace capillary equation solution to the experimental area/volume data which included large drops and extended liquid masses with vapor bubble

breakthrough. Thus the area/volume relationship used to reduce the data implicitly included both deviations from the equilibrium shape and vapor bubble breakthrough.

The ability of the Laplace capillary equation to describe the area/volume relationship for non-equilibrium drops (Figures 8 through 11) is thought to be due to the surface tension forces as mentioned previously. Namely, for small drops when the drop thickness is clearly not uniform and deviations in drop shape from the equilibrium would strongly effect the area/volume relationship, the drops assume essentially the equilibrium shape because the liquid interface is relatively rigid, whereas, for large drops, when the aspect ratio (drop diameter divided by drop thickness) is large and the drop thickness is essentially uniform, the shape of the drop is relatively unimportant to the area/volume relationship.

The assumed drop geometry employed in the present study (section 1 of Chapter 3) is the same shape as that of Baumeister [20] (viz. a right circular disk). Since the aspect ratio of the drops is above 5 for dimensionless drop volumes in excess of 75, the present model is only thought to be applicable for dimensionless drop volumes above 75 (i.e., large drops and extended liquid masses). Baumeister et al. [23], however, applied the disk-shaped model over the entire range of drop sizes with some success. Thus, the same principles used in developing the present model might be applicable to drops of dimensionless volume less than 75.

The liquid-solid contact phenomenon may be regular and somewhat periodic as in the case of Figure 26 or irregular as in the case of Figure 27. The regularity (or irregularity) of the contact phenomenon is in part reflected by the standard deviations in the experimental quantities listed in parentheses in Tables 10 and 11. From a modeling perspective one short contact followed by one long contact may not necessarily produce the same result as two contacts of average duration. Thus estimates of enhanced heat flux based on average contact quantities (especially average quantities having significant standard deviations) will necessarily have only limited success (ie. Figures 67 through 74).

In Figure 67 the computed heat transfer coefficients ("stars") were based on contact data similar to that in Figure 27 (i.e., all of the contact data used to compute the heat transfer coefficients represented by the stars in Figure 67 and the strip chart in Figure 27 correspond to bulk surface temperature below the BMFBT but above the LMFBT). In Figure 27 film boiling persisted for 36 time divisions before the LMFBT was reached at which time the boiling process became quasi-nucleate boiling (which persisted until complete vaporization). In Figure 67 the octagons represent heat transfer coefficients that were computed from drop vaporization rate data (for large drops and extended liquid masses, $V^* > 75$). The lower 3 octagons which are in a vertical line above 575°C represent heat transfer coefficients computed from vaporization data early in the drop lifetime (which is analogous to the left side of the strip chart in Figure 27), whereas the upper 2 octagons represent heat transfer coefficients computed from vaporization data later in the drop lifetime (which is analogous to the right side of the strip chart in Figure 27). Recognizing that all of the stars in Figure 67 represent metastable liquid-solid contact ("metastable" liquid-solid contact was defined in the second section of Chapter 6 as relating to the case where film boiling only occurs over a portion of the drop lifetime), the experimental heat transfer coefficients (as computed from drop vaporization rates) and the calculated heat transfer coefficients (based on contact duration and period data) are in reasonable agreement since only the lower 5 octagons are applicable in the comparison to the 10 stars). This same situation (metastable liquid-solid contact) is present with the data in Figure 71. The agreement

between experimental and calculated heat transfer coefficients (octagons and stars respectively) in Figures 68, 69, 79, 72, 73, and 74 is apparent in the Figures.

As stated in section 3 of Chapter 5, both contact duration and period were used by computer program 2-D PINT to calculate the heat transfer coefficients plotted using stars in Figures 67 through 74. All of the analyses reviewed which dealt with heat flux during liquid-solid contact (viz. [4], [5], [6], [37], and [51]) except one (viz. [51]) either assumed that contact duration equals contact period or ignored the fact that there is a finite "OFF" time during the contact period. The contact durations measured in the present study (as listed in Tables 10 and 11) ranged from 26% to 84% of the illustrated in Figure 28), and 4) that large temperature depressions across the pins can occur even in film boiling when intermittent liquid-solid contact is present.

Some further aspects of the present model can be seen from the contact Nusselt number (Equation 6-6), the contact Biot number (Equation 6-9), and the conduction parameter, Q (Equation 6-8). These quantities were computed from drop vaporization data rather than contact data; thus, they are not directly connected to any assumptions concerning the character of liquid-solid contact, but only to the assumption that all the increase in heat flux on the macro-roughened surfaces is attributable to liquid-solid contact.

The contact Nusselt number, Nuc, was typically varied less than one-half order of magnitude throughout a single drop lifetime. For instance see column 15 of Table 15 (the maximum value of "NUC" is 3.165, entry #1 and the minimum is 1.067, entry #30). The drop volume in Table 15 varies over 3 orders of magnitude. Since the contact Nusselt number is defined by $Nuc = hc\delta/kg$, this indicates that the contact heat transfer coefficient, he, is roughly proportional to the inverse of the computed vapor layer thickness, (Equation 3-30).

The conduction parameter, Ω, is defined by $\Omega = \delta ks/\varepsilon kg$ and is therefore equal to a constant times the computed vapor layer thickness for a given liquid and macro-roughened surface. The physical significance of the conduction parameter, Ω, is that it represents the ratio of the conduction thermal resistance of the vapor layer to the conduction thermal resistance of the macro-roughness 116 contact period. The present data is the only data for both duration and period of liquid-solid contact in film boiling known to the author at the present time. Since knowledge (or assumption) of contact duration as well as period is essential to any analysis of contact heat transfer (regardless of the particular theory used) the absence of such data in the literature is disturbing.

Also it is implicitly assumed that the instrumented thermocouple/pin is typical and representative of any pin on the surface such that what is measured there is assumed to occur in like manner elsewhere. This is not strictly the case, as the instrumented pins are, in fact, different from the other pins by virtue of the instrumentation. Also in the case of SHP2612 only the instrumented pin was pressed into the surface while all the other macro-roughness elements were an integral part of the surface itself.

The success in computing heat transfer coefficients from contact data (as compared to that which was determined from drop vaporization rates) may be seen in Figures 67 through 74. It would appear that the present modeling is somewhat consistent with the actual phenomenon. In particular the model predicts 1) that the effect of liquid-solid contact is most pronounced near the MFBT and of diminishing importance with increasing temperature, 2) that film boiling may occur for a short period of time even on a macro-roughened surface whose bulk temperature is

below the BMFBT (provided it is above the LMFBT) as illustrated in Figure 27, 3) that the boiling process may degenerate rapidly into quasi-nucleate boiling characterized by continuous liquid-solid contact (as elements. The values of n ("OMEGA") listed in column 17 of Table 15 range from 202 to 979. These large values of n indicate that the major thermal resistance between the heating surface and the liquid (in Leidenfrost film boiling on macro-roughened surfaces) is that associated with the vapor and not the macro-roughness elements.

The contact Biot number is the ratio of the computed contact heat transfer coefficient to the specific thermal conductance of the pin (for one-dimensional steady heat flow). Values of the contact Biot number listed in column 18 of Table 15 range from 0.0032 to 0.011 (when weighted by the ratio of the cross sectional area of the pins to the total area of the heating surface this range would be 0.016 to 0.055). While these small values of contact Biot number would suggest that a lumped system model of the pins would be sufficient for these "micro" phenomena (e.g., [62]), a two-dimensional model was used in the present study for generality (see details of computer program 2-D PINT in Appendix c. Computed heat transfer coefficients based on a one-dimensional analysis are illustrated for comparison with the two-dimensional results in Figure 68 (these were also computed using program 2-D PINT with radial variations removed).

The computed relative contributions to the overall heat flux of convection, liquid-solid contact, and radiation were plotted for the 3596 data points taken in the present study using computer program PLOT:FRC (a total of 125 plots). A sample of these 125 plots for a smooth and macro-roughened surface is given in Figures 75 and 76 respectively. These figures show radiation less than 30% of the 119 total heat flux for the smooth surface and less than 20% for the macro-roughened surface (note that both Figure 75 and 76 are for relatively high surface temperatures). Figure 76 shows liquid-solid contact 50% to 80% of the total heat flux for the macro-roughened surface. Two points should be noted here concerning the present model for the Leidenfrost phenomenon on macro-roughened surfaces: 1) the conservative estimate of radiation heat flux and 2) the decrease in convective heat flux with increasing total heat flux.

The relationship used for radiation heat flux (Equation 3-45) is conservative in that it will over-estimate the radiative heat flux, since blackbody radiation is the theoretical maximum. This over-estimation of the radiation heat flux, as determined from tabulated values of emissivities from various sources (e.g., [50]), was as small as 6% and as large as 24%. Since the contribution of radiation to the total heat flux was always an over-estimate and always less than 20% on the macro-roughened surfaces (this being the case regardless of how the remaining heat transfer is divided between contact and convection) the error in calculating radiative heat flux is thought to be between 1% and 5% of the total heat flux to the drops for the conditions in the present study. Note also that the present model is only applied to drops having an aspect ratio greater than 5 ($V^*>75$) so that the radiation view factor from the top of the drops to the heating surface is effectively zero as was assumed in section 4 of Chapter 3.

As the total heat flux to the drop increases, the average mass flux, $\underline{G}$, from the drop (due to vaporization) increases proportionately (Equation 3-32). The computed vapor layer thickness, $\underline{\delta}$, (Equation 3-30) also increases as $\underline{G}$ increases. This may be explained in terms of increased "blowing" from the bottom of the drop lifting the drop farther from the surface. The dimensionless enthalpy flux parameter, B, is equal to a constant times the product of $\underline{G}$ and $\underline{\delta}$ (Equation 3-19). The convective heat transfer coefficient (Equation 3-40) decreases with increasing $\underline{\delta}$ and with increasing $\underline{G}$. Thus, as the total heat flux increases the convective heat flux decreases and the relative contribution of convection decreases even more. An example of the

recognition of this decrease in convection with increasing total heat transfer is given in the radiation correction factor employed by Baumeister, Keshock, and Pucci [31]. This correction factor is given in Chapter 5, Equation 5-6.

The dimensionless enthalpy flux parameter B= $\underline{\delta}$CpgG/kg, is listed in column 11 of Table 15 (ethanol on surface SCG02 at 450°C). The maximum value of B listed in Table 15 is 3.916 (entry #1) and the minimum value is 1.893 (entry #32). Throughout a single drop life time the dimensionless enthalpy flux parameter, B, was typically constant within a factor of 2. The dimensionless enthalpy flux parameter, B, is related to the convective Nusselt number, Nu_F = $h_F\underline{\delta}$/kg, by Equations 3-41 and 3-42. As illustrated by the values of Nu_F listed in column 13 of Table 14 and column 14 of Table 15, the convective Nusselt number is also constant within a factor of 2 121 throughout a single drop lifetime whether on the smooth surface (Table 14) or a macro-roughened surface (Table 15). Since B is approximately constant throughout a drop lifetime and thus Nu_F is also approximately constant throughout a drop lifetime (by Equation 3-42), this indicates that the mass flux, G, and the convective heat transfer coefficient, hp, are both approximately proportional to the inverse of o whether on the smooth surface or a macro-roughened surface. Therefore, the computed vapor layer thickness, δ, is a parameter which relates both convective heat transfer and contact heat transfer (as detailed previously through the contact Nusselt number, Nuc), since both quantities (viz. h_F and he) are approximately proportional to the inverse of $\underline{\delta}$. This relationship between o, hp, and he further reinforces the postulate that the effect of the surface macro-roughness on Leidenfrost film boiling is directly related to the vapor layer thickness and the macro-roughness height.

Chapter 8. Conclusions

1. Liquid-solid contact does occur on macro-roughened surfaces even at bulk surface temperatures significantly above the smooth surface minimum film boiling temperature.
2. The liquid-solid contact period was found to be on the same order of magnitude as the period of the Taylor most dangerous instability.
3. Substantial variations in contact duration and period were measured throughout a single drop lifetime indicating that the liquid-solid contact phenomenon investigated is irregular and not strictly periodic.
4. Substantial temperature depressions across the relatively short distance between the top of the instrumented pins and the location where the bulk surface temperature were measured. These substantial temperature differences indicate that relatively large heat fluxes (approaching the critical heat flux) occurred in some cases during film boiling on the macro-roughened surfaces. Calculations based on temperature differences, contact period, contact duration, and drop vaporization agreed that near critical heat fluxes can, in fact, occur over small areas during Leidenfrost film boiling on a macro-roughened surface even if the surface temperature is significantly above the critical heat flux temperature.
5. Substantial increases in heat flux were measured on the macro-roughened surfaces (over that which was measured on the smooth surface). The evidence of pin tip temperature depressions, contact period, and contact duration as well as calculations based on this evidence indicate that this increase in heat flux appears to be a result of increased liquid-solid contact on the macro-roughened surfaces.
6. The probability of liquid-solid contact occurring for a Leidenfrost drop at rest on a surface appears to be increased with decreasing computed layer thickness (or increasing macro-roughness height) and decreased with increasing computed layer thickness (or decreasing macro-roughness height.
7. The relative increase in heat flux on the macro-roughened surfaces (as compared to the smooth surface) was seen to diminish with increasing surface temperature and become larger with decreasing surface temperature. This is postulated to be a result of an increase in vapor layer thickness with increasing surface temperature and a decrease in vapor layer thickness with decreasing surface temperature since the heat flux appears to increase with increasing liquid-solid contact and liquid-solid contact appears to increase with decreasing vapor layer thickness.
8. The BMFBT (bulk minimum film boiling temperature) was measured on two macro-roughened surfaces and found to be higher than the LMFBT (significantly higher in the case of water). The difference between the BMFBT and the LMFBT is postulated to result from conduction of heat from the bulk of the heating surface through the macro-roughness elements and to the liquid, specifically at the points where liquid-solid contact occurs (i.e., the LMFBT and BMFBT would be equal only if the thermal conductivity of the heating surface were infinite).
9. The contact heat fluxes as calculated using the modification of the error function solution for the contact of two semi-infinite static media were on the same order as those based on

experimental drop vaporization rates on the macro-roughened surfaces indicating that this approximation for the contact heat flux is a reasonable model for the contact phenomenon.

Chapter 9 Recommendations

The vapor flow pattern beneath the drop on a macro-roughened surface, the average vapor layer thickness, and the contact area were all assumed in the present analysis. Experimental measurement of any or all of these quantities would greatly add to the basic understanding of film boiling on macro-roughened surfaces and more particularly liquid-solid contact in film boiling. It is recommended that studies be made of these basic quantities before more general quantities (such as the effects of ambient pressure) are investigated so that the theoretical understanding of the phenomenon can be more firmly established. The logical extension of the present study would be to investigate non-cylindrical macro-roughness. Tetrahedral macro-roughness should be strongly considered in such a study as this can be produced by a simple milling process similar to that used in producing the hexagonal pins in the present study. The difficulty of instrumenting a tetrahedron would be a major obstacle in such a study. Experiments similar to the present ones should also be carried out for pool and flow film boiling when liquid-solid contact in film boiling of Leidenfrost drops is more fully understood. Additional investigations should be undertaken to identify non-dimensional groups that would permit all of the variables influencing heat transfer enhancement due to surface macro-roughness to be accurately accounted for in a generalized fashion.

List of References

1. Bromley, L. A., "Heat Transfer in Stable Film Boiling," Chemical Engineering Progress, Vol. 46, No. 5, May, 1959, pp. 221-227.

2. Leidenfrost, J. G., "On the Fixation of Water in Diverse Fire," trans. Carolyn Wares, International Journal of Heat and Mass Transfer, Vol. 9, November, 1966, pp. 1153-1166.

3. Baumeister, K. J., Hendricks, R. C., and Hamill, T. D., "Metastable Leidenfrost States," NASA TND-3226, April, 1966.

4. Bradfield, W. S., "Liquid-Solid Contact in Stable Film Boiling," Industrial and Engineering Chemistry: Fundamentals, Vol. 5, No. 2, May 1966, pp. 200-204.

5. Nishio, S. and Hirata, M., "Direct Contact Phenomenon Between a Liquid Droplet and High Temperature Solid Surface," Proceedings of the Sixth International Heat Transfer Conference, Toronto, Canada, August 1978, pp 245-250.

6. Yao, S. C. and Henry, R. E., "Experiments of Quenching Under Pressure," Proceedings of the Sixth International Heat Transfer Conference, Toronto, Canada, August, 1978, pp. 263-267.

7. Taylor, Sir G., "The Instability of Liquid Surfaces When Accelerated in a Direction Perpendicular to Their Planes I," Proceedings of the Royal Society of London, Vol. 201, Series A., 1950, pp. 192-196.

8. Tevepaugh, J. A. and Keshock, E. G., "Influence of Artificial Surface Projections on Film Boiling Heat Transfer," Proceedings of the Eighteenth National Heat Transfer Conference: Advances in Enhanced Heat Transfer, San Diego, California, August 1979, pp. 133-140.

9. Knobel, D. H. and Yeh, Y. C., "The Effect of Artificial Surface Projections on Film-Boiling Heat Transfer," Proceedings of the AIChE-ASME National Heat Transfer Conference, Salt Lake City, Utah, August, 1977.

10. Yao, S. C. and Henry, R. E., "An Investigation of the Minimum Film Boiling Temperature on Horizontal Surfaces," ASME Journal of Heat Transfer, Vol. 100, May, 1978, pp. 260-267.

11. Seki, M., Kawamura, H., and Sanokawa, K., "Transient Temperature Profile of a Hot Wall Due to an Impinging Liquid Droplet," ASME Journal of Heat Transfer, Vol. 100, February 1978, pp. 167-169.

12. Gorton, C. W., "Heat Transfer to Drops in the Spheroidal State," Ph. D. Thesis, Purdue University, July 1953.

13. Wachters, L. H. J., "Heat Transfer from a Hot Wall to Drops in a Spheroidal State," trans. H. Houtsager, Ph. D. Thesis, Technische Hogeschool, Delft, The Netherlands, 1965.

14. Bell, K. J., "The Leidenfrost Phenomenon: A Survey," Chemical Engineering Progress Symposium Series, Vol. 63, No. 79, 1967, PP• 74-85.

15. Gottfried, B. S., Lee, C. J., and Bell, K. J., "The Leidenfrost Phenomenon: Film Boiling of Liquid Droplets on a Flat Plate," International Journal of Heat and Mass Transfer, Vol. 9, 1966, pp. 1167-1187.

16. Gottfried, B. S., "The Evaporation of Small Drops on a Flat Plate in the Film Boiling Regime," Ph. D. Thesis, Case Institute of Technology, May 1962.

17. Lee, C. J., "The Leidenfrost Phenomenon for Small Droplets," Ph. D. Thesis, Oklahoma State University, Stillwater, Oklahoma, 1965.

18. Wachters, L. H. J., Bonne, H., and van Nouhuis, H. J., "The Heat Transfer from a Hot Horizontal Plate to Sessile Drops in the Spheroidal State," Chemical Engineering Science, Vol. 21, 1966, pp. 923-936.

19. Wachters, L. H. J. and Westerling, N. A. J., "The Heat Transfer from a Hot Wall to Impinging Water Drops in the Spheroidal State," Chemical Engineering Science, Vol. 21, 1966, pp. 147-1056.

20. Baumeister, K. J., "Heat Transfer to Water Droplets on a Flat Plate in the Film Boiling Regime," Ph. D. Thesis, University of Florida, Gainesville, Florida, 1964.

21. Baumeister, K. J., Hamill, T. D., Schwarts, F. L., and Schoessow, G. J., "Film Boiling Heat Transfer to Water Drops on a Flat Plate," Proceedings of the Third International Heat Transfer Conference, Chicago, Illinois, August, 1966.

22. Baumeister, K. J. and Hamill, T. D., "Creeping Flow Solution of the Leidenfrost Phenomenon," NASA TND-3133, December 1965.

23. Baumeister, K. J., Hamill, T. D., and Schoessow, G. J., "A Generalized Correlation of Vaporization Times of Drops in Film Boiling on a Flat Plate," Proceedings of the Third International Heat Transfer Conference, Chicago, Illinois, August, 1966.

24. Patel, B. M., "The Leidenfrost Phenomenon for Extended Liquid Masses," Ph. D. Thesis, Oklahoma State University, Stillwater, Oklahoma, 1965.

25. Patel, B. M. and Bell, K. J., "The Leidenfrost Phenomenon for Extended Liquid Masses," Proceedings of the Third International Heat Transfer Conference, Chicago, Illinois, August 1966.

26. Keshock, E. G., "Leidenfrost Film Boiling of Intermediate and Extended Bubbly Masses of Liquid Nitrogen," Ph. D. Thesis, Oklahoma State University, Stillwater, Oklahoma, May 1968.

27. Keshock, E. G. and Bell, K. J., "Heat Transfer Coefficient Measurements of Liquid Nitrogen drops Undergoing Film Boiling," Advances in Cryogenic Engineering, Vol. 15, 1979, pp. 271-282.

28. Hendricks, R. C. and Baumeister, K. J., "Liquid or Solid on Liquid in Leidenfrost Film Boiling," Advances in Cryogenic Engineering, Vol. 16, 1971, pp. 445-466.

29. Baumeister, K. J. and Simon, F. F., "Leidenfrost Temperature -Its Correlation for liquid Metals, Cryogens, Hydrocarbons, and Water," ASME Journal of Heat Transfer, May 1973, pp. 166-173.

30. Schoessow, G. J., Jones, D. R., and Baumeister, K. J., "Leidenfrost Film Boiling of Drops on a Moving Surface," Chemical Engineering Progress Symposium Series, Vol. 64, No. 82, 1966, pp. 95-101.

31. Baumeister, K. J., Keshock, E. G., and Pucci, D. A., "Anomalous Behavior of Liquid Nitrogen Drops in Film Boiling," NASA TMX-52800, June, 1970.

32. Henry, R. E., "A Correlation for the Minimum Film Boiling Temperature," AIChE Symposium Series, Vol. 70, No. 138, 1974, pp. 81-90.

33. Hall, W. B., "The Stability of Leidenfrost Drops," Proceedings of the Fifth International Heat Transfer Conference, Tokyo, Japan, 1974, pp. 125-129.

34. Berghmans, J., "The Minimum Heat Flux During Film Boiling," Proceedings of the Sixth International Heat Transfer Conference, Toronto, Canada, 1978, pp. 233-237.

35. Bankoff, S. G., Maeshima, M., Segev, A., and Sharon, A., "Destabilization of Film Boiling in Liquid-Liquid Systems," Proceedings of the Sixty International Heat Transfer Conference, Toronto, Canada, 1978, pp. 269-274.

36. Baumeister, K. J., Hendricks, R. C., and Schoessow, G. J., "Thermally Driven Oscillations and Wave motion of a Drop," NASA TMX-73635, August, 1977.

37. Bankoff, S. G. and Mehra, V. S., "A Quenching Theory for Transition Boiling," Industrial and Engineering Chemistry: Fundamentals, Vol. 1, No. 1, February 1962, pp. 38-40.

38. Berenson, P. J., "Film-Boiling Heat Transfer from a Horizontal Surface," ASME Journal of Heat Transfer, August 1961, pp. 351-358.

39. Blander, M. and Katz, J. L., "Bubble Nucleation Liquids," AIChE Journal, Vol. 21, No. 5, September, 1975, pp. 833-848.

40. Hsu, Y. Y., "On the Size Range of Active Nucleation Cavities on a Heating Surface," ASME Journal of Heat Transfer, August 1962, pp. 207-216.

41. Shourki, M. and Judd, R. L., "Nucleation Site Activation in Saturated Boiling," ASME Journal of Heat Transfer, February, 1975, pp. 93-98.

42. Singh, A. Mikic, B. B., and Rohsenow, W. M., "Active Sites in Boiling," ASME Journal of Heat Transfer, August 1976, pp. 401-406.

43. Han, C. Y. and Griffith, P., "The Mechanism of Heat Transfer in Nucleate Pool Boiling," International Journal of Heat Mass Transfer, Vol. 8, 1965, pp. 887-904.

44. K.utateladze, s. S., "Boiling Heat Transfer," International Journal of Heat and Mass Transfer, Vol. 4, 1961, pp. 31-45.

45. Hartland, S. and Hartley, R. W., Axisymmetric Fluid-Liquid Interfaces, Elsevier Scientific, Amsterdam, 1976.

46. Morikawa, A. and Keii, T., "Change in Interfacial Tension During Mass Transfer I," Chemical Engineering Science, Vol. 20, 1965, pp. 225-259.

47. Morikawa, A. and Keii, T., "Change in Interfacial Tension During Mass Transfer II," Chemical Engineering Science, Vol. 22, 1965, pp. 127-133.

48. Bakker, C. A. P., van Buytensen, P.M., and Beek, W. J., "Interfacial Phenomenon and Mass Transfer," Chemical Engineering Science, Vol. 21, 1966, pp. 1039-1046.

49. Baumeister, K. J. and Schoessow, G. J., "Diffusive and Radiative Effects on Vaporization times of Drops in Film Boiling," AIChE Symposium Series, Vol. 69, No. 131, 1969, pp. 10-17.

50. Eckert, E. R. G. and Drake, R. M. Jr., Heat and Mass Transfer, 2nd Ed., McGraw-Hill, New York, 1959.

51. Gunnerson, F. S. and Cronenberg, A. W., "A Prediction of the Minimum Film Boiling Conditions for Spherical and Horizontal Flat Plate Heaters," Proceedings of ASME/AIChE Eighteenth National Heat Transfer Conference, San Diego, California, August 1979.

52. Henry, R. E., Quinn, D. J., and Sleha, E. A., "An Experimental Study of the Minimum Film Boiling point for Liquid-Liquid Systems," Proceedings of the Fifth International Heat Transfer Conference, Tokyo, Japan, 1974, pp. 101-104.

53. Chen, J. C., Sundaran, R. K., and Ozkaynak, F. T., "A Phenomenological Correlation for Post-CHF Heat Transfer," NUREG-0237, 1977.

54. Grigoriev, V. A., Klimenko, V. V., Pavlov, Yu. M., and Ametistov, Ye. V., "The Influence of Some Heating Surface Properties on the Critical Heat Flux In Cryogenic Liquids in Boiling," Proceedings of the Sixth International Heat Transfer conference, Toronto, Canada, August, 1978, pp. 215-220.

55. Mikic, B. B. and Rohsenow, w. M., "A New Correlation of Pool-Boiling Data Including the Effect of Heating Surface Characteristics," ASME Journal of Heat Transfer, May 1969, pp. 245-250.

56. Zhukov, V. M., Kazakov, G. M., Kovalev, S. A., and Kuzma-Kichta, Yu. A., "Heat Transfer in Boiling of Liquids on Surfaces Coated with Low Thermal Conductivity Films," Heat Transfer Soviet Research, Vol. 7, No. 3, May-June, 197s:- pp. 16-26.

57. Chester, M., "Second Sound in Solids," Physical Review, Vol. 131, No. 5, September 1963, pp. 2013-2015.

58. Weymann, H. D., "Finite Speed of Propagation in Heat Conduction, Diffusion, and Viscous Shear Motion," American Journal of Physics, Vol. 35, No. 6, June 1967, pp. 488-496.

59. Baumeister, K. J. and Hamill, T. D., "Hyperbolic Heat-Conduction Equation: A Solution for the Semi-Infinite Body Problem," ASME Journal of Heat Transfer, November 1969, pp. 543-548.

60. Cho, D. H. and Chan, S. H., "Effect of Internal Thermal Radiation on the Contact Interface Temperature," Letters in Heat and Mass Transfer, Vol. 4, 1977, pp. 465-475.

61. Rice, J. R., The Approximation of Functions, Addison-Wesley, Reading, Massachusetts, 1964.

62. Adams, J. A. and Rogers, D. F., Computer-Aided Heat Transfer Analysis, McGraw-Hill, New York, 1973.

63. Ortega, J. M. and Rheinboldt, W. C., Iterative Solution of Nonlinear Equations in Several Variables, Academic Press, New York, 1973.

64. Lambert, J. D., Computational Methods in Ordinary Differential Equations, John Wiley and Sons, Chichester, New Jersey, 1973.

65. Zuber, N., Tribus, M., and Westwater, J. W., "The Hydrodynamic Crisis in Pool Boiling of Saturated and Subcooled Liquids," Proceedings of the Second International Heat Transfer Conference, Denver, Colorado, 1961.

66. Weast, R. C., ed., CRC Handbook of Chemistry and Physics, 54th ed., CRC Press, Cleveland, Ohio, 1973.

67. Hildebrand, F. B., Advanced Calculus for Applications, 2nd ed., Prentice-Hall, Englewood Cliffs, New Jersey, 1976.

68. Hildebrand, F. B., Introduction to Numerical Analysis, 2nd ed., McGraw-Hill, New York, 1974.

69. White, F. M. Fluid Mechanics, McGraw-Hill, New York, 1979.

Appendix A. Tables

Table 1. Summary of Strip Charts for Surface CP54

Strip	Liquid	Initial Surface Temp.	Initial Drop Volume	Initial Liquid Temp.	Mode of Boiling
7	H2O	510°C	10 cc	100°C	F&QNB
4	H2O	502°C	10 cc	100°C	F&ONB
1	H2O	498°C	10 cc	100°C	F&OMB
3	H2O	497°C	10 cc	100°C	F&ONB
6	H2O	495°C	2 cc	100°C	F
2	H2O	494°C	5 cc	0°C	QNB
5	H2O	487°C	5 cc	100°C	F&QNB
16	H2O	453°C	5 cc	0°C	QNB
18	H2O	445°C	10 cc	100°C	QNB
17	H2O	440°C	5 cc	100°C	F&QNB
19	H2O	433°C	10 cc	100°C	QNB
20	H2O	432°C	10 cc	100°C	QNB
32	H2O	345°C	10 cc	100°C	QNB
31	H2O	335°C	10 cc	100°C	QNB
41	H2O	295°C	10 cc	100°C	QNB
40	H2O	290°C	10 cc	100°C	QNB
42	H2O	285°C	10 cc	100°C	QNB
11	EA	515°C	5 cc	78°C	F
8	EA	500°C	5 cc	78°C	F
21	EA	450°C	5 cc	78°C	F
24	EA	405°C	5 cc	78°C	F
28	EA	385°C	5 cc	78°C	F
33	EA	350°C	10 cc	78°C	F
36	EA	325°C	5 cc	78°C	F&QNB
43	EA	285°C	5 cc	78°C	QNB
12	IP	515°C	5 cc	83°C	F
13	IP	510°C	5 cc	83°C	F
9	IP	495°C	5 cc	83°C	F
22	IP	440°C	5 cc	83°C	F
25	IP	405°C	5 cc	83°C	F
29	IP	380°C	5 cc	83°C	F
34	IP	360°C	5 cc	83°C	F&QNB
44	IP	280°C	5 cc	83°C	F&QNB
15	EC	515°C	5 cc	84°C	F
14	EC	510C	5 cc	84C	F
10	EC	490°C	5 cc	84°C	F
23	EC	437°C	5 cc	84°C	F
27	EC	410°C	5 cc	84°C	F
26	EC	405°C	5 cc	84°C	F
30	EC	385°C	5 cc	84°C	F
35	EC	350°C	10 cc	84°C	F
38	EC	340°C	5 cc	84°C	F
39	EC	320°C	5 cc	84°C	F&QNB
45	EC	275°C	5 cc	84°C	F&QNB

EA=Ethanol, IP=Isopropanol, EC=Ethylene-Chloride
F=Film Boiling (with intermittent liquid/solid contact)
QNB=Quasi-Nucleate Boil. (w/ continuous lqd./s. contact)

Table 2. Summary of Strip Charts for Surface SHP2612

Strip	Liquid	Initial Surface Temp.	Initial Drop Volume	Initial Liquid Temp.	Mode of Boiling
46	H2O	530 C	10 cc	100 C	F&QNB
47	H2O	465 C	10 cc	100 C	F&QNB
48	H2O	395 C	10 cc	100 C	F&QNB
49	H2O	345 C	10 cc	100 C	F&QNB
50	H2O	260 C	10 cc	100 C	QNB
51	EA	480 C	10 cc	78 C	F
52	EA	420 C	10 cc	78 C	F
53	EA	360 C	10 cc	78 C	F
54	EA	289 C	15 cc	78 C	F
55	EA	235 C	10 cc	78 C	F
57	EA	230 C	10 cc	78 C	F&QNB
58	EA	200 C	10 cc	78 C	QNB
59	IP	500 C	10 cc	83 C	F
60	IP	410 C	10 cc	83 C	F
61	IP	400 C	10 cc	83 C	F
62	IP	370 C	10 cc	83 C	F
63	IP	290 C	10 cc	83 C	F
64	IP	250 C	10 cc	83 C	F
65	IP	210 C	10 cc	83 C	F&QNB
66	IP	200 C	10 cc	83 C	QNB
67	IP	190 C	10 cc	83 C	QNB
68	EC	480 C	10 cc	84 C	F
69	EC	460 C	10 cc	84 C	F
70	EC	430 C	10 cc	84 C	F
71	EC	365 C	10 cc	84 C	F
72	EC	275 C	10 cc	84 C	F
73	EC	255 C	10 cc	84 C	F
74	EC	220 C	10 cc	84 C	F&QNB
75	EC	180 C	10 cc	84 C	QNB

EA=Ethanol, IP=Isopropanol, EC=Ethylene-Chloride
F=Film Boiling (with intermittent liquid/solid contact)
QNB=Quasi-Nucleate Boil. (w/ continuous lqd./s. contact)

Table 3. Summary of Data on Surface SMTH

Strip	Seq.	Liquid	Initial Surface Temp.	Initial Liquid Temp.	Mode of Boiling
12	83	H2O	240 C	100 C	F
12	81	H2O	300 C	100 C	F
12	79	H2O	345 C	100 C	F
12	77	H2O	400 C	100 C	F
12	75	H2O	450 C	100 C	F
12	73	H2O	500 C	100 C	F
12	71	H2O	535 C	100 C	F
12	84	EA	190 C	78 C	F
12	82	EA	240 C	78 C	F
12	80	EA	300 C	78 C	F
12	78	EA	350 C	78 C	F
12	76	EA	400 C	78 C	F
12	74	EA	450 C	78 C	F
12	72	EA	500 C	78 C	F
12	70	EA	530 C	78 C	F
12	107	IP	180 C	83 C	F
12	109	IP	240 C	83 C	F
12	111	IP	290 C	83 C	F
12	116	IP	330 C	83 C	F
12	120	IP	380 C	83 C	F
12	123	IP	440 C	83 C	F
12	126	IP	500 C	83 C	F
12	108	EC	190 C	84 C	F
12	110	EC	250 C	84 C	F
12	112	EC	300 C	84 C	F
12	118	EC	330 C	84 C	F
12	121	EC	380 C	84 C	F
12	124	EC	440 C	84 C	F
12	127	EC	490 C	84 C	F

EA=Ethanol, IP=Isopropanol, EC=Ethylene-Chloride
F=Film Boiling

Table 4. Summary of Data on Surface CG01

Strip	Seq.	Liquid	Initial Surface Temp.	Initial Liquid Temp.	Mode of Boiling
12	65	H2O	350 C	100 C	F&QNB
12	64	H2O	400 C	100 C	F&QNB
12	61	H2O	450 C	100 C	F&QNB
12	63	H2O	500 C	100 C	F
12	69	EA	200 C	78 C	F&QNB
12	68	EA	230 C	78 C	F&QNB
12	66	EA	300 C	78 C	F&QNB
12	58	EA	350 C	78 C	F
12	59	EA	400 C	78 C	F
12	60	EA	450 C	78 C	F
12	62	EA	500 C	78 C	F
12	147	IP	190 C	83 C	F&QNB
12	145	IP	240 C	83 C	F&QNB
12	143	IP	300 C	83 C	F&QNB
12	141	IP	320 C	83 C	F&QNB
12	138	IP	370 C	83 C	F
12	132	IP	440 C	83 C	F
12	135	IP	460 C	83 C	F
12	129	IP	500 C	83 C	F
12	148	EC	190 C	84 C	F&QNB
12	146	EC	240 C	84 C	F&QNB
12	144	EC	300 C	84 C	F&QNB
12	142	EC	320 C	84 C	F&QNB
12	139	EC	370 C	84 C	F
12	133	EC	410 C	84 C	F
12	136	EC	460 C	84 C	F
12	130	EC	500 C	84 C	F

EA=Ethanol, IP=Isopropanol, EC=Ethylene-Chloride
F=Film Boiling (with intermittent liquid/solid contact)
QNB=Quasi-Nucleate Boil. (w/ continuous lqd./s. contact)

Table 5. Summary of Data on Surface SCG02

Strip	Seq.	Liquid	Initial Surface Temp.	Initial Liquid Temp.	Mode of Boiling
13	18	H2O	450 C	100 C	F&QNB
13	43	H2O	525 C	100 C	F&QNB
13	40	EA	210 C	78 C	F&QNB
13	37	EA	260 C	78 C	F&QNB
13	34	EA	300 C	78 C	F&QNB
13	31	EA	350 C	78 C	F
13	28	EA	410 C	78 C	F
13	23	EA	450 C	78 C	F
13	19	EA	500 C	78 C	F
13	41	IP	210 C	83 C	F&QNB
13	38	IP	260 C	83 C	F&QNB
13	35	IP	300 C	83 C	F&QNB
13	32	IP	350 C	83 C	F
13	29	IP	410 C	83 C	F
13	24	IP	450 C	83 C	F
13	20	IP	500 C	83 C	F
13	42	EC	235 C	84 C	F&QNB
13	39	EC	260 C	84 C	F&QNB
13	36	EC	300 C	84 C	F&QNB
13	33	EC	350 C	84 C	F
13	30	EC	410 C	84 C	F
13	25	EC	450 C	84 C	F
13	21	EC	500 C	84 C	F

EA=Ethanol, IP=Isopropanol, EC=Ethylene-Chloride
F=Film Boiling (with intermittent liquid/solid contact)
QNB=Quasi-Nucleate Boil. (w/ continuous lqd./s. contact)

Table 6. Summary of Data on Surface CP54

Strip	Seq.	Liquid	Initial Surface Temp.	Initial Liquid Temp.	Mode of Boiling
13	63	H2O	575 C	100 C	F&QNB
13	64	H2O	620 C	100 C	F&QNB
13	62	EA	220 C	78 C	F&QNB
13	56	EA	260 C	78 C	F&QNB
13	53	EA	310 C	78 C	F&QNB
13	52	EA	380 C	78 C	F&QNB
13	49	EA	430 C	78 C	F&QNB
13	46	EA	490 C	78 C	F
13	61	IP	220 C	83 C	F&QNB
13	57	IP	270 C	83 C	F&QNB
13	54	IP	310 C	83 C	F&QNB
13	51	IP	370 C	83 C	F&QNB
13	48	IP	430 C	83 C	F&QNB
13	45	IP	490 C	83 C	F
13	59	EC	220 C	84 C	F&QNB
13	58	EC	270 C	84 C	F&QNB
13	55	EC	310 C	84 C	F&QNB
13	50	EC	380 C	84 C	F&QNB
13	47	EC	440 C	84 C	F&QNB
13	44	EC	470 C	84 C	F&QNB
13	144	EC	480 C	84 C	F

EA=Ethanol, IP=Isopropanol, EC=Ethylene-Chloride
F=Film Boiling (with intermittent liquid/solid contact)
QNB=Quasi-Nucleate Boil. (w/ continuous lqd./s. contact)

Table 7. Summary of Data on Surface SHP2612

Strip	Seq.	Liquid	Initial Surface Temp.	Initial Liquid Temp.	Mode of Boiling
19	8	H2O	410 C	100 C	F&QNB
19	1	H2O	550 C	100 C	F&QNB
19	24	EA	200 C	78 C	F&QNB
19	21	EA	250 C	78 C	F&QNB
19	18	EA	300 C	78 C	F&QNB
19	15	EA	355 C	78 C	F&QNB
19	11	EA	410 C	78 C	F&QNB
19	7	EA	440 C	78 C	F&QNB
19	2	EA	550 C	78 C	F
19	23	IP	210 C	83 C	F&QNB
19	20	IP	260 C	83 C	F&QNB
19	17	IP	315 C	83 C	F&QNB
19	14	IP	355 C	83 C	F&QNB
19	10	IP	415 C	83 C	F&QNB
19	6	IP	465 C	83 C	F&QNB
19	3	IP	550 C	83 C	F
19	22	EC	215 C	84 C	F&QNB
19	19	EC	265 C	84 C	F&QNB
19	16	EC	320 C	84 C	F&QNB
19	13	EC	370 C	84 C	F&QNB
19	9	EC	425 C	84 C	F&QNB
19	5	EC	465 C	84 C	F&QNB
19	4	EC	550 C	84 C	F

EA=Ethanol, IP=Isopropanol, EC=Ethylene-Chloride
F=Film Boiling (with intermittent liquid/solid contact)
QNB=Quasi-Nucleate Boil. (w/ continuous lqd./s. contact)

Table 8. Sample Output of Program DATABASE for a Smooth Surface

λ	Cpg	κg	ρf	ρg	μg	κs	ε	Tsat	Hfg	ΔA	
0.219	2.03	2.76E-04	0.9583	0.0006	0.00012	0.00E+00	0.52	100	2257	5.6%	
T	A	As	-d(ln(As))/dt	A*	V*	V	L	Hexp	Hx/Hs	Nuv	H
sec	cm²	cm²	1/sec	-	-	cm³	cm	W/cm³/C	-	-	-
0	7.240	6.616	0.01820	138.1	240.1	2.518	0.381	0.01200	0.665	59.4	21.4
10	6.290	6.240	0.01800	130.2	225.8	2.368	0.379	0.01320	0.723	63.9	23.0
20	5.330	5.853	0.01770	122.1	211.0	2.214	0.378	0.01440	0.776	67.9	24.4
30	5.240	5.460	0.01740	113.9	196.1	2.057	0.377	0.01550	0.826	71.5	25.7
40	5.120	5.066	0.01700	105.7	181.2	1.901	0.375	0.01660	0.871	74.5	26.8
50	4.390	4.676	0.01670	97.6	166.5	1.747	0.374	0.01770	0.913	77.1	27.7
60	4.310	4.295	0.01640	89.6	152.2	1.596	0.372	0.01870	0.950	79.2	28.5
70	3.900	3.925	0.01600	81.9	138.3	1.450	0.369	0.01970	0.983	80.7	29.0
80	3.520	3.569	0.01560	74.5	124.9	1.311	0.367	0.02060	1.012	81.9	29.4
90	3.290	3.230	0.01520	67.4	112.3	1.178	0.365	0.02160	1.037	82.5	29.7
100	2.960	2.910	0.01490	60.7	100.4	1.053	0.362	0.02240	1.058	82.8	29.8
110	2.640	2.610	0.01450	54.5	89.3	0.936	0.359	0.02330	1.075	82.6	29.7
120	2.670	2.330	0.01410	48.6	79.0	0.828	0.355	0.02410	1.088	82.0	29.5
130	2.200	2.071	0.01370	43.2	69.5	0.729	0.352	0.02490	1.097	81.1	29.2
140	1.910	1.833	0.01330	38.3	60.8	0.638	0.348	0.02560	1.102	79.8	28.7
150	1.670	1.616	0.01290	33.7	52.9	0.555	0.343	0.02620	1.104	78.2	28.1
160	1.400	1.419	0.01250	29.6	45.8	0.481	0.339	0.02690	1.102	76.3	27.4
170	1.150	1.242	0.01210	25.9	39.5	0.414	0.333	0.02740	1.097	74.1	26.7
180	1.100	1.082	0.01180	22.6	33.8	0.355	0.328	0.02790	1.089	71.7	25.8
190	0.66	0.939	0.01140	19.6	28.8	0.302	0.322	0.02840	1.077	69.0	24.8
200	0.83	0.813	0.01100	17.0	24.4	0.256	0.315	0.02880	1.062	66.2	23.8
210	0.73	0.701	0.01070	14.6	20.5	0.215	0.307	0.02910	1.044	63.1	22.7
220	0.64	0.602	0.01030	12.6	17.2	0.180	0.299	0.02930	1.024	59.9	21.6
230	0.530	0.516	0.01000	10.8	14.3	0.150	0.291	0.02940	1.000	56.6	20.4
240	0.45	0.441	0.00970	9.2	11.8	0.124	0.281	0.02940	0.973	53.2	19.1
250	0.4	0.375	0.00940	7.8	9.7	0.102	0.272	0.02930	0.943	49.6	17.9
260	0.34	0.319	0.00910	6.6	7.9	0.083	0.260	0.02910	0.910	46.0	16.6
270	0.29	0.27	0.00880	5.6	6.4	0.067	0.248	0.02870	0.874	42.4	15.3
280	0.2	0.228	0.00850	4.8	5.2	0.054	0.237	0.02830	0.836	38.8	14.0

Table 9. Sample Output of Program DATABASE for a Macro-Roughened Surface

λ	Cpg	κg	ρf	ρg	μg	κs	ε	Tsat	Hfg	ΔA	
0.119	1.98	2.71E-04	0.739	0.00163	1.03E-04	5.08E-02	0.16	78.4	854.6	8.8%	
T	A	Asmth	-d(ln(As))/dt	A*	V*	V	L	Hexp	Hx/Hs	Nuv	H
sec	cm²	cm²	1/sec	-	-	cm³	cm	W/cm³/C	-	-	-
0	37.628	43.249	0.03440	3049.0	5783.7	9.771	0.226	0.02600	2.694	205.1	176.6
2	36.113	37.952	0.03320	2675.5	5064.7	8.556	0.225	0.02490	2.523	188.2	162.0
4	32.420	33.472	0.03200	2359.7	4457.5	7.531	0.225	0.02400	2.369	173.3	149.2
6	30.898	29.657	0.03100	2090.8	3941.4	6.659	0.225	0.02310	2.231	160.1	137.9
8	27.179	26.388	0.03000	1860.3	3499.6	5.912	0.224	0.02230	2.107	148.5	127.9
10	24.843	23.568	0.02910	1661.5	3119.1	5.269	0.224	0.02150	1.996	138.3	119.1
12	22.852	21.119	0.02830	1488.9	2789.2	4.712	0.223	0.02090	1.898	129.3	111.4
14	18.636	18.980	0.02750	1338.1	2501.4	4.226	0.223	0.02040	1.811	121.5	104.6
16	19.020	17.100	0.02670	1205.5	2248.8	3.799	0.222	0.01990	1.735	114.5	98.6
18	16.395	15.438	0.02600	1088.4	2025.8	3.422	0.222	0.01950	1.669	108.5	93.4
20	14.749	13.960	0.02530	984.1	1827.8	3.088	0.221	0.01920	1.612	103.2	88.9
22	13.158	12.638	0.02470	891.0	1651.0	2.789	0.221	0.01900	1.564	98.7	85.0
24	11.538	11.450	0.02400	807.2	1492.3	2.521	0.220	0.01890	1.523	94.8	81.6
26	10.745	10.378	0.02340	731.6	1349.3	2.279	0.220	0.01880	1.490	91.4	78.7
28	9.103	9.404	0.02280	663.0	1219.7	2.061	0.219	0.01880	1.464	88.5	76.2
30	8.280	8.518	0.02220	600.5	1101.8	1.861	0.218	0.01900	1.444	86.1	74.1
32	8.624	7.707	0.02170	543.3	994.3	1.680	0.218	0.01910	1.431	84.0	72.3
34	6.478	6.964	0.02110	491.0	895.8	1.513	0.217	0.01940	1.422	82.3	70.8
36	6.224	6.281	0.02050	442.8	805.6	1.361	0.217	0.01980	1.418	80.8	69.6
38	5.28	5.653	0.02000	398.5	722.6	1.221	0.216	0.02020	1.419	79.7	68.6
40	4.952	5.073	0.01940	357.7	646.3	1.092	0.215	0.02070	1.423	78.7	67.7
42	3.672	4.539	0.01890	320.0	576.1	0.973	0.214	0.02130	1.431	77.8	67.0
44	4.793	4.047	0.01830	285.3	511.5	0.864	0.213	0.02190	1.441	77.1	66.4
46	3.116	3.594	0.01780	253.4	452.3	0.764	0.213	0.02270	1.454	76.5	65.8
48	3.327	3.177	0.01720	224.0	398.0	0.672	0.212	0.02350	1.468	75.9	65.3
50	2.323	2.796	0.01670	197.1	348.3	0.588	0.210	0.02430	1.483	75.3	64.8
52	2.677	2.447	0.01610	172.5	303.1	0.512	0.209	0.02530	1.499	74.6	64.2
54	1.836	2.129	0.01560	150.1	262.1	0.443	0.208	0.02630	1.515	73.9	63.6
56	1.784	1.842	0.01500	129.8	225.1	0.380	0.206	0.02730	1.530	73.1	62.9
58	1.362	1.583	0.01450	111.6	191.8	0.324	0.205	0.02850	1.545	72.2	62.1
60	1.323	1.35	0.01390	95.2	162.2	0.274	0.203	0.02960	1.557	71.1	61.2
62	1.086	1.144	0.01330	80.6	136.0	0.230	0.201	0.03090	1.567	69.8	60.1
64	1.073	0.961	0.01280	67.8	112.9	0.191	0.199	0.03210	1.575	68.3	58.8
66	0.832	0.801	0.01220	56.5	92.9	0.157	0.196	0.03340	1.579	66.6	57.3
68	0.677	0.662	0.01170	46.7	75.5	0.128	0.193	0.03480	1.579	64.6	55.6
70	0.629	0.542	0.01110	38.2	60.7	0.103	0.190	0.03610	1.574	62.4	53.7
72	0.561	0.44	0.01060	31.0	48.2	0.081	0.184	0.03740	1.565	59.9	51.6
74	0.485	0.353	0.01010	24.9	37.7	0.064	0.181	0.03870	1.550	57.1	49.1
76	0.305	0.28	0.00960	19.8	29.1	0.049	0.175	0.04000	1.528	54.0	46.5
78	0.19	0.22	0.00910	15.5	22.0	0.037	0.168	0.04110	1.499	50.6	43.6
80	0.167	0.171	0.00860	12.1	16.4	0.028	0.164	0.04200	1.462	46.9	40.4
82	0.116	0.132	0.00820	9.3	11.9	0.020	0.152	0.04260	1.414	42.8	36.9
84	0.084	0.1	0.00770	7.0	8.5	0.014	0.140	0.04290	1.355	38.5	33.2

Table 10. Summary of Thermocouple/Pin Data for Surface CP54

S#	Lqd	#C	τ sec	στ sec	θ sec	σθ sec	Tw °C	Tr °C	σTr °C	Tq °C	σTq °C	Tp °C	σTp °C	ΔTp °C	ΔTc °C
1a	H2O	16	0.150	0.054	0.440	0.220	495	430	23	420	15	425	20	70	10
1b	H2O	11	0.120	0.054	0.360	0.200	485	795	7	389	7	392	7	93	6
1c	H2O	7	0.096	0.072	0.310	0.130	475	381	2	376	3	378	4	97	5
1d	H2O	8	0.100	0.033	0.420	0.130	465	362	6	357	7	359	7	106	5
1e	H2O	11	0.087	0.036	0.410	0.150	450	337	8	330	12	333	11	117	7
1f	H2O	13	0.086	0.028	0.360	0.170	425	290	15	281	17	286	16	139	9
17a	H2O	7	0.240	0.096	0.430	0.300	430	362	37	341	29	358	33	72	21
17b	H2O	6	0.083	0.026	0.590	0.210	420	315	9	306	9	310	10	110	9
17c	H2O	5	0.160	0.120	0.380	0.210	410	284	16	369	13	277	16	133	15
17d	H2O	3	0.080	0.012	0.400	0.320	400	258	8	248	8	253	8	147	10
11a	EA	17	0.250	0.120	0.550	0.230	520	474	12	469	7	472	7	48	5
11b	EA	17	0.160	0.052	0.580	0.220	515	459	7	457	6	458	7	57	2
11c	EA	19	0.200	0.120	0.550	0.200	510	451	3	449	3	450	3	60	2
24a	EA	11	0.210	0.100	0.840	0.210	405	381	7	378	3	380	5	25	3
24b	EA	11	0.170	0.045	0.500	0.190	405	374	1	373	1	374	1	31	1
24c	EA	11	0.210	0.130	0.520	0.120	405	375	1	373	2	374	2	31	2
24d	EA	11	0.220	0.087	0.560	0.210	400	372	3	370	2	371	2	29	2
28a	EA	21	0.210	0.100	0.540	0.220	385	358	7	355	5	357	6	28	3
28b	EA	26	0.160	0.060	0.580	0.150	380	348	2	347	3	348	2	32	1
28c	EA	14	0.220	0.082	0.560	0.220	375	340	4	338	4	339	4	36	2
28d	EA	11	0.210	0.054	0.530	0.093	370	339	1	337	1	338	1	32	2
36a	EA	10	0.240	0.190	0.600	0.270	325	304	10	296	16	392	10	23	5
36b	EA	10	0.300	0.200	0.430	0.220	320	296	2	294	3	295	2	25	2
12a	IP	24	0.220	0.100	0.520	0.260	515	461	10	456	3	459	8	56	5
12b	IP	16	0.210	0.110	0.530	0.210	510	451	4	447	3	494	4	61	4
12c	IP	8	0.210	0.091	0.420	0.210	505	444	3	442	2	443	3	62	2
12d	IP	6	0.300	0.210	0.460	0.170	500	439	2	436	2	438	3	62	3
12e	IP	8	0.230	0.100	0.460	0.250	495	438	2	435	2	436	3	59	3
26a	IP	26	0.160	0.120	0.440	0.260	405	380	8	377	6	378	7	27	2
25b	IP	26	0.170	0.060	0.500	0.190	400	369	2	368	2	368	3	32	2
25c	IP	11	0.220	0.120	0.440	0.230	395	365	3	363	2	364	3	31	2
25d	IP	15	0.180	0.895	0.340	0.240	390	363	2	361	1	362	7	38	2
25e	IP	5	0.160	0.025	0.510	0.450	385	361	2	359	2	360	3	25	2
29a	IP	26	0.190	0.071	0.490	0.320	380	348	7	346	5	347	6	33	2
29b	IP	26	0.150	0.071	0.500	0.210	370	339	3	338	3	339	3	31	1
29c	IP	26	0.180	0.100	0.470	0.250	360	332	4	331	4	332	4	28	2
37	IP	15	0.290	0.140	0.520	0.260	325	300	6	297	3	299	5	26	4
14a	EC	13	0.170	0.120	0.550	0.270	505	486	11	483	11	486	11	20	3
14b	EC	4	0.110	0.035	0.260	0.160	506	470	2	469	2	469	2	36	1
14c	EC	15	0.160	0.059	0.530	0.290	500	463	2	462	2	463	2	37	2
14d	EC	17	0.110	0.052	0.440	0.200	495	463	1	462	1	462	1	33	1
27a	EC	11	0.220	0.220	0.530	0.190	405	392	6	389	6	391	6	14	3
27b	EC	14	0.130	0.045	0.540	0.260	405	379	3	378	3	378	3	27	1
27c	EC	10	0.140	0.094	0.520	0.220	405	374	1	373	1	373	1	32	1
27d	EC	12	0.120	0.062	0.470	0.170	400	377	3	375	1	376	2	24	2
27e	CC	6	0.170	0.042	0.500	0.270	400	375	2	373	1	374	2	26	2
30a	EC	22	0.200	0.110	0.540	0.260	385	365	2	364	7	365	2	20	2
30b	EC	16	0.250	0.086	0.490	0.210	380	352	4	351	3	352	4	28	2
30c	EC	14	0.160	0.035	0.440	0.190	380	353	1	352	1	352	1	28	1
30d	EC	11	0.170	0.055	0.390	0.190	375	350	2	349	1	349	2	28	1
38a	EC	4	0.430	0.180	0.620	0.180	335	314	10	305	7	309	9	28	9
38b	EC	11	0.230	0.091	0.500	0.200	330	303	3	301	1	302	2	28	2
38c	EC	16	0.160	0.062	0.590	0.240	330	302	1	300	1	301	1	29	1
38d	EC	6	0.190	0.092	0.440	0.230	325	303	3	300	2	301	3	24	3
39a	EC	11	0.160	0.045	0.650	0.350	320	299	7	297	4	298	5	22	3
39b	EC	28	0.170	0.062	0.430	0.240	310	291	2	290	2	290	2	20	1

S#=strip number, #C=number of contacts, τ=contact period, σ=standard deviation
θ=contact duration/period, Tq=quench temperature, ΔTp=pin temperature depression
Tr=recovery temperature, ΔTc=temperature change during contact
EA=Ethanol, IP=Isopropanol, EC=Ethylene-Chloride

Table 11. Summary of Thermocouple/Pin Data for Surface SHP2612

S#	Lqd	#C	τ sec	στ sec	θ sec	σθ sec	Tw °C	Tr °C	σTr °C	Tq °C	σTq °C	Tp °C	σTp °C	ΔTp °C	ΔTc °C
46a	WA	8	0.310	0.130	0.41	0.26	525	470	40	444	46	460	45	65	31
46b	WA	8	0.110	0.094	0.56	0.33	475	344	32	310	34	327	37	148	23
46c	WA	7	0.058	0.026	0.77	0.20	425	296	66	261	65	279	65	148	35
46d	WA	4	0.085	0.060	0.67	0.31	420	274	65	205	39	239	62	181	70
47a	WA	9	0.150	0.084	0.54	0.35	465	408	24	385	24	397	26	68	23
47b	WA	8	0.082	0.038	0.53	0.21	455	277	75	232	64	254	71	201	44
48	WA	7	0.082	0.040	0.62	0.35	395	331	53	293	75	312	66	83	39
49a	WA	8	0.140	0.087	0.28	0.15	340	281	46	238	62	259	57	81	43
49b	WA	11	0.082	0.068	0.53	0.26	335	187	38	158	33	172	38	163	29
51a	EA	30	0.140	0.058	0.51	0.23	475	461	6	459	5	460	6	15	3
51b	EA	30	0.085	0.042	0.42	0.24	465	451	3	450	2	450	3	15	1
51c	EA	30	0.092	0.045	0.41	0.26	455	446	2	445	2	446	2	9	2
51d	EA	30	0.120	0.055	0.46	0.22	450	440	4	438	3	439	4	11	2
51e	EA	30	0.110	0.057	0.47	0.20	445	434	2	432	2	433	2	12	2
51f	EA	38	0.140	0.096	0.50	0.22	440	430	4	427	4	428	4	12	3
52a	EA	30	0.075	0.028	0.45	0.21	415	404	5	402	4	403	5	12	2
52b	EA	30	0.088	0.031	0.48	0.26	410	394	2	303	2	393	2	17	1
52c	EA	30	0.110	0.043	0.48	0.31	405	390	2	388	2	389	2	16	1
52d	EA	30	0.092	0.027	0.49	0.21	400	384	2	382	2	383	2	17	1
52e	EA	30	0.099	0.051	0.46	0.23	395	381	3	379	3	380	3	15	2
52f	EA	30	0.110	0.042	0.49	0.25	390	375	2	374	2	375	2	15	2
53a	EA	20	0.120	0.050	0.50	0.15	350	331	2	329	2	330	3	20	2
53b	EA	20	0.100	0.055	0.57	0.23	345	326	1	324	1	325	2	20	2
54a	EA	30	0.120	0.078	0.54	0.28	280	260	9	257	8	258	9	22	3
54b	EA	29	0.100	0.035	0.44	0.22	270	248	3	246	3	247	3	23	2
54c	EA	30	0.110	0.038	0.52	0.17	265	236	3	234	3	235	3	30	2
54d	EA	30	0.110	0.035	0.55	0.26	260	233	3	230	3	232	3	28	2
55	EA	12	0.120	0.057	0.61	0.18	225	211	8	206	6	209	7	16	5
56	EA	20	0.097	0.038	0.59	0.26	225	201	6	198	5	200	6	25	3
59a	IP	30	0.120	0.043	0.57	0.25	495	477	7	475	6	476	7	19	2
59b	IP	30	0.094	0.071	0.54	0.31	485	469	3	467	3	468	3	17	2
59c	IP	30	0.100	0.046	0.47	0.22	480	463	3	461	3	462	3	18	2
59d	IP	27	0.110	0.063	0.58	0.23	475	454	4	452	3	453	4	22	2
60a	IP	30	0.130	0.066	0.51	0.20	410	394	7	392	6	393	3	17	2
60b	IP	30	0.092	0.039	0.57	0.19	400	378	3	377	3	378	3	22	1
60c	IP	30	0.120	0.057	0.56	0.26	395	376	2	374	2	375	2	20	2
60d	IP	30	0.110	0.037	0.53	0.20	390	373	3	372	3	373	3	17	2
60e	IP	18	0.160	0.062	0.69	0.17	385	363	3	361	3	362	3	23	2
62a	IP	30	0.150	0.094	0.60	0.23	365	348	9	345	7	347	8	18	2
62b	IP	30	0.120	0.054	0.54	0.19	355	337	3	335	3	336	3	19	2
62c	IP	39	0.150	0.064	0.52	0.27	350	329	3	326	3	327	4	23	2
64a	IP	30	0.140	0.069	0.65	0.47	250	226	6	224	5	225	5	25	2
64b	IP	31	0.095	0.041	0.51	0.22	245	217	2	215	2	216	2	29	1
64c	IP	30	0.091	0.035	0.52	0.24	240	212	3	211	3	211	4	29	2
54d	IP	30	0.100	0.048	0.52	0.25	235	204	3	202	3	203	3	32	2
64e	IP	30	0.130	0.072	0.46	0.38	235	205	2	203	2	204	2	31	2
64f	IP	23	0.097	0.047	0.53	0.21	230	203	2	201	2	202	2	20	2
65a	IP	16	0.130	0.051	0.62	0.22	210	190	8	187	7	189	8	21	3
65b	IP	17	0.100	0.038	0.53	0.18	210	173	5	170	5	171	5	39	3
66	IP	16	0.190	0.120	0.59	0.19	205	192	7	187	10	289	9	18	4
68a	EC	26	0.110	0.053	0.55	0.25	475	467	6	455	5	456	0	19	2
68b	EC	12	0.120	0.048	0.54	0.28	465	454	5	452	5	453	5	12	2
69a	EC	30	0.120	0.053	0.57	0.26	455	442	7	440	6	441	7	14	2
69b	EC	31	0.099	0.031	0.60	0.10	445	431	2	430	2	431	2	14	1
69c	EC	33	0.130	0.060	0.54	0.22	440	426	2	424	2	426	2	16	2
71a	EC	20	0.080	0.054	0.48	0.34	360	368	4	356	3	367	3	3	1
71b	EC	30	0.110	0.050	0.66	0.10	366	360	2	349	6	349	0	6	1
71c	EC	30	0.110	0.045	0.54	0.25	355	347	1	346	1	340	1	9	1
71d	EC	30	0.100	0.034	0.59	0.24	350	342	1	341	1	342	1	8	1
71e	EC	27	0.150	0.059	0.63	0.27	345	336	2	335	2	336	2	9	1
72a	EC	30	0.130	0.057	0.66	0.26	275	264	6	263	6	264	6	11	1
72b	EC	23	0.140	0.062	0.52	0.17	270	255	2	254	1	254	2	16	1
73a	EC	30	0.110	0.059	0.58	0.22	255	238	4	237	4	237	4	10	1
73b	EC	30	0.093	0.035	0.57	0.21	250	231	2	230	2	231	2	19	1
73c	EC	31	0.110	0.030	0.56	0.22	250	226	2	225	2	226	2	24	1
73d	EC	31	0.120	0.053	0.62	0.26	245	225	2	224	2	225	2	20	1
74	EC	28	0.140	0.072	0.56	0.29	215	197	13	193	13	196	13	20	3

θ=contact duration/period, Tq=quench temperature, ΔTp=pin temperature depression
Tr=recovery temperature, ΔTc=temperature change during contact
EA=Ethanol, IP=Isopropanol, EC=Ethylene-Chloride

Table 12. Sample Output of Program 2-D PINT

time	T1		T2		T3		T4		T5	T6	T7	T8		T9	T10	T11	T12		T13	T14	T15	T16		T17	T18	T19	T20		Tmx	Hpin	Havg
sec	°C		°C		°C		°C		°C	°C	°C	°C		°C	°C	°C	°C		°C	°C	°C	°C		°C	°C	°C	°C		°C	W/cm²/°C	W/cm²/°C
0.00	620		620		620		620		620	620	620	620		620	620	620	620		620	620	620	620		620	620	620	620		620	N/A	N/A
0.01	533	C	536	C	548	C	522	C	614	612	583	558	C	620	620	600	602	F	620	620	617	615	F	620	620	619	619	F	620	2.47417	0.67060
0.02	508	C	513	C	530	C	514	C	603	598	561	544	C	619	617	591	586	F	620	619	607	606	F	620	620	614	615	F	620	1.87033	0.43013
0.03	500	C	505	C	522	C	511	C	592	584	549	536	C	617	614	578	574	F	619	616	597	596	F	620	618	607	608	F	620	1.66964	0.36917
0.04	496	C	501	C	517	C	508	C	581	572	541	531	C	616	609	568	566	F	618	613	587	586	F	619	616	599	600	F	619	1.38091	0.32595
0.05	518	F	522	F	534	F	534	F	573	564	545	544	F	611	604	563	562	F	617	609	580	579	F	618	613	591	592	F	618	1.11763	0.26666
0.06	532	F	535	F	543	F	544	F	568	561	550	550	F	608	599	563	562	F	615	604	575	574	F	617	609	584	585	F	617	0.94201	0.22551
0.07	542	F	544	F	549	F	550	F	566	560	554	554	F	604	595	563	562	F	612	600	572	571	F	615	606	579	580	F	615	0.91667	0.10607
0.08	548	F	549	F	553	F	554	F	565	560	557	557	F	600	591	564	563	F	609	596	570	570	F	613	602	576	576	F	613	0.72268	0.17543
0.09	552	F	553	F	556	F	556	F	564	560	559	558	F	597	588	564	563	F	606	593	569	568	F	610	598	573	574	F	610	0.64959	0.15876
0.10	552	C	553	C	555	C	553	C	564	561	560	557	C	594	585	564	563	F	603	590	568	567	F	607	594	572	572	F	607	0.62614	0.15342
0.11	476	C	479	C	492	C	470	C	558	554	526	503	C	590	582	552	546	F	600	587	564	563	F	604	591	570	570	F	604	0.76550	0.10519
0.12	457	C	462	C	479	C	466	C	549	542	507	493	C	587	578	537	532	F	597	583	555	554	F	602	588	565	566	F	602	0.79453	0.19182
0.13	452	C	457	C	473	C	464	C	539	530	498	487	C	583	573	526	522	F	593	579	545	544	F	598	584	557	559	F	598	0.79919	0.19288
0.14	451	C	455	C	471	C	463	C	530	520	492	483	C	579	567	516	515	F	590	574	537	536	F	595	580	550	551	F	595	0.79370	0.19163
0.15	472	F	475	F	487	F	487	F	523	514	497	496	F	574	561	514	513	F	586	568	530	530	F	592	576	542	544	F	592	0.74458	0.18042
0.16	486	F	488	F	496	F	497	F	519	511	503	502	F	569	556	514	514	F	581	563	526	526	F	588	571	536	538	F	588	0.70163	0.17063
0.17	495	F	496	F	502	F	502	F	518	511	507	506	F	564	551	515	515	F	577	558	524	524	F	584	566	532	534	F	584	0.66375	0.16199
0.18	501	F	502	F	506	F	506	F	517	512	510	509	F	559	547	516	515	F	573	554	523	522	F	580	561	530	531	F	580	0.63008	0.15432
0.19	505	F	506	F	509	F	509	F	517	513	512	511	F	556	543	517	516	F	568	550	522	522	F	576	557	527	529	F	576	0.99970	0.14746
0.20	506	C	506	C	509	C	507	C	517	514	513	511	C	551	540	517	517	F	564	546	522	521	F	571	553	527	527	F	571	0.58850	0.14407
0.21	436	C	439	C	451	C	432	C	512	508	482	462	C	548	537	507	501	F	560	543	519	517	F	567	549	525	526	F	567	0.65265	0.15946
0.22	420	C	424	C	440	C	428	C	503	497	465	453	C	544	533	493	489	F	556	539	510	509	F	563	546	521	522	F	563	0.66837	0.16304
0.23	416	C	420	C	435	C	427	C	495	486	457	448	C	540	528	483	480	F	552	535	502	501	F	559	542	514	516	F	559	0.67266	0.16402
0.24	415	C	419	C	433	C	426	C	487	476	453	445	C	535	523	476	473	F	548	530	494	493	F	555	538	507	509	F	555	0.67166	0.16379
0.25	435	F	438	F	448	F	449	F	481	472	457	457	F	530	517	473	472	F	544	525	488	488	F	551	533	501	503	F	551	0.64685	0.15814
0.26	448	F	450	F	457	F	458	F	478	470	463	463	F	525	512	474	473	F	539	520	485	485	F	547	528	496	498	F	547	0.62397	0.15293
0.27	456	F	458	F	463	F	463	F	476	470	467	467	F	521	508	475	474	F	535	515	484	483	F	543	524	492	494	F	543	0.60278	0.14811
0.28	462	F	463	F	467	F	467	F	476	471	470	470	F	516	504	476	476	F	530	511	483	483	F	539	519	490	492	F	539	0.50312	0.14363
0.29	466	F	467	F	470	F	470	F	476	472	472	472	F	512	501	477	477	F	526	508	483	482	F	534	515	489	490	F	534	0.56482	0.13947
0.30	468	F	469	F	472	F	472	F	476	473	474	473	F	509	498	476	477	F	522	504	483	482	F	530	510	488	490	F	530	0.64775	0.13559
0.31	405	C	408	C	419	C	402	C	472	468	446	429	C	505	493	469	466	F	516	500	480	479	F	526	505	487	489	F	526	0.58690	0.14449
0.32	390	C	394	C	408	C	398	C	465	459	431	420	C	502	490	456	462	F	514	497	473	472	F	522	503	483	485	F	522	0.59687	0.14676
0.33	387	C	391	C	404	C	397	C	457	450	424	416	C	498	483	446	445	F	510	494	465	464	F	518	500	477	480	F	518	0.59988	0.14744
0.34	386	C	390	C	402	C	396	C	450	442	420	413	C	494	477	441	439	F	507	490	459	458	F	515	496	471	474	F	515	0.59955	0.14737
0.35	404	F	407	F	417	F	417	F	445	437	425	424	F	490	470	439	438	F	503	486	455	453	F	511	492	466	468	F	511	0.58376	0.14378
0.36	416	F	418	F	425	F	425	F	442	436	430	430	F	485	466	440	440	F	499	481	451	451	F	507	490	461	464	F	507	0.56886	0.14039
0.37	424	F	426	F	430	F	431	F	441	436	434	434	F	481	463	441	441	F	495	477	450	448	F	503	486	457	461	F	503	0.65476	0.13710
0.38	429	F	430	F	434	F	434	F	441	437	437	437	F	477	461	443	442	F	491	474	450	449	F	499	482	455	459	F	499	0.64144	0.13415
0.39	433	F	434	F	437	F	437	F	441	438	439	439	F	474	464	444	444	F	487	471	453	450	F	495	479	456	460	F	495	0.62879	0.13120
0.40	434	C	435	C	437	C	435	C	442	439	441	439	C	471	462	445	445	F	483	468	450	451	F	492	476	457	460	F	492	0.60325	0.13002
0.41	375	C	378	C	389	C	373	C	438	435	414	398	C	468	459	430	431	F	480	466	447	447	F	488	473	456	458	F	488	0.54926	0.13593
0.42	362	C	366	C	380	C	371	C	431	426	401	391	C	465	455	424	421	F	477	463	440	440	F	485	470	450	454	F	485	0.65673	0.13740
0.43	360	C	364	C	377	C	370	C	424	417	396	387	C	461	451	417	414	F	473	461	434	433	F	481	467	446	449	F	481	0.66761	0.13701
0.44	360	C	364	C	375	C	370	C	418	411	391	385	C	458	448	411	409	F	470	458	428	427	F	476	464	440	444	F	476	0.65708	0.13768
0.45	371	F	380	F	389	F	389	F	413	407	396	396	F	454	444	410	409	F	470	457	425	423	F	475	460	436	438	F	475	0.64660	0.13510

pin height=0.1270 cm; pin diameter=0.1650 cm; pin spacing=0.3450; E0=0.3050
contact period=0.1 sec; contact duration=0.04 sec; time step=0.001 sec; output printed every 10 time steps
buld surface temperature=620°C; surface material=steel; liquid=water
Tchf=123.8°C; Qchf=142.35 [W/cm²/°C]; TMFBN=288.4°C; QMFB=3.55 [W/cm²/°C]

Table 13. Experimental and Calculated Contact Temperature

strips	surface	lqd	To °C	Te °C	Tc °C
1	CP54	H2O	498	453	453
3	CP54	H2O	497	460	452
4	CP54	H2O	502	460	456
5	CP54	H2O	487	439	443
6	CP54	H2O	495	432	450
17	CP54	H2O	440	410	401
18	CP54	H2O	445	407	405
19	CP54	H2O	433	379	395
20	CP54	H2O	432	378	394
46	CP54	H2O	505	420	445
47	SHP2612	H2O	460	420	430
47	SHP2612	H2O	405	360	358
48	SHP2612	H2O	395	353	350
49	SHP2612	H2O	330	280	292

To=initial temperature
Te=experimental contact temperature
Tc=calculated contact temperature

Table 14. Sample Output of Program SMOOTH

λ	Cpg	κg	ρf	ρg	μg	κs	ε	Tsat	Hfg	ΔA		
0.219	2.03	2.76E-04	0.9583	0.0006	0.00012	0.00E+00	0.52	100	2257	5.6%		
time	A	As	-d(ln(As))/dt	A*	V*	V	L	Hexp	Hx/Hs	Nuv	H	B
sec	cm²	cm²	1/sec	-	-	cm³	cm	W/cm³/C	-	-	-	-
0	7.240	6.616	0.0182	138.1	240.1	2.518	0.381	0.0120	0.665	59.4	21.4	0.430
10	6.290	6.240	0.0180	130.2	225.8	2.368	0.379	0.0132	0.723	63.9	23.0	0.429
20	5.330	5.853	0.0177	122.1	211.0	2.214	0.378	0.0144	0.776	67.9	24.4	0.427
30	5.240	5.460	0.0174	113.9	196.1	2.057	0.377	0.0155	0.826	71.5	25.7	0.425
40	5.120	5.066	0.0170	105.7	181.2	1.901	0.375	0.0166	0.871	74.5	26.8	0.423
50	4.390	4.676	0.0167	97.6	166.5	1.747	0.374	0.0177	0.913	77.1	27.7	0.421
60	4.310	4.295	0.0164	89.6	152.2	1.596	0.372	0.0187	0.950	79.2	28.5	0.419
70	3.900	3.925	0.0160	81.9	138.3	1.450	0.369	0.0197	0.983	80.7	29.0	0.417
80	3.520	3.569	0.0156	74.5	124.9	1.311	0.367	0.0206	1.012	81.9	29.4	0.415
90	3.290	3.230	0.0152	67.4	112.3	1.178	0.365	0.0216	1.037	82.5	29.7	0.413
100	2.960	2.910	0.0149	60.7	100.4	1.053	0.362	0.0224	1.058	82.8	29.8	0.411
110	2.640	2.610	0.0145	54.5	89.3	0.936	0.359	0.0233	1.075	82.6	29.7	0.409
120	2.670	2.330	0.0141	48.6	79.0	0.828	0.355	0.0241	1.088	82.0	29.5	0.406
130	2.200	2.071	0.0137	43.2	69.5	0.729	0.352	0.0249	1.097	81.1	29.2	0.404
140	1.910	1.833	0.0133	38.3	60.8	0.638	0.348	0.0256	1.102	79.8	28.7	0.402
150	1.670	1.616	0.0129	33.7	52.9	0.555	0.343	0.0262	1.104	78.2	28.1	0.400
160	1.400	1.419	0.0125	29.6	45.8	0.481	0.339	0.0269	1.102	76.3	27.4	0.397
170	1.150	1.242	0.0121	25.9	39.5	0.414	0.333	0.0274	1.097	74.1	26.7	0.395
180	1.100	1.082	0.0118	22.6	33.8	0.355	0.328	0.0279	1.089	71.7	25.8	0.393
190	0.657	0.939	0.0114	19.6	28.8	0.302	0.322	0.0284	1.077	69.0	24.8	0.391
200	0.828	0.813	0.0110	17.0	24.4	0.256	0.315	0.0288	1.062	66.2	23.8	0.389
210	0.733	0.701	0.0107	14.6	20.5	0.215	0.307	0.0291	1.044	63.1	22.7	0.387
220	0.642	0.602	0.0103	12.6	17.2	0.180	0.299	0.0293	1.024	59.9	21.6	0.385
230	0.530	0.516	0.0100	10.8	14.3	0.150	0.291	0.0294	1.000	56.6	20.4	0.383
240	0.448	0.441	0.0097	9.2	11.8	0.124	0.281	0.0294	0.973	53.2	19.1	0.381
250	0.397	0.375	0.0094	7.8	9.7	0.102	0.272	0.0293	0.943	49.6	17.9	0.380
260	0.336	0.319	0.0091	6.6	7.9	0.083	0.260	0.0291	0.910	46.0	16.6	0.378
270	0.285	0.270	0.0088	5.6	6.4	0.067	0.248	0.0287	0.874	42.4	15.3	0.376
280	0.203	0.228	0.0085	4.8	5.2	0.054	0.237	0.0283	0.836	38.8	14.0	0.375

Table 15. Sample Output of Program ROUGH

time	A	Asm	A*	V*	V	δ	Hexp	Hx/Hs	Nuv	H	B
sec	cm²	cm²	-	-	cm³	cm	W/cm³/C	-	-	-	-
0	37.628	43.249	3049.0	5783.7	9.771	0.0344	0.0260	2.694	205.1	176.6	1.054
2	36.113	37.952	2675.5	5064.7	8.556	0.0332	0.0249	2.523	188.2	162.0	1.041
4	32.420	33.472	2359.7	4457.5	7.531	0.0320	0.0240	2.369	173.3	149.2	1.030
6	30.898	29.657	2090.8	3941.4	6.659	0.0310	0.0231	2.231	160.1	137.9	1.019
8	27.179	26.388	1860.3	3499.6	5.912	0.0300	0.0223	2.107	148.5	127.9	1.009
10	24.843	23.568	1661.5	3119.1	5.269	0.0291	0.0215	1.996	138.3	119.1	0.999
12	22.852	21.119	1488.9	2789.2	4.712	0.0283	0.0209	1.898	129.3	111.4	0.990
14	18.636	18.980	1338.1	2501.4	4.226	0.0275	0.0204	1.811	121.5	104.6	0.982
16	19.020	17.100	1205.5	2248.8	3.799	0.0267	0.0199	1.735	114.5	98.6	0.974
18	16.395	15.438	1088.4	2025.8	3.422	0.0260	0.0195	1.669	108.5	93.4	0.967
20	14.749	13.960	984.1	1827.8	3.088	0.0253	0.0192	1.612	103.2	88.9	0.960
22	13.158	12.638	891.0	1651.0	2.789	0.0247	0.0190	1.564	98.7	85.0	0.953
24	11.538	11.450	807.2	1492.3	2.521	0.0240	0.0189	1.523	94.8	81.6	0.946
26	10.745	10.378	731.6	1349.3	2.279	0.0234	0.0188	1.490	91.4	78.7	0.940
28	9.103	9.404	663.0	1219.7	2.061	0.0228	0.0188	1.464	88.5	76.2	0.934
30	8.280	8.518	600.5	1101.8	1.861	0.0222	0.0190	1.444	86.1	74.1	0.927
32	8.624	7.707	543.3	994.3	1.680	0.0217	0.0191	1.431	84.0	72.3	0.921
34	6.478	6.964	491.0	895.8	1.513	0.0211	0.0194	1.422	82.3	70.8	0.916
36	6.224	6.281	442.8	805.6	1.361	0.0205	0.0198	1.418	80.8	69.6	0.910
38	5.280	5.653	398.5	722.6	1.221	0.0200	0.0202	1.419	79.7	68.6	0.904
40	4.952	5.073	357.7	646.3	1.092	0.0194	0.0207	1.423	78.7	67.7	0.898
42	3.672	4.539	320.0	576.1	0.973	0.0189	0.0213	1.431	77.8	67.0	0.893
44	4.793	4.047	285.3	511.5	0.864	0.0183	0.0219	1.441	77.1	66.4	0.887
46	3.116	3.594	253.4	452.3	0.764	0.0178	0.0227	1.454	76.5	65.8	0.881
48	3.327	3.177	224.0	398.0	0.672	0.0172	0.0235	1.468	75.9	65.3	0.875
50	2.323	2.796	197.1	348.3	0.588	0.0167	0.0243	1.483	75.3	64.8	0.870
52	2.677	2.447	172.5	303.1	0.512	0.0161	0.0253	1.499	74.6	64.2	0.864
54	1.836	2.129	150.1	262.1	0.443	0.0156	0.0263	1.515	73.9	63.6	0.858
56	1.784	1.842	129.8	225.1	0.380	0.0150	0.0273	1.530	73.1	62.9	0.852
58	1.362	1.583	111.6	191.8	0.324	0.0145	0.0285	1.545	72.2	62.1	0.847
60	1.323	1.350	95.2	162.2	0.274	0.0139	0.0296	1.557	71.1	61.2	0.841
62	1.086	1.144	80.6	136.0	0.230	0.0133	0.0309	1.567	69.8	60.1	0.835
64	1.073	0.961	67.8	112.9	0.191	0.0128	0.0321	1.575	68.3	58.8	0.829
66	0.832	0.801	56.5	92.9	0.157	0.0122	0.0334	1.579	66.6	57.3	0.824
68	0.677	0.662	46.7	75.5	0.128	0.0117	0.0348	1.579	64.6	55.6	0.818
70	0.629	0.542	38.2	60.7	0.103	0.0111	0.0361	1.574	62.4	53.7	0.812
72	0.561	0.440	31.0	48.2	0.081	0.0106	0.0374	1.565	59.9	51.6	0.807
74	0.485	0.353	24.9	37.7	0.064	0.0101	0.0387	1.550	57.1	49.1	0.801
76	0.305	0.280	19.8	29.1	0.049	0.0096	0.0400	1.528	54.0	46.5	0.796
78	0.190	0.220	15.5	22.0	0.037	0.0091	0.0411	1.499	50.6	43.6	0.791
80	0.167	0.171	12.1	16.4	0.028	0.0086	0.0420	1.462	46.9	40.4	0.786
82	0.116	0.132	9.3	11.9	0.020	0.0082	0.0426	1.414	42.8	36.9	0.781
84	0.084	0.100	7.0	8.5	0.014	0.0077	0.0429	1.355	38.5	33.2	0.777

Appendix B. Figures

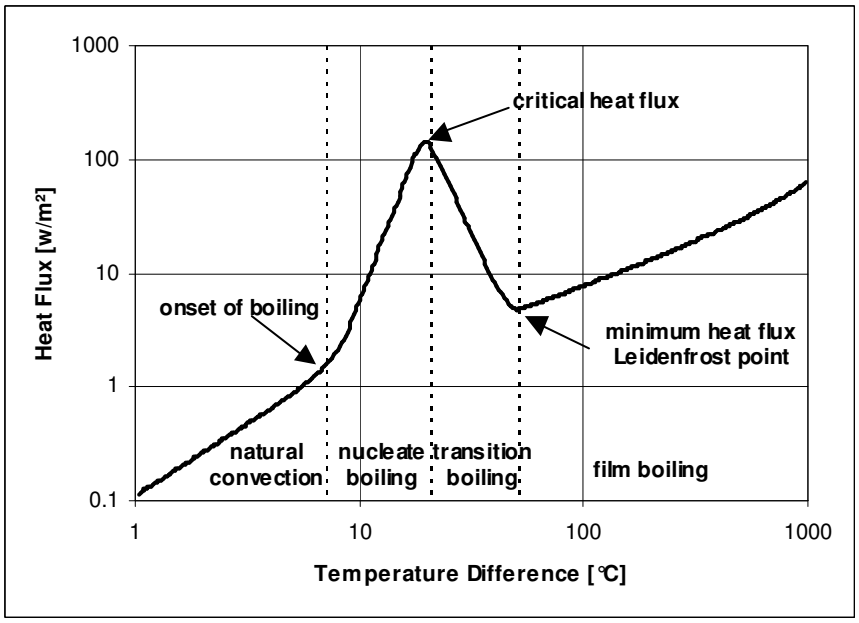

Figure 1. Typical Boiling Curve (Water)

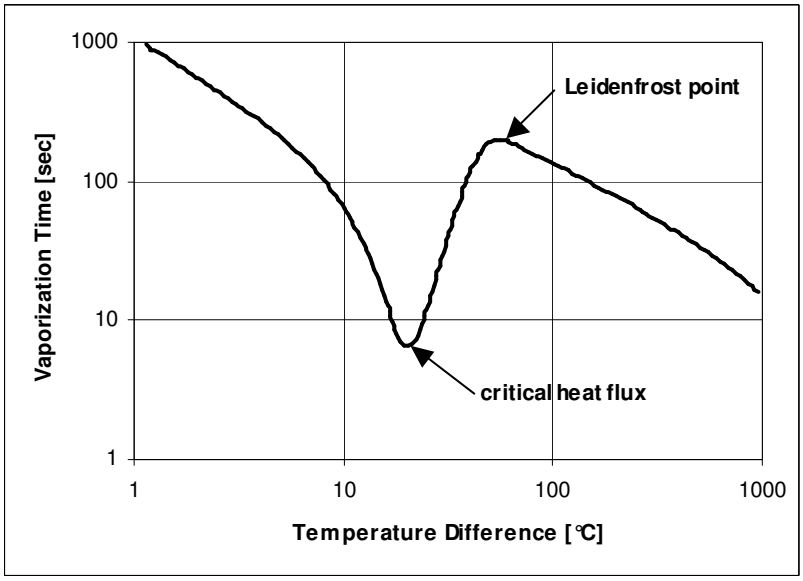

Figure 2. Typical Vaporization Curve (Water)

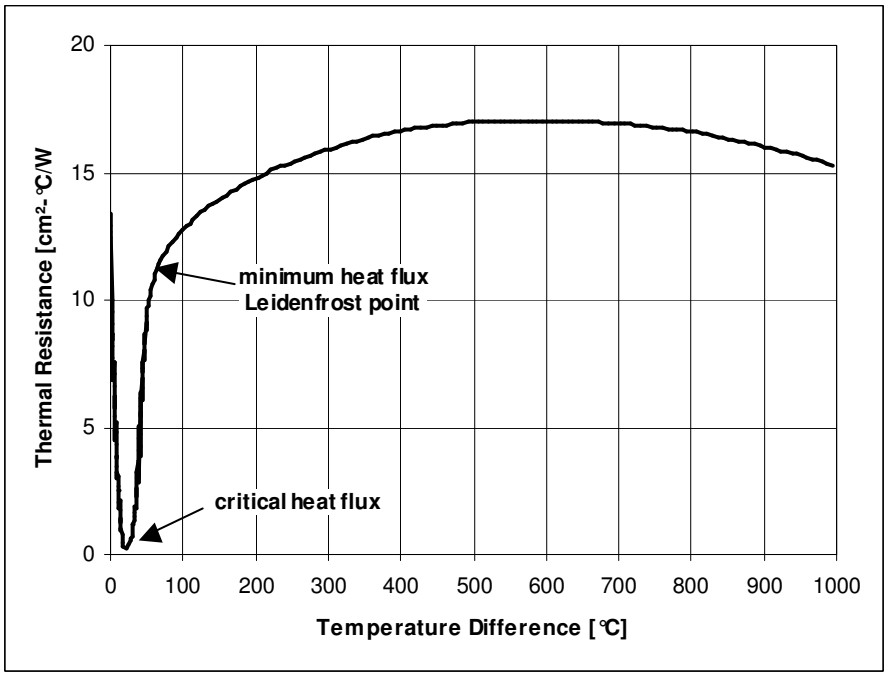

Figure 3. Typical Boiling Specific Thermal Resistance (Water)

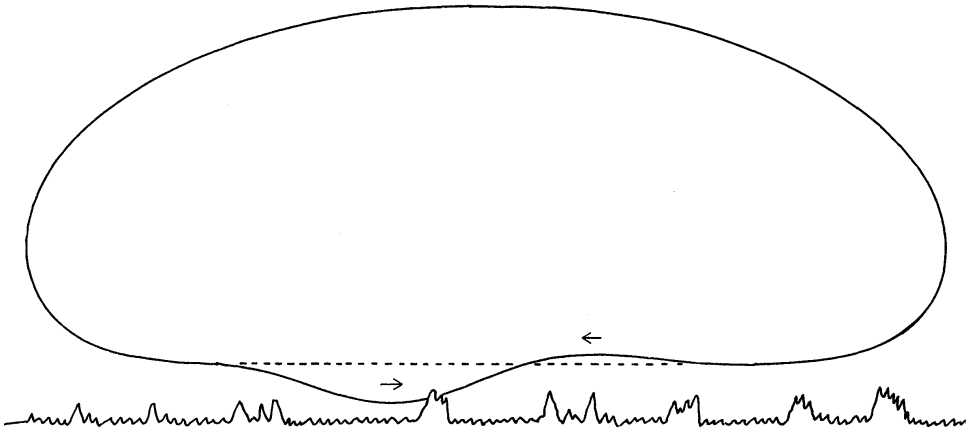

Figure 4. Taylor Instability Propagating Across Droplet Interface

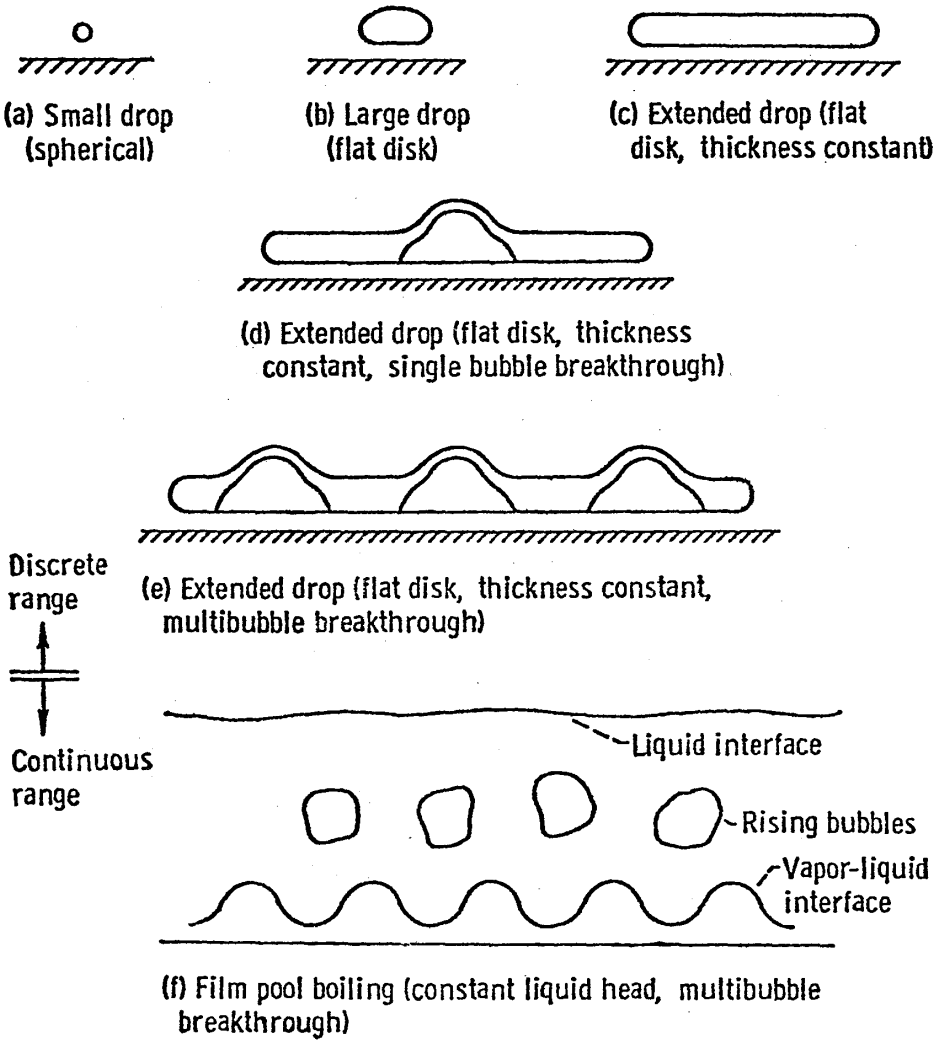

Figure 5. Film Boiling States (after Baumeister [20])

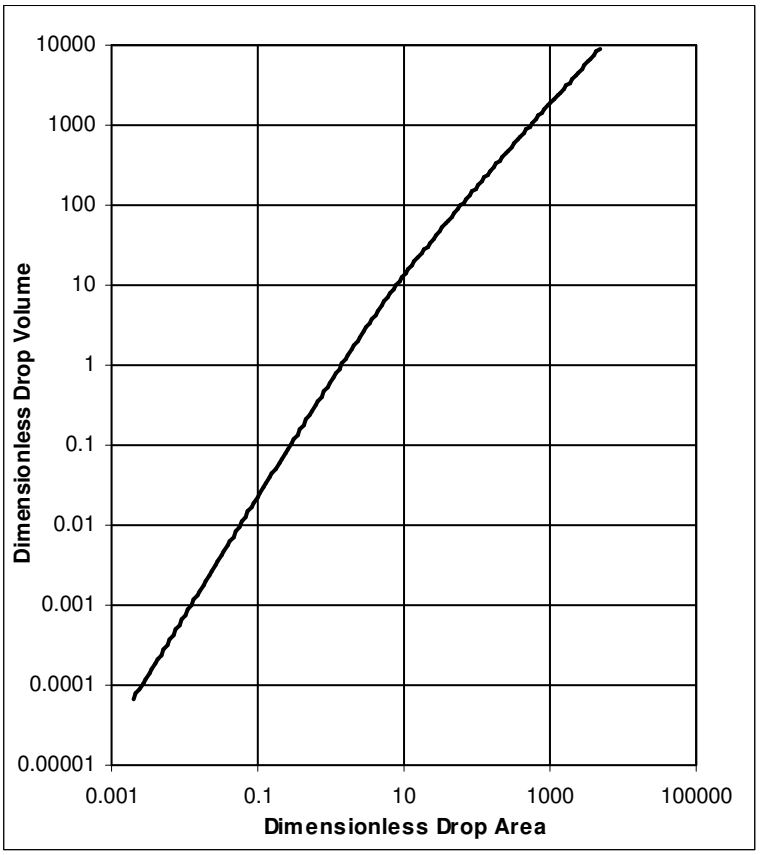

Figure 6. Area/Volume Relationship from Laplace Capillary Equation

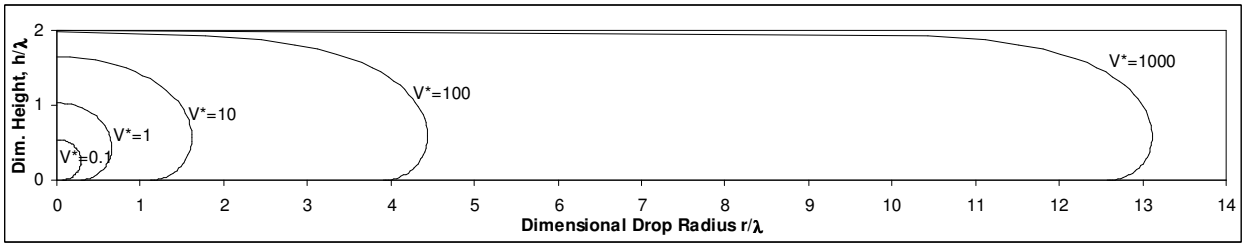

Figure 7. Computed Drop Cross-Sections

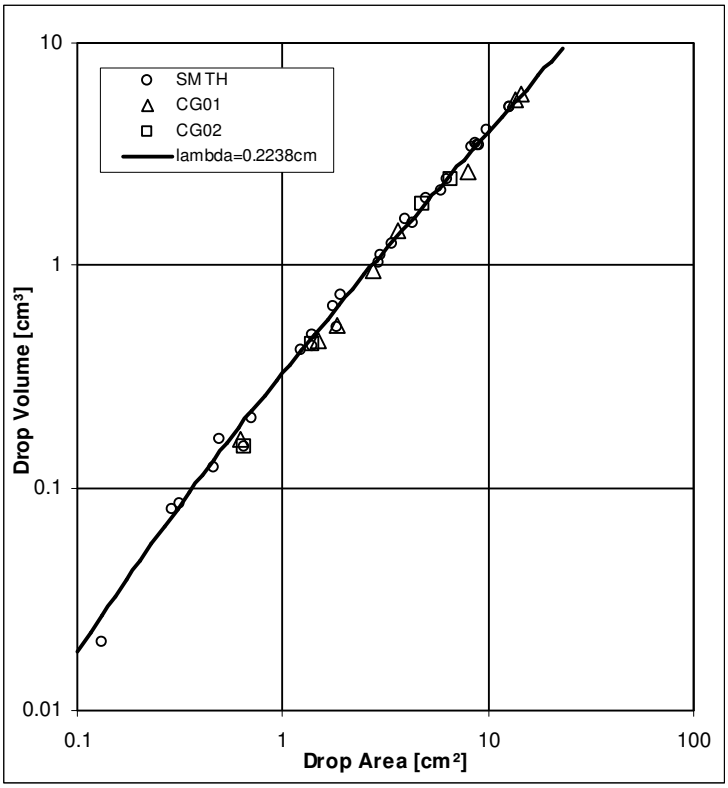

Figure 8. Area/Volume Data for Water

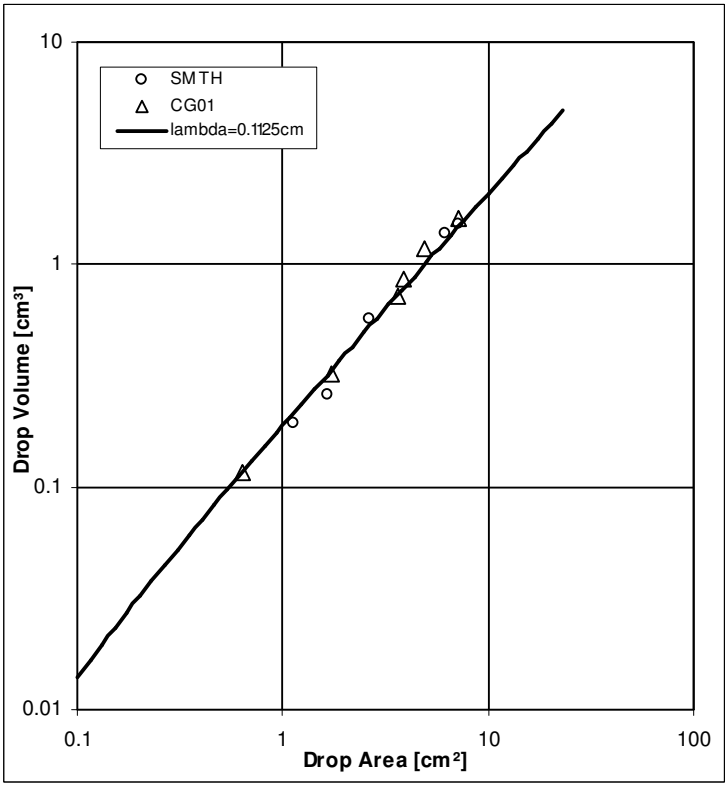

Figure 9. Area/Volume Data for Ethanol

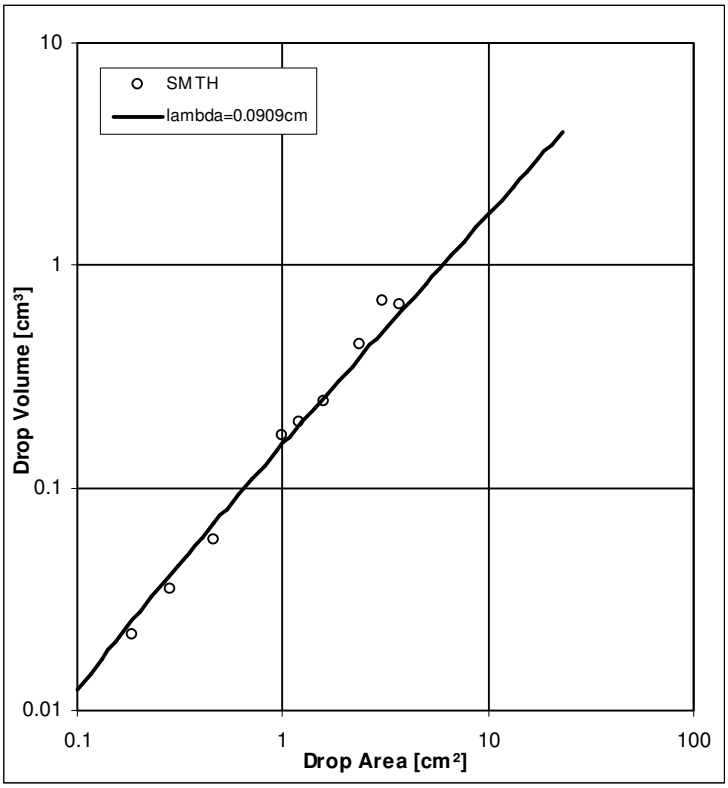

Figure 10. Area/Volume Data for Isopropanol

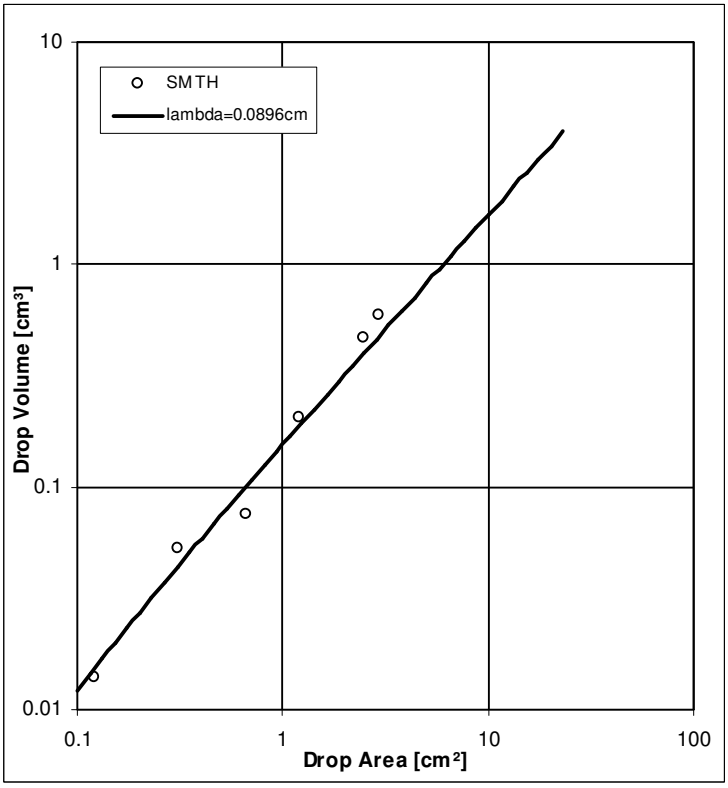

Figure 11. Area/Volume Data for Ethylene-Chloride

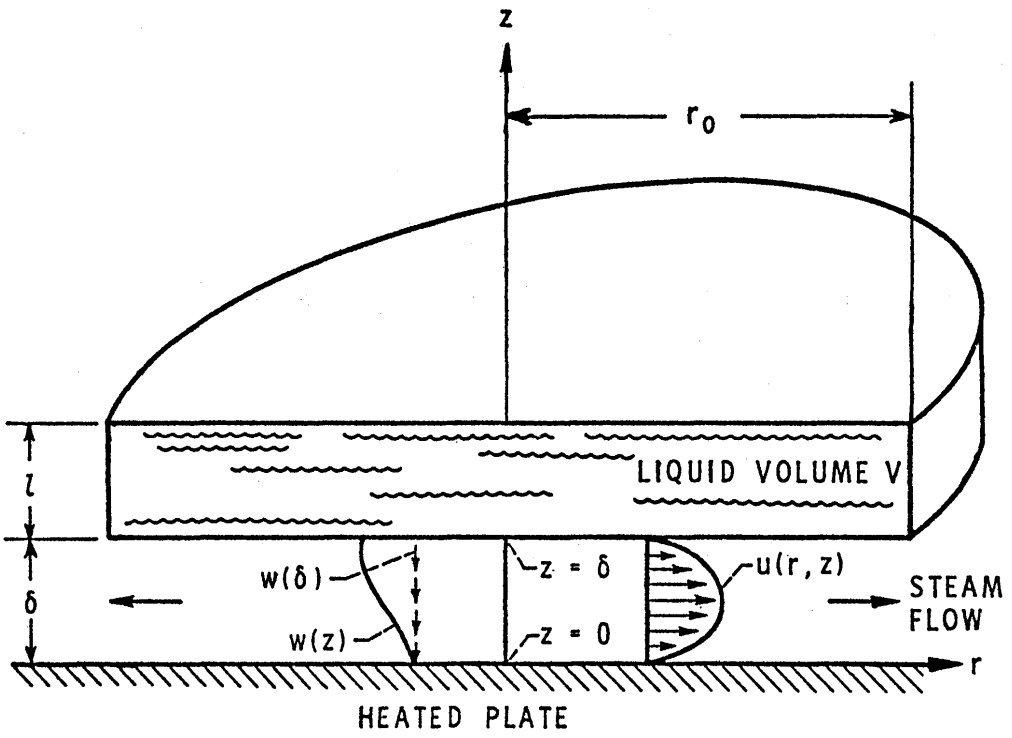

Figure 12. Baumeister's Disk Model (Reference 20)

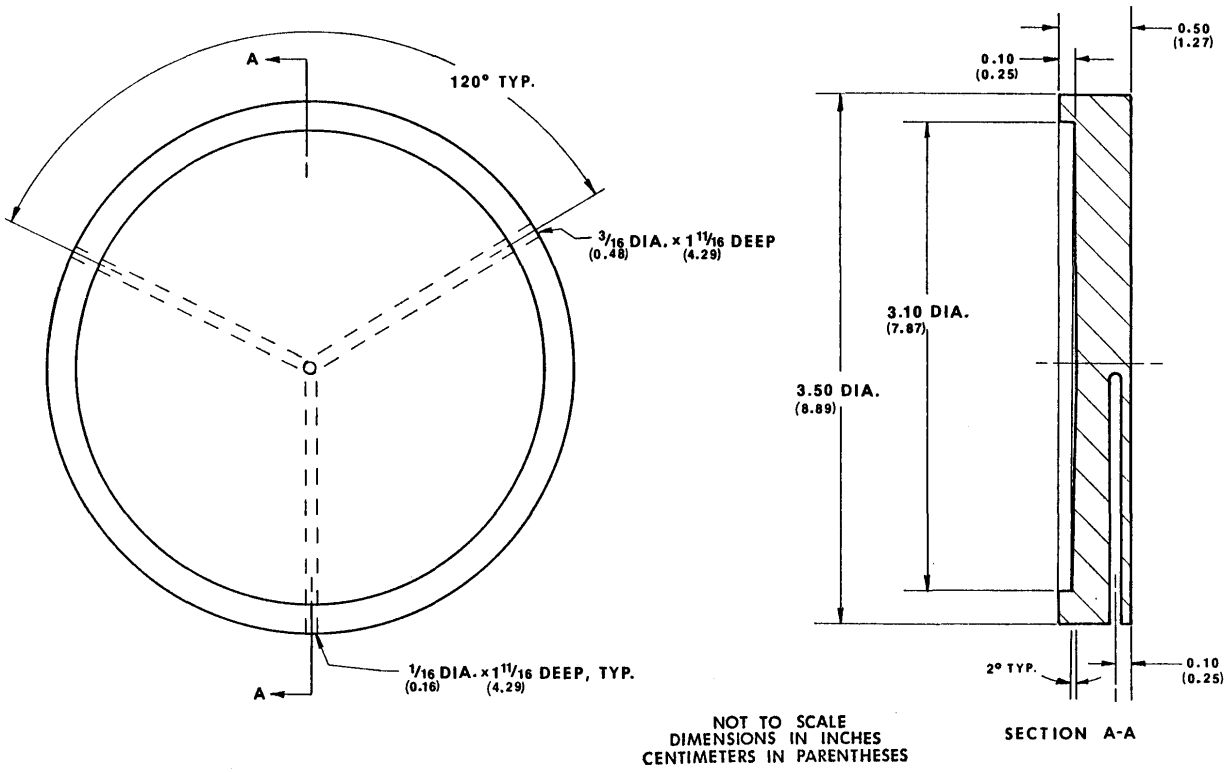

Figure 13. Details of Surface SMTH

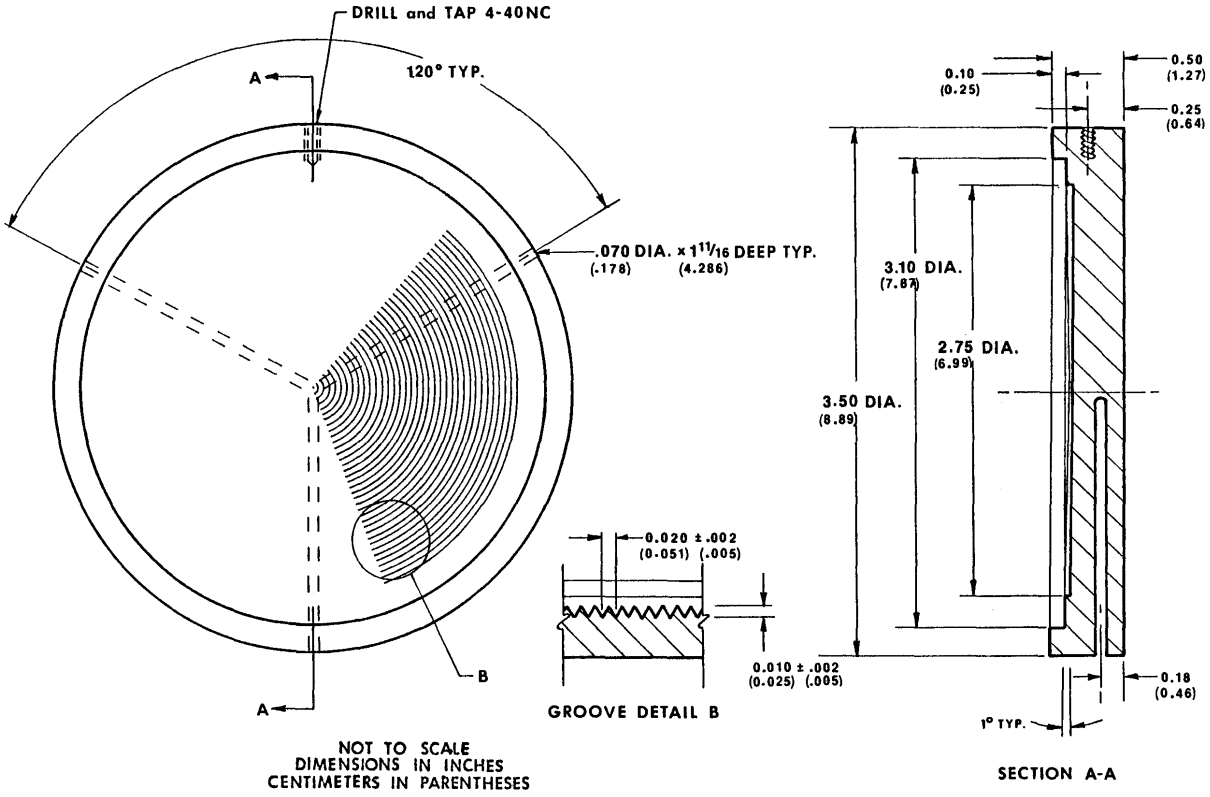

Figure 14. Details of Surface CG01

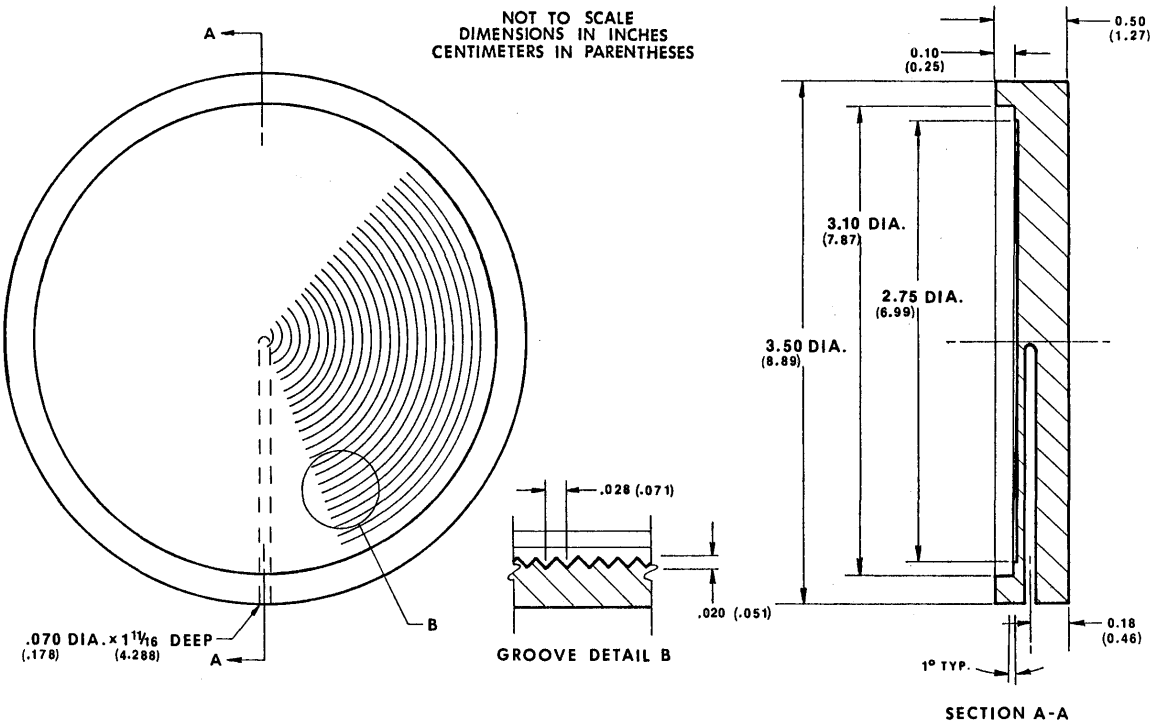

Figure 15. Details of Surface SCG02

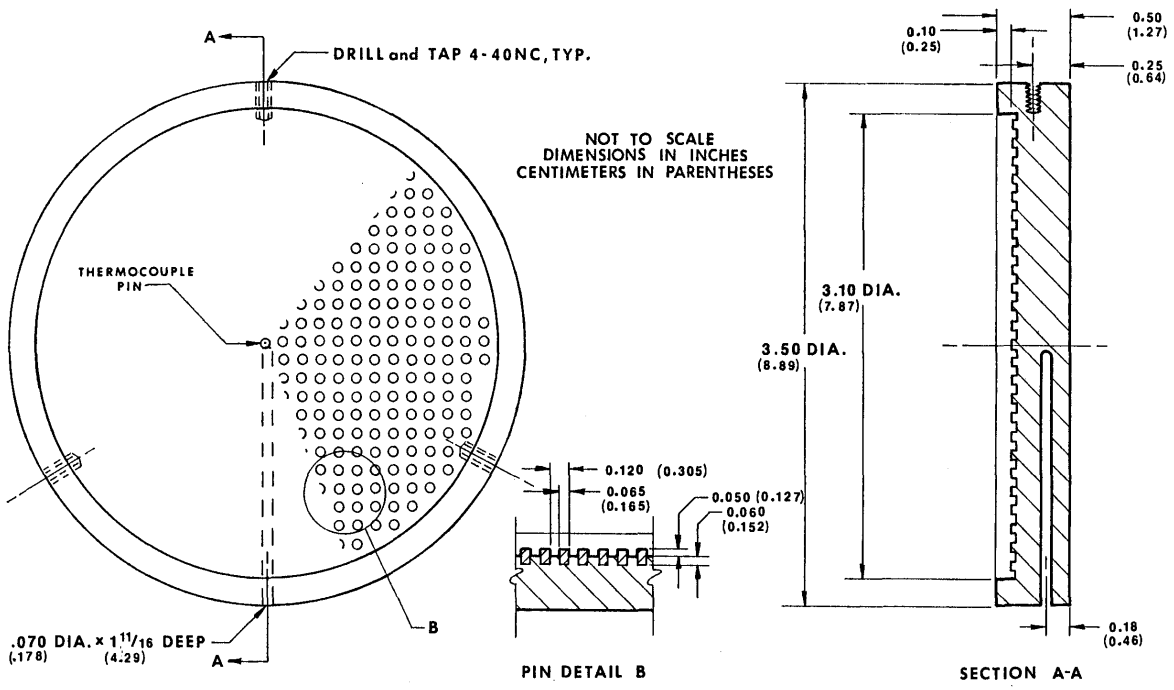

Figure 16. Details of Surface CP54

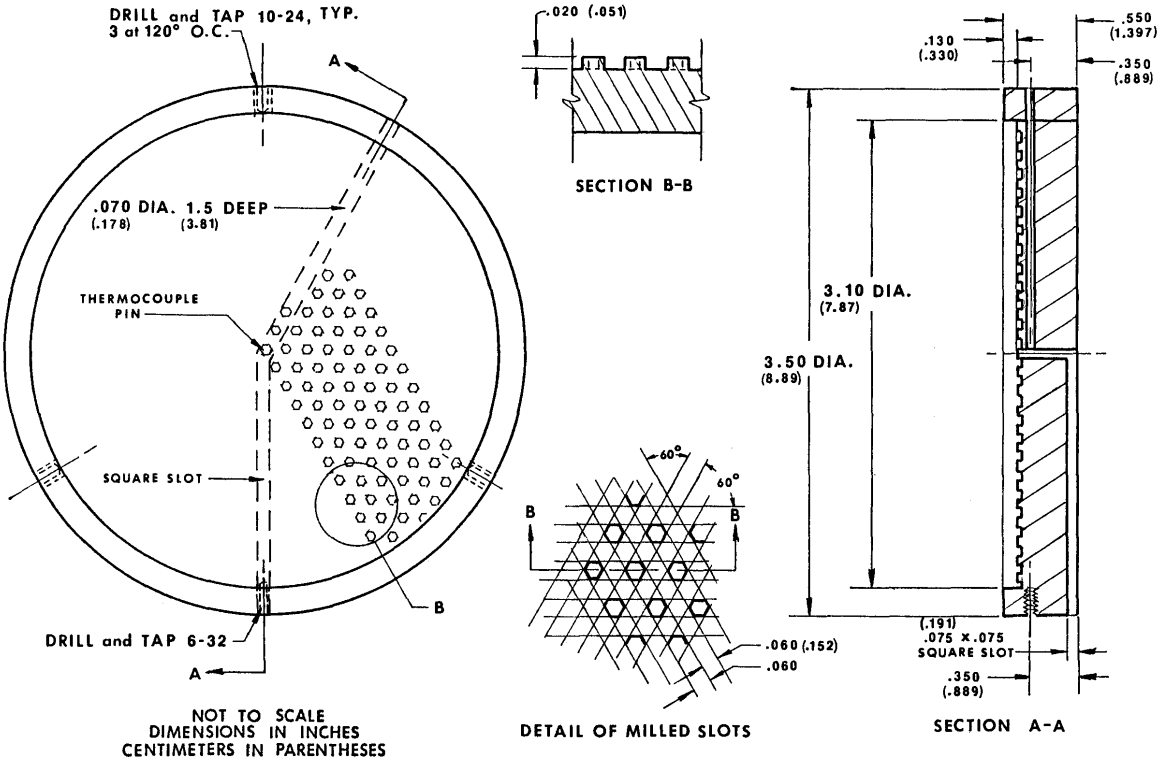

Figure 17. Details of Surface SHP2612

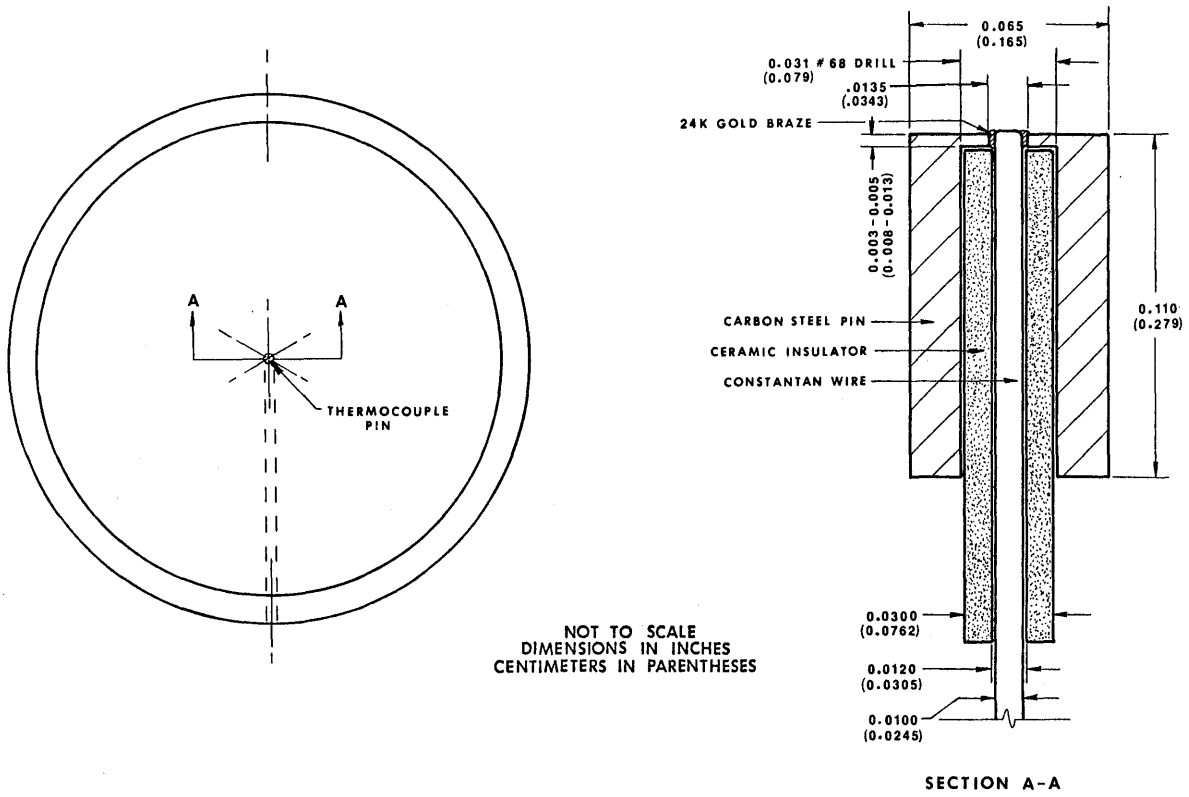

Figure 18. Details of Micro-Thermocouple/Pin for Surface CP54

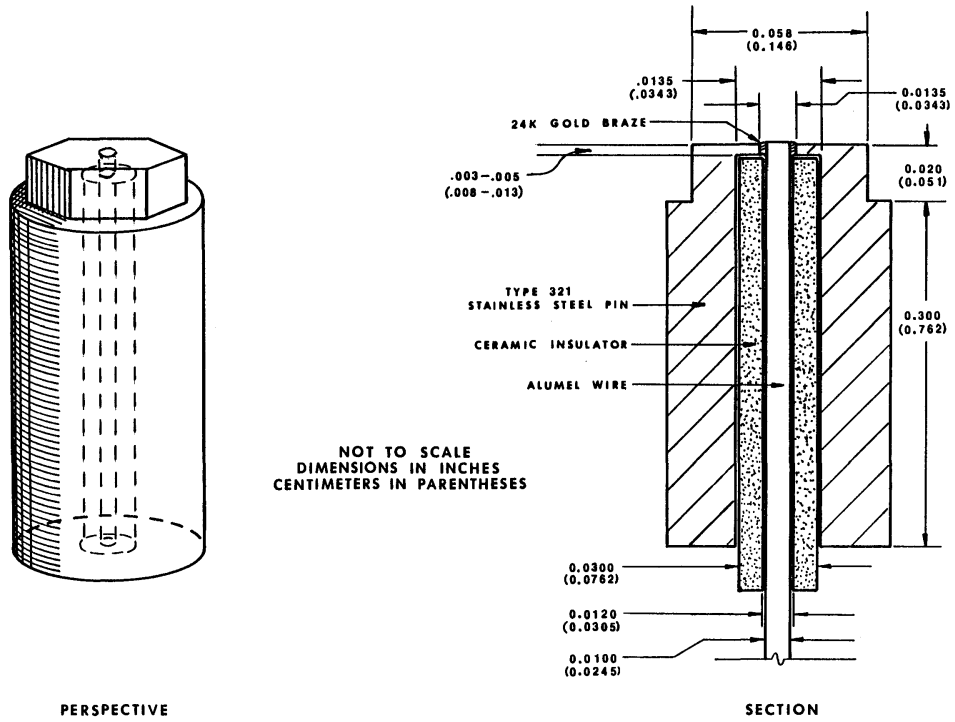

Figure 19. Details of Micro-Thermocouple/Pin for Surface SHP2612

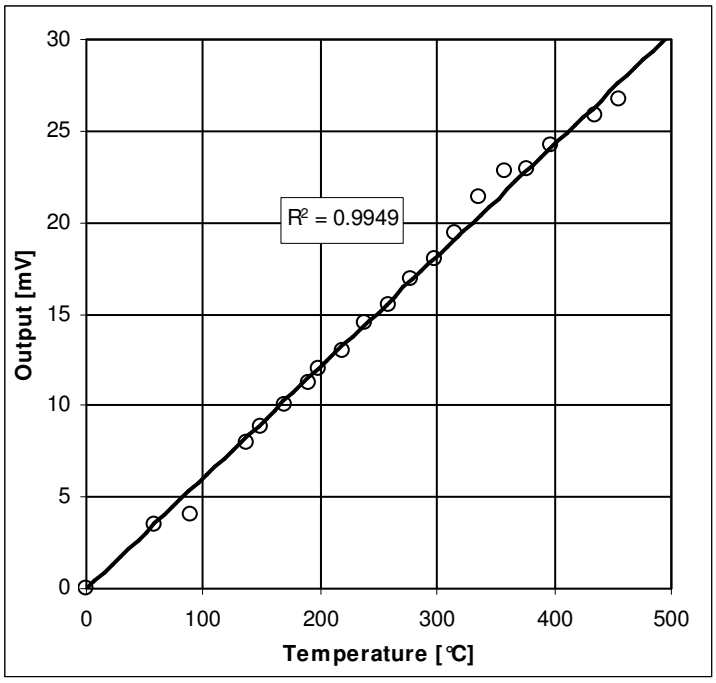

Figure 20. CP54 Thermocouple Calibration Curve

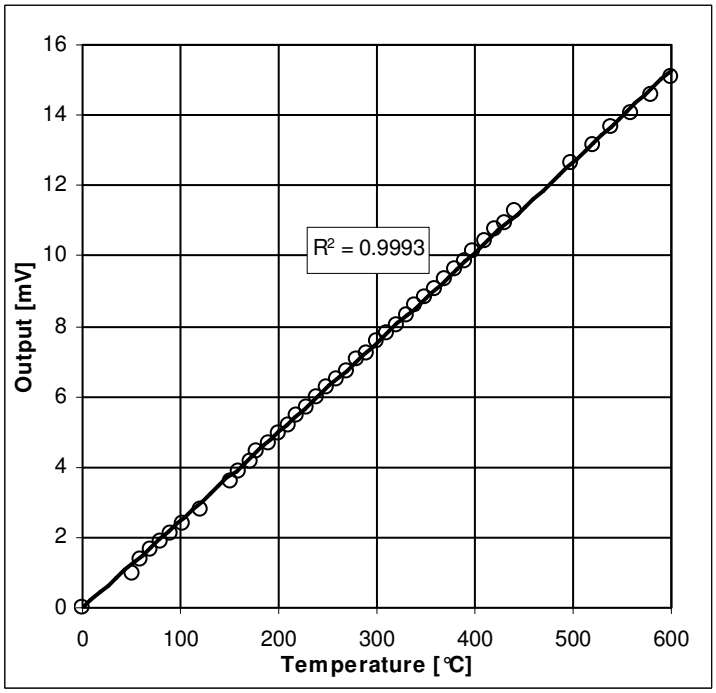

Figure 21. SHP2612 Thermocouple Calibration Curve

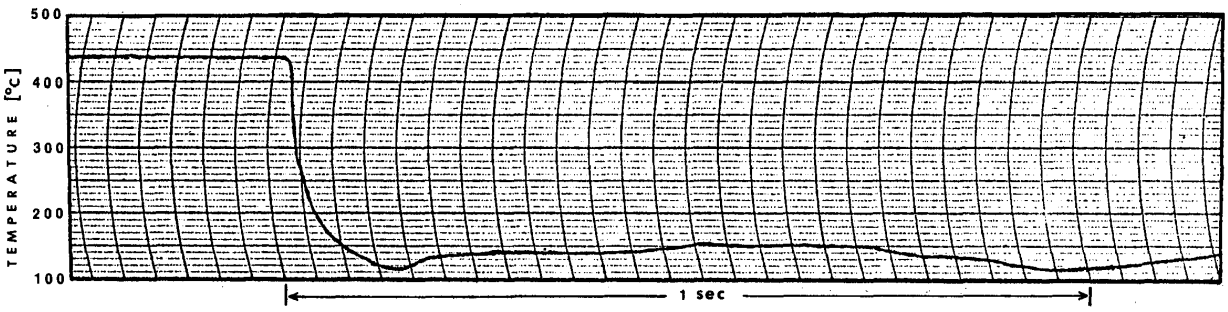

Figure 22. Response of CP54 Thermocouple/Pin to Water at 0°C

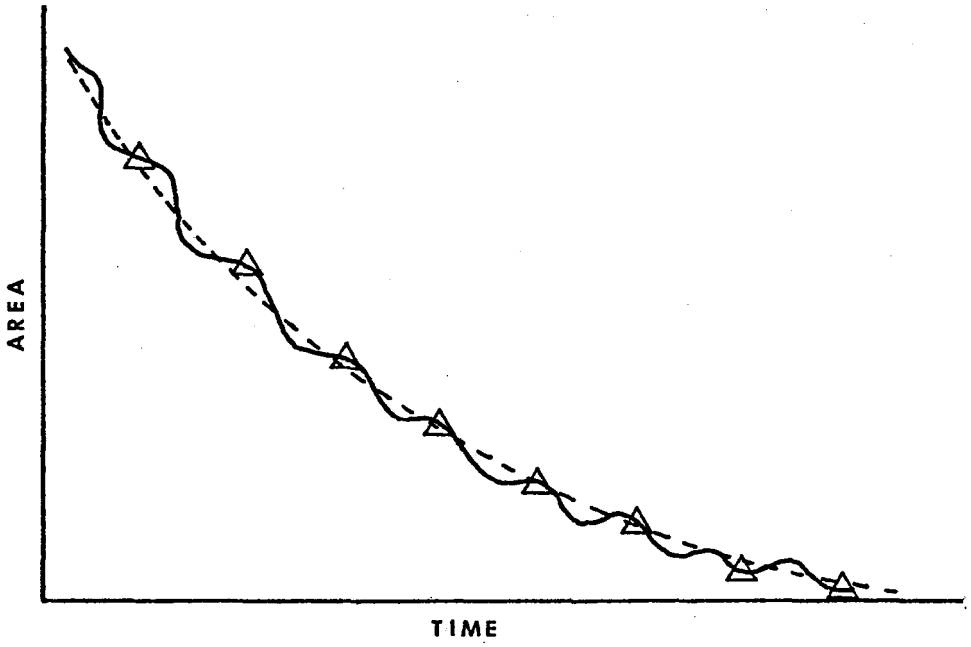

Figure 23. Typical Area/Time Plot with Sampling

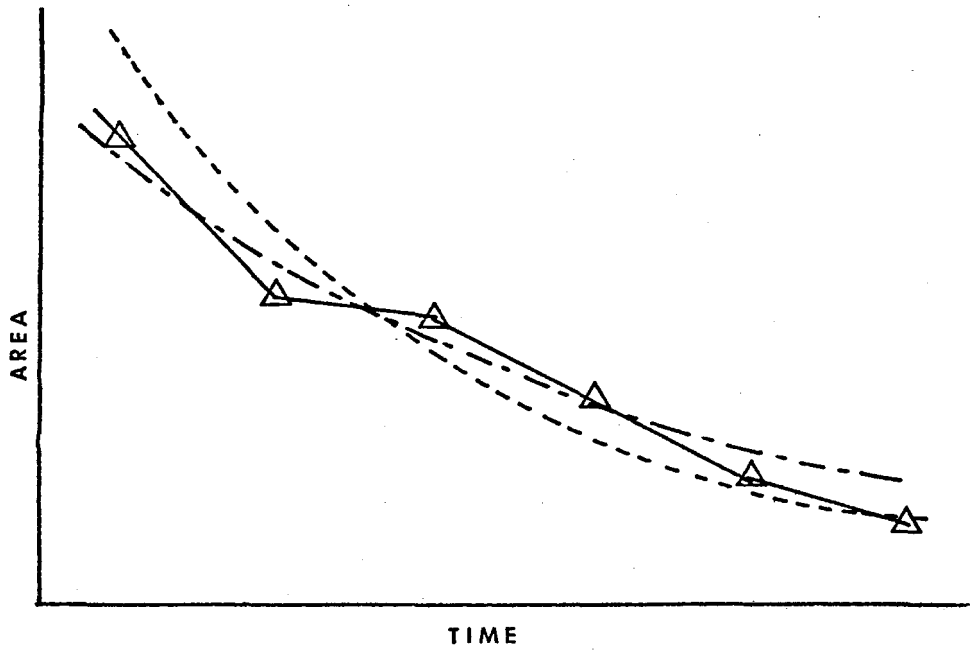

Figure 24. Are/Time Plot Showing Possible Curves

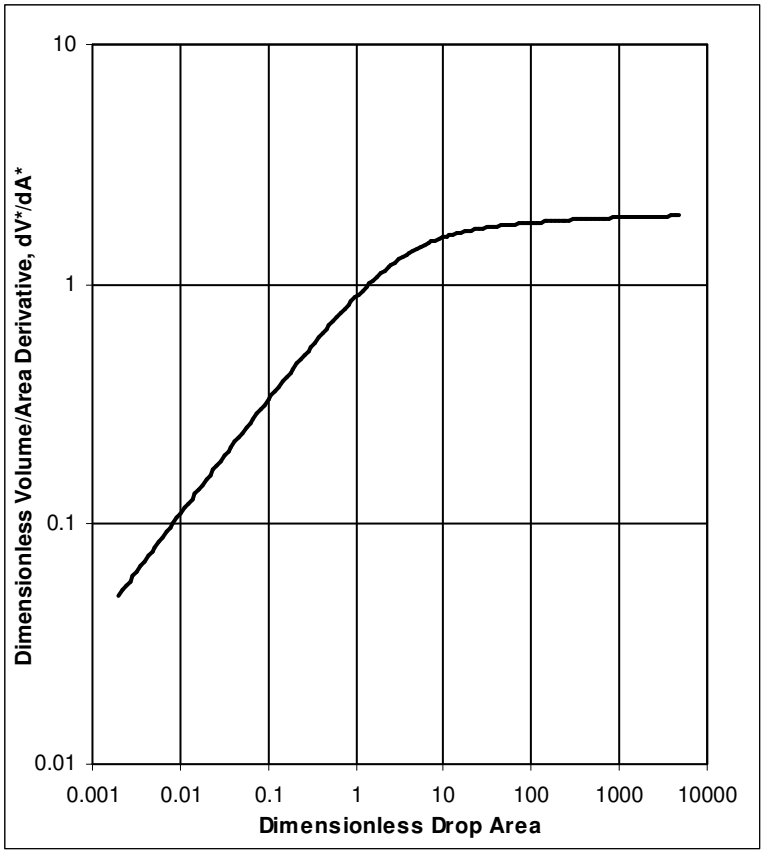

Figure 25. Dimensionless Volume/Area Derivative

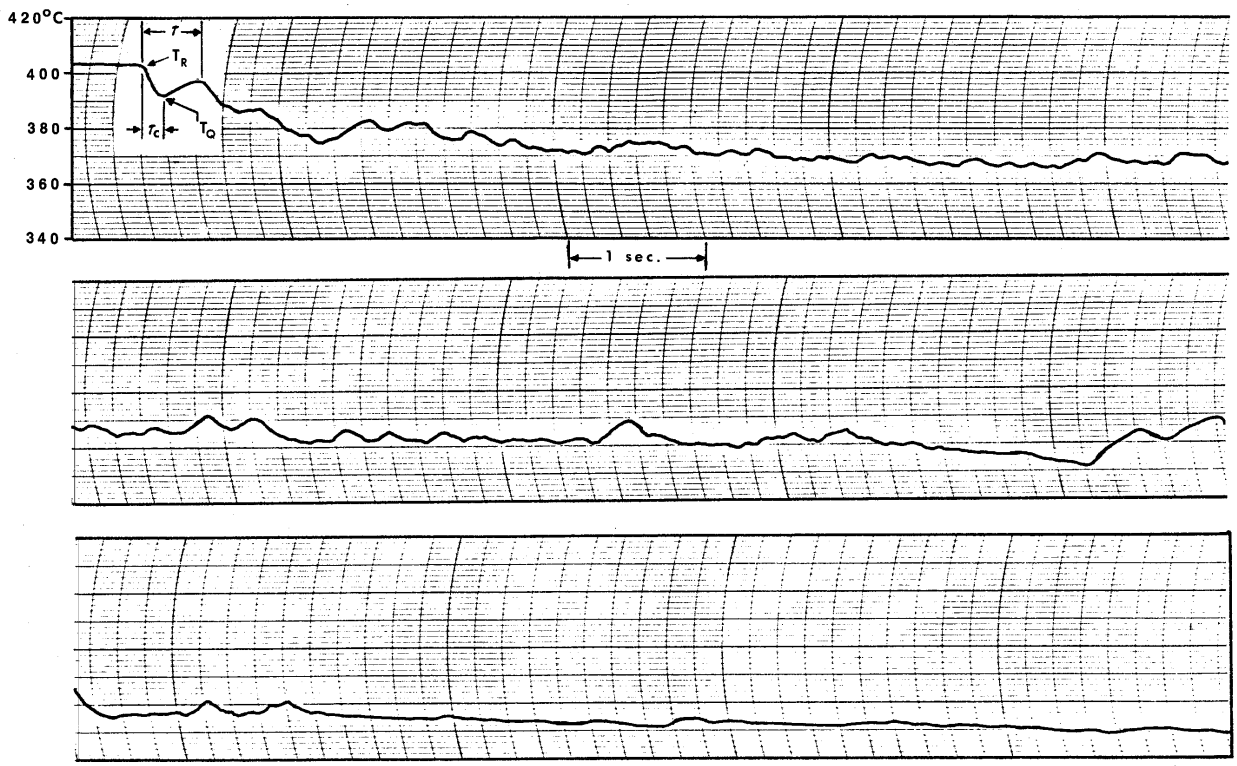

Figure 26. Isopropanol on Surface CP54 (Strip #25)

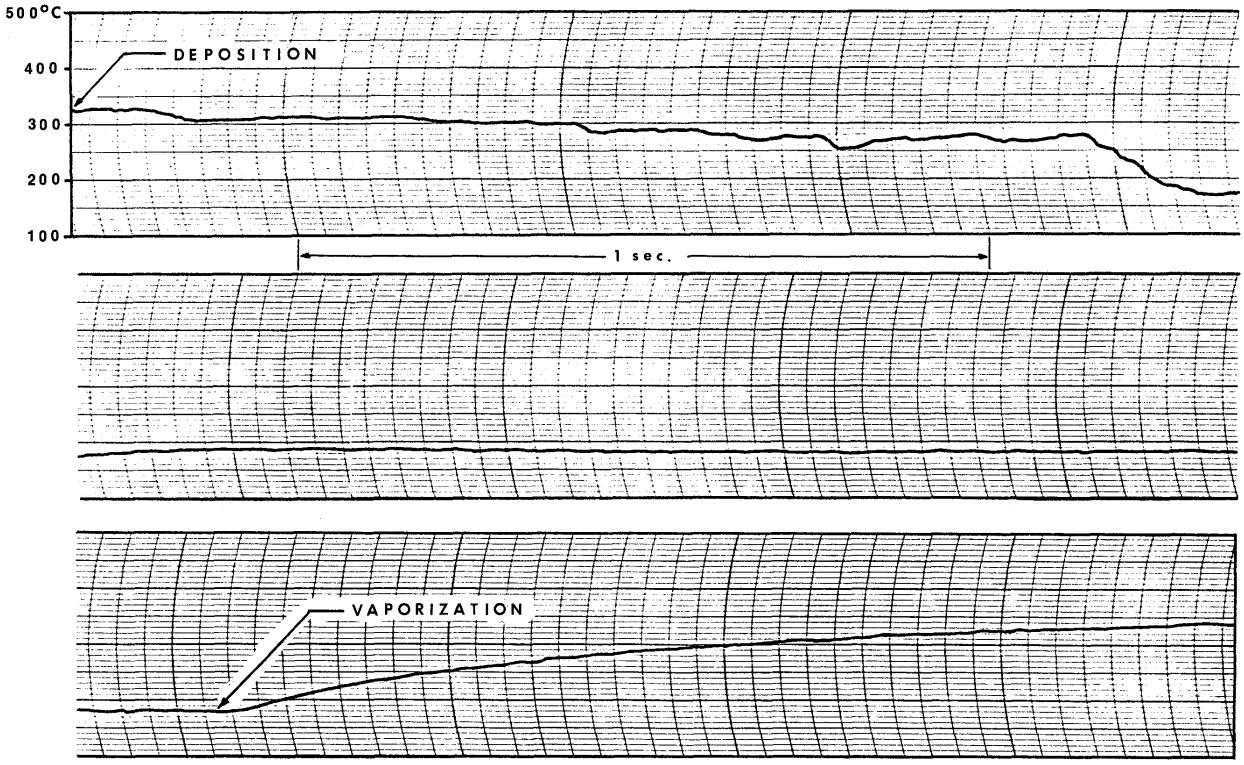

Figure 27. Water on Surface CP54 (Strip #31)

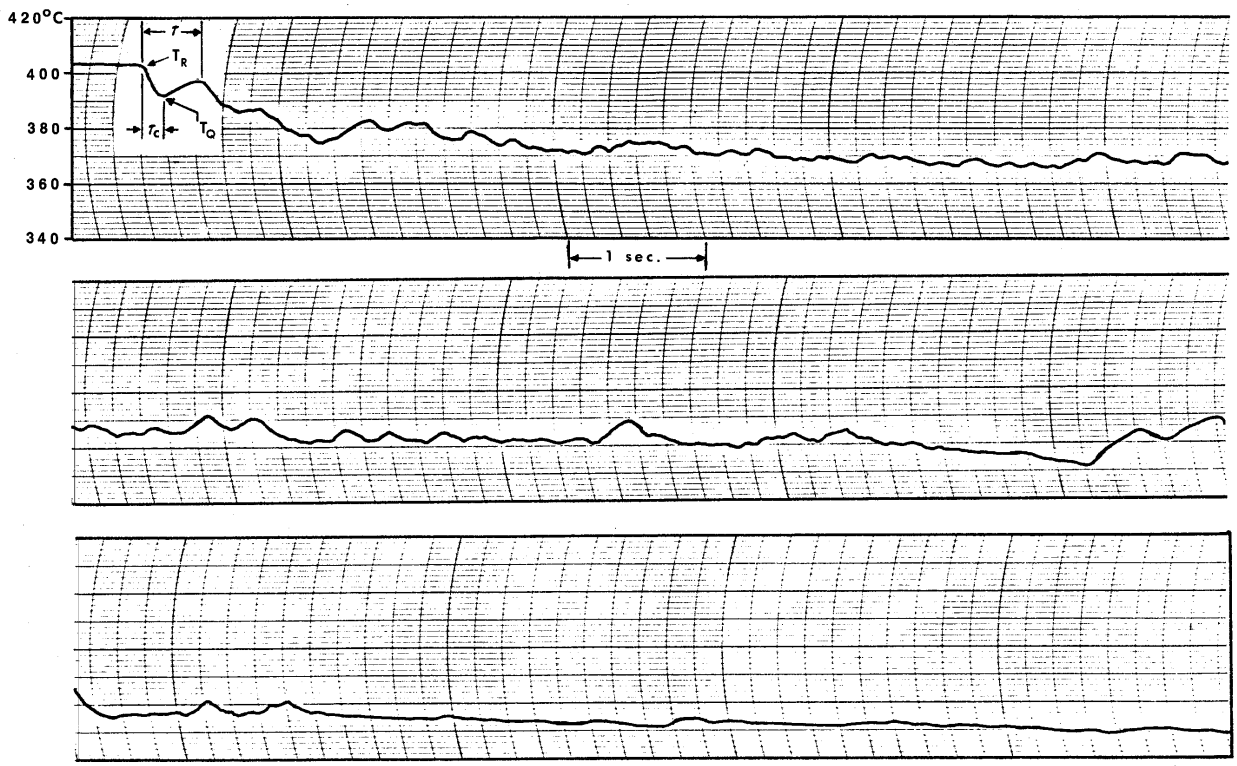

Figure 28. Water on Surface CP54 (Strip #41)

CREATE FINITE DIFFERENCE PROGRAM TO DETERMINE THE TRANSIENT TEMPERATURE OF A CYLINDRICAL PIN SUBJECTED TO PULSE-LIKE PERIODIC LIQUID-SOLID CONTACT

MODELING THE PHENOMENA:

1. CIRCUMFERENTIAL SYMMETRY IS ASSUMED
2. THE SUBSTRATA IS ASSUMED TO BE ISOTHERMAL
3. THE LIQUID-SOLID CONTACT IS ASSUMED TO PULSE-LIKE PERIODIC WITH PERIOD TAU AND DURATION TAUC
4. WHERE LIQUID-SOLID CONTACT OCCURS A CONTACT-TYPE HEAT FLUX IS IMPOSED
5. WHERE LIQUID-SOLID CONTACT DOES NOT OCCUR A POOL BOILING HEAT FLUX IS IMPOSED
6. THE ENTIRE BOILING CURVE IS USED TO DETERMINE HEAT FLUX DEPENDING ON THE LOCAL TEMPERATURE
7. THE IMPOSED HEAT FLUX VARIES WITH TIME, TEMPERATURE, AND NODAL POINT LOCATION
8. THE THERMOPHYSICAL PROPERTIES OF THE SOLID ARE ALLOWED TO VARY WITH TEMPERATURE
9. THE CERAMIC INSULATOR OCCUPIES NODES 5, 6, 9, 10, 13, 14, 17, & 18

DESCRIPTION OF PROGRAM:

1. 20 NODES ARE USED
2. FOURTH ORDER RUNGE-KUTTA INTEGRATION IS USED

LOCATION OF NODAL POINTS:

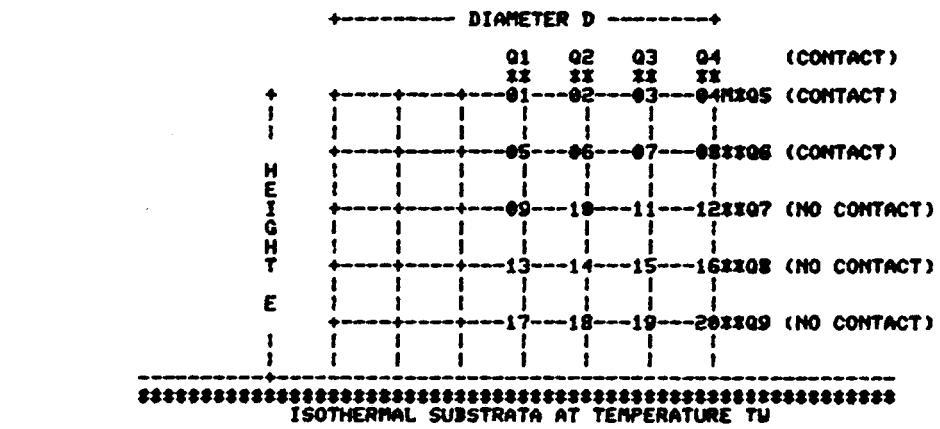

HEAT FLUX DISTRIBUTION:

1. CONTACT IS ASSUMED TO OCCUR ONLY AT NODES 1-4 AND 8 (THUS Q1-Q6)
2. SINCE THE LIQUID WETS THE SURFACE DURING INTIMATE LIQUID-SOLID CONTACT IT SEEMS REASONABLE TO INCLUDE NODE 8 IN THE CONTACT PROCESS. THIS MEANS THAT ONE-THIRD OF THE PIN HEIGHT IS SUBJECTED TO CONTACT
3. IF THE LOCAL TEMPERATURE FALLS BELOW THE MFBT THEN THE NODE IS SUBJECTED TO THE USUAL POOL BOILING HEAT FLUX

Figure 29. Details of Finite Difference Model 2DPINT

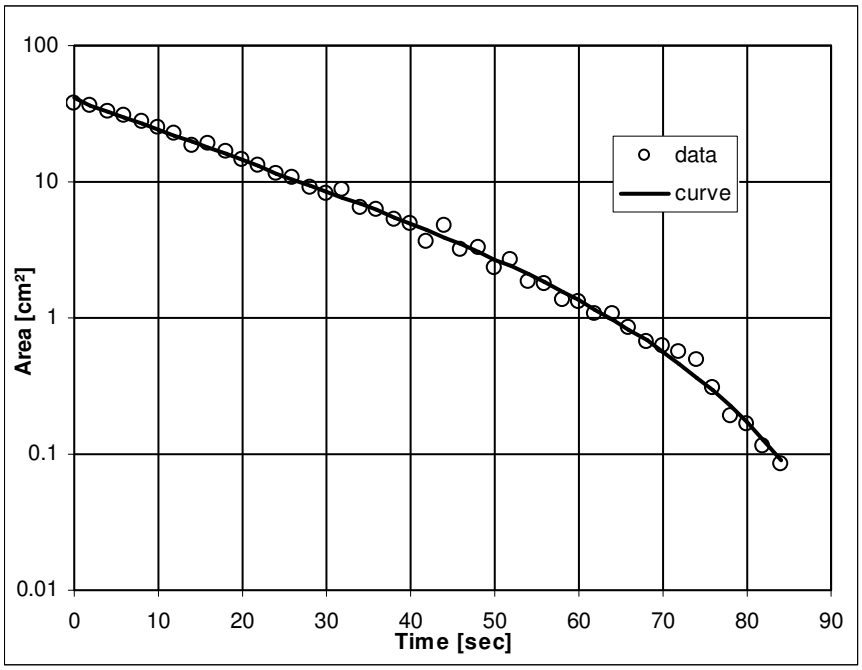

Figure 30. Typical Experimental Data (EA/SCG02/450°C)

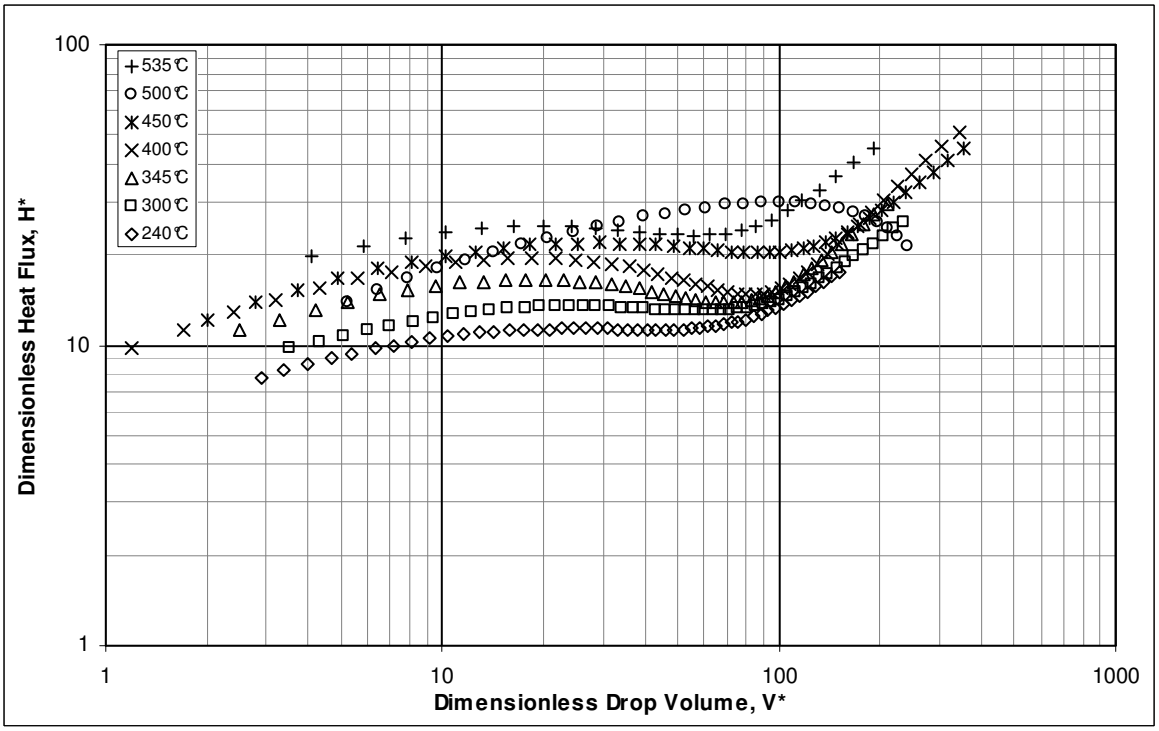

Figure 31. Dimensionless Heat Flux (Water on SMTH)

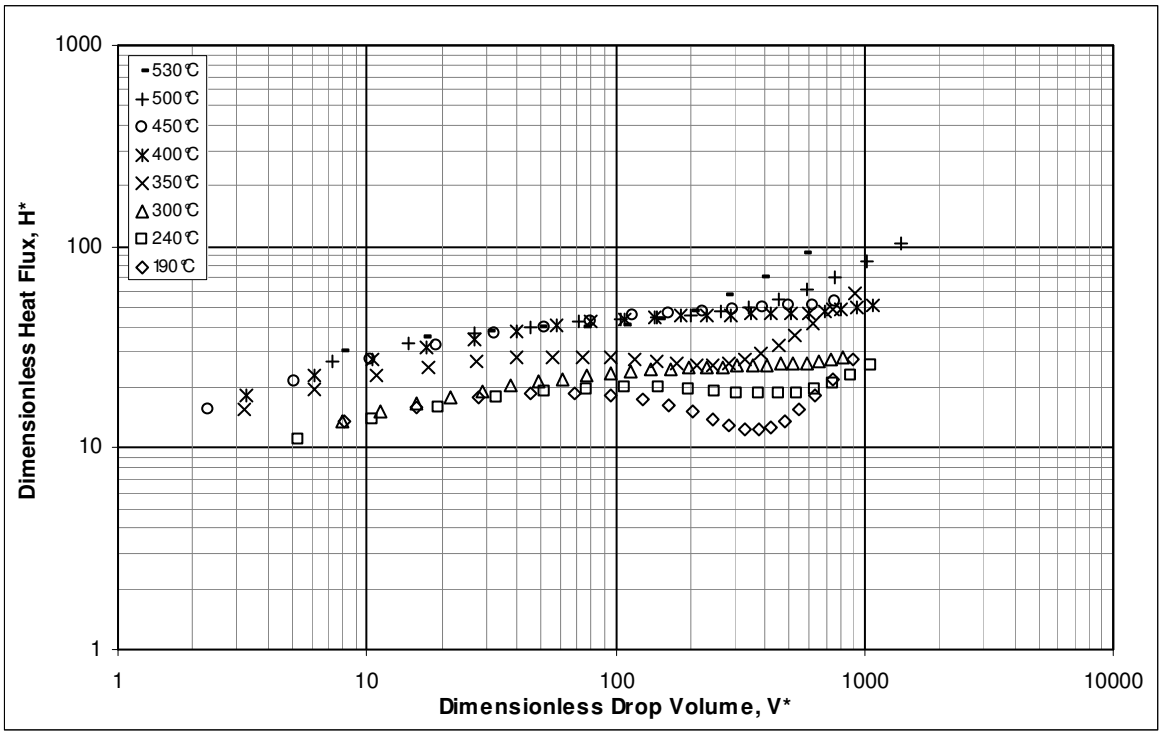

Figure 32. Dimensionless Heat Flux (Ethanol on SMTH)

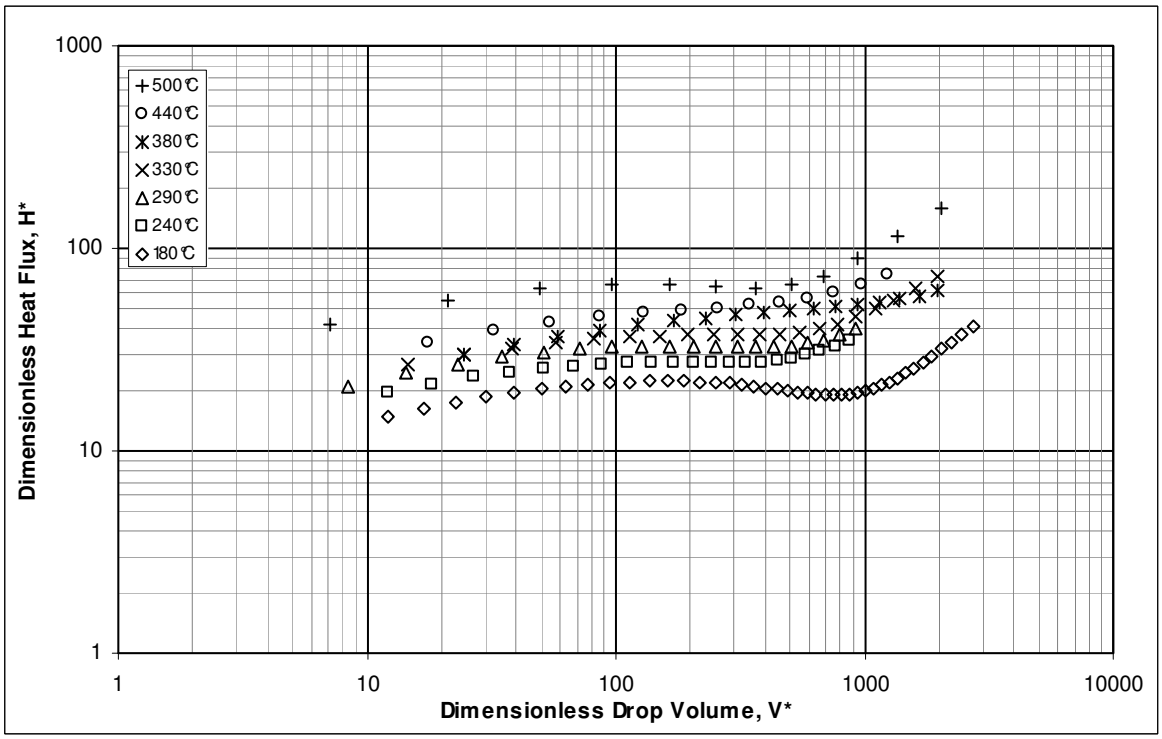

Figure 33. Dimensionless Heat Flux (Isopropanol on SMH)

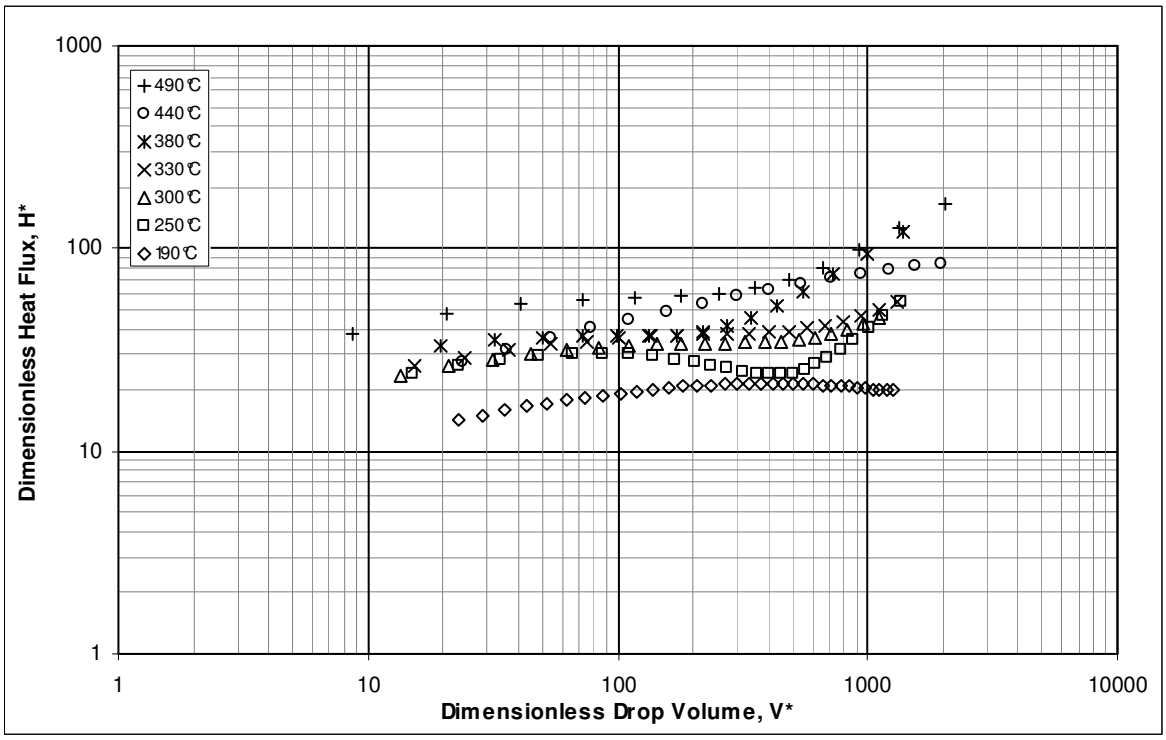

Figure 34. Dimensionless Heat Flux (Ethylene-Chloride on SMTH)

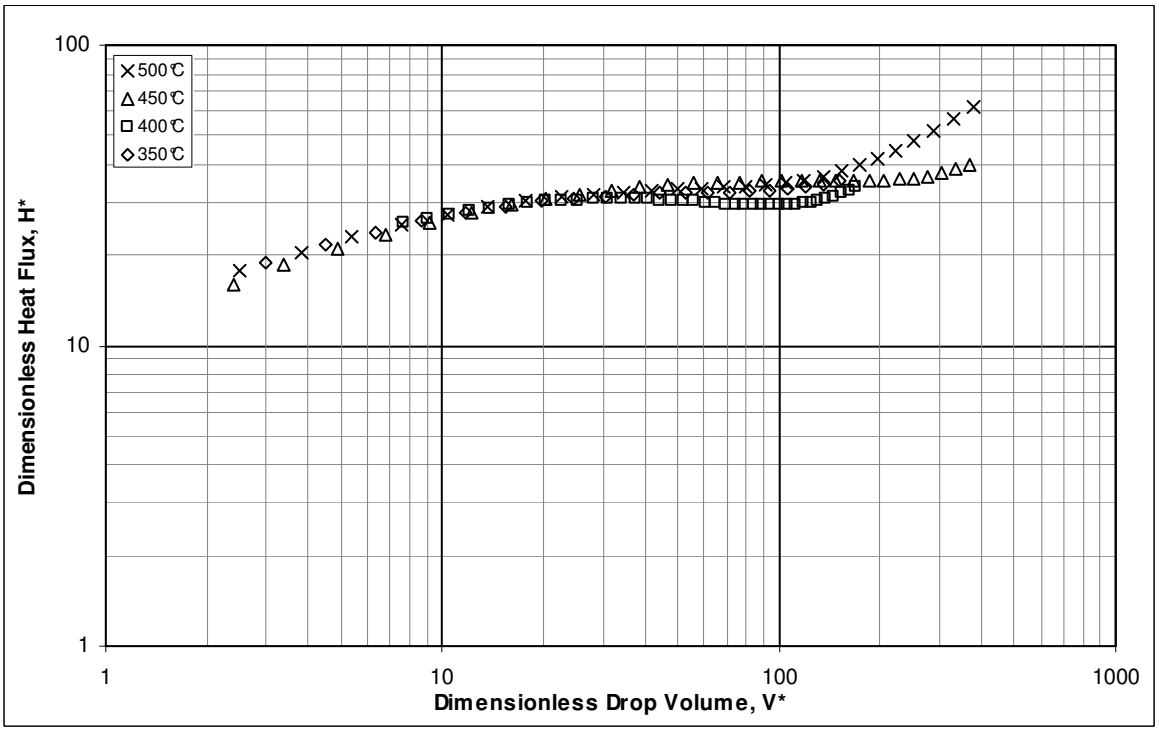

Figure 35. Dimensionless Heat Flux (Water on CG01)

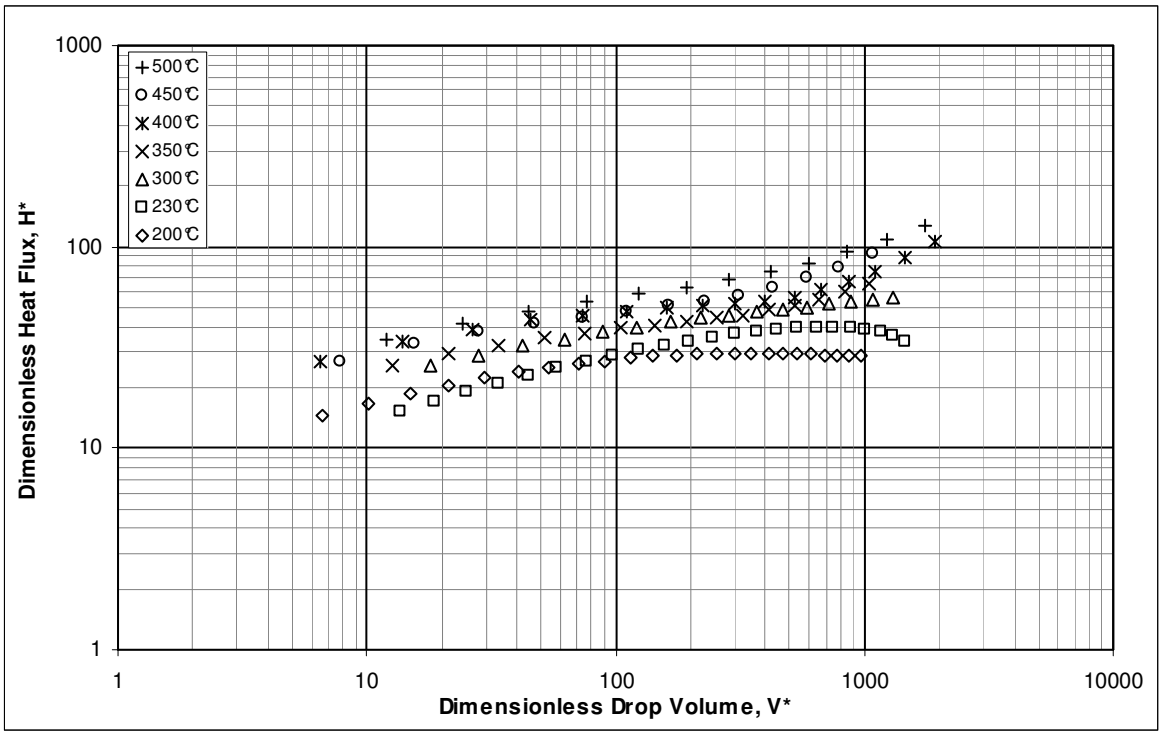

Figure 36. Dimensionless Heat Flux (Ethanol on CG01)

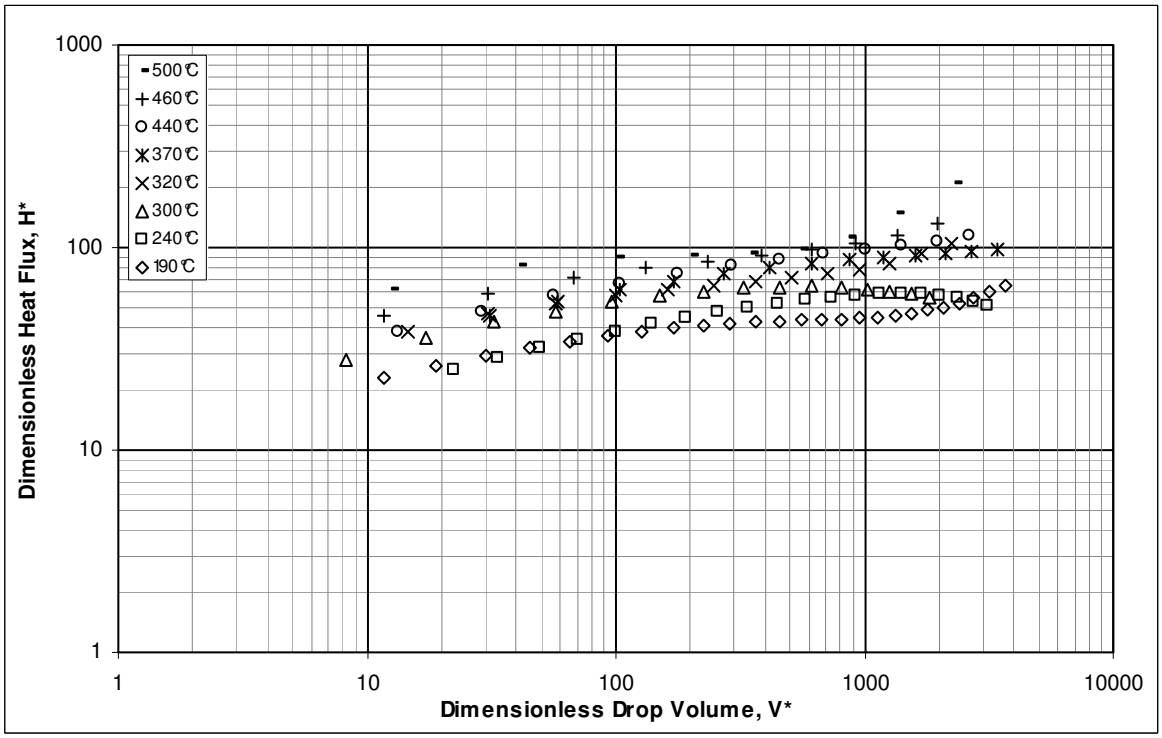

Figure 37. Dimensionless Heat Flux (Isopropanol on CG01)

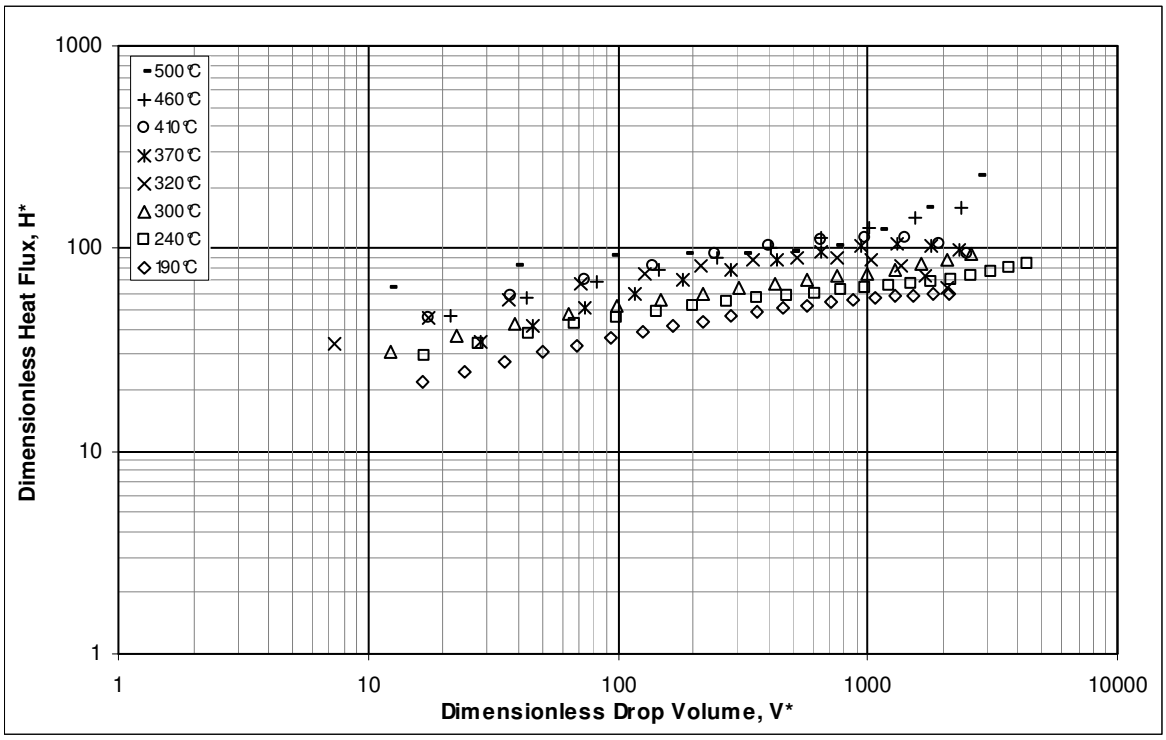

Figure 38. Dimensionless Heat Flux (Ethylene-Chloride on CG01)

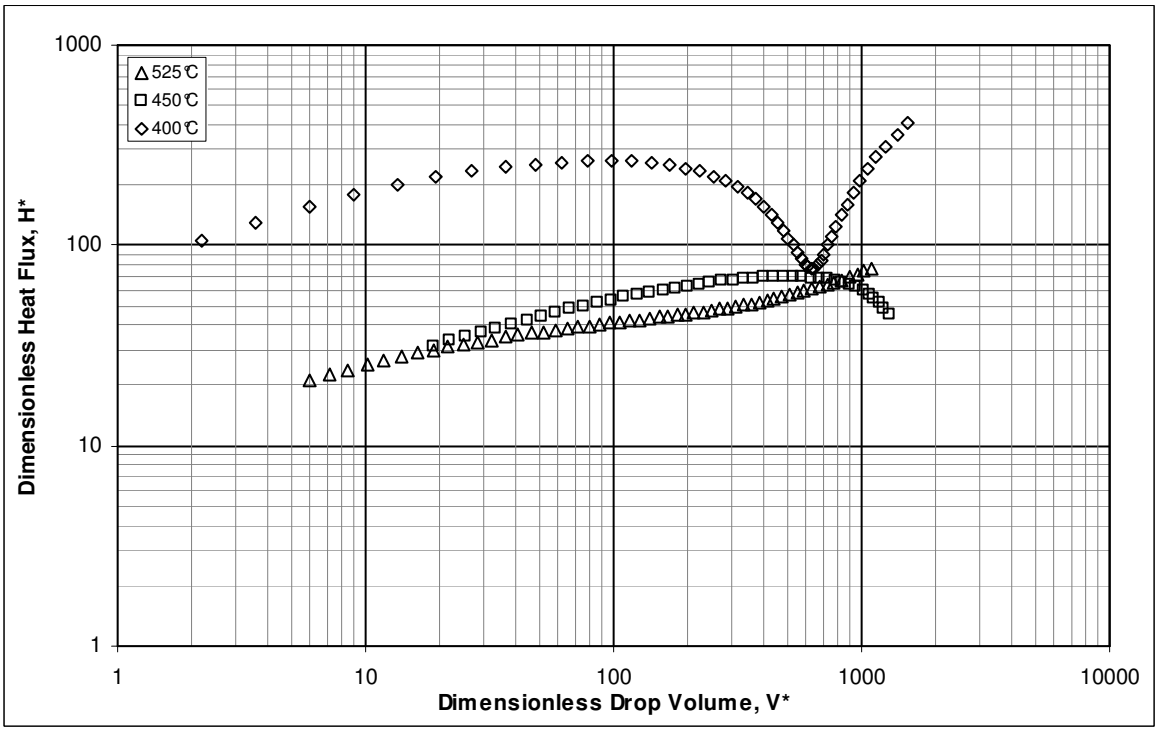

Figure 39. Dimensionless Heat Flux (Water on SCG02)

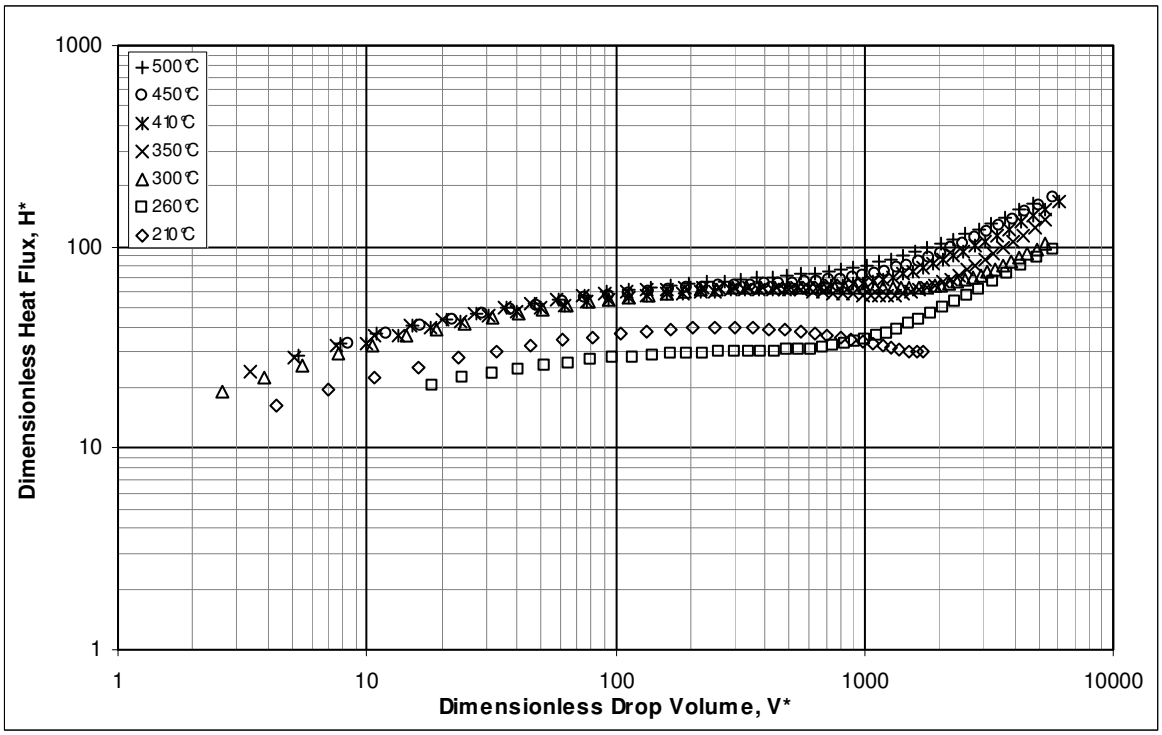

Figure 40. Dimensionless Heat Flux (Ethanol on SCG02)

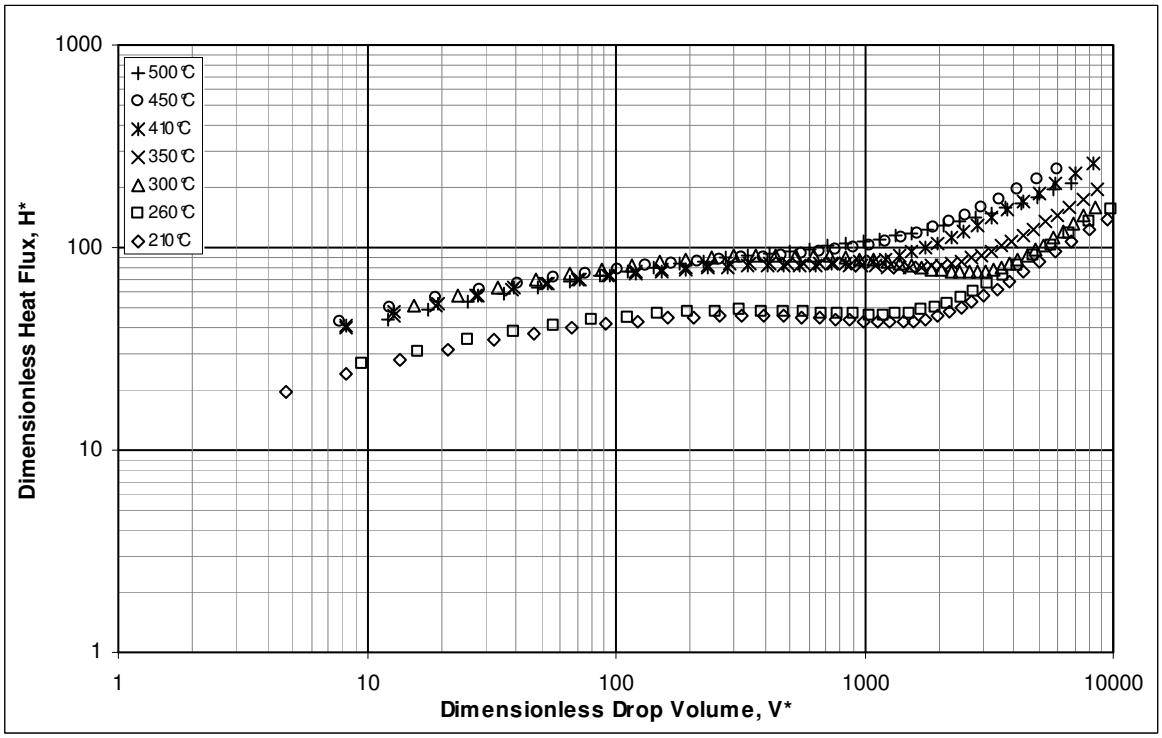

Figure 41. Dimensionless Heat Flux (Isopropanol on SCG02)

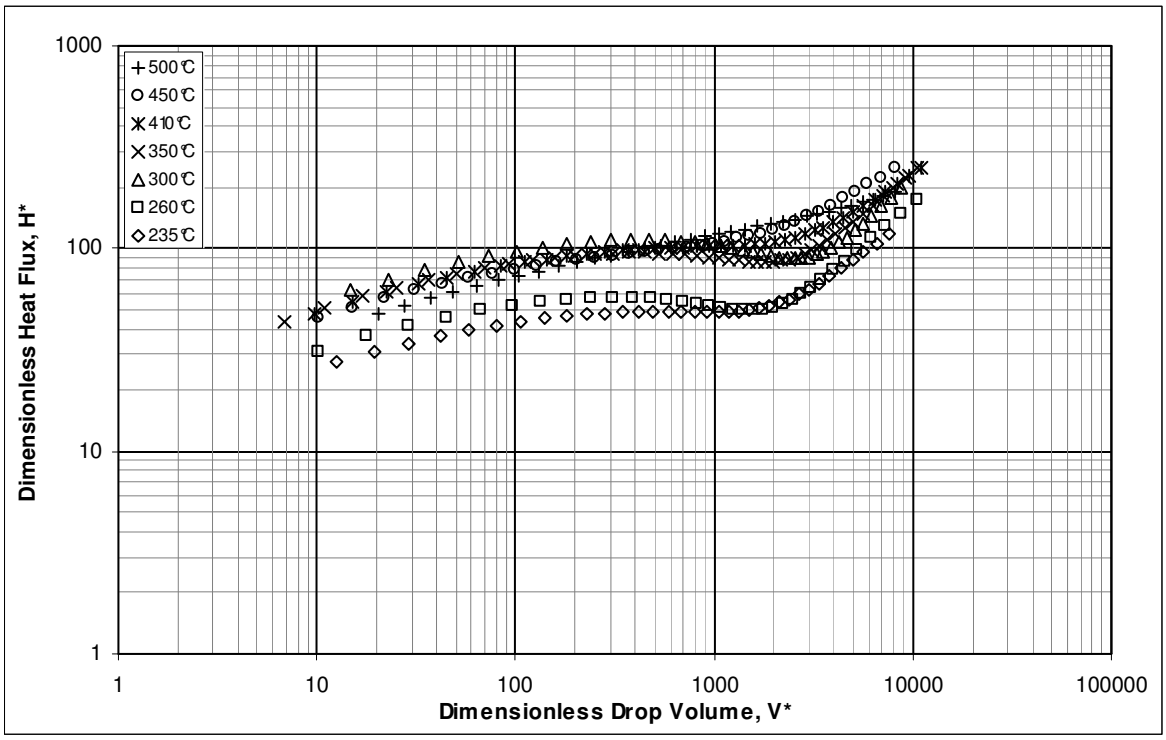

Figure 42. Dimensionless Heat Flux (Ethylene-Chloride on SCG02)

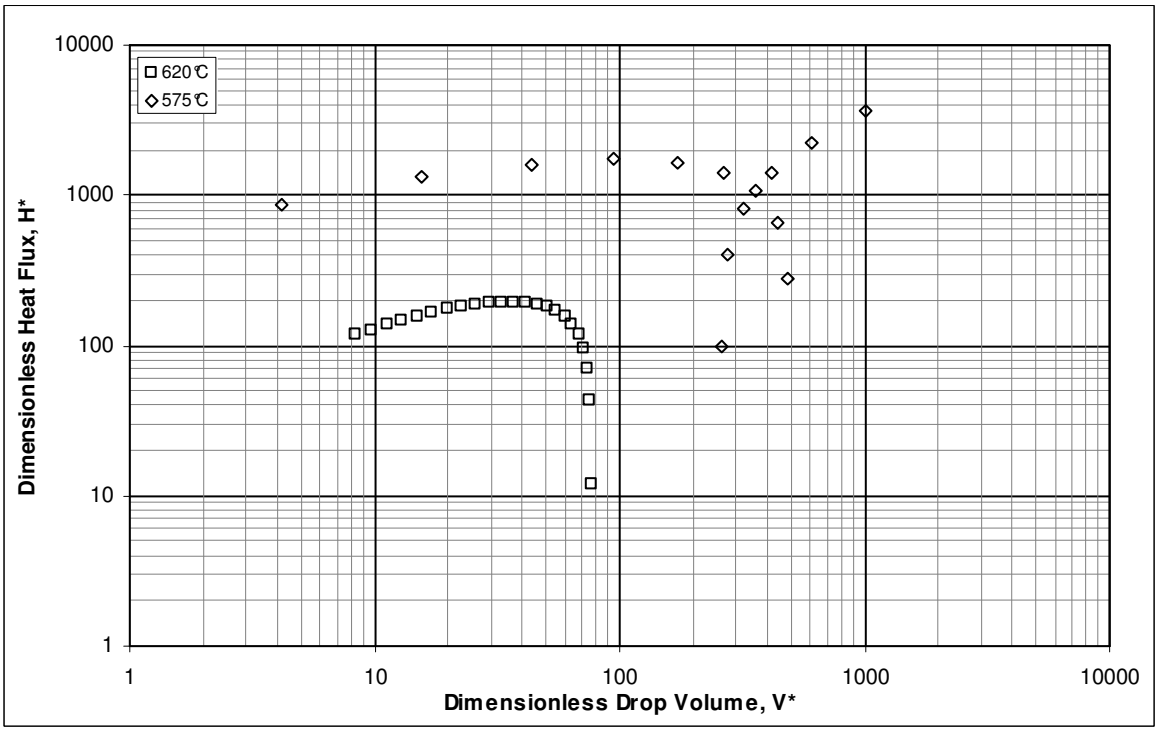

Figure 43. Dimensionless Heat Flux (Water on CP54)

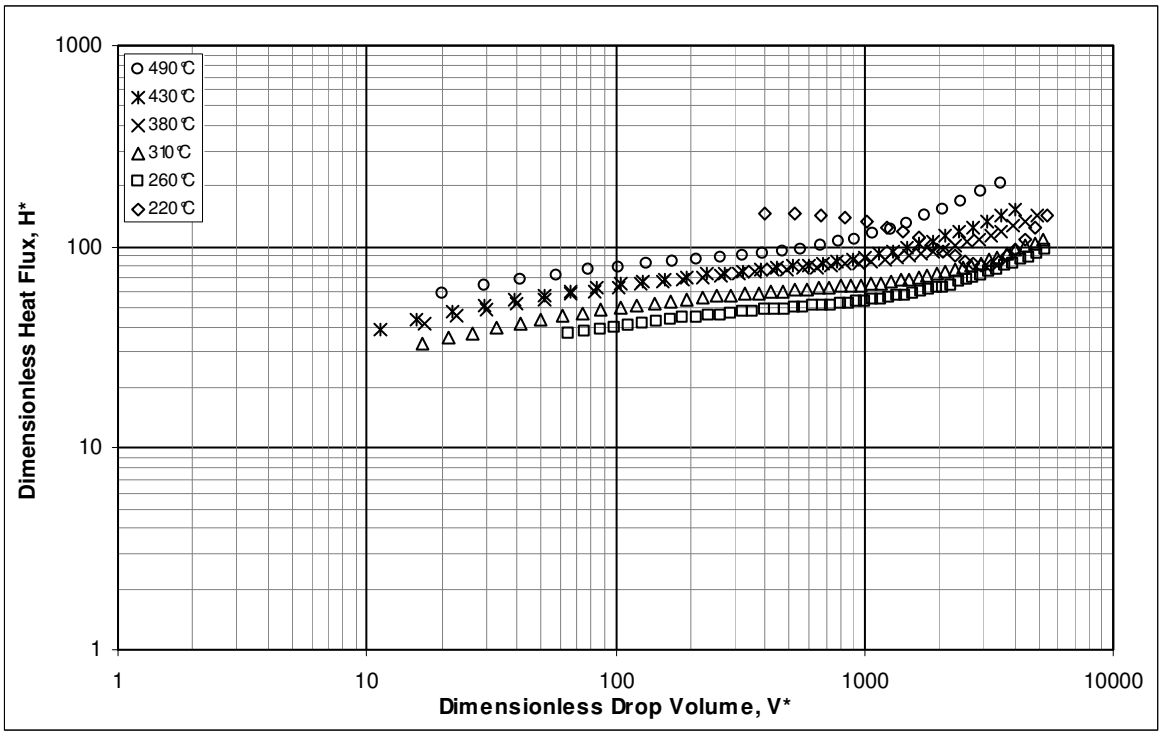

Figure 44. Dimensionless Heat Flux (Ethanol on CP54)

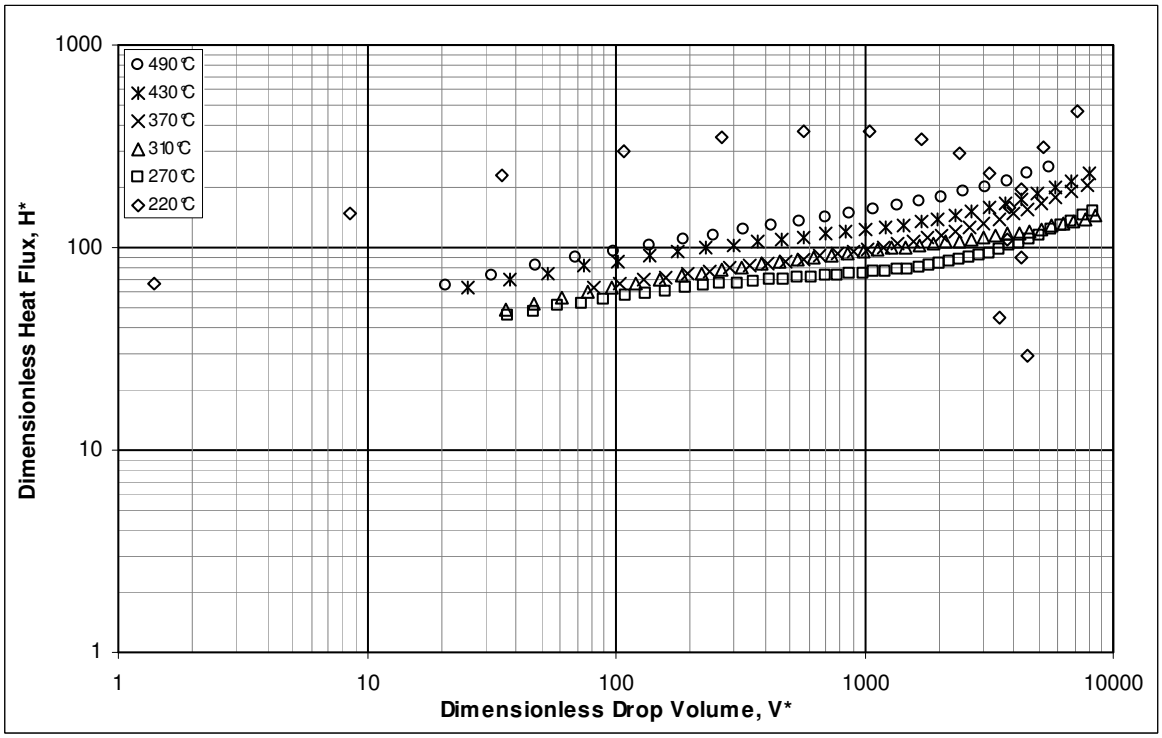

Figure 45. Dimensionless Heat Flux (Isopropanol on CP54)

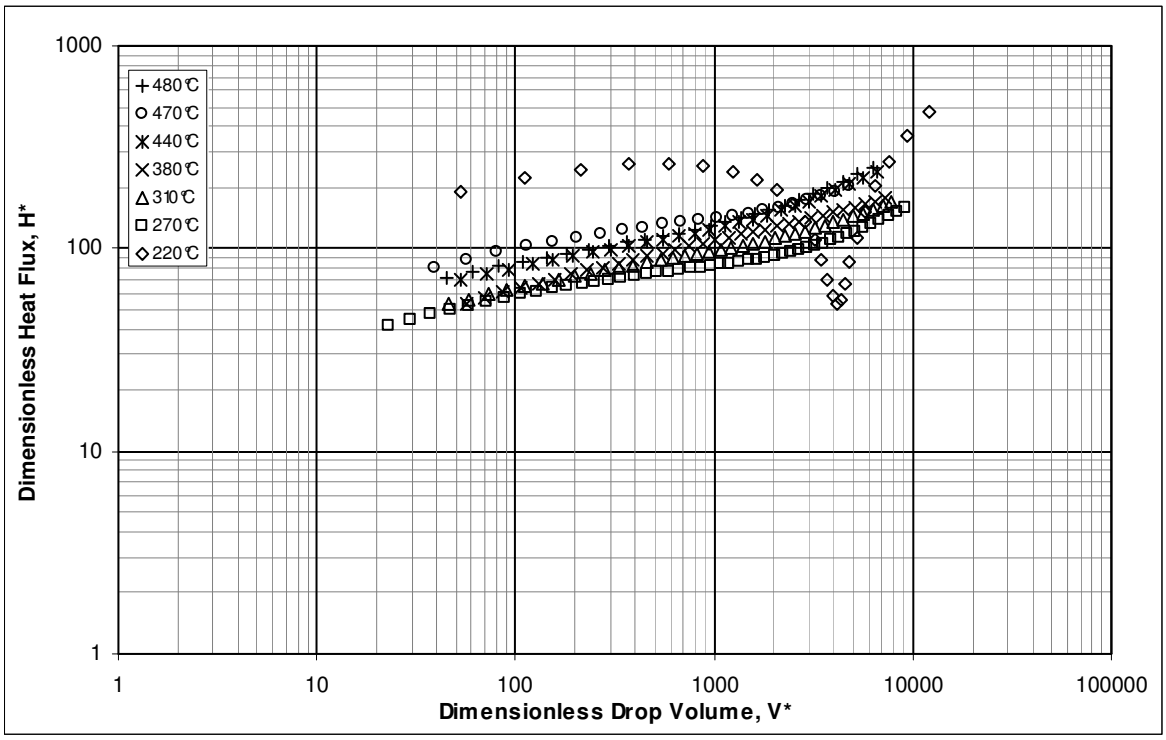

Figure 46. Dimensionless Heat Flux (Ethylene-Chloride on CP54)

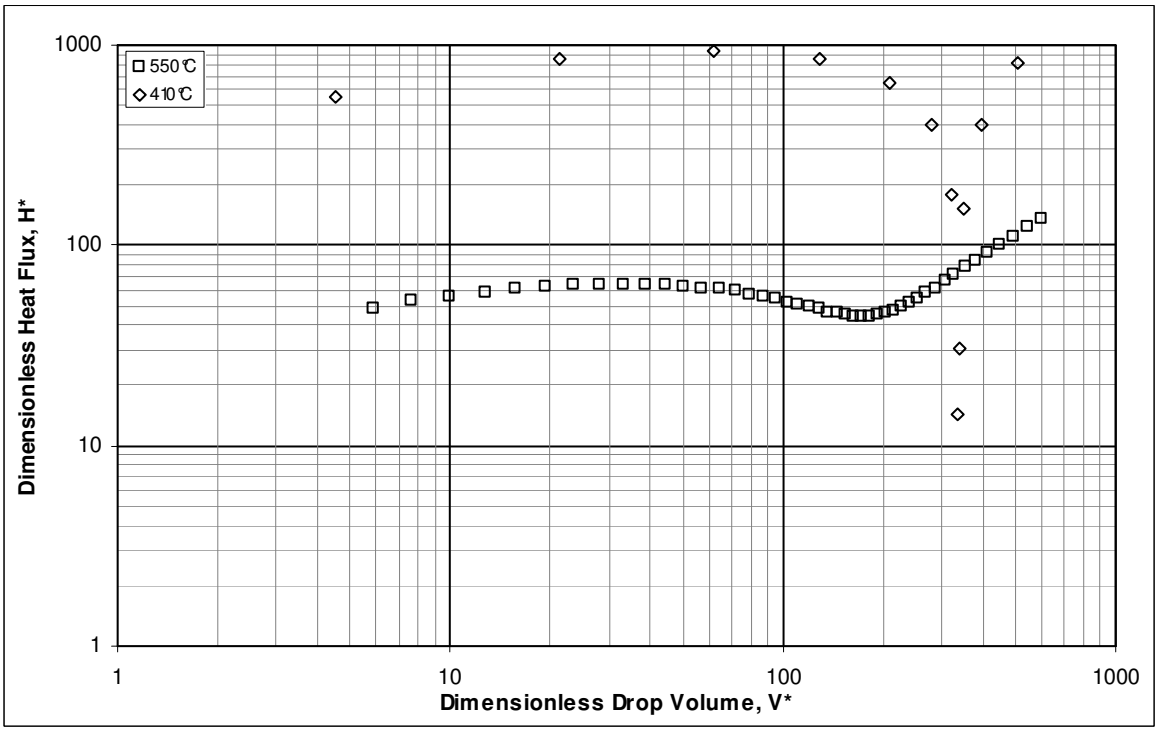

Figure 47. Dimensionless Heat Flux (Water on SHP2612)

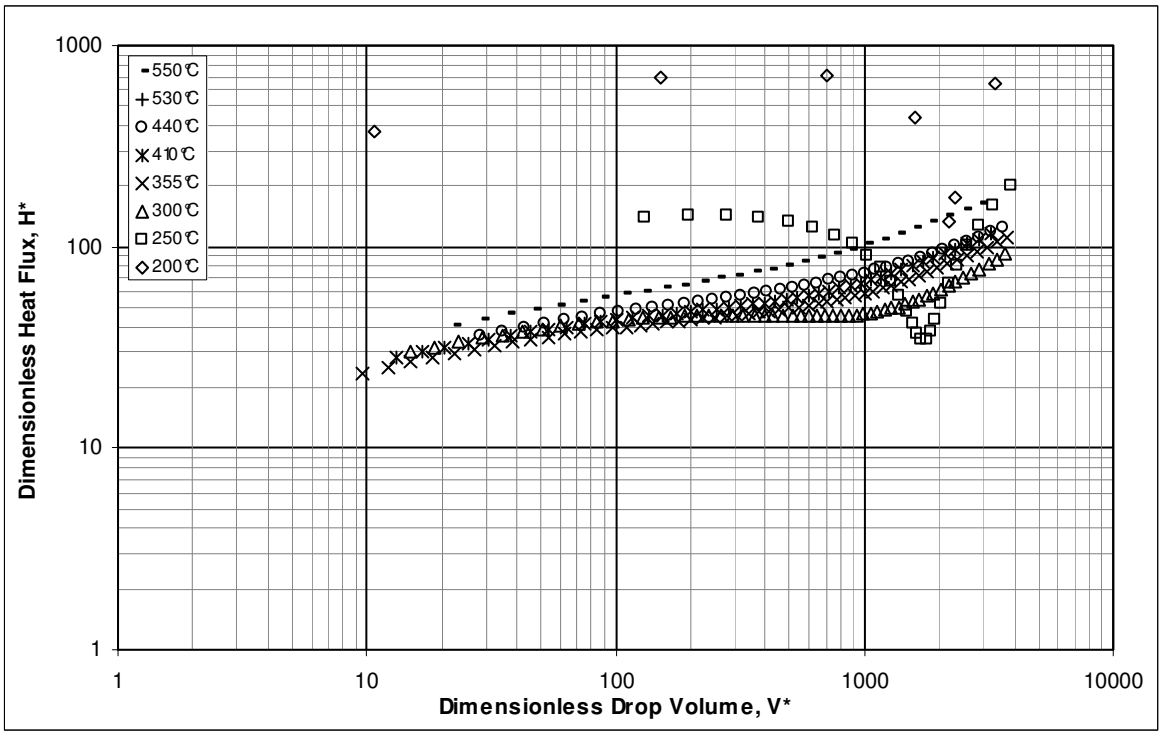

Figure 48. Dimensionless Heat Flux (Ethanol on SHP2612)

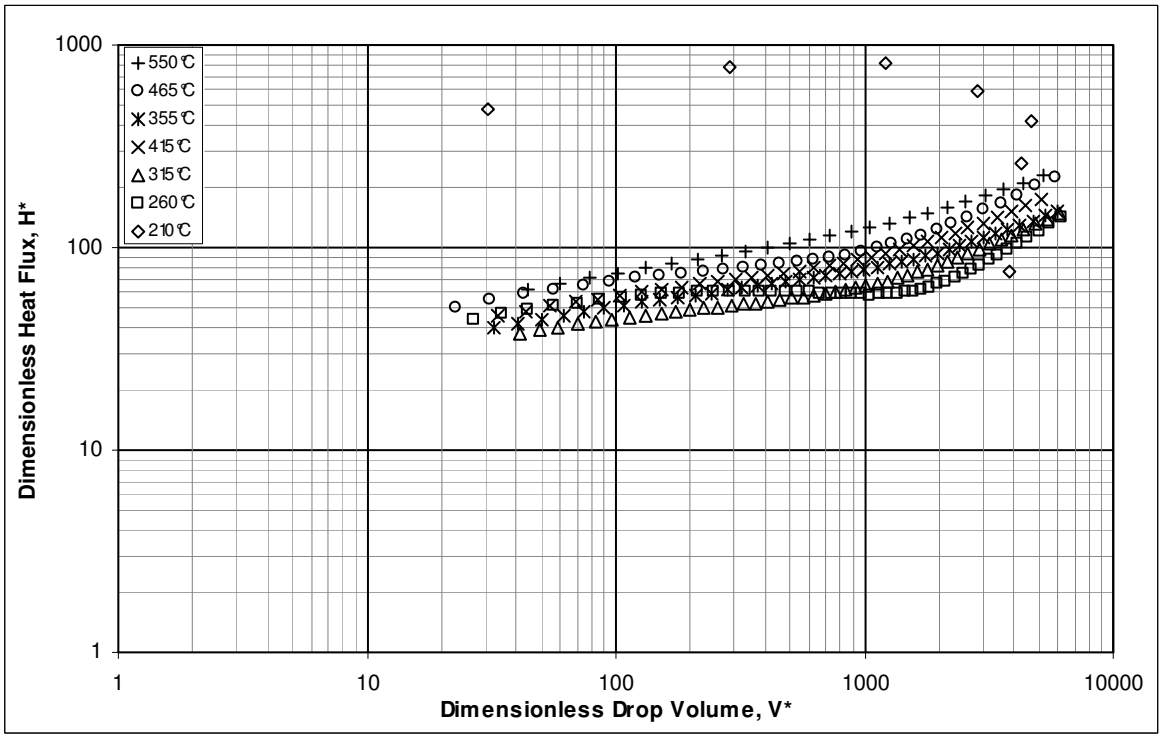

Figure 49. Dimensionless Heat Flux (Isopropanol on SHP2612)

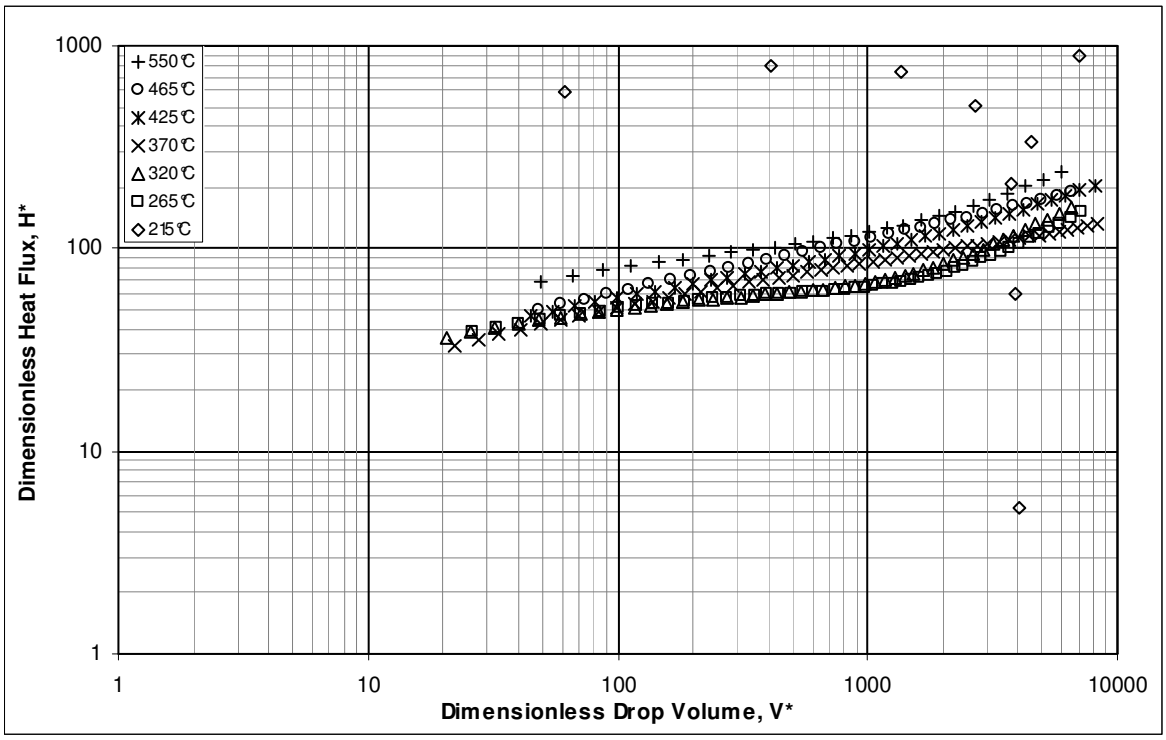

Figure 50. Dimensionless Heat Flux (Ethylene-Chloride on SHP2612)

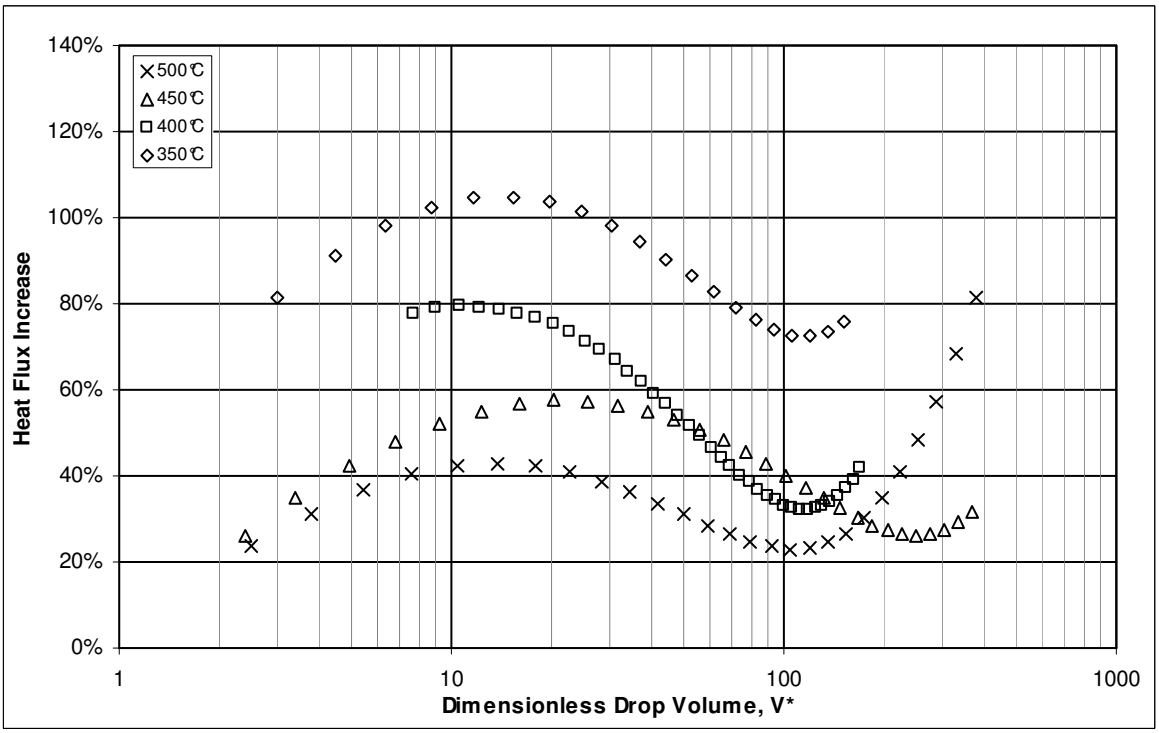

Figure 51. Increase in Heat Flux (Water on CG01)

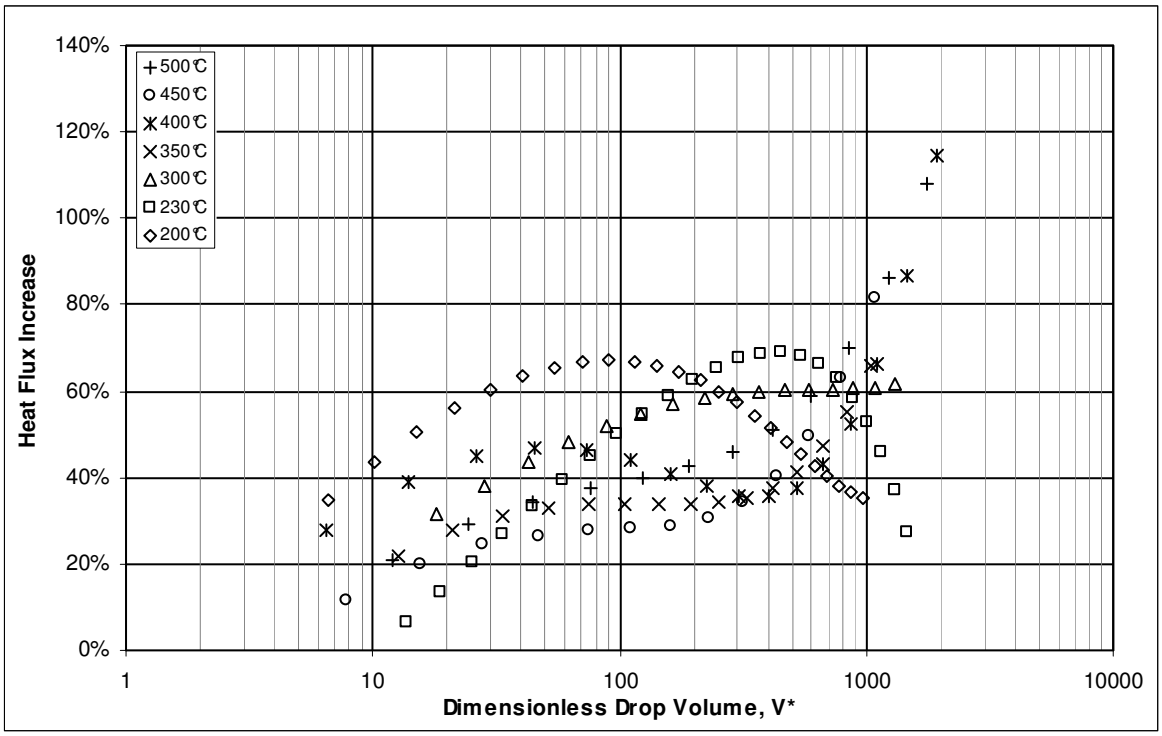

Figure 52. Increase in Heat Flux (Ethanol on CG01)

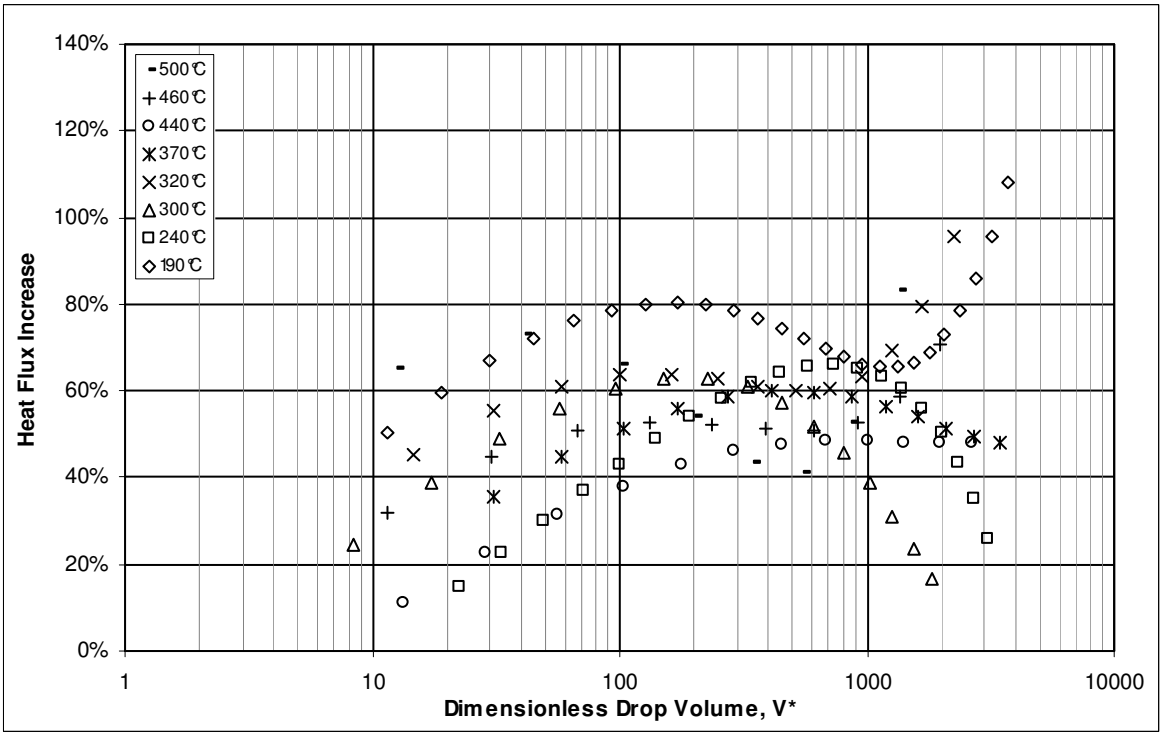

Figure 53. Increase in Heat Flux (Isopropanol on CG01)

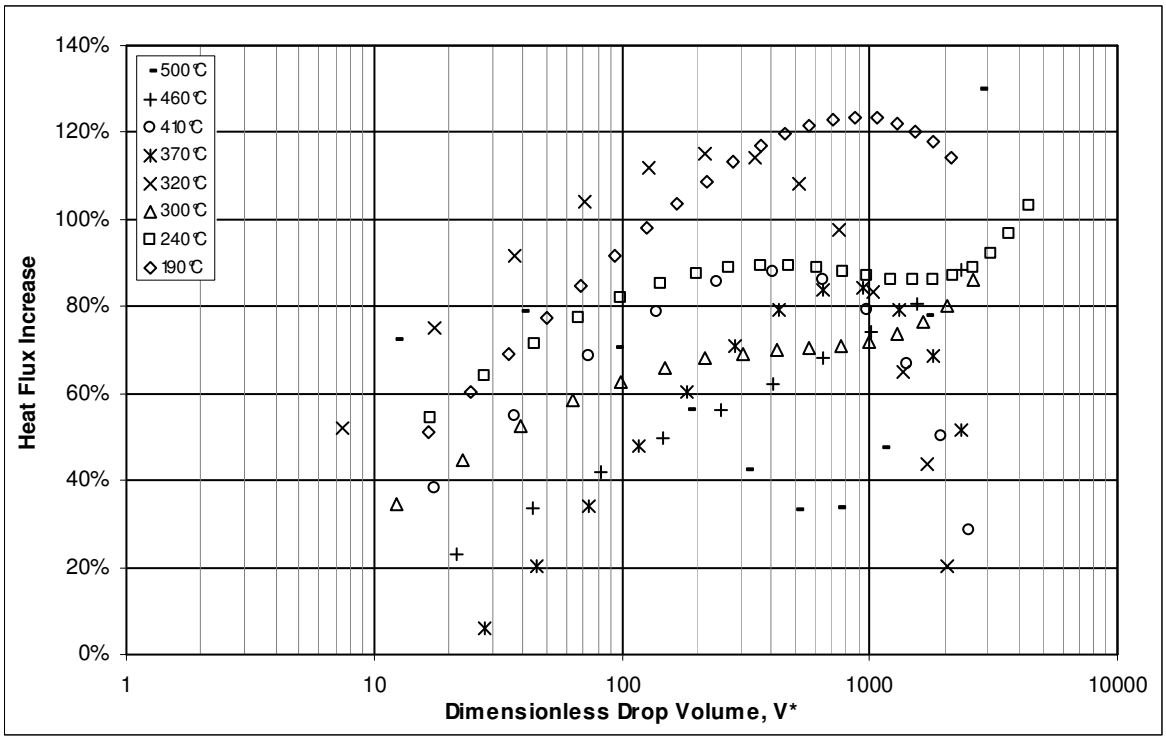

Figure 54. Increase in Heat Flux (Ethylene-Chloride on CG01)

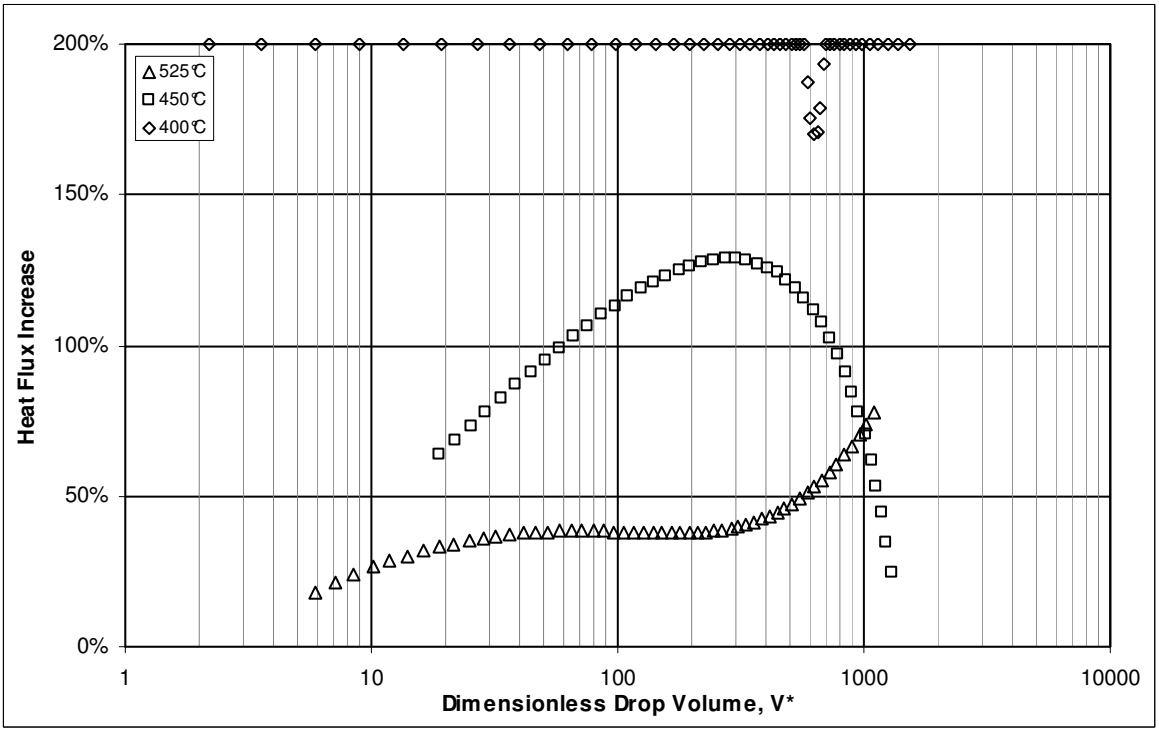

Figure 55. Increase in Heat Flux (Water on SCG02)

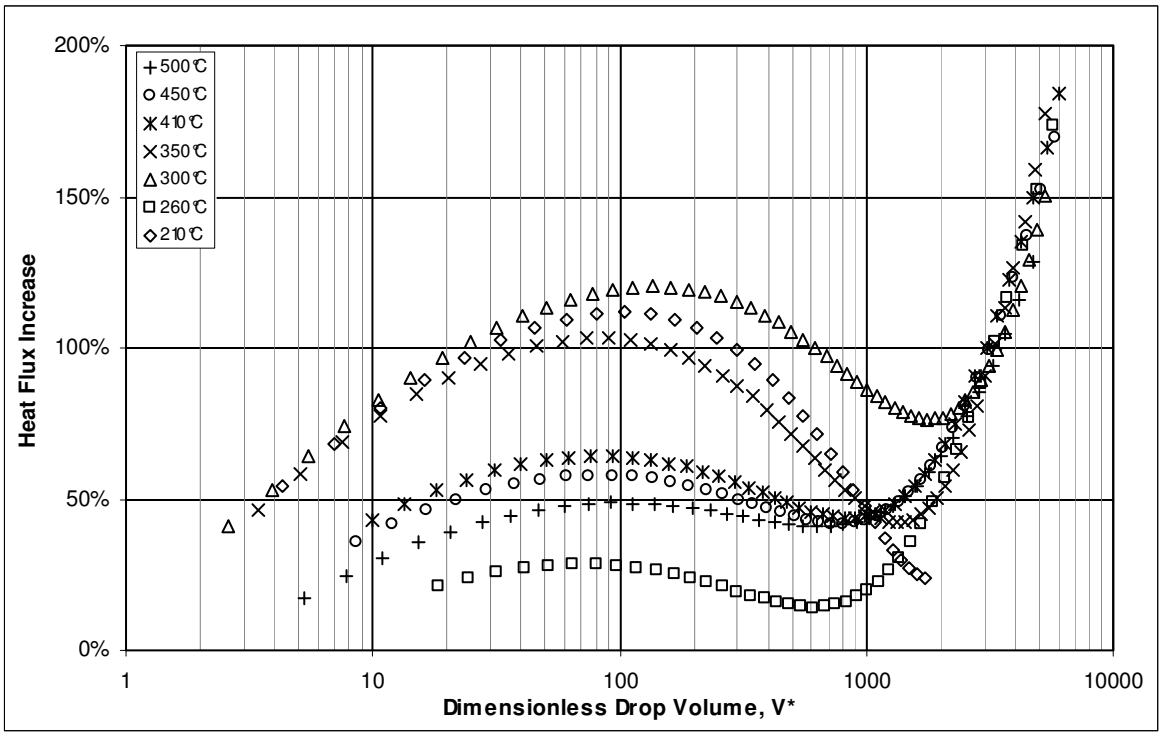

Figure 56. Increase in Heat Flux (Ethanol on SCG02)

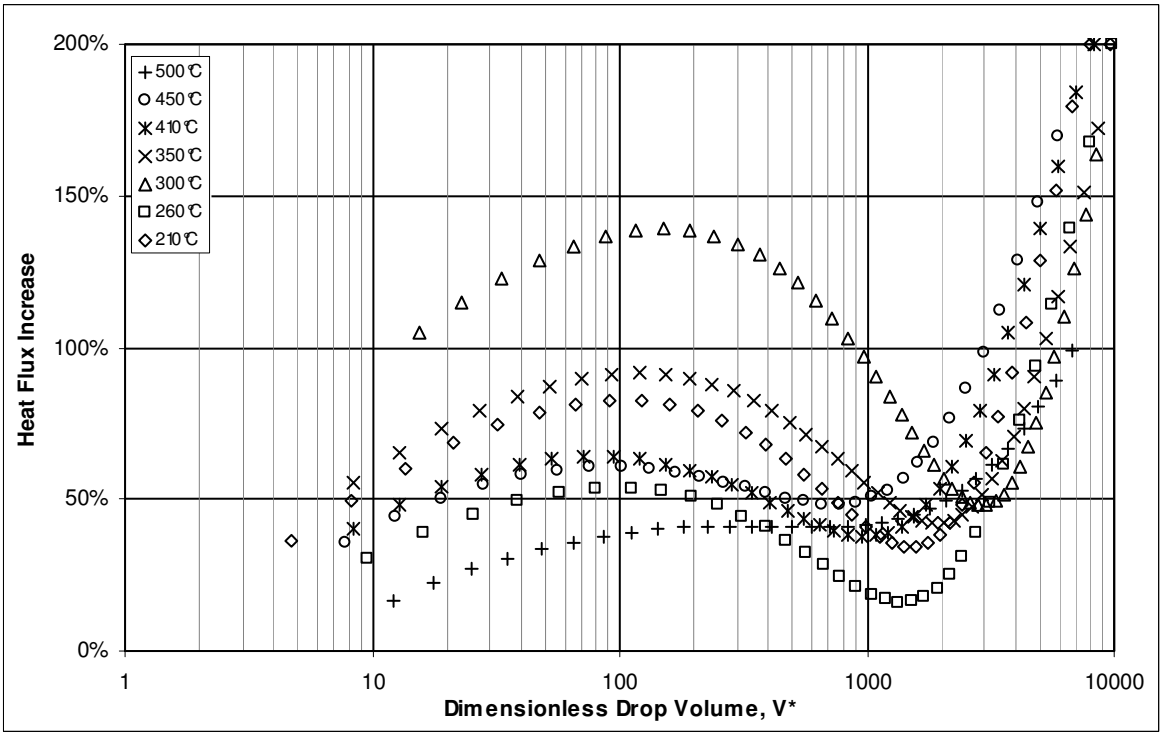

Figure 57. Increase in Heat Flux (Isopropanol on SCG02)

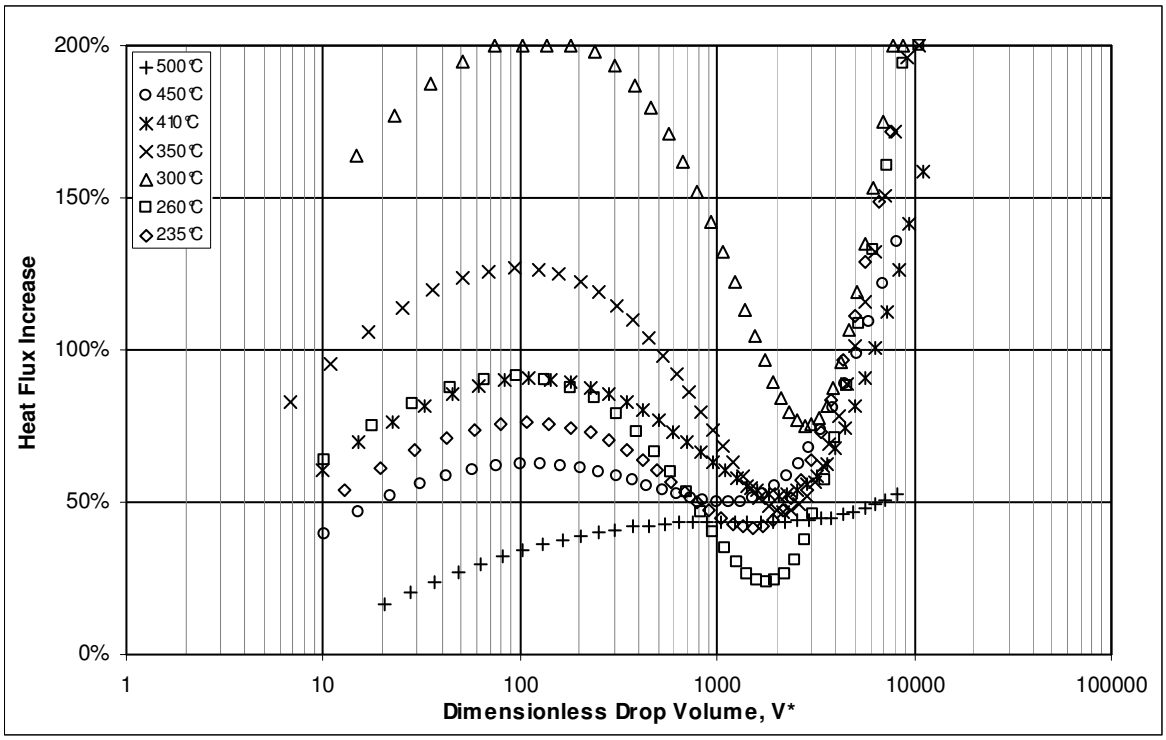

Figure 58. Increase in Heat Flux (Ethylene-Chloride on SCG02)

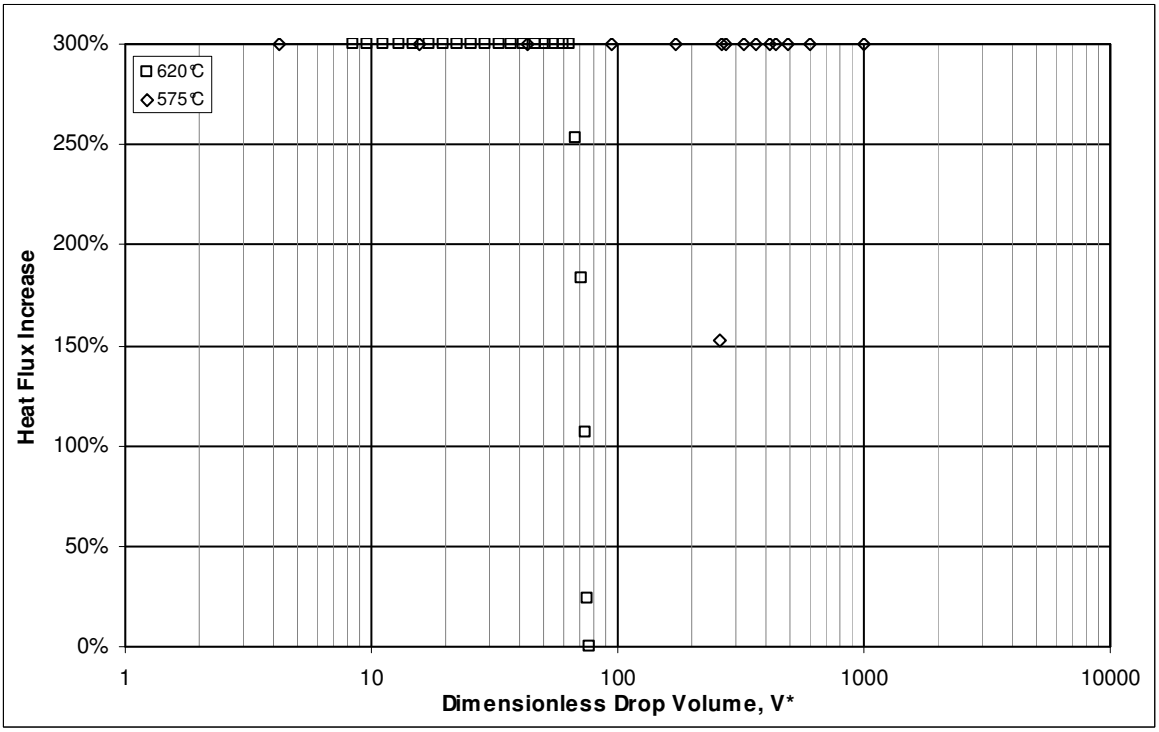

Figure 59. Increase in Heat Flux (Water on CP54)

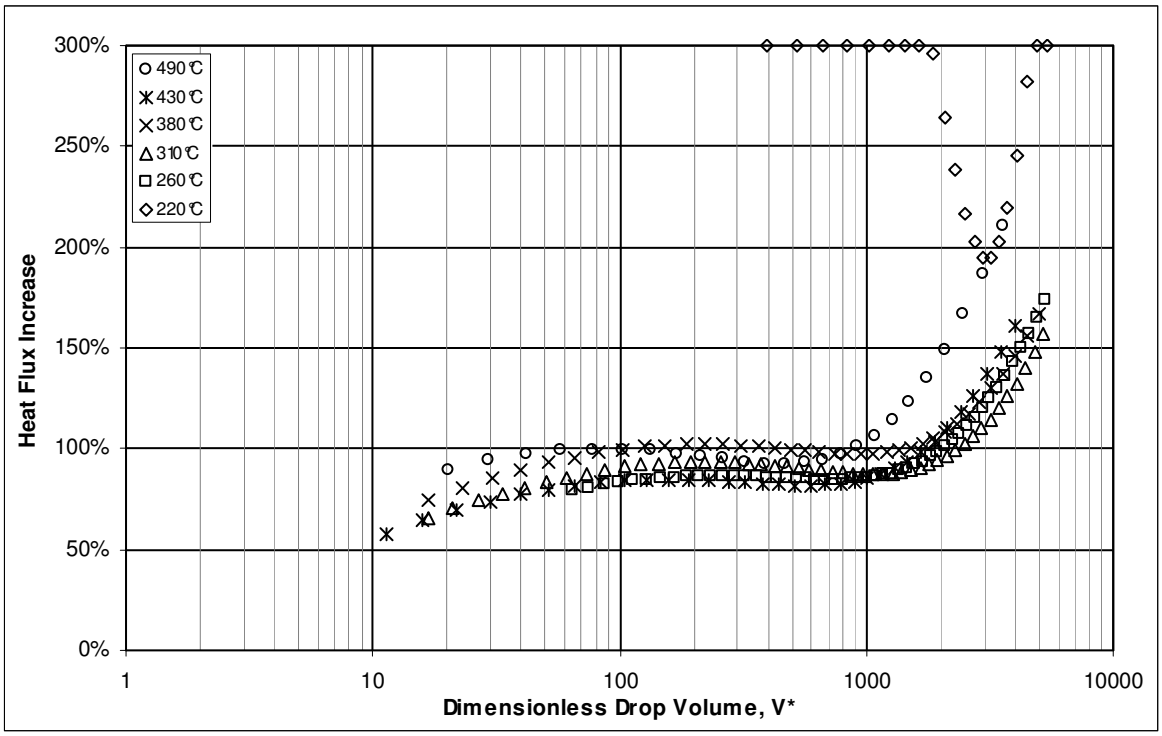

Figure 60. Increase in Heat Flux (Ethanol on CP54)

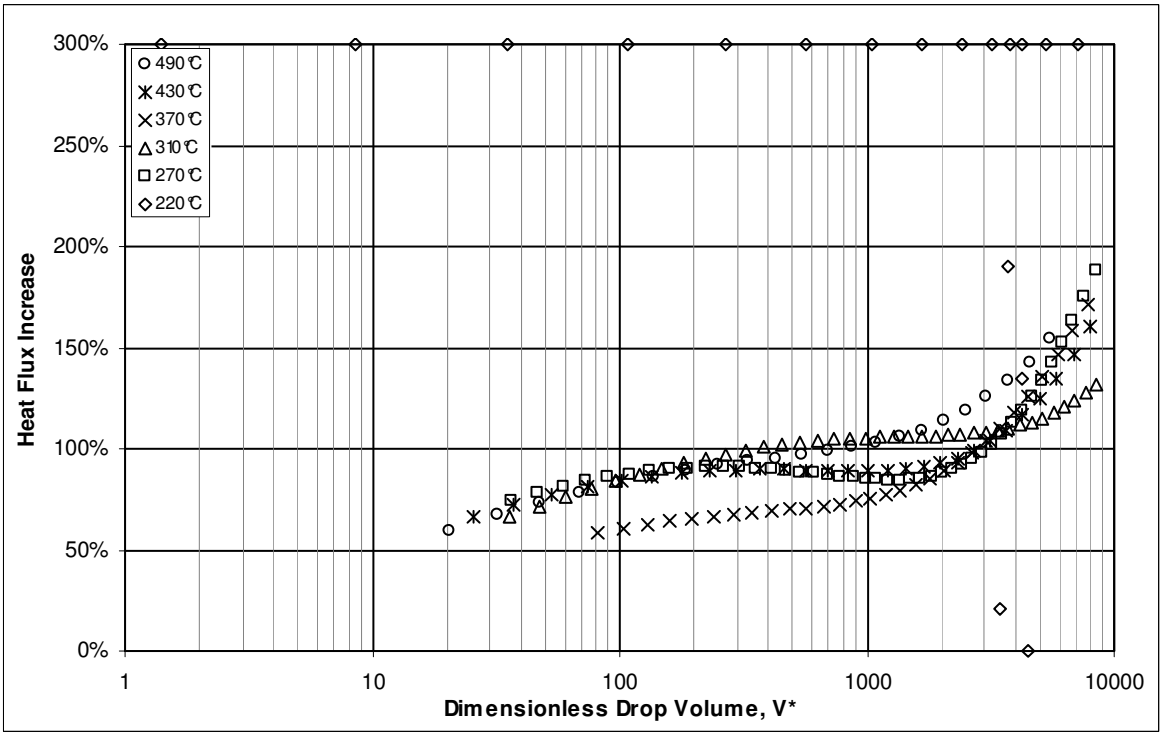

Figure 61. Increase in Heat Flux (Isopropanol on CP54)

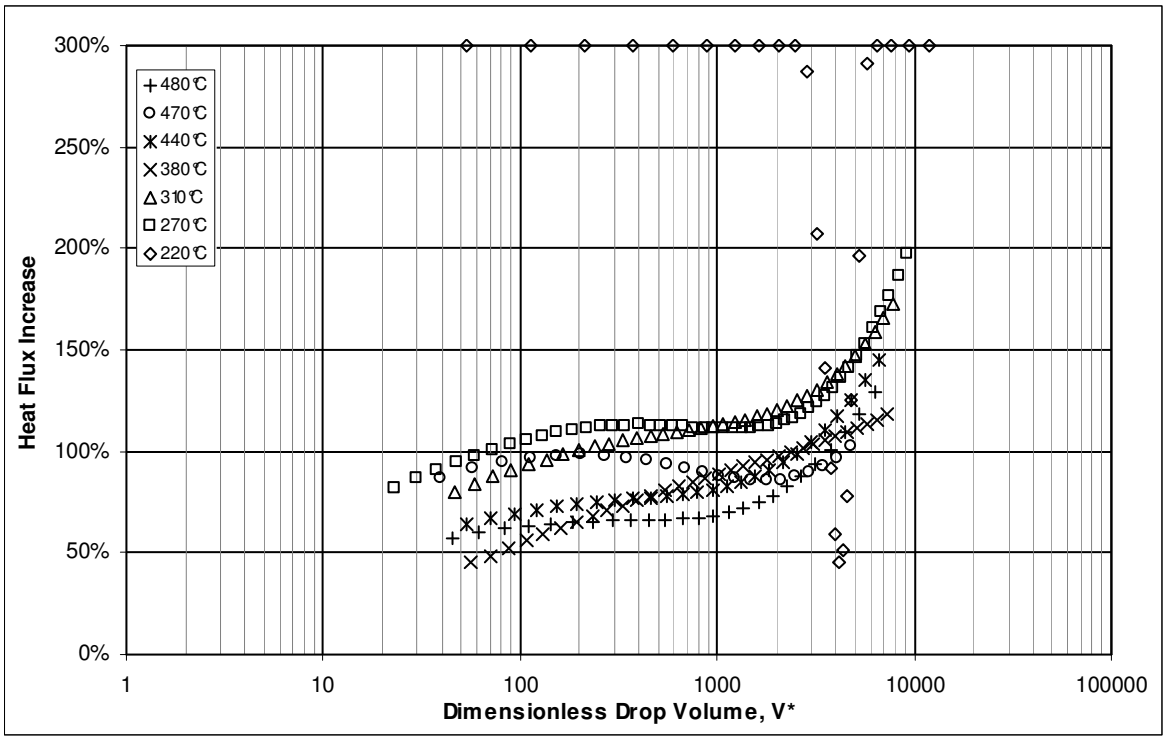

Figure 62. Increase in Heat Flux (Ethylene-Chloride on CP54)

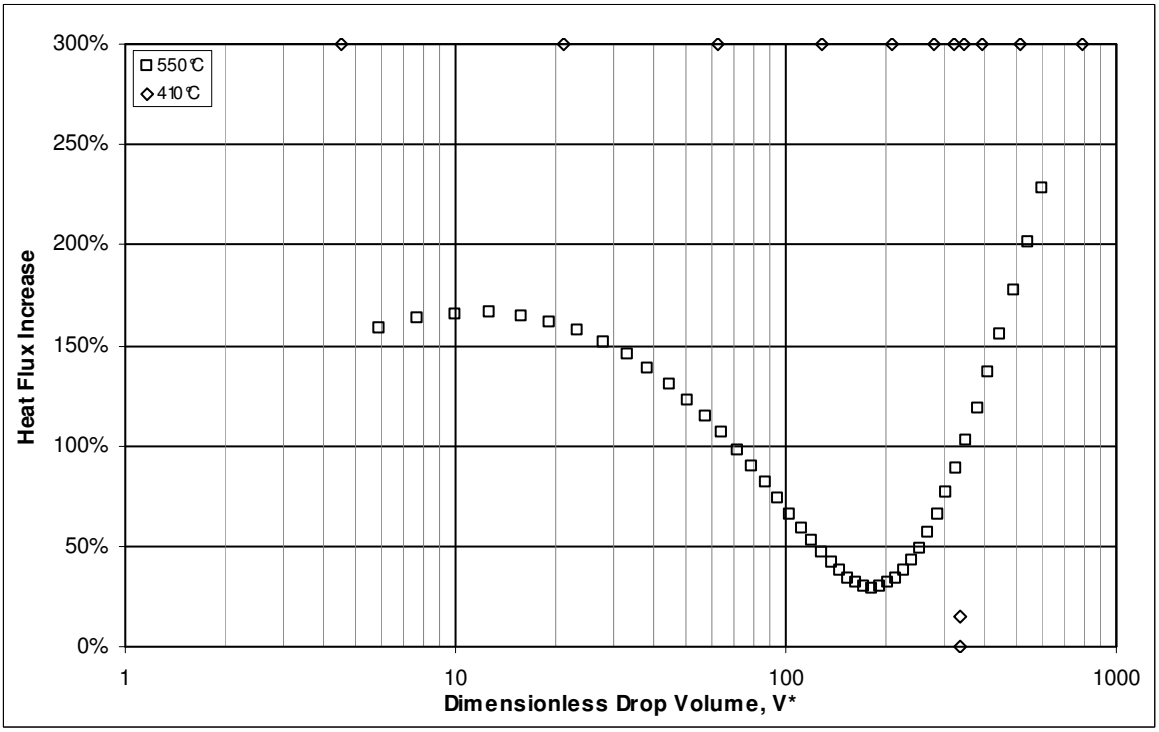

Figure 63. Increase in Heat Flux (Water on SHP2612)

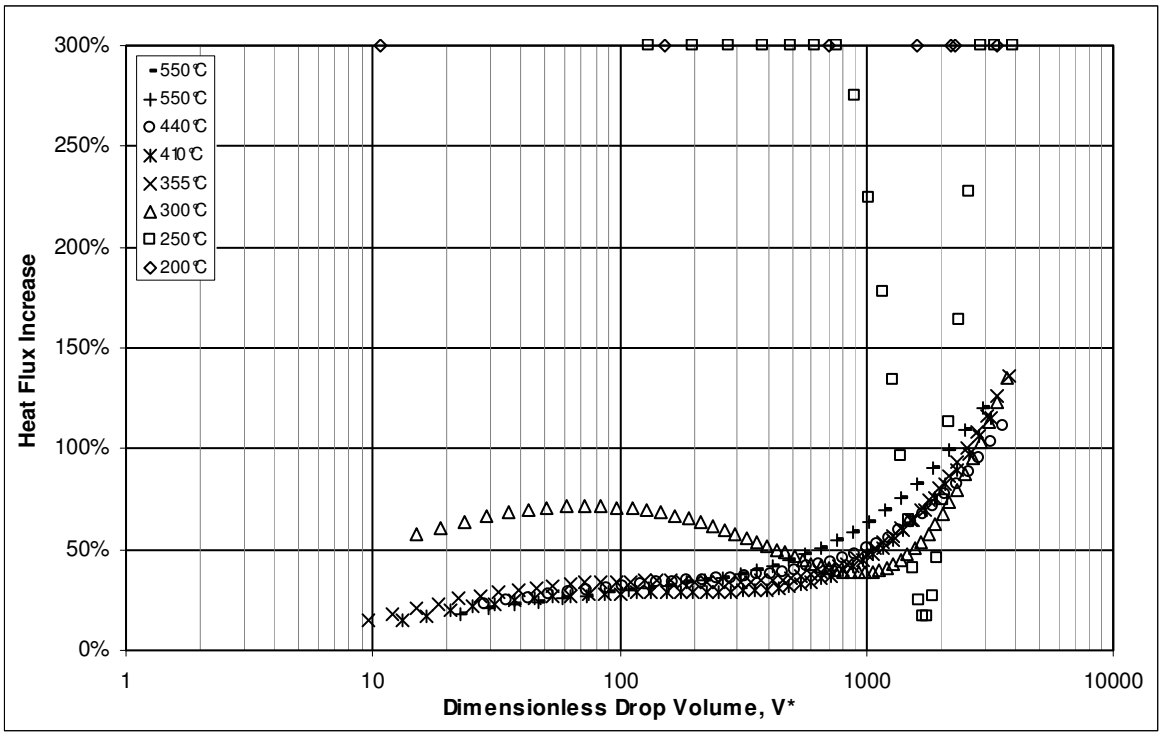

Figure 64. Increase in Heat Flux (Ethanol on SHP2612)

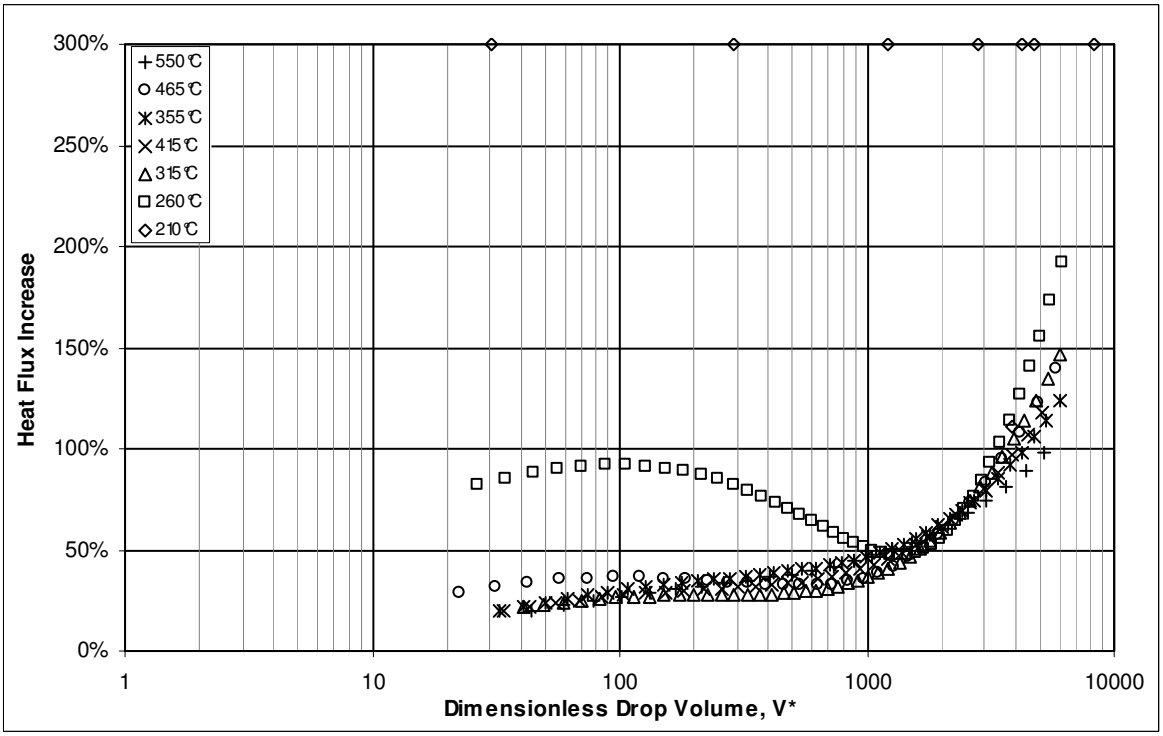

Figure 65. Increase in Heat Flux (Isopropanol on SHP2612)

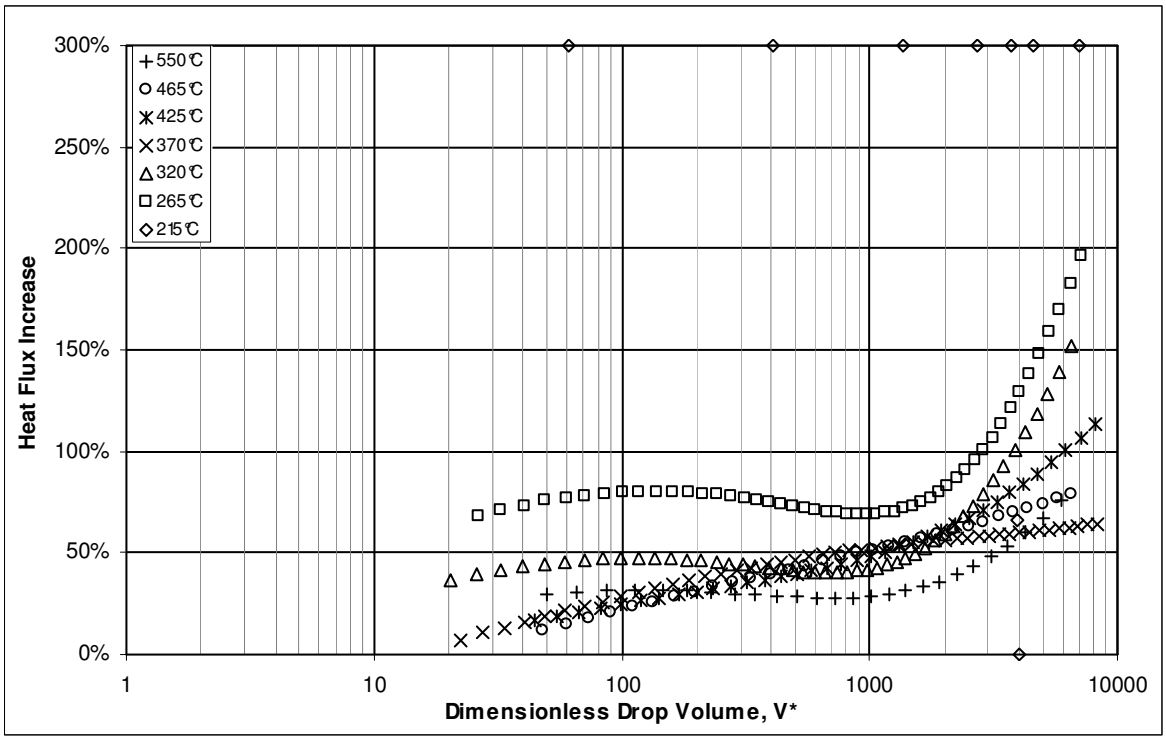

Figure 66. Increase in Heat Flux (Ethylene-Chloride on SHP2612)

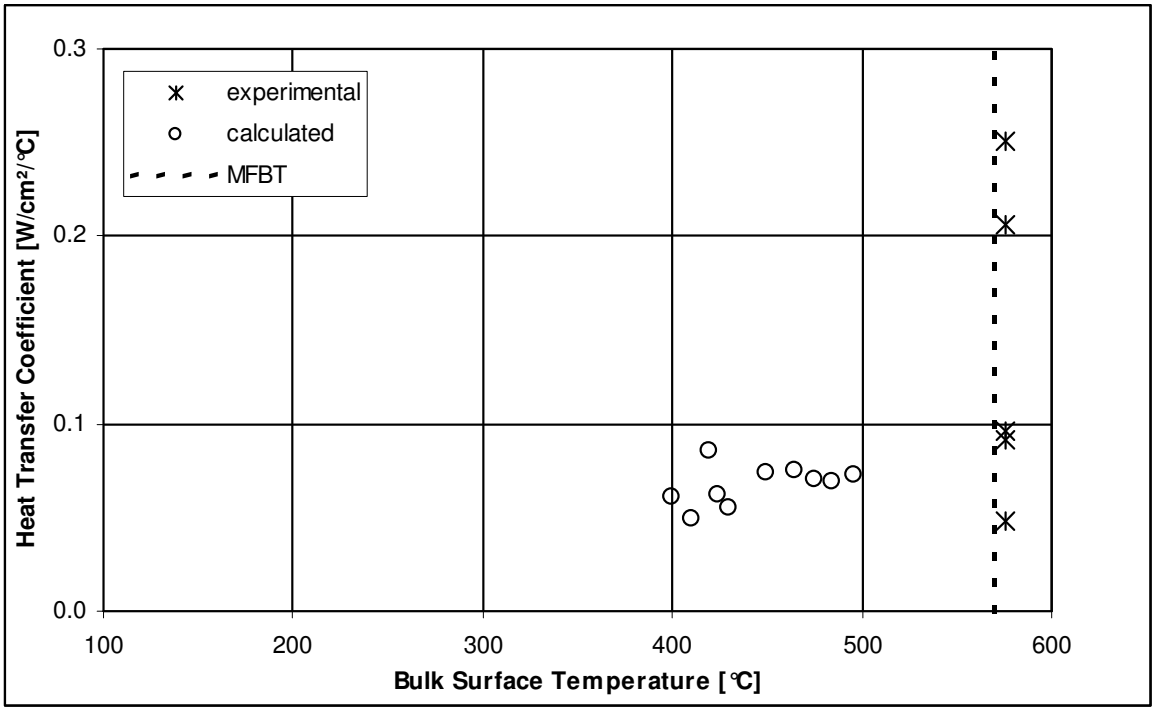

Figure 67. Experimental & Calculated HTC (Water on CP54)

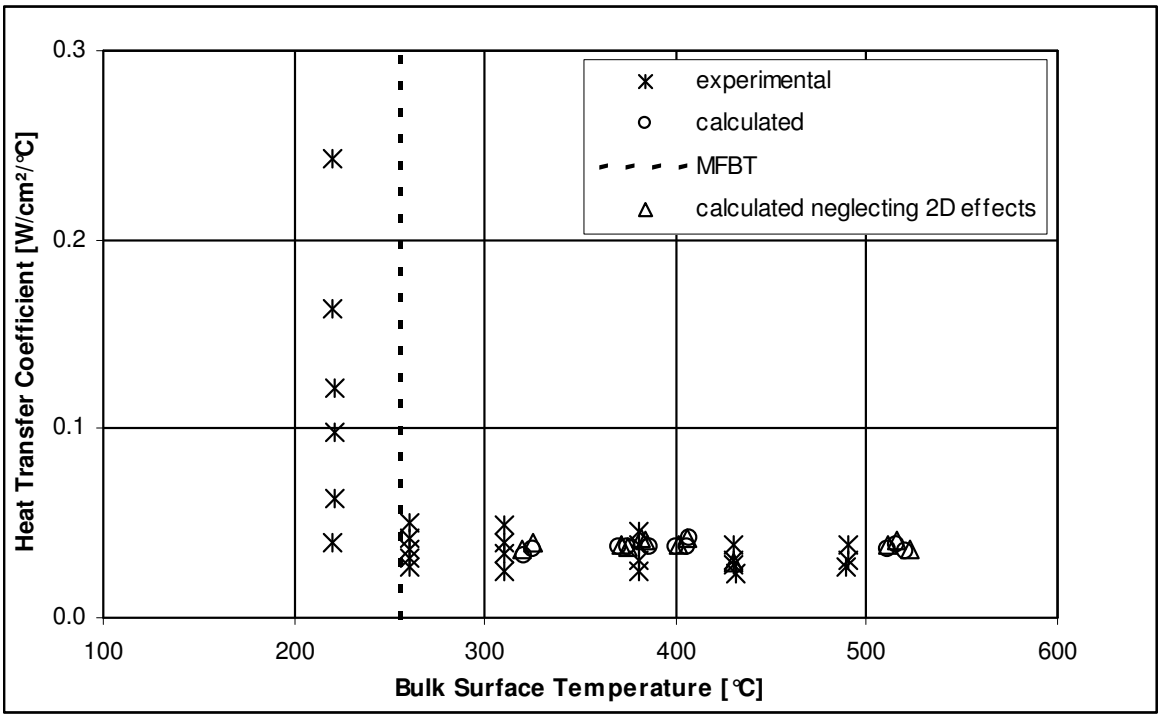

Figure 68. Experimental & Calculated HTC (Ethanol on CP54)

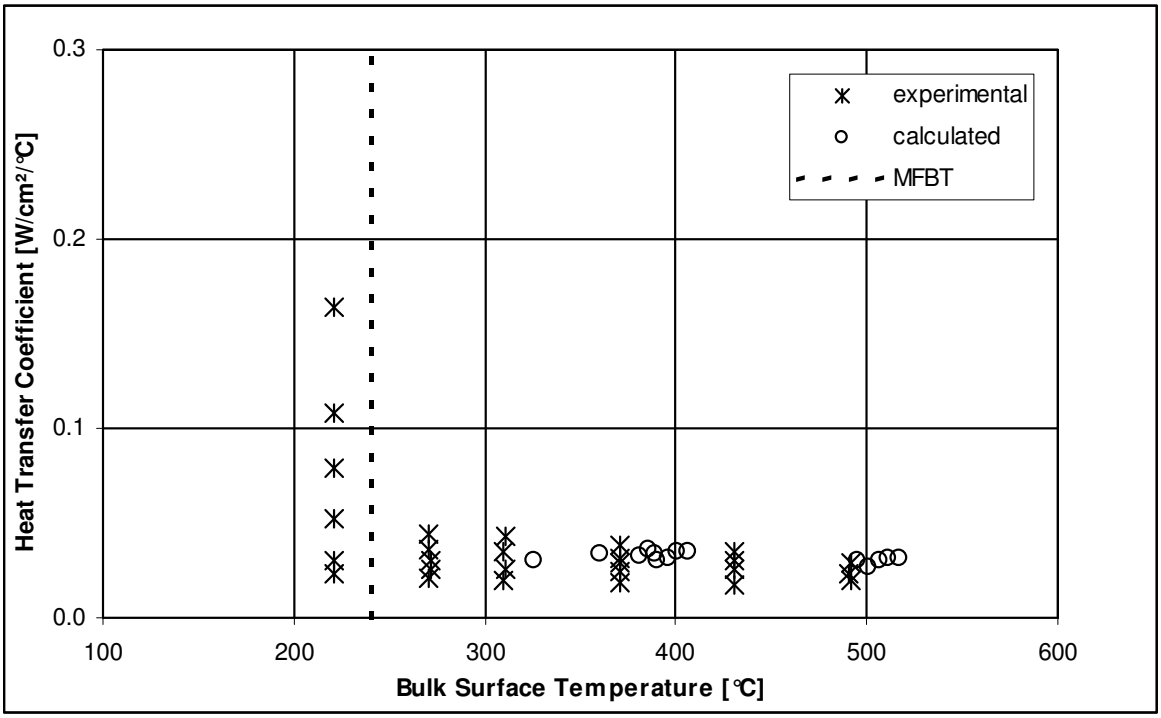

Figure 69. Experimental & Calculated HTC (Isopropanol on CP54)

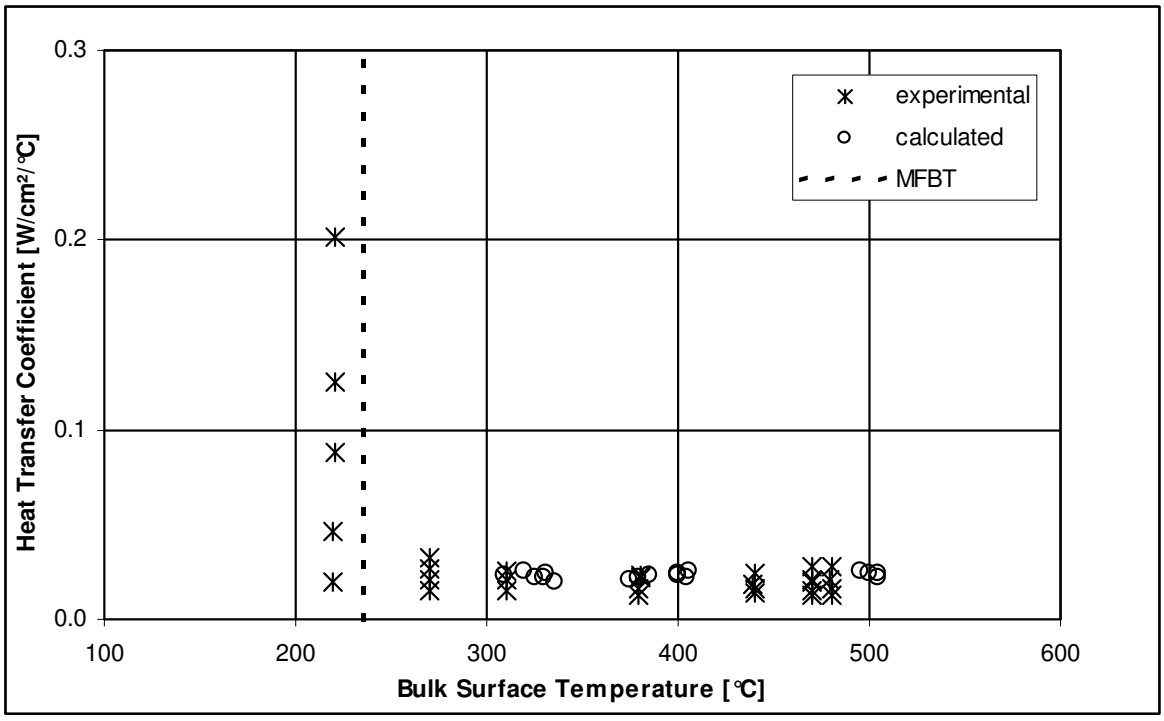

Figure 70. Experimental & Calculated HTC (Ethylene-Chloride on CP54)

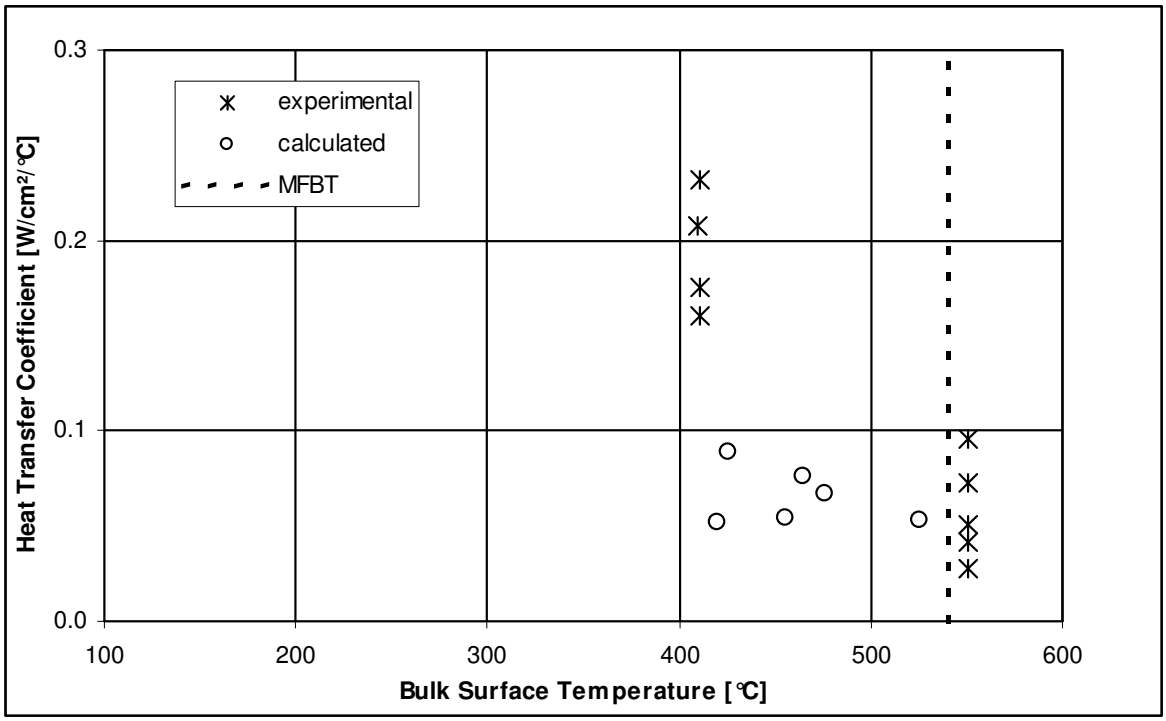

Figure 71. Experimental & Calculated HTC (Water on SHP2612)

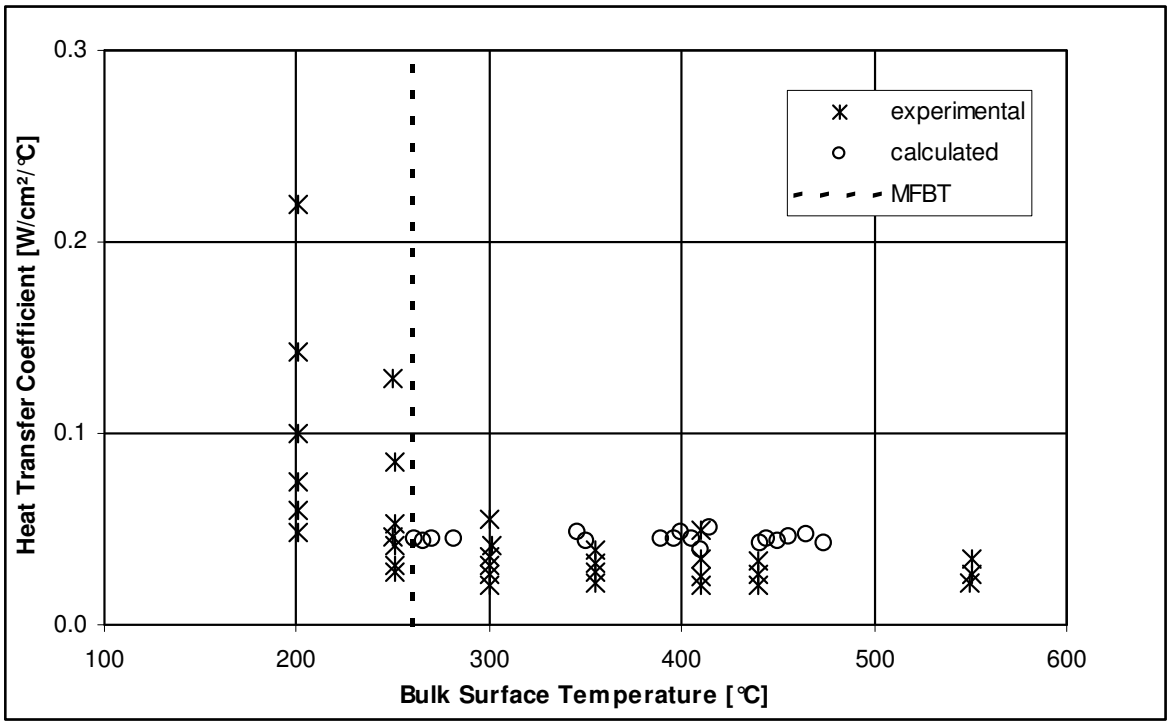

Figure 72. Experimental & Calculated HTC (Ethanol on SHP2612)

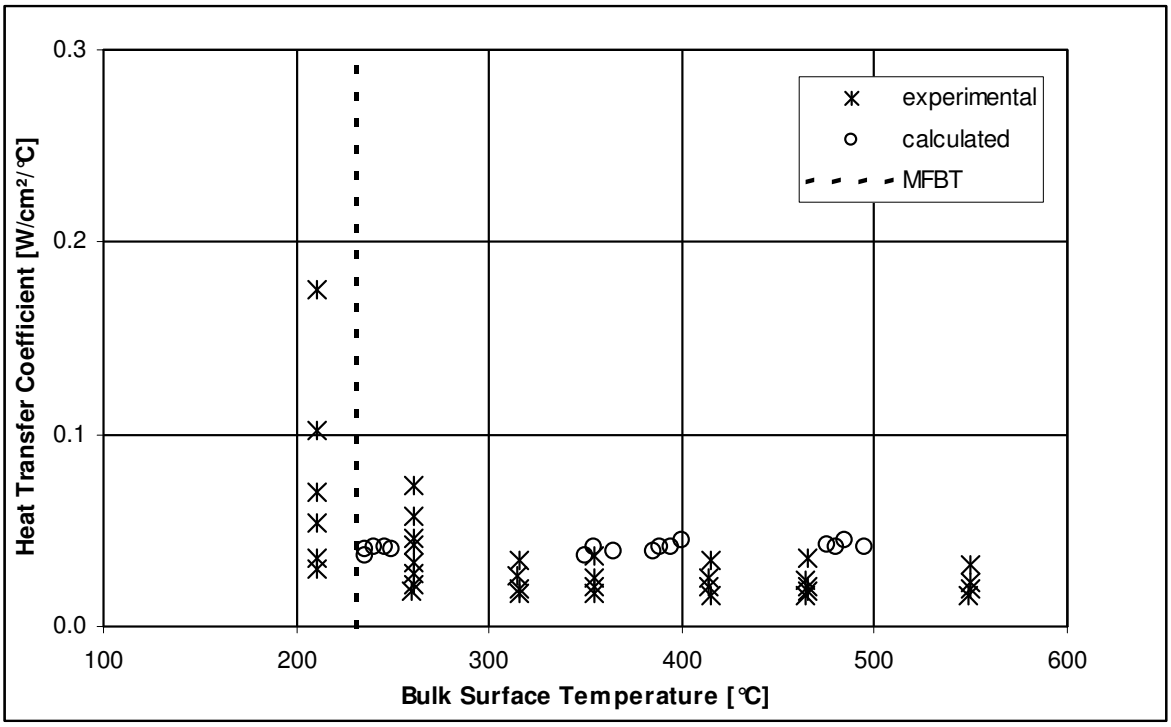

Figure 73. Experimental & Calculated HTC (Isopropanol on SHP2612)

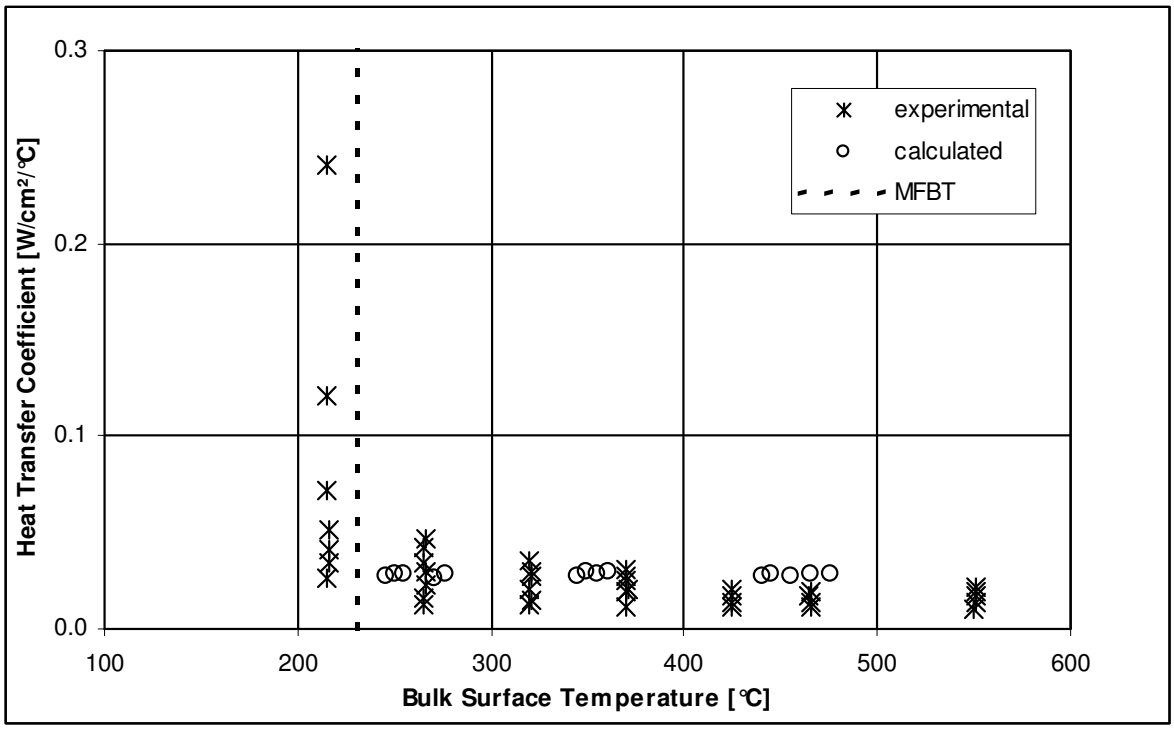

Figure 74. Experimental & Calculated HTC (Ethylene-Chloride on SHP2612)

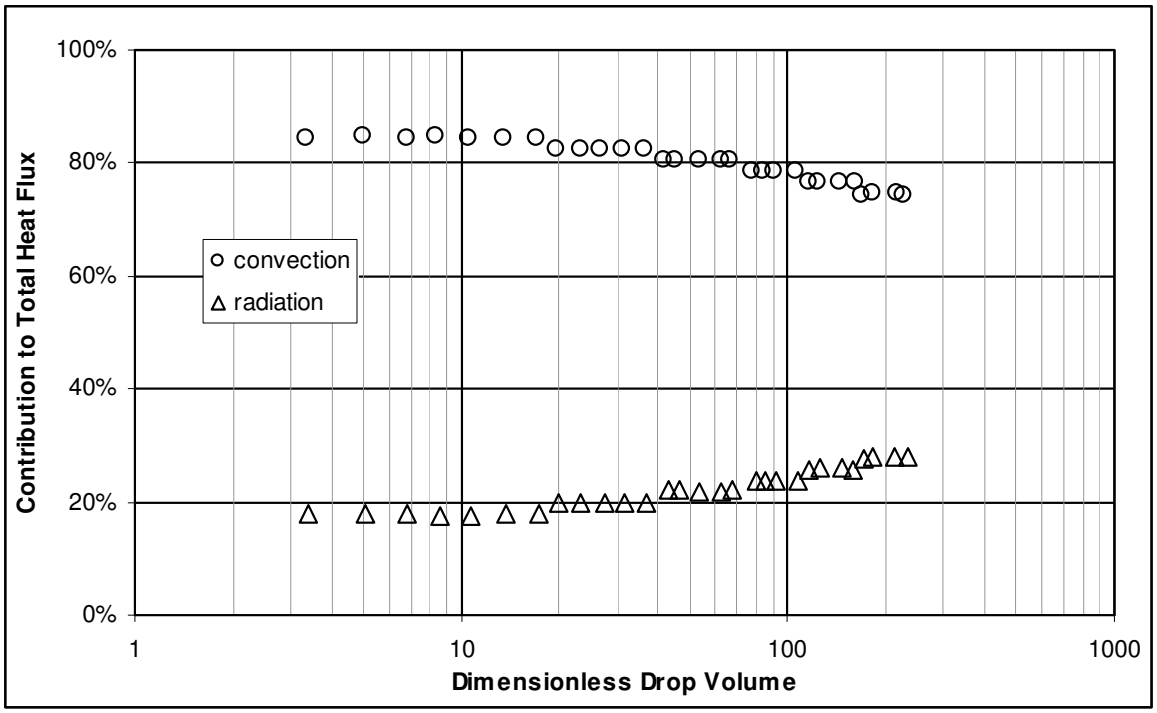

Figure 75. Sample Program Output for Smooth Surface

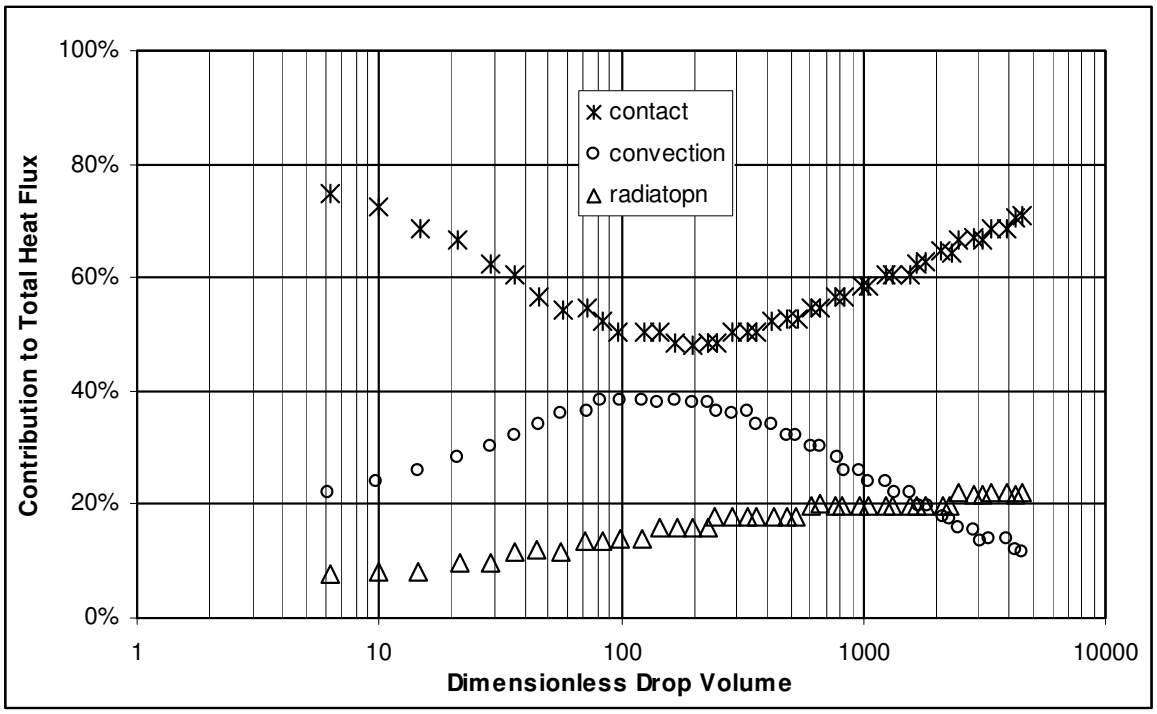

Figure 76. Sample Program Output for Rough Surface

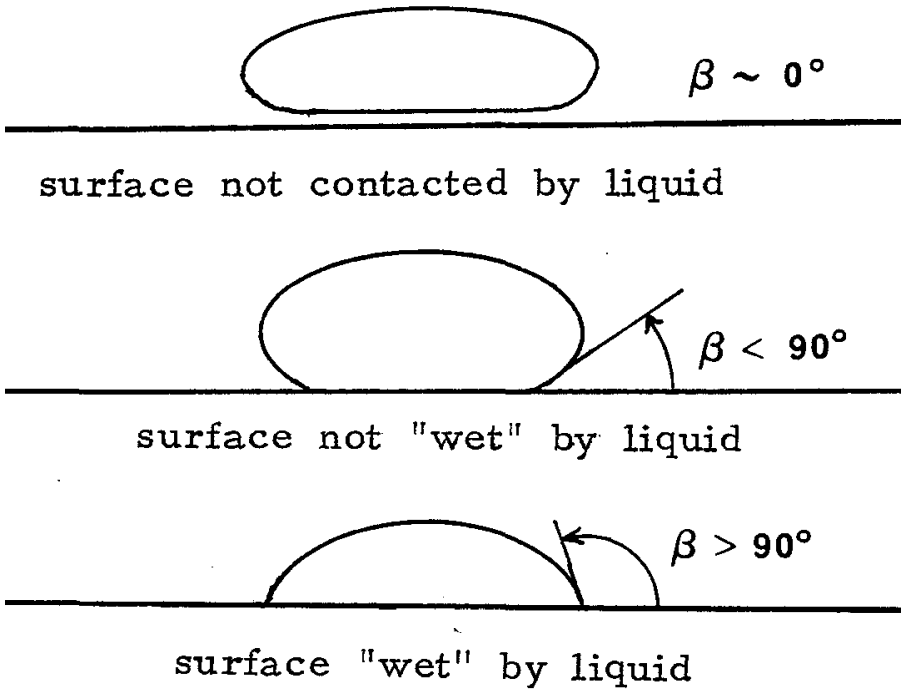

Figure 77. Surface Wetting and the Contact Angle

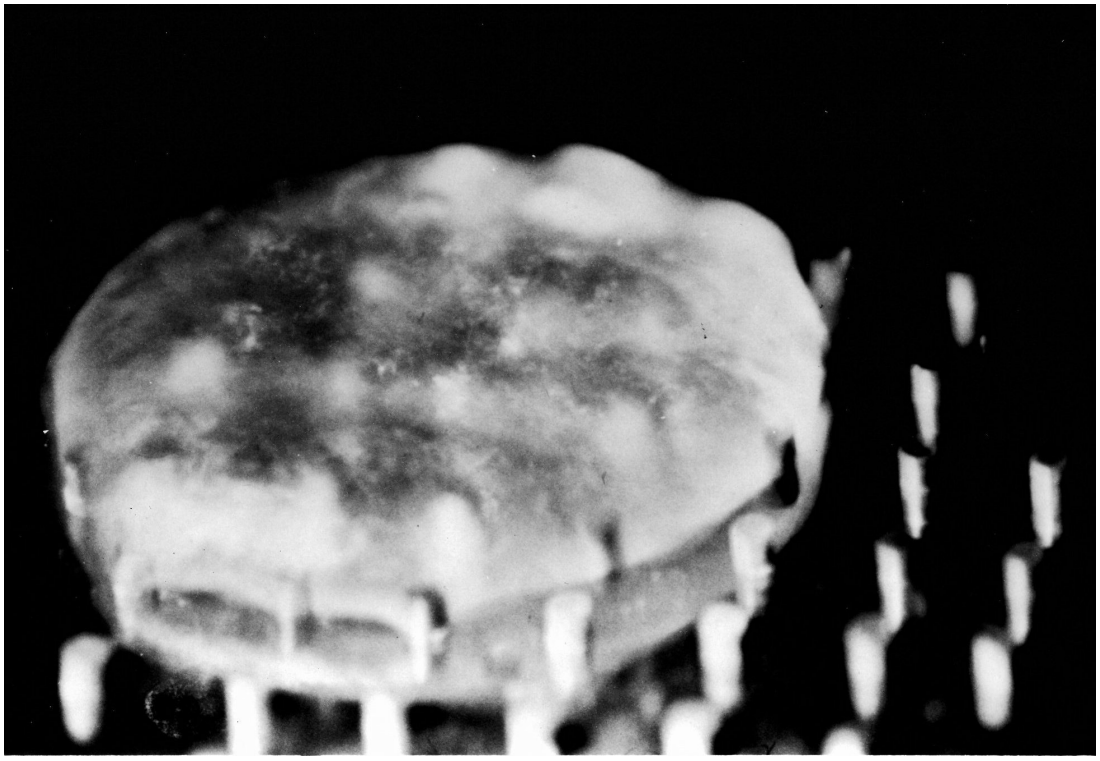

Figure 78. Water Drop Engulfing Cylindrical Pins

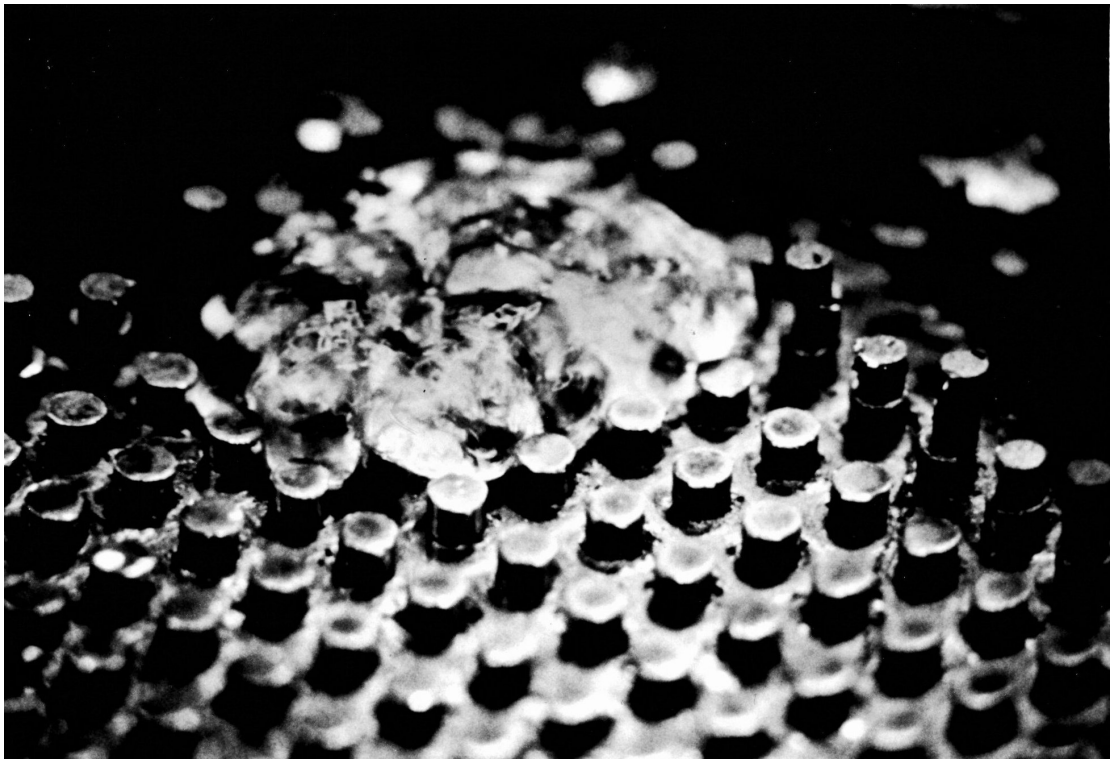

Figure 79. Ethanol Drop Resting on Cylindrical Pins

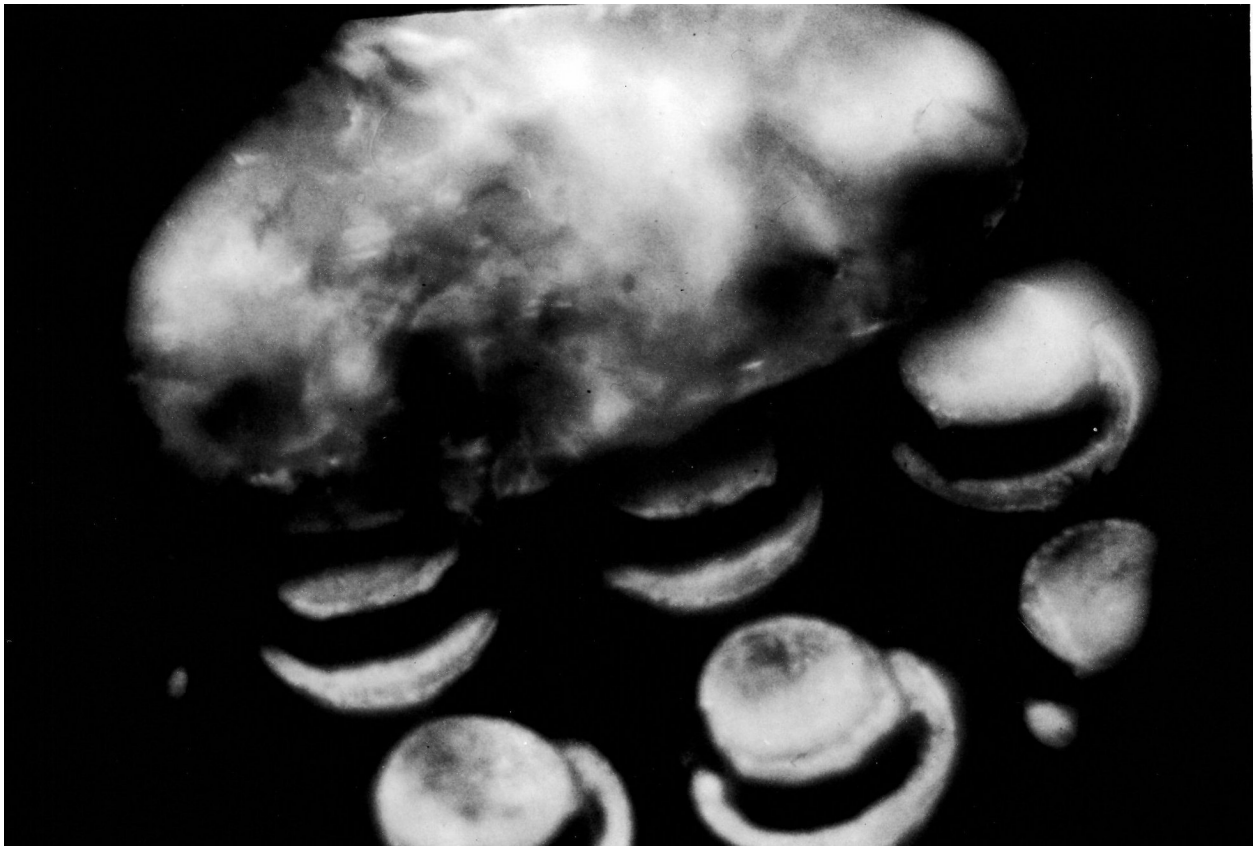

Figure 80. Edge of Ethanol Drop on Cylindrical Pins

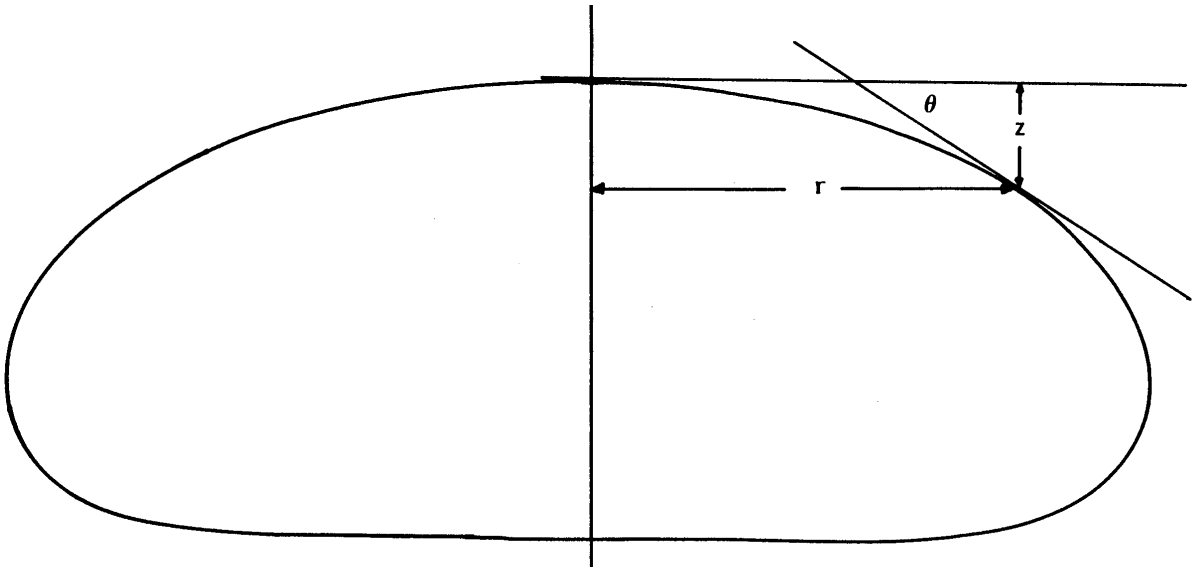

Figure 81. Sessile Drop Variables

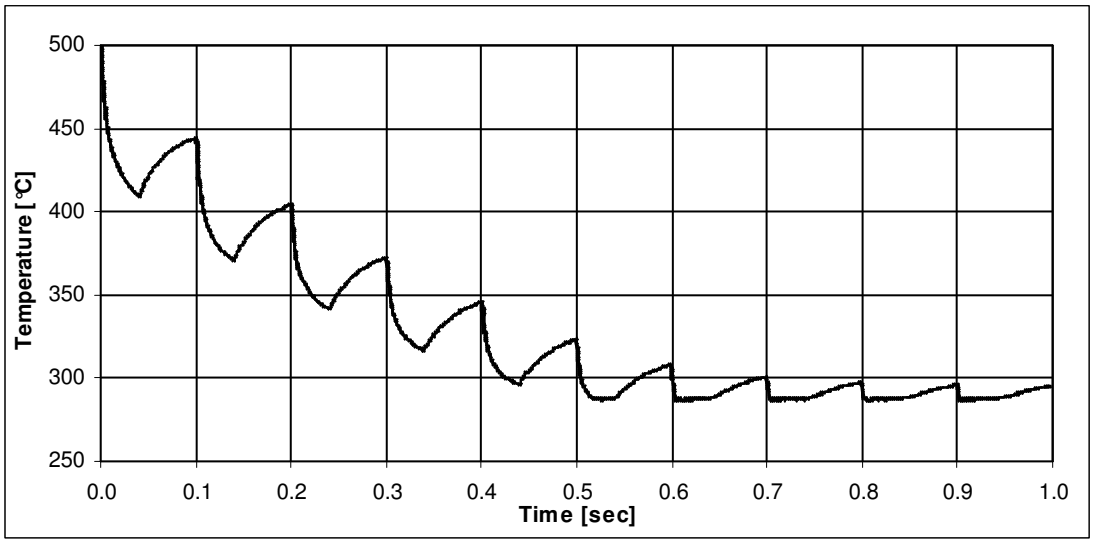

Figure 82. Computed Thermocouple Temperature

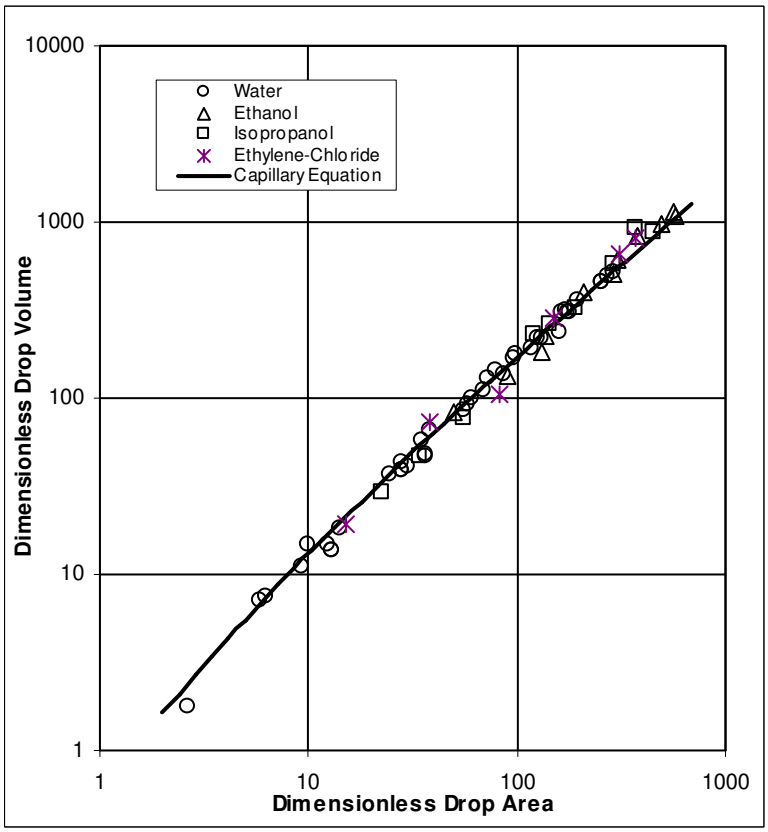

Figure 83. Comparison of All Drops to Capillary Equation

Appendix C Computer Programs

Descriptions and listings of the following computer programs are presented in this appendix in alphabetical order:

1) DATABASE (performs primary reduction of drop vaporization data, computes heat flux from drop area vs. time, and generates the database used by computer programs PLOT:FRC, PLOT:HF%, PLOT:HV, ROUGH, and SMOOTH).

2) LAMBDA (determines the value of the characteristic length parameter A, Equation 1-1, which provides the best correlation of drop volume vs. area through the numerical solution to the Laplace capillary equation as pro vided by computer program VOLUME).

3) PLOT:FRC (computes and plots the apparent relative contributions of convection, radiation, and contact to the total heat flux as a function of dimensionless superheat and dimensionless drop volume).

4) PLOT:HF% (computes and plots the percent increase in heat flux on the macro-roughened surfaces as a function of dimensionless superheat and dimensionless drop volume).

5) PLOT:HV (plots the dimensionless heat flux as a function of dimensionless superheat and dimensionless drop volume).

6) ROUGH (macro-roughened surface data reduction–computes hf, he, hR, o, B, Nuv, Nun, Nup, NuR, Q, and Bic).

7) SMOOTH (smooth surface data reduction–computes hp, hR, 5, B, Nuv, Nup, and NuR)

8) VOLUME (numerical solution to the Laplace capillary equation –computes the size and shape of sessile drops).

9) 2-D PINT (2-dimensional finite difference model for the temperature response of a cylindrical pin to pulse-like periodic liquid-solid contact)

The description of each program precedes the respective listing. All programs are coded in FORTRAN V.

Program DATABASE

Program DATABASE generates a database (card deck) of time smoothened vertically projected drop area, drop volume, and dimensionless heat flux at specified discrete time intervals throughout a drop lifetime (from deposition to complete vaporization) from fluid thermophysical properties, bulk heating surface temperature, and experimental area/time data. A sample of the output of program DATABASE is given in Tables 8 and 9 for a smooth and macro-roughened surface respectively.

The area/time approximating function is determined in program DATABASE by subroutine FINDC. Subroutine FINDC uses a modification of the method of steepest descent to solve the non-linear, constrained minimization problem associated with approximating the experimental data. The LAR (least-absolute-relative) fit was selected for the reasons given in section 6 Chapter 5. Also mentioned in Chapter 5 is the fact that this problem cannot be solved in a finite number of steps (as is the case with any set of simultaneous non-linear equations). This mathematical dilemma is discussed in some detail in Reference 63.

The method of steepest descent (which was modified for use in subroutine FINDC) follows the gradient of a specified residual until a minimum is found (Reference 63, pp. 245-247). The residual in this case is the sum of the absolute-relative discrepancies between the experimental area/time data and the corresponding values of the approximating function (Equation 5-17). Minimizing this residual produces, by its definition, the LAR fit (Reference 63, p. 25). This minimization problem is analogous to location the minimum elevation of a relief map. The major differences between the present minimization problem and the relief map analogy are: 1) there are more than the two variables of latitude and longitude involved in determining what is analogous to elevation and 2) the entire relief map cannot be viewed at any one time (analogously, the elevation at any specified point may be computed but the elevation is only known at a finite number of discrete points rather than over a continuous region).

This application of the method of steepest descent requires solving a set of non-linear simultaneous equations at each step (specified location above). Damped Newton iteration (Reference 63, pp. 181-187) is used to solve these sets of equations. The method of steepest descent must be modified for the present application for two reasons: 1) certain constraints are placed on the solution (Equation 5-18) and 2) the gradient of the residual may become discontinuous at an indeterminate number of locations (viz. whenever the absolute value of the relative discrepancy at any one point passes through zero).

Since the gradient of the residual may become discontinuous, the gradient of the gradient (which is the tensor matrix called the Hessian, (e.g., [63]) will become indeterminate and thus non-invertible. (Newton iteration requires the solution of a set of simultaneous equations that involves the inversion of the Hessian matrix. If the Hessian matrix is non-invertible the next step in the iteration can not be computed.). This discontinuity in the gradient of the residual (which results in the Hessian matrix becoming non-invertible) frequently occurs as a minimum is approached. Thus the method of steepest descent can rarely locate a minimum. The relief map analogy is illustrative at this point. The present minimization problem is analogous to a relief map having one large valley whose sides are marked by many deep ruts (which may not necessarily lead anywhere near the bottom of the valley).

The present algorithm is written such that when one of these mathematical ruts is encountered the method of steepest descent is abandoned and the method of random

displacements is activated. The method of displacements "displaces" the solution randomly from the location of the rut. In the event that the program is unable to get out of the rut in 100 iterations the execution is terminated (this problem never occurred in reducing the 125 data sequences in the present study). Of course, if the program never encounters one of these mathematical ruts the method of steepest descent will iterate to a specified convergence. The following is a listing of program DATABASE. Comments are provided in the listing at various points to detail the specifics of program operation.

```
CREATE PROGRAM TO REDUCE LEIDENFROST FILM BOILING DATA
C
      DIMENSION C(4),A(99),AL(99),ALS(99),T(99)                          DATABASE
      INTEGER TITLE(40)                                                  DATABASE
      REAL LAMBDA,KG,MUG,KS,KF,NUV,L                                     DATABASE
C  DEFINE PHYSICAL CONSTANTS                                             DATABASE
      DATA PI,G,SIGMA/3.14159,980.,5.6688E-12/                           DATABASE
C  CONVERGENCE INFORMATION WILL BE PRINTED FOR IPRT>1                     DATABASE
C  PLOT OF EXPERIMENTAL AND SMOOTHENED AREA VS. TIME WILL BE PRINTED      DATABASE
C  FOR IPRT>0                                                            DATABASE
      IPRT=0                                                             DATABASE
      IPRT=1                                                             DATABASE
      IPRT=2                                                             DATABASE
C  DATABASE (CARD DECK) WILL BE PUNCHED FOR IPUNCH>0                      DATABASE
      IPUNCH=0                                                           DATABASE
      IPUNCH=1                                                           DATABASE
C  READ IN THE ROLL#, SEQUENCE#, THE NUMBER OF POINTS, THE TIME STEP      DATABASE
C  AND THE BULK SURFACE TEMPERATURE                                       DATABASE
    1 READ(5,1000) NROLL,NSEQ,NPOINT,DT,TW                               DATABASE
 1000 FORMAT(I2,1X,I3,1X,I2,1X,F3.0,1X,F4.0)                             DATABASE
      IF(NROLL.LE.0.OR.NPOINT.LT.2.OR.NPOINT.GT.99) STOP                 DATABASE
C  PUNCH NEW IDENTIFIER CARD                                             DATABASE
      IF(IPUNCH.NE.0) WRITE(7,1000) NROLL,NSEQ,NPOINT,DT,TW              DATABASE
C  READ IN TITLE                                                         DATABASE
      READ(5,2000) (TITLE(I),I=1,40)                                     DATABASE
 2000 FORMAT(40A2)                                                       DATABASE
C  PUNCH NEW TITLE CARD                                                  DATABASE
      IF(IPUNCH.NE.0) WRITE(7,2000) (TITLE(I),I=1,40)                    DATABASE
C  READ IN THERMOPHYSICAL PROPERTIES                                     DATABASE
      READ(5,3000) LAMBDA,CPG,KG,RHOF,RHOG,MUG,KS,EPS,TL,HFG,KF         DATABASE
 3000 FORMAT(F6.4,F5.3,E9.3,F6.4,F7.6,E9.3,F5.4,F7.5,F5.1,F6.1,E9.3)     DATABASE
C  PUNCH NEW THERMOPHYSICAL PROPERTY CARD                                DATABASE
      IF(IPUNCH.NE.0) WRITE(7,3000) LAMBDA,CPG,KG,RHOF,RHOG,MUG,KS,EPS,  DATABASE
     >TL,HFG,KF                                                          DATABASE
C  CALCULATE DIMENSIONLESS SUPERHEAT                                     DATABASE
      SH=CPG*(TW-TL)/HFG                                                 DATABASE
C  CALCULATE RADIATION HEAT TRANSFER COEFFICIENT                         DATABASE
      HR=SIGMA*((TW+273.15)**4-(TL+273.15)**4)/(TW-TL)                   DATABASE
C  READ IN AREA DATA                                                     DATABASE
      READ(5,4000) (A(I),I=1,NPOINT)                                     DATABASE
 4000 FORMAT(10F8.3)                                                     DATABASE
C  CALCULATE TIME VECTOR                                                 DATABASE
      DO 2 I=1,NPOINT                                                    DATABASE
    2 T(I)=DT*FLOAT(I-1)                                                 DATABASE
C  FIND THE COEFFICIENTS WHICH CORRESPOND TO A BEST-FIT OF THE DATA       DATABASE
      CALL FINDC(A,T,DT,NPOINT,C,DMIN,IPRT,AL)                           DATABASE
C  WRITE HEADING ON NEW PAGE                                             DATABASE
      WRITE(6,5000) NROLL,NSEQ,(TITLE(I),I=1,40)                         DATABASE
 5000 FORMAT(1H1,32X,39HLEIDENFROST FILM BOILING DATA REDUCTION.//,      DATABASE
     >42X,4HROLL,I3,3X,8HSEQUENCE,I4,/,12X,40A2,//)                      DATABASE
      WRITE(6,5100) (C(I),I=1,4),DMIN                                    DATABASE
 5100 FORMAT(5X,67HCURVE FIT OF AREA(TIME) DATA BY LEAST ABSOLUTE RELATI DATABASE
     >VE DISCREPANCY.                                                    DATABASE
     >/,5X,33HA(T)=EXP(C1*(C2-T)*(C3-T)/(C4-T)),/,                       DATABASE
     >5X,3HC1=,E12.6,3X,3HC2=,E12.6,3X,3HC3=,E12.6,3X,3HC4=,E12.6,       DATABASE
     >3X,12HDISCREPANCY=,F4.1,1H%,//)                                    DATABASE
      WRITE(6,5200) LAMBDA,CPG,KG,RHOF,RHOG,MUG,KS,EPS,TL,HFG,KF         DATABASE
 5200 FORMAT(5X,6HLAMBDA,6X,3HCPG,10X,2HKG,8X,4HRHOF,7X,4HRHOG,10X,     DATABASE
     >3HMUG,9X,2HKS,7X,7HEPSILON,6X,4HTSAT,5X,3HHFG,10X,2HKF,/,          DATABASE
     >5X,F6.4,5X,F5.3,5X,E9.3,4X,F6.4,4X,F7.6,6X,E9.3,4X,F5.4,6X,F7.5,  DATABASE
     >5X,F5.1,4X,F6.1,5X,E9.3,//)                                        DATABASE
      WRITE(6,5300)                                                      DATABASE
 5300 FORMAT(8X,1HT,7X,1HA,6X,5HASMTH,3X,13H-D(LN(AS))/DT,4X,2HA*,4X,    DATABASE
     >2HV*,7X,1HV,6X,1HL,7X,4HHEXP,6X,5HHE/HB,3X,3HNUV,4X,1HH,/,         DATABASE
     >6X,5H(SEC),2X,7H(CM**2),2X,7H(CM**2),4X,9H(SEC**-1),18X,           DATABASE
     >7H(CM**3),2X,4H(CM),2X,11H(V/CM**2/C))                             DATABASE
      DO 4 I=1,NPOINT                                                    DATABASE
C  CALCULATE SMOOTHENED AREA                                             DATABASE
      ALS(I)=C(1)*(T(I)-C(2))*(T(I)-C(3))/(C(4)-T(I))                    DATABASE
      AS=EXP(ALS(I))                                                     DATABASE
C  CALCULATE DERIVITIVE OF LN(AREA) WITH RESPECT TO TIME                 DATABASE
      DLNADT=-(C(1)*((T(I)-C(2))+(T(I)-C(3)))+ALS(I))/(C(4)-T(I))        DATABASE
C  CALCULATE DIMENSIONLESS AREA                                          DATABASE
      ASTAR=AS/LAMBDA**2                                                 DATABASE
C  DETERMINE DIMENSIONLESS VOLUME FROM DIMENSIONLESS AREA                DATABASE
      VSTAR=VOFA(ASTAR)                                                  DATABASE
C  CALCULATE VOLUME                                                      DATABASE
      V=VSTAR*LAMBDA**3                                                  DATABASE
C  CALCULATE DROP THICKNESS                                              DATABASE
      L=V/AS                                                             DATABASE
C  CALCULATE EXPERIMENTAL HEAT TRANSFER COEFFICIENT                      DATABASE
      HEXP=RHOF*HFG*DVDA(ASTAR)*LAMBDA*DLNADT/(TW-TL)                    DATABASE
      B=SH                                                               DATABASE
```

```
      DG=B*KF/CPG                                                       DATABASE
      DO 3 ITER=1,10                                                    DATABASE
      DELTA=((3 +9 *DG/20 /MUG)*DG*MUG*AS**2/                           DATABASE
     )(2 *PI*G*RHOG*(RHOF-RHOG)*U))**.25                                DATABASE
      DG=(KF/F(B)+HR*DELTA)*(TU-TL)/HFG                                 DATABASE
    3 B=DG*CPG/KF                                                       DATABASE
      HB=B*KF/DELTA/SH                                                  DATABASE
C  CALCULATE THE RATIO OF THE EXPERIMENTAL HEAT TRANSFER COEFFICIENT    DATABASE
C  TO THE THEORETICAL VALUE FOR A SMOOTH SURFACE                        DATABASE
      HEHB=AMIN1(99.9,HEXP/HB)                                          DATABASE
C  CALCULATE THE EXPERIMENTAL NUSSELT NUMBER BASED ON THE DROP VOLUME   DATABASE
      NUV=HEXP*V** .333333/KG                                           DATABASE
C  CALCULATE DIMENSIONLESS HEAT FLUX BASED ON DROP VOLUME               DATABASE
      H=NUV*SH                                                          DATABASE
C  WRITE EXPERIMENTAL AND CALCULATED VALUES TO LINE PRINTER             DATABASE
      WRITE(6,6000) T(I),A(I),AS,DLNADT,ASTAR,VSTAR,V,L,HEXP,HEHB,      DATABASE
     )NUV,H                                                             DATABASE
 6000 FORMAT(5X,F6.0,F8.3,F9.3,F13.5,F10.1,F7.1,F8.3,F7.3,F11.5,F9.3,   DATABASE
     )F7.1,F6.1)                                                        DATABASE
C  PUNCH DATABASE (CARD DECK)                                           DATABASE
    4 IF(IPUNCH.NE.0) WRITE(7,7000) NROLL,NSEQ,I,SH,VSTAR,HEHB,H        DATABASE
 7000 FORMAT(I2,1X,I3,1X,I2,F6.3,F8.2,F6.3,F7.2)                        DATABASE
C  PLOT EXPERIMENTAL AND TIME SMOOTHENED AREA VS. TIME                  DATABASE
      IF(IPRT.GT.0) CALL APLOT(TITLE,AL,ALS,NPOINT,DT)                  DATABASE
      GO TO 1                                                           DATABASE
      END                                                               DATABASE
      SUBROUTINE FINDC(A,T,DT,NPOINT,CMIN,DMIN,IPRT,AL)                 FINDC
C  FINDC LOCATES THE VECTOR 'CMIN' WHICH CORRESPONDS TO A MINIMUM       FINDC
C  AVERAGE ABSOLUTE RELATIVE DISCREPANCY BETWEEN THE EXPERIMENTAL       FINDC
C  DATA AND THE APPROXIMATING FUNCTION                                  FINDC
      DIMENSION AL(99),C(4),DFDC(4),D2FDC2(4,4),S(4),JPIVOT(4),         FINDC
     )C2T(99),C3T(99),C4T(99),A(99),T(99),CMIN(4)                       FINDC
C  SET-UP LOG(AREA) VECTOR                                              FINDC
      DO 1 I=1,NPOINT                                                   FINDC
C  CHECK FOR AREA OUT OF RANGE                                          FINDC
      IF(A(I).GT..0001.AND.A(I).LT.100.) GO TO 1                        FINDC
      WRITE(6,1000)                                                     FINDC
 1000 FORMAT(5X,31H***** AREA OUT OF RANGE *****)                       FINDC
      STOP                                                              FINDC
    1 AL(I)=ALOG(A(I))                                                  FINDC
C  INITIALIZATION ALGORITHM FOR VECTOR 'C'                              FINDC
      IC2=0                                                             FINDC
      DO 2 I=2,NPOINT                                                   FINDC
    2 IF(AL(I-1)*AL(I).LE.0.) IC2=I                                     FINDC
      IF(IC2.NE.0) C(2)=T(IC2)                                          FINDC
      IF(IC2.EQ.0.AND.AL(1).LT.0.) C(2)=-DT                             FINDC
      IF(IC2.EQ.0.AND.AL(1).GT.0.) C(2)=T(NPOINT)+DT                    FINDC
      C(4)=T(NPOINT)+DT                                                 FINDC
      C(3)=3.*C(4)-2.*C(2)                                              FINDC
      C(1)=AL(1)*C(4)/C(2)/C(3)                                         FINDC
C  INITIALIZE MINIMUM ERROR                                             FINDC
C  INITIALIZE DIFFERENCE EQUATIONS AND GRADIENT VECTOR                  FINDC
      DO 3 I=1,NPOINT                                                   FINDC
      C2T(I)=C(2)-T(I)                                                  FINDC
      C3T(I)=C(3)-T(I)                                                  FINDC
    3 C4T(I)=C(4)-T(I)                                                  FINDC
      CALL GRAD(C(1),C2T,C3T,C4T,AL,NPOINT,DFDC)                        FINDC
C  DETERMINE THE AVERAGE ABSOLUTE RELATIVE DISCREPANCY CORRESPONDING    FINDC
C  TO THE INITIAL ESTIMATE                                              FINDC
      DMIN=AARD(C,A,T,DT,NPOINT)                                        FINDC
C  INITIALIZE THE CMIN VECTOR                                           FINDC
      DO 4 I=1,4                                                        FINDC
    4 CMIN(I)=C(I)                                                      FINDC
C  WRITE HEADING ON NEW PAGE TO KEEP TRACK OF THE CONVERGENCE           FINDC
      IF(IPRT.GT.1) WRITE(6,2000)                                       FINDC
 2000 FORMAT(1H1,7X,4HC(1),10X,4HC(2),10X,4HC(3),10X,4HC(4),10X,        FINDC
     )4HG(1),10X,4HG(2),10X,4HG(3),10X,4HG(4),8X,4HAARD,8X,3HIER)       FINDC
C  LIST INITIAL VECTORS AND CORRESPONDING DISCREPANCY                   FINDC
      IF(IPRT.GT.1) WRITE(6,2100) (C(I),I=1,4),(DFDC(I),I=1,4),DMIN,IER FINDC
 2100 FORMAT(2X,9G14.6,2X,I2)                                           FINDC
      DAMP=.5                                                           FINDC
      DO 10 ITER=1,100                                                  FINDC
C  DETERMINE HESSIAN MATRIX                                             FINDC
      CALL HESS(C(1),C2T,C3T,C4T,AL,NPOINT,D2FDC2)                      FINDC
C  DETERMINE NEXT STEP IN STEEPEST DESCENT                              FINDC
      CALL GAUSSP(D2FDC2,4,DFDC,4,S,4,JPIVOT,4,4,RLOGD,DSIGN,IER)       FINDC
C  COMPUTE NEW VALUE OF VECTOR 'C'                                      FINDC
C  (WHEN NEWTON ITERATION DIVERGES THE METHOD OF DISPLACEMENTS          FINDC
C   WILL AUTOMATICALLY BE ACTIVATED)                                    FINDC
      DO 5 I=1,4                                                        FINDC
      DC=DT                                                             FINDC
      IF(I.EQ.1) DC=.2*C(1)                                             FINDC
    5 C(I)=C(I)-DAMP*SIGN(AMIN1(DC,ABS(S(I))),DFDC(I))                  FINDC
```

```
      C2=C(2)                                                           FINDC
      C(2)=AMIN1(C(2),C(3))                                             FINDC
      C(3)=AMAX1(C2,C(3))                                               FINDC
      C(2)=AMIN1(C(2),C(4)-DT)                                          FINDC
      C(3)=AMAX1(C(3),C(4)+DT)                                          FINDC
      C(3)=AMIN1(C(3),5.*C(4)-4.*C(2))                                  FINDC
      C(1)=AMAX1(.1*AL(1)/C(4),AMIN1(10.*AL(1)/C(4),C(1)))              FINDC
C  DETERMINE NEW AVERAGE ABSOLUTE RELATIVE DISCREPANCY                  FINDC
      DIS=AARD(C,A,T,DT,NPOINT)                                         FINDC
C  IF THE ERROR IS LESS THAN THE PREVIOUS MINIMUM ERROR SAVE THE NEW    FINDC
C  VALUES OF C IN THE VECTOR 'CMIN'                                     FINDC
      IF(DIS.GE.DMIN) GO TO 7                                           FINDC
      DMIN=DIS                                                          FINDC
      DO 6 I=1,4                                                        FINDC
    6 CMIN(I)=C(I)                                                      FINDC
C  DETERMINE NEW DIFFERENCE EQUATIONS                                   FINDC
    7 DO 8 I=1,NPOINT                                                   FINDC
      C2T(I)=C(2)-T(I)                                                  FINDC
      C3T(I)=C(3)-T(I)                                                  FINDC
    8 C4T(I)=C(4)-T(I)                                                  FINDC
C  DETERMINE NEW GRADIENT                                               FINDC
      CALL GRAD(C(1),C2T,C3T,C4T,AL,NPOINT,DFDC)                        FINDC
C  DETERMINE THE MAGNITUDE OF THE GRADIENT VECTOR                       FINDC
      GM=0.                                                             FINDC
      DO 9 I=1,4                                                        FINDC
    9 GM=GM+ABS(DFDC(I))                                                FINDC
C  WRITE UPDATE ON CONVERGENCE OF ITERATIONS                            FINDC
      IF(IPRT.GT.1) WRITE(6,2100) (C(I),I=1,4),(DFDC(I),I=1,4),DIS,IER  FINDC
C  IF CONVERGENCE HAS NOT BEEN REACHED IN 50 ITERATIONS REDUCE          FINDC
C  DAMPING FACTOR. RE-INITIALIZE 'C', AND RESTART ITERATIONS            FINDC
      IF(ITER.NE.50) GO TO 10                                           FINDC
      DAMP=.1                                                           FINDC
      C(4)=T(NPOINT)+DT                                                 FINDC
      C(3)=3.*C(4)-2.*C(2)                                              FINDC
      C(1)=AL(1)*C(4)/C(2)/C(3)                                         FINDC
C  END ITERATIONS IF THE MAGNITUDE OF THE GRADIENT IS WITHIN THE        FINDC
C  SPECIFIED TOLERANCE                                                  FINDC
   10 IF(GM.LE.1.E-6) RETURN                                            FINDC
C  IF CONVERGENCE HAS NOT BEEN ATTAINED IN 100 ITERATIONS ABANDON       FINDC
C  THE METHOD OF STEEPEST DESCENT AND COMMENCE DIRECTIONAL SEARCH       FINDC
C  ALONG 'C4'                                                           FINDC
      C(4)=FLOAT(NPOINT-1)                                              FINDC
      DFDC(1)=DT*C(4)*(C(4)+1.)/2.                                      FINDC
      DFDC(2)=DT*DFDC(1)*(2.*C(4)+1.)/3.                                FINDC
      DFDC(3)=DT*DFDC(1)**2                                             FINDC
      DFDC(4)=DT**2*DFDC(2)*(3.*C(4)**2+3.*C(4)-1.)/5.                  FINDC
      C(4)=C(4)+1.                                                      FINDC
      C(1)=C(4)*(DFDC(2)*DFDC(4)-DFDC(3)**2)-DFDC(1)*DFDC(4))           FINDC
     )-DFDC(2)**3+2.*DFDC(1)*DFDC(2)*DFDC(3)                            FINDC
      D2FDC2(1,1)=(DFDC(2)*DFDC(4)-DFDC(3)**2)/C(1)                     FINDC
      D2FDC2(1,2)=(DFDC(2)*DFDC(3)-DFDC(1)*DFDC(4))/C(1)                FINDC
      D2FDC2(1,3)=(DFDC(1)*DFDC(3)-DFDC(2)**2)/C(1)                     FINDC
      D2FDC2(2,1)=D2FDC2(1,2)                                           FINDC
      D2FDC2(2,2)=(C(4)*DFDC(4)-DFDC(2)**2)/C(1)                        FINDC
      D2FDC2(2,3)=(DFDC(1)*DFDC(2)-C(4)*DFDC(3))/C(1)                   FINDC
      D2FDC2(3,1)=D2FDC2(1,3)                                           FINDC
      D2FDC2(3,2)=D2FDC2(2,3)                                           FINDC
      D2FDC2(3,3)=(C(4)*DFDC(2)-DFDC(1)**2)/C(1)                        FINDC
      C(4)=T(NPOINT)                                                    FINDC
      DO 16 ITER=1,100                                                  FINDC
      C(4)=C(4)+DT/10.                                                  FINDC
      DO 11 I=1,3                                                       FINDC
   11 C(I)=0.                                                           FINDC
      DO 12 I=1,NPOINT                                                  FINDC
      DC=AL(I)*(C(4)-T(I))                                              FINDC
      DO 12 J=1,3                                                       FINDC
      C(J)=C(J)+DC                                                      FINDC
   12 DC=DC*T(I)                                                        FINDC
      DO 13 I=1,3                                                       FINDC
      DFDC(I)=0.                                                        FINDC
      DO 13 J=1,3                                                       FINDC
   13 DFDC(I)=DFDC(I)+D2FDC2(I,J)*C(J)                                  FINDC
      C(1)=DFDC(3)                                                      FINDC
      IF(C(1).LT.1.E-6) GO TO 16                                        FINDC
      DFDC(1)=DFDC(1)/DFDC(3)                                           FINDC
      DFDC(2)=-DFDC(2)/DFDC(3)                                          FINDC
      DFDC(4)=DFDC(2)*DFDC(2)-4.*DFDC(1)                                FINDC
      IF(DFDC(4).LE.0.) GO TO 16                                        FINDC
      DFDC(4)=SQRT(DFDC(4))                                             FINDC
      C(3)=(DFDC(2)+DFDC(4))/2.                                         FINDC
      IF(C(3).LT.C(4)+DT) GO TO 16                                      FINDC
      C(2)=DFDC(1)/C(3)                                                 FINDC
      IF(C(2).GT.C(4)-DT) GO TO 16                                      FINDC
```

```
      DIS=AARD(C,A,T,DT,NPOINT)                                          FINDC
      IF(DIS.GE.DMIN) GO TO 15                                           FINDC
      DMIN=DIS                                                           FINDC
      DO 14 I=1,4                                                        FINDC
   14 CMIN(I)=C(I)                                                       FINDC
   15 IF(IPRT.GT.1) WRITE(6,2200) (C(I),I=1,4),DIS                       FINDC
 2200 FORMAT(2X,4G14.6,56X,G14.6)                                        FINDC
   16 CONTINUE                                                           FINDC
      RETURN                                                             FINDC
      END                                                                FINDC
      SUBROUTINE GRAD(C1,C2T,C3T,C4T,AL,NPOINT,DFDC)                     GRADIENT
C  GRAD DETERMINES THE GRADIENT OF THE RESIDUAL                          GRADIENT
      DIMENSION C2T(99),C3T(99),C4T(99),AL(99),DFDC(4)                   GRADIENT
      DO 1 I=1,4                                                         GRADIENT
    1 DFDC(I)=0.                                                         GRADIENT
      DO 2 I=1,NPOINT                                                    GRADIENT
      DFDC(1)=DFDC(1)+2.*C1*C2T(I)*C2T(I)*C3T(I)*C3T(I)/C4T(I)/C4T(I)-   GRADIENT
     >2.*AL(I)*C2T(I)*C3T(I)/C4T(I)                                      GRADIENT
      DFDC(2)=DFDC(2)+2.*C1*C1*C2T(I)*C3T(I)*C3T(I)/C4T(I)/C4T(I)-       GRADIENT
     >2.*AL(I)*C1*C3T(I)/C4T(I)                                          GRADIENT
      DFDC(3)=DFDC(3)+2.*C1*C1*C2T(I)*C2T(I)*C3T(I)/C4T(I)/C4T(I)-       GRADIENT
     >2.*AL(I)*C1*C2T(I)/C4T(I)                                          GRADIENT
    2 DFDC(4)=DFDC(4)-2.*C1*C1*C2T(I)*C2T(I)*C3T(I)*C3T(I)/C4T(I)/       GRADIENT
     >C4T(I)/C4T(I)+2.*AL(I)*C1*C2T(I)*C3T(I)/C4T(I)/C4T(I)              GRADIENT
      DO 3 I=1,4                                                         GRADIENT
    3 DFDC(I)=DFDC(I)/FLOAT(NPOINT)                                      GRADIENT
      RETURN                                                             GRADIENT
      END                                                                GRADIENT
      SUBROUTINE HESS(C1,C2T,C3T,C4T,AL,NPOINT,D2FDC2)                   HESSIAN
C  HESS DETERMINES THE HESSIAN MATRIX (RESIDUAL TENSOR)                  HESSIAN
      DIMENSION C2T(99),C3T(99),C4T(99),AL(99),D2FDC2(4,4)               HESSIAN
      DO 1 I=1,4                                                         HESSIAN
      DO 1 J=1,4                                                         HESSIAN
    1 D2FDC2(I,J)=0.                                                     HESSIAN
      DO 2 I=1,NPOINT                                                    HESSIAN
      D2FDC2(1,1)=D2FDC2(1,1)+2.*C2T(I)*C2T(I)*C3T(I)*C3T(I)/C4T(I)/     HESSIAN
     >C4T(I)                                                             HESSIAN
      D2FDC2(1,2)=D2FDC2(1,2)+4.*C1*C2T(I)*C3T(I)*C3T(I)/C4T(I)/C4T(I)-  HESSIAN
     >2.*AL(I)*C3T(I)/C4T(I)                                             HESSIAN
      D2FDC2(1,3)=D2FDC2(1,3)+4.*C1*C2T(I)*C2T(I)*C3T(I)/C4T(I)/C4T(I)-  HESSIAN
     >2.*AL(I)*C2T(I)/C4T(I)                                             HESSIAN
      D2FDC2(1,4)=D2FDC2(1,4)-4.*C1*C2T(I)*C2T(I)*C3T(I)*C3T(I)/C4T(I)/  HESSIAN
     >C4T(I)/C4T(I)+2.*AL(I)*C2T(I)*C3T(I)/C4T(I)/C4T(I)                 HESSIAN
      D2FDC2(2,2)=D2FDC2(2,2)+2.*C1*C1*C3T(I)*C3T(I)/C4T(I)/C4T(I)       HESSIAN
      D2FDC2(2,3)=D2FDC2(2,3)+4.*C1*C1*C2T(I)*C3T(I)/C4T(I)/C4T(I)-      HESSIAN
     >2.*AL(I)*C1/C4T(I)                                                 HESSIAN
      D2FDC2(2,4)=D2FDC2(2,4)-4.*C1*C1*C2T(I)*C3T(I)*C3T(I)/C4T(I)/      HESSIAN
     >C4T(I)/C4T(I)+2.*AL(I)*C1*C3T(I)/C4T(I)/C4T(I)                     HESSIAN
      D2FDC2(3,3)=D2FDC2(3,3)+2.*C1*C1*C2T(I)*C2T(I)/C4T(I)/C4T(I)       HESSIAN
      D2FDC2(3,4)=D2FDC2(3,4)-4.*C1*C1*C2T(I)*C2T(I)*C3T(I)/C4T(I)/      HESSIAN
     >C4T(I)/C4T(I)+2.*AL(I)*C1*C2T(I)/C4T(I)/C4T(I)                     HESSIAN
    2 D2FDC2(4,4)=D2FDC2(4,4)+6.*C1*C1*C2T(I)*C2T(I)*C3T(I)*C3T(I)/      HESSIAN
     >C4T(I)/C4T(I)/C4T(I)/C4T(I)-4.*AL(I)*C1*C2T(I)*C3T(I)/C4T(I)/      HESSIAN
     >C4T(I)                                                             HESSIAN
      DO 3 I=1,3                                                         HESSIAN
      I1=I+1                                                             HESSIAN
      DO 3 J=I1,4                                                        HESSIAN
    3 D2FDC2(J,I)=D2FDC2(I,J)                                            HESSIAN
      DO 4 I=1,4                                                         HESSIAN
      DO 4 J=1,4                                                         HESSIAN
    4 D2FDC2(I,J)=D2FDC2(I,J)/FLOAT(NPOINT)                              HESSIAN
      RETURN                                                             HESSIAN
      END                                                                HESSIAN
      FUNCTION AARD(C,A,T,DT,NPOINT)                                     ADISCREP
C  AARD CALCULATES THE AVERAGE ABSOLUTE RELATIVE DISCREPANCY BETWEEN     ADISCREP
C  THE EXPERIMENTAL DATA AND THE APPROXIMATING FUNCTION                  ADISCREP
      DIMENSION C(4),A(99),T(99)                                         ADISCREP
      AARD=0.                                                            ADISCREP
      DO 1 I=1,NPOINT                                                    ADISCREP
C  DETERMINE THE SMOOTHENED AREA FROM THE APPROXIMATING FUNCTION         ADISCREP
      ASL=C(1)*(C(2)-T(I))*(C(3)-T(I))/(C(4)-T(I))                       ADISCREP
      AS=EXP(AMAX1(-10.,AMIN1(10.,ASL)))                                 ADISCREP
C  ACCUMULATE THE ABSOLUTE VALUE OF THE RELATIVE DISCREPANCY             ADISCREP
    1 AARD=AARD+ABS((A(I)-AS)/A(I))                                      ADISCREP
C  DIVIDE BY THE NUMBER OF POINTS TO DETERMINE THE AVERAGE               ADISCREP
      AARD=100.*AARD/FLOAT(NPOINT)                                       ADISCREP
      RETURN                                                             ADISCREP
      END                                                                ADISCREP
      FUNCTION VOFA(A)                                                   V%(A%)
      DATA C1,C2,C3/-.117976129,-.102198064,.102842212/                  V%(A%)
      AL=ALOG10(A)                                                       V%(A%)
      VL=1.25*AL-C1-SQRT(.0625*AL*AL+C2*AL+C3)                           V%(A%)
```

```
      VOFA=10.**VL                                                      V#(A#)
      RETURN                                                            V#(A#)
      END                                                               V#(A#)
      FUNCTION DVDA(A)                                                  DV#/DA#
      DATA C1,C2,C3/-.117976129,-.102198064,.102842212/                 DV#/DA#
      V=VOFA(A)                                                         DV#/DA#
      AL=ALOG10(A)                                                      DV#/DA#
      DVDA=V#(1.25-(.0625*AL+.5*C2)/SQRT(.0625*AL*AL+C2*AL+C3))/A       DV#/DA#
      RETURN                                                            DV#/DA#
      END                                                               DV#/DA#
      FUNCTION F(B)                                                     F(B)
      F=1.+EXP(.5*B)                                                    F(B)
      DO 1 I=1,99                                                       F(B)
      Z=.01*FLOAT(I)                                                    F(B)
    1 F=F+2.*EXP(.5*B*(1.-Z*Z*Z*(2.-Z)))                                F(B)
      F=.005*F                                                          F(B)
      RETURN                                                            F(B)
      END                                                               F(B)
      SUBROUTINE GAUSSP(A,NA,B,NB,X,NX,JPIVOT,NJP,N,RLOGD,DSIGN,IER)    GAUSSP
C  GAUSSP PERFORMS GAUSS ELIMINATION WITH FULL COLUMN PIVOTING          GAUSSP
      DIMENSION A(NA,NA),B(NB),X(NX),JPIVOT(NJP)                        GAUSSP
      IER=0                                                             GAUSSP
      IF(N.GT.NA.OR.N.GT.NB.OR.N.GT.NX.OR.N.GT.NJP.OR.N.LT.2) IER=1     GAUSSP
      IF(IER.NE.0) RETURN                                               GAUSSP
      DELTA=1.E-30                                                      GAUSSP
      DSIGN=1.                                                          GAUSSP
      RLOGD=0.                                                          GAUSSP
      N1=N-1                                                            GAUSSP
      DO 10 I=1,N                                                       GAUSSP
   10 JPIVOT(I)=I                                                       GAUSSP
      DO 90 K=1,N1                                                      GAUSSP
      K1=K+1                                                            GAUSSP
      IPIVOT=K                                                          GAUSSP
      JTEMP=K                                                           GAUSSP
      RMAX=ABS(A(K,K))                                                  GAUSSP
      DO 20 I=K,N                                                       GAUSSP
      DO 20 J=K,N                                                       GAUSSP
      IF(ABS(A(I,J)).LE.RMAX) GO TO 20                                  GAUSSP
      RMAX=ABS(A(I,J))                                                  GAUSSP
      IPIVOT=I                                                          GAUSSP
      JTEMP=J                                                           GAUSSP
   20 CONTINUE                                                          GAUSSP
      IF(IPIVOT.EQ.K) GO TO 40                                          GAUSSP
      IF(RMAX.LT.DELTA) GO TO 120                                       GAUSSP
      DSIGN=-DSIGN                                                      GAUSSP
      BTEMP=B(K)                                                        GAUSSP
      B(K)=B(IPIVOT)                                                    GAUSSP
      B(IPIVOT)=BTEMP                                                   GAUSSP
      DO 30 J=K,N                                                       GAUSSP
      ATEMP=A(K,J)                                                      GAUSSP
      A(K,J)=A(IPIVOT,J)                                                GAUSSP
   30 A(IPIVOT,J)=ATEMP                                                 GAUSSP
   40 IF(JTEMP.EQ.K) GO TO 60                                           GAUSSP
      DSIGN=-DSIGN                                                      GAUSSP
      JTP=JPIVOT(JTEMP)                                                 GAUSSP
      JPIVOT(JTEMP)=JPIVOT(K)                                           GAUSSP
      JPIVOT(K)=JTP                                                     GAUSSP
      DO 50 I=1,N                                                       GAUSSP
      ATEMP=A(I,JTEMP)                                                  GAUSSP
      A(I,JTEMP)=A(I,K)                                                 GAUSSP
   50 A(I,K)=ATEMP                                                      GAUSSP
   60 RLOGD=RLOGD+ALOG10(ABS(A(K,K)))                                   GAUSSP
      IF(A(K,K).LT.0.) DSIGN=-DSIGN                                     GAUSSP
      DO 80 I=K1,N                                                      GAUSSP
      AR=A(I,K)/A(K,K)                                                  GAUSSP
      IF(ABS(AR).LT.DELTA) GO TO 80                                     GAUSSP
      B(I)=B(I)-AR*B(K)                                                 GAUSSP
      DO 70 J=K1,N                                                      GAUSSP
   70 A(I,J)=A(I,J)-AR*A(K,J)                                           GAUSSP
   80 CONTINUE                                                          GAUSSP
   90 CONTINUE                                                          GAUSSP
      IF(ABS(A(N,N)).LT.DELTA) GO TO 120                                GAUSSP
      RLOGD=RLOGD+ALOG10(ABS(A(N,N)))                                   GAUSSP
      IF(A(N,N).LT.0.) DSIGN=-DSIGN                                     GAUSSP
      X(JPIVOT(N))=B(N)/A(N,N)                                          GAUSSP
      DO 110 IN=2,N                                                     GAUSSP
      I=N+1-IN                                                          GAUSSP
      X(JPIVOT(I))=B(I)                                                 GAUSSP
      I1=I+1                                                            GAUSSP
      DO 100 J=I1,N                                                     GAUSSP
  100 X(JPIVOT(I))=X(JPIVOT(I))-A(I,J)*X(JPIVOT(J))                     GAUSSP
  110 X(JPIVOT(I))=X(JPIVOT(I))/A(I,I)                                  GAUSSP
```

```
      RETURN                                                            GAUSSP
  120 IER=1                                                             GAUSSP
      DSIGN=0.                                                          GAUSSP
      RLOGD=0.                                                          GAUSSP
      RETURN                                                            GAUSSP
      END                                                               GAUSSP
      SUBROUTINE APLOT(TITLE,AL,ALS,NPOINT,DT)                          AREAPLOT
      DIMENSION AL(99),ALS(99),LA(99),LAS(99),IT(99)                    AREAPLOT
      INTEGER TITLE(40),ROW(126),PLUS,V,H,BLANK,E,S                     AREAPLOT
      DATA PLUS,V,H,BLANK,E,S/1H+,1H^,1H-,1H ,1HE,1HS/                  AREAPLOT
      WRITE(6,1000) (TITLE(I),I=1,40)                                   AREAPLOT
 1000 FORMAT(1H1,29X,40A2,//,1X,4HAREA,/,7H 100. +,124(1H-),1H+)        AREAPLOT
      DO 1 I=1,NPOINT                                                   AREAPLOT
      IT(I)=INT(2.5+123.*FLOAT(I-1)/FLOAT(NPOINT-1))                    AREAPLOT
      LA(I)=21-INT(.5+4.342945*AL(I))                                   AREAPLOT
    1 LAS(I)=21-INT(.5+4.342945*ALS(I))                                 AREAPLOT
      DO 7 IY=2,51                                                      AREAPLOT
      MIY=MOD(IY+9,10)                                                  AREAPLOT
      DO 2 J=2,125                                                      AREAPLOT
      ROW(J)=BLANK                                                      AREAPLOT
    2 IF(MIY.EQ.0) ROW(J)=H                                             AREAPLOT
      ROW(1)=V                                                          AREAPLOT
      IF(MIY.EQ.0) ROW(1)=PLUS                                          AREAPLOT
      ROW(126)=V                                                        AREAPLOT
      IF(MIY.EQ.0) ROW(126)=PLUS                                        AREAPLOT
      WRITE(6,2000) (ROW(J),J=1,126)                                    AREAPLOT
 2000 FORMAT(6X,126A1)                                                  AREAPLOT
      DO 3 I=1,126                                                      AREAPLOT
    3 ROW(I)=BLANK                                                      AREAPLOT
      IPRT=0                                                            AREAPLOT
      DO 4 I=1,NPOINT                                                   AREAPLOT
      IF(LA(I).NE.IY) GO TO 4                                           AREAPLOT
      IPRT=1                                                            AREAPLOT
      ROW(IT(I))=E                                                      AREAPLOT
    4 CONTINUE                                                          AREAPLOT
      IF(IPRT.NE.0) WRITE(6,2100) (ROW(J),J=1,126)                      AREAPLOT
 2100 FORMAT(1H+,5X,126A1)                                              AREAPLOT
      DO 5 I=1,126                                                      AREAPLOT
    5 ROW(I)=BLANK                                                      AREAPLOT
      IPRT=0                                                            AREAPLOT
      DO 6 I=1,NPOINT                                                   AREAPLOT
      IF(LAS(I).NE.IY) GO TO 6                                          AREAPLOT
      ROW(IT(I))=S                                                      AREAPLOT
      IPRT=1                                                            AREAPLOT
    6 CONTINUE                                                          AREAPLOT
      IF(IPRT.NE.0) WRITE(6,2100) (ROW(J),J=1,126)                      AREAPLOT
      IF(IY.EQ.3) WRITE(6,3003)                                         AREAPLOT
 3003 FORMAT(1H+,112X,14HE=EXPERIMENTAL)                                AREAPLOT
      IF(IY.EQ.4) WRITE(6,3004)                                         AREAPLOT
 3004 FORMAT(1H+,112X,12HS=SMOOTHENED)                                  AREAPLOT
      IF(IY.EQ.11) WRITE(6,3011)                                        AREAPLOT
 3011 FORMAT(1H+,4H 10.)                                                AREAPLOT
      IF(IY.EQ.21) WRITE(6,3021)                                        AREAPLOT
 3021 FORMAT(1H+,4H 1.0)                                                AREAPLOT
      IF(IY.EQ.31) WRITE(6,3031)                                        AREAPLOT
 3031 FORMAT(1H+,4H 0.1)                                                AREAPLOT
      IF(IY.EQ.41) WRITE(6,3041)                                        AREAPLOT
 3041 FORMAT(1H+,4H0.01)                                                AREAPLOT
    7 IF(IY.EQ.51) WRITE(6,3051)                                        AREAPLOT
 3051 FORMAT(1H+,4H.001)                                                AREAPLOT
      TNP=DT*FLOAT(NPOINT-1)                                            AREAPLOT
      WRITE(6,4000) TNP                                                 AREAPLOT
 4000 FORMAT(6X,2H0.,58X,9HTIME(SEC),53X,F5.1)                          AREAPLOT
      RETURN                                                            AREAPLOT
      END                                                               AREAPLOT
```

Program LAMBDA

Program LAMBDA determines the value of A (Equation 1-1) that provides the best correlation between experimental drop area/volume data and the numerical solution to the Laplace capillary equation (detailed in Chapter 3). The algorithm used in the program is the step-search method. In the step-search method the value of A is incremented until a minimum is over-stepped, the value of A is reduced by twice the increment size, and the search is continued with smaller increments until a desired accuracy is obtained. The values of A generated by this program were used to plot the solid lines in Figures 8 through·11 (which are a comparison of the experimental and theoretical drop area/volume relationship). The following is a listing of program LAMBDA. Comments are provided in the listing at various points to detail the specifics of program operation.

```
CREATE PROGRAM TO DETERMINE LAMBDA FROM AREA VOLUME DATA
C
      REAL LAMBDA                                                          LAMBDA
      INTEGER TITLE(39)                                                    LAMBDA
      DIMENSION A(50),V(50)                                                LAMBDA
C  READ IN THE NUMBER OF DATA POINTS AND THE TITLE                         LAMBDA
    1 READ(5,1000) N,(TITLE(I),I=1,39)                                     LAMBDA
 1000 FORMAT(I2,39A2)                                                      LAMBDA
      IF(N.EQ.0) STOP 1000                                                 LAMBDA
C  READ IN THE AREA DATA                                                   LAMBDA
      READ(5,1010) (A(I),I=1,N)                                            LAMBDA
 1010 FORMAT(10F8.3)                                                       LAMBDA
C  READ IN THE VOLUME DATA                                                 LAMBDA
      READ(5,1010) (V(I),I=1,N)                                            LAMBDA
      ENEW=1.E10                                                           LAMBDA
C  INITIALIZE THE VALUE OF LAMBDA AND THE STEP SIZE                        LAMBDA
      LAMBDA=0.                                                            LAMBDA
      DL=.1                                                                LAMBDA
C  SET THE NUMBER OF FURTHER DIGITS OF SEARCH                              LAMBDA
      IDIGIT=4                                                             LAMBDA
      DO 3 I=1,IDIGIT                                                      LAMBDA
C  INCREMENT THE DECIMAL ACCURACY OF THE STEP SIZE                         LAMBDA
      DL=DL/10.                                                            LAMBDA
C  INCREMENT LAMBDA                                                        LAMBDA
    2 LAMBDA=LAMBDA+DL                                                     LAMBDA
C  STOP FOR LAMBDA OUT OF RANGE                                            LAMBDA
      IF(LAMBDA.GT.1.) STOP 2222                                           LAMBDA
      EOLD=ENEW                                                            LAMBDA
      ENEW=ERR(A,V,LAMBDA,N)                                               LAMBDA
C  DETERMINE IF THERE IS A REDUCTION IN ERROR WITH THIS STEP               LAMBDA
C  IF SO, CONTINUE STEPPING LAMBDA                                         LAMBDA
C  IF NOT, BACK-UP AND STEP WITH SMALLER INCREMENTS                        LAMBDA
      IF(ENEW.LT.EOLD) GO TO 2                                             LAMBDA
      IF(I.EQ.IDIGIT) GO TO 3                                              LAMBDA
C  TAKE TWO STEPS BACK IN LAMBDA AND CONTINUE WITH SMALLER STEPS           LAMBDA
      LAMBDA=LAMBDA-2.*DL                                                  LAMBDA
    3 CONTINUE                                                             LAMBDA
C  THE BEST VALUE OF LAMBDA HAS BEEN OVERSTEPPED BY ONE INCREMENT          LAMBDA
C  STEP BACK ONE INCREMENT IN LAMBDA AND PRINT OUT RESULTS                 LAMBDA
      LAMBDA=LAMBDA-DL                                                     LAMBDA
      WRITE(6,2000) (TITLE(I),I=1,39),LAMBDA                               LAMBDA
 2000 FORMAT(1H1,10X,32HDATA REDUCTION, LAMBDA FROM DATA,/,10X,39A2,/,     LAMBDA
     >10X,7HLAMBDA=,F7.5,//,11X,4HAREA,11X,6HVOLUME,10X,6H%ERROR,/,       LAMBDA
     >20X,8HMEASURED,2X,10HCALCULATED)                                     LAMBDA
      EMAX=0.                                                              LAMBDA
      EAVE=0.                                                              LAMBDA
C  COMPUTE THE ERROR IN VOLUME FOR EACK DATA POINT                         LAMBDA
      DO 4 I=1,N                                                           LAMBDA
      AS=A(I)/LAMBDA**2                                                    LAMBDA
      VS=VOFA(AS)                                                          LAMBDA
      VC=VS*LAMBDA**3                                                      LAMBDA
      ER=100.*(V(I)-VC)/V(I)                                               LAMBDA
      IF(ABS(ER).GT.ABS(EMAX)) EMAX=ER                                     LAMBDA
      EAVE=EAVE+ABS(ER)                                                    LAMBDA
    4 WRITE(6,2010) A(I),V(I),VC,ER                                        LAMBDA
 2010 FORMAT(10X,F6.3,5X,F6.4,5X,F6.4,4X,F5.1)                             LAMBDA
C  WRITE SUMMARY DATA (MAXIMUM AND AVERAGE ERRORS)                         LAMBDA
      EAVE=EAVE/FLOAT(N)                                                   LAMBDA
      WRITE(6,2020) EMAX,EAVE                                              LAMBDA
 2020 FORMAT(//,10X,14HMAXIMUM ERROR=,F5.1,1H%,/,                          LAMBDA
     >10X,14HAVERAGE ERROR=,F4.1,1H%)                                      LAMBDA
      GO TO 1                                                              LAMBDA
      END                                                                  LAMBDA
      FUNCTION ERR(A,V,R,N)                                                ERROR
      DIMENSION A(50),V(50)                                                ERROR
      ERR=0.                                                               ERROR
      DO 1 I=1,N                                                           ERROR
      AS=A(I)/R/R                                                          ERROR
      VS=VOFA(AS)                                                          ERROR
      VC=VS*R*R*R                                                          ERROR
      ER=ABS(V(I)-VC)*100./V(I)                                            ERROR
    1 ERR=ERR+ER                                                           ERROR
      RETURN                                                               ERROR
      END                                                                  ERROR
      FUNCTION VOFA(A)                                                     V(A)
      DATA C1,C2,C3/-.117976129,-.102198064,.102842212/                    V(A)
      AL=ALOG10(A)                                                         V(A)
      VL=1.25*AL-C1-SQRT(.0625*AL*AL+C2*AL+C3)                             V(A)
      VOFA=10.**VL                                                         V(A)
      RETURN                                                               V(A)
      END                                                                  V(A)
```

Program PLOT:FRC

Program PLOT:FRC was used to generate plots of the computed relative contribution to the overall heat flux of convection (F, flow), radiation (R), and intermittent liquid-solid contact (C) for each data point in each data sequence. Program_ PLOT:FRC reads the database (generated by program DATABASE) to produce the plots. The computed relative contributions were determined by solving Equations 3-30, 3-34 through 3-41, and 3-45 simultaneously. Program PLOT:FRC was written to process both smooth and macro-roughened surface data without modification. An example of the plots generated by program PLOT:FRC for the smooth surface and a macro-roughened surface are given in Figures 75 and 76 respectively. The following is a listing of program PLOT:FRC. Comments are provided in the listing at various points to detail the specifics of program operation.

```
CREATE PROGRAM TO PLOT THE RELATIVE CONTRIBUTION OF CONVECTION (FLOW),
C  RADIATION, AND CONTACT AS A FUNCTION OF DIMENSIONLESS DROP VOLUME
C
      DIMENSION JX(99),IY(99,3)                                          PLOT·FRC
      REAL LAMBDA,MUV,MUD,MUR,MUC,MUF,KG,KS,MUG,KF                       PLOT·FRC
      INTEGER TITLE(80),SMTH(2)                                          PLOT·FRC
      DATA SMTH/1HS,1HM/                                                 PLOT·FRC
C  DEFINE PHYSICAL CONSTANTS                                            PLOT·FRC
      DATA PI,G,SIGMA/3.14159,980.,5.6688E-12/                           PLOT·FRC
C  READ IN THE ROLL#, THE NUMBER OF POINTS IN THE SEQUENCE, AND THE     PLOT·FRC
C  BULK SURFACE TEMPERATURE                                             PLOT·FRC
    1 READ(5,1000) NROLL,NPOINT,TW                                       PLOT·FRC
 1000 FORMAT(I2,5X,I2,5X,F4.0)                                           PLOT·FRC
      IF(NROLL.LE.0) STOP                                                PLOT·FRC
C  READ IN TITLE CARD                                                   PLOT·FRC
      READ(5,1010) (TITLE(I),I=1,80)                                     PLOT·FRC
 1010 FORMAT(80A1)                                                       PLOT·FRC
C  READ IN THERMOPHYSICAL PROPERTY CARD                                 PLOT·FRC
      READ(5,1020) LAMBDA,CPG,KG,RHOF,RHOG,MUG,KS,EPS,TS,HFG,KF          PLOT·FRC
 1020 FORMAT(F6.4,F5.3,E9.3,F6.4,F7.6,E9.3,F5.4,F7.5,F5.1,F6.1,E9.3)     PLOT·FRC
C  DETERMINE IF SURFACE IS SMOOTH OR ROUGH                              PLOT·FRC
      NSMTH=0                                                            PLOT·FRC
      DO 2 I=1,79                                                        PLOT·FRC
      IF(TITLE(I).EQ.SMTH(1).AND.TITLE(I+1).EQ.SMTH(2)) GO TO 3          PLOT·FRC
    2 CONTINUE                                                           PLOT·FRC
      GO TO 4                                                            PLOT·FRC
    3 NSMTH=1                                                            PLOT·FRC
    4 DO 8 I=1,NPOINT                                                    PLOT·FRC
C  READ IN THE DATA ONE CARD AT A TIME                                  PLOT·FRC
      READ(5,2000) NROLL,NSEQ,NDATA,SH,VSTAR,HEHB,H                      PLOT·FRC
 2000 FORMAT(I2,1X,I3,1X,I2,F6.3,F8.2,F6.3,F7.2)                         PLOT·FRC
      IF(I.NE.1) GO TO 5                                                 PLOT·FRC
C  CALCULATE THE RADIATIVE HEAT TRANSFER COEFFICIENT                    PLOT·FRC
      HR=SIGMA*((TW+273.)**4-(TS+273.)**4)/(TW-TS)                       PLOT·FRC
C  CALCULATE DROP VOLUME                                                PLOT·FRC
    5 V=VSTAR*LAMBDA**3                                                  PLOT·FRC
C  CALCULATE DROP HEAT TRANSFER COEFFICIENT FROM DIMENSIONLESS HEAT FLUXPLOT·FRC
      HD=H*KG/SH/V**.333333                                              PLOT·FRC
C  DETERMINE DIMENSIONLESS DROP AREA                                    PLOT·FRC
      ASTAR=AOFV(VSTAR)                                                  PLOT·FRC
C  CALCULATE DROP AREA                                                  PLOT·FRC
      A=ASTAR*LAMBDA**2                                                  PLOT·FRC
C  CALCULATE MASS FLUX                                                  PLOT·FRC
      GG=HD*(TW-TS)/HFG                                                  PLOT·FRC
C  CALCULATE VAPOR LAYER THICKNESS                                      PLOT·FRC
      DELTA=0.                                                           PLOT·FRC
      DO 6 ITER=1,5                                                      PLOT·FRC
    6 DELTA=(GG*MUG*A*A*(9.*GG*DELTA/20./MUG+3.)/                        PLOT·FRC
     >(2.*PI*G*RHOG*(RHOF-RHOG)*V))**.333333                             PLOT·FRC
C  CALCULATE DIMENSIONLESS PARAMETER B                                  PLOT·FRC
      B=GG*CPG*DELTA/KG                                                  PLOT·FRC
C  CALCULATE DROP NUSSELT NUMBER                                        PLOT·FRC
      NUV=H/SH                                                           PLOT·FRC
      NUD=HD*DELTA/KG                                                    PLOT·FRC
C  CALCULATE THE NUSSELT NUMBER FOR THE CONVECTIVE TRANSPORT            PLOT·FRC
      NUF=KF/KG/F(B*KG/KF)                                               PLOT·FRC
C  CALCULATE THE RELATIVE CONTRIBUTION TO HEAT TRANSFER DUE TO THE FLOW PLOT·FRC
      FLOW=NUF/NUD                                                       PLOT·FRC
C  CALCULATE THE RADIATIVE NUSSELT NUMBER                               PLOT·FRC
      NUR=HR*DELTA/KG                                                    PLOT·FRC
C  CALCULATE THE RELATIVE CONTRIBUTION TO HEAT TRANSFER DUE TO          PLOT·FRC
C  RADIATION                                                            PLOT·FRC
      RAD=NUR/NUD                                                        PLOT·FRC
C  CALCULATE THE CONTACT NUSSELT NUMBER                                 PLOT·FRC
      NUC=NUD-NUF-NUR                                                    PLOT·FRC
C  CALCULATE THE RELATIVE CONTRIBUTION TO HEAT TRANSFER DUE TO CONTACT  PLOT·FRC
      CON=NUC/NUD                                                        PLOT·FRC
      IF(NSMTH.EQ.0) GO TO 7                                             PLOT·FRC
      CON=0.                                                             PLOT·FRC
      FLOW=FLOW/(FLOW+RAD)                                               PLOT·FRC
      RAD=1.-FLOW                                                        PLOT·FRC
    7 JX(I)=MAX0(1,MIN0(121,IFIX(1.+30.*ALOG10(VSTAR))))                 PLOT·FRC
      IY(I,1)=MAX0(1,MIN0(51,IFIX(1.+50.*(1.-FLOW))))                    PLOT·FRC
      IY(I,2)=MAX0(1,MIN0(51,IFIX(1.+50.*(1.-RAD))))                     PLOT·FRC
    8 IY(I,3)=MAX0(1,MIN0(51,IFIX(1.+50.*(1.-CON))))                     PLOT·FRC
      CALL PLOT(JX,IY,TITLE,NPOINT,NSMTH)                                PLOT·FRC
      GO TO 1                                                            PLOT·FRC
      END                                                                PLOT·FRC
      FUNCTION AOFV(V)                                                   A*(V*)
      DATA C1,C2,C3/-.397138,-.569978,.691262/                           A*(V*)
      VL=ALOG10(V)                                                       A*(V*)
      ALOGA=((2.5*VL+C1)*SQRT(.25*VL*VL+C2*VL+C3))/3.                    A*(V*)
      AOFV=10.**ALOGA                                                    A*(V*)
```

```
      RETURN                                                                AX(VX)
      END                                                                   AX(VX)
      FUNCTION F(B)                                                         F(B)
      F=1.+EXP(.5*B)                                                        F(B)
      DO 1 I=1,99                                                           F(B)
      Z=.01*FLOAT(I)                                                        F(B)
    1 F=F+2.*EXP(.5*B*(1.-Z*Z*Z*(2.-Z)))                                    F(B)
      F=.005*F                                                              F(B)
      RETURN                                                                F(B)
      END                                                                   F(B)
      SUBROUTINE PLOT(JX,IY,TITLE,NPOINT,NSMTH)                             SUB PLOT
      INTEGER SYMBOL(3),V,H,BLANK,PLUS,TITLE(80),YHEAD(51)                  SUB PLOT
      DIMENSION JX(99),IY(99,3),LINE(121),NAMEX(6,5)                        SUB PLOT
      DATA V,H,BLANK,PLUS/1H|,1H-,1H ,1H+/                                  SUB PLOT
      DATA SYMBOL/1HF,1HR,1HC/                                              SUB PLOT
      DATA NAMEX/1H1,1H ,1H ,1H ,1H ,1H ,1H ,1H ,1H ,1H ,1H1,1H0,           SUB PLOT
     ) 1H ,1H ,1H ,1H1,1H0,1H0,1H ,1H ,1H1,1H0,1H0,1H0,                     SUB PLOT
     )1H1,1H0,1H,,1H0,1H0,1H0/                                              SUB PLOT
      DATA YHEAD/                                                           SUB PLOT
     )1H ,1H ,1H ,1H ,1H ,1H ,1H ,1H ,1H ,1H ,                              SUB PLOT
     )1H ,1H ,1H ,1H ,1H ,1H ,1H ,1H ,1H ,1H ,                              SUB PLOT
     )1H ,1H ,1H ,1H ,1H ,1H ,1H ,1H ,1H ,1H ,                              SUB PLOT
     )1H ,1H ,1H ,1H ,1H ,1H ,1H ,1H ,1H ,1H ,                              SUB PLOT
     )1H ,1H ,1H ,1H ,1H ,1H ,1H ,1H ,1H ,1H ,1H /                          SUB PLOT
C  CENTER TITLE ABOVE PLOT                                                 SUB PLOT
      DO 1 I1=1,80                                                          SUB PLOT
      IF(TITLE(I1).NE.BLANK) GO TO 2                                        SUB PLOT
    1 CONTINUE                                                              SUB PLOT
      STOP 1111                                                             SUB PLOT
    2 DO 3 I=1,80                                                           SUB PLOT
      I2=81-I                                                               SUB PLOT
      IF(TITLE(I2).NE.BLANK) GO TO 4                                        SUB PLOT
    3 CONTINUE                                                              SUB PLOT
      STOP 2222                                                             SUB PLOT
    4 N=I2-I1+1                                                             SUB PLOT
      DO 5 I=1,121                                                          SUB PLOT
    5 LINE(I)=BLANK                                                         SUB PLOT
      M=(121-N)/2                                                           SUB PLOT
      IF(M.LT.1) STOP 3333                                                  SUB PLOT
      DO 6 I=1,N                                                            SUB PLOT
    6 LINE(M+I)=TITLE(I1-1+I)                                               SUB PLOT
      WRITE(6,1000) (LINE(I),I=1,121)                                       SUB PLOT
 1000 FORMAT(1H1,10X,121A1,//)                                              SUB PLOT
C  WRITE LEGEND FOR ROUGH SURFACE                                           SUB PLOT
      IF(NSMTH.EQ.0) WRITE(6,1010)                                          SUB PLOT
 1010 FORMAT(18X,107HCONTRIBUTION DUE TO FLOW INDICATED BY F, DUE TO RADSUB PLOT
     )IATION INDICATED BY R, AND DUE TO CONTACT INDICATED BY C)             SUB PLOT
C  WRITE LEGEND FOR SMOOTH SURFACE                                          SUB PLOT
      IF(NSMTH.NE.0) WRITE(6,1020)                                          SUB PLOT
 1020 FORMAT(35X,75HCONTRIBUTION DUE TO FLOW INDICATED BY F AND DUE TO RSUB PLOT
     )ADIATION INDICATED BY R)                                              SUB PLOT
      LY=0                                                                  SUB PLOT
      NAMEY=100                                                             SUB PLOT
      N=3                                                                   SUB PLOT
      IF(NSMTH.NE.0) N=2                                                    SUB PLOT
      DO 16 I=1,51                                                          SUB PLOT
      IF(MOD(I+9,10).NE.0) GO TO 10                                         SUB PLOT
C  WRITE VERTICAL HEADING AND HORIZONTAL DIVISION                           SUB PLOT
      LY=LY+1                                                               SUB PLOT
      DO 8 J=1,121                                                          SUB PLOT
    8 LINE(J)=H                                                             SUB PLOT
      DO 9 J=1,121,30                                                       SUB PLOT
    9 LINE(J)=PLUS                                                          SUB PLOT
      WRITE(6,2000) YHEAD(I),NAMEY,(LINE(J),J=1,121)                        SUB PLOT
 2000 FORMAT(3X,A1,2X,I3,1H%,1X,121A1)                                      SUB PLOT
      NAMEY=NAMEY-20                                                        SUB PLOT
      GO TO 13                                                              SUB PLOT
C  WRITE VERTICAL DIVISION                                                  SUB PLOT
   10 DO 11 J=1,121                                                         SUB PLOT
   11 LINE(J)=BLANK                                                         SUB PLOT
      DO 12 J=1,121,30                                                      SUB PLOT
   12 LINE(J)=V                                                             SUB PLOT
      WRITE(6,2010) (LINE(J),J=1,121)                                       SUB PLOT
 2010 FORMAT(11X,121A1)                                                     SUB PLOT
C  SET-UP DATA POINTS AND WRITE ON TOP OF GRID                              SUB PLOT
   13 DO 16 K=1,N                                                           SUB PLOT
      DO 14 J=1,121                                                         SUB PLOT
   14 LINE(J)=BLANK                                                         SUB PLOT
      IPRT=0                                                                SUB PLOT
      DO 15 IPOINT=1,NPOINT                                                 SUB PLOT
      IF(IY(IPOINT,K).NE.I) GO TO 15                                        SUB PLOT
      IPRT=1                                                                SUB PLOT
```

```
      LINE(JX(IPOINT))=SYMBOL(K)                                        SUB PLOT
   15 CONTINUE                                                          SUB PLOT
   16 IF(IPRT.EQ.1) WRITE(6,2020) (LINE(J),J=1,121)                     SUB PLOT
 2020 FORMAT(1H+,10X,121A1)                                             SUB PLOT
C  WRITE NAMEX ALONG THE BOTTOM OF THE GRAPH                           SUB PLOT
      WRITE(6,3000) ((NAMEX(I,J),I=1,6),J=1,5)                          SUB PLOT
 3000 FORMAT(11X,6A1,19X,6A1,3(24X,6A1))                                SUB PLOT
C  WRITE SUBTITLE                                                      SUB PLOT
      WRITE(6,3010)                                                     SUB PLOT
 3010 FORMAT(/,59X,25HDIMENSIONLESS DROP VOLUME)                        SUB PLOT
      RETURN                                                            SUB PLOT
      END                                                               SUB PLOT
```

Program PLOT:HF%

Program PLOT:HF% was used to generate plots of the increase in heat flux on the macro-roughened surfaces as compared to that which would theoretically occur for the same size drop of the same liquid on a smooth surface at the same bulk surface temperature. It should be noted that the increase in heat flux so defined is equivalent to the increase in heat transfer coefficient (since the temperature difference is the same).As mentioned in Chapter 6, the corresponding smooth surface heat transfer was calculated by solving Equations 3-38, 3-40, and 3-45 simultaneously (The agreement between experimentally determined smooth surface heat flux and the theoretically determined value was also given in Chapter 6.). The percent increase in heat flux on the macro-roughened surfaces was provided to program PLOT:HF% by the database (generated by program DATABASE). Program DATABASE computes the quantity "HERB" (Chapter6) which is the ratio of the experimentally determined heat flux on the macro-roughened surface to the theoretical smooth surface heat flux. This quantity HERB is also punched on the database along with the dimensionless drop volume, V*, and the dimensionless superheat, A • The percent increase on the macro-roughened surface is then calculated from Equation C-1.

$$increase = 100\,(HEHB - 1) \tag{C-1}$$

Examples of the plots generated by program PLOT:HF% are Figures 57 through 66. The following is a listing of program PLOT:HF%. Comments are provided in the listing at various points to detail the specifics of program operation.

```
CREATE PROGRAM TO PLOT THE PERCENT INCREASE IN HEAT FLUX ON A
C  MACRO-ROUGHENED SURFACE OVER THAT ON A SMOOTH SURFACE UNDER THE
C  SAME CONDINTION (ALL PLOT ARE SUPERIMPOSED)
C
      DIMENSION JX(99,10),IY(99,10),SH(10),NPOINT(10)                    PLOT·HF%
      INTEGER TITLE(80)                                                  PLOT·HF%
      DO 3 NSET=1,4                                                      PLOT·HF%
C  RESET THE NUMBER OF SEQUENCES                                         PLOT·HF%
      NSEQ=0                                                             PLOT·HF%
C  DETERMINE THE NUMBER OF POINTS IN THE SEQUENCE                        PLOT·HF%
    1 READ(5,1000) NROLL,NP,TW                                           PLOT·HF%
 1000 FORMAT(I2,5X,I2,5X,F4.0)                                           PLOT·HF%
      IF(NROLL.LE.0) GO TO 3                                             PLOT·HF%
C  INCREMENT THE NUMBER OF SEQUENCES                                     PLOT·HF%
      NSEQ=NSEQ+1                                                        PLOT·HF%
      NPOINT(NSEQ)=NP                                                    PLOT·HF%
C  READ IN TITLE                                                         PLOT·HF%
      READ(5,1010) (TITLE(I),I=1,80)                                     PLOT·HF%
 1010 FORMAT(80A1)                                                       PLOT·HF%
C  SKIP THERMOPHYSIACL PROPERTY CARD                                     PLOT·HF%
      READ(5,1010) IDUMMY                                                PLOT·HF%
      DO 2 I=1,NP                                                        PLOT·HF%
C  READ IN THE DATA ONE CARD AT A TIME                                   PLOT·HF%
      READ(5,1030) NR,NS,ND,SH(NSEQ),USTAR,HEHB,H                        PLOT·HF%
 1030 FORMAT(I2,1X,I3,1X,I2,F6.3,F8.2,F6.3,F7.2)                         PLOT·HF%
      JX(I,NSEQ)=MAX0(1,MIN0(121,IFIX(1.+30.*ALOG10(USTAR))))            PLOT·HF%
    2 IY(I,NSEQ)=MAX0(1,MIN0(51,IFIX(1.+10.*(5.-(HEHB-1.)))))           PLOT·HF%
      GO TO 1                                                            PLOT·HF%
    3 CALL PLOT(JX,IY,SH,NSEQ,NPOINT,TITLE)                              PLOT·HF%
      STOP                                                               PLOT·HF%
      END                                                                PLOT·HF%
      SUBROUTINE PLOT(JX,IY,SH,NSEQ,NPOINT,TITLE)                        SUB PLOT
      INTEGER SYMBOL(10),U,H,BLANK,PLUS,TITLE(80),AT                     SUB PLOT
      DIMENSION JX(99,10),IY(99,10),SH(10),NPOINT(10),LINE(121),         SUB PLOT
     >NAMEX(6,5),NAME(16)                                                SUB PLOT
      DATA U,H,BLANK,PLUS,AT/1H^,1H-,1H ,1H+,1H@/                        SUB PLOT
      DATA SYMBOL/1H0,1H1,1H2,1H3,1H4,1H5,1H6,1H7,1H8,1H9/               SUB PLOT
      DATA NAMEX/1H1,1H ,1H ,1H ,1H ,1H ,1H ,1H ,1H ,1H1,1H0,            SUB PLOT
     > 1H ,1H ,1H ,1H1,1H0,1H0,1H ,1H ,1H1,1H0,1H0,1H0,                  SUB PLOT
     >1H1,1H0,1H.,1H0,1H0,1H0/                                           SUB PLOT
      DATA NAME/1HF,1HI,1HL,1HM,1H ,1HB,1HO,1HI,1HL,1HI,1HN,1HG,1H ,     SUB PLOT
     >1HO,1HF,1H /                                                       SUB PLOT
C  CENTER TITLE ABOVE PLOT                                               SUB PLOT
      DO 1 II=1,80                                                       SUB PLOT
      IF(TITLE(I1).NE.BLANK) GO TO 2                                     SUB PLOT
    1 CONTINUE                                                           SUB PLOT
      STOP 1111                                                          SUB PLOT
    2 DO 2 IN=2,80                                                       SUB PLOT
      I2=80-IN                                                           SUB PLOT
      IF(TITLE(I2+1).EQ.AT) GO TO 4                                      SUB PLOT
    3 CONTINUE                                                           SUB PLOT
      STOP 2222                                                          SUB PLOT
    4 M=I2-I1+1                                                          SUB PLOT
      M=(121-M-16)/2                                                     SUB PLOT
      IF(M.LT.1.OR.M.LT.1) STOP 3333                                     SUB PLOT
      DO 5 I=1,121                                                       SUB PLOT
    5 LINE(I)=BLANK                                                      SUB PLOT
      DO 6 I=1,16                                                        SUB PLOT
    6 LINE(M+I)=NAME(I)                                                  SUB PLOT
      DO 7 I=1,M                                                         SUB PLOT
    7 LINE(M+16+I)=TITLE(I1+I-1)                                         SUB PLOT
      WRITE(6,1000) (LINE(I),I=1,121)                                    SUB PLOT
 1000 FORMAT(1H1,10X,121A1,//)                                           SUB PLOT
      NAMEY=600                                                          SUB PLOT
C  WRITE SYMBOL TABLE                                                    SUB PLOT
      WRITE(6,1010) (SYMBOL(I),SH(I),I=1,NSEQ)                           SUB PLOT
 1010 FORMAT(14X,16HSYMBOL·SUPERHEAT,10(3X,A1,1H·,F5.3))                 SUB PLOT
      DO 16 I=1,51                                                       SUB PLOT
      IF(MOD(I+9,10).NE.0) GO TO 10                                      SUB PLOT
C  WRITE NAMEY AND HORIZONTAL DIVISION                                   SUB PLOT
      NAMEY=NAMEY-100                                                    SUB PLOT
      DO 8 J=1,121                                                       SUB PLOT
    8 LINE(J)=H                                                          SUB PLOT
      DO 9 J=1,121,30                                                    SUB PLOT
    9 LINE(J)=PLUS                                                       SUB PLOT
      WRITE(6,1020) NAMEY,(LINE(J),J=1,121)                              SUB PLOT
 1020 FORMAT(6X,I3,2H% ,121A1)                                           SUB PLOT
      GO TO 13                                                           SUB PLOT
C  WRITE VERTICAL DIVISION                                               SUB PLOT
   10 DO 11 J=1,121                                                      SUB PLOT
   11 LINE(J)=BLANK                                                      SUB PLOT
      DO 12 J=1,121,30                                                   SUB PLOT
   12 LINE(J)=U                                                          SUB PLOT
```

```
      WRITE(6,1030) (LINE(J),J=1,121)                                   SUB PLOT
 1030 FORMAT(11X,121A1)                                                 SUB PLOT
C  SET-UP DATA POINTS AND WRITE ON TOP OF GRID                         SUB PLOT
   13 DO 16 ISEQ=1,NSEQ                                                 SUB PLOT
      DO 14 J=1,121                                                     SUB PLOT
   14 LINE(J)=BLANK                                                     SUB PLOT
      NP=NPOINT(ISEQ)                                                   SUB PLOT
      IPRT=0                                                            SUB PLOT
      DO 15 IPOINT=1,NP                                                 SUB PLOT
      IF(IY(IPOINT,ISEQ).NE.I) GO TO 15                                 SUB PLOT
      IPRT=1                                                            SUB PLOT
      LINE(JX(IPOINT,ISEQ))=SYMBOL(ISEQ)                                SUB PLOT
   15 CONTINUE                                                          SUB PLOT
   16 IF(IPRT.EQ.1) WRITE(6,1040) (LINE(J),J=1,121)                     SUB PLOT
 1040 FORMAT(1H+,10X,121A1)                                             SUB PLOT
C  WRITE NAMEX ALONG THE BOTTOM OF THE GRAPH                            SUB PLOT
      WRITE(6,1050) ((NAMEX(I,J),I=1,6),J=1,5)                          SUB PLOT
 1050 FORMAT(11X,6A1,19X,6A1,3(24X,6A1))                                SUB PLOT
C  WRITE SUBTITLE                                                       SUB PLOT
      WRITE(6,1060)                                                     SUB PLOT
 1060 FORMAT(/,60X,25HDIMENSIONLESS DROP VOLUME)                        SUB PLOT
      RETURN                                                            SUB PLOT
      END                                                               SUB PLOT
```

Program PLOT:HV

Program PLOT:HV was used to generate plots of the dimensionless heat flux, H (Equation 6-3), as a function of dimensionless drop volume, V*, and dimensionless superheat, A. Dimensionless heat flux, drop volume, and superheat were all supplied to program PLOT:HV by the database (generated by program DATABASE). Examples of the plots generated by program PLOT:HV are Figures 31 through 50. The following is a listing of program PLOT:HV. Comments are provided in the listing at various points to detail the specifics of program operation.

```
CREATE PROGRAM TO PLOT DIMENSIONLESS HEAT FLUX AS A FUNCTION OF
C  DIMENSIONLESS DROP VOLUME FOR DIFFERENT VALUES OF DIMENSIONLESS
C  SUPERHEAT (ALL PLOTS ARE SUPERIMPOSED)
C
      DIMENSION JX(99,10),IY(99,10),SH(10),NPOINT(10)                    PLOT·HV
      INTEGER TITLE(80)                                                  PLOT·HV
      DO 5 NSET=1,4                                                      PLOT·HV
C  RESET THE NUMBER OF SEQUENCES                                         PLOT·HV
      NSEQ=0                                                             PLOT·HV
C  DETERMINE THE NUMBER OF POINTS IN THE SEQUENCE                        PLOT·HV
    1 READ(5,1000) NROLL,NP                                              PLOT·HV
 1000 FORMAT(I2,5X,I2)                                                   PLOT·HV
      IF(NROLL.LE.0) GO TO 3                                             PLOT·HV
C  INCREMENT THE NUMBER OF SEQUENCES                                     PLOT·HV
      NSEQ=NSEQ+1                                                        PLOT·HV
      NPOINT(NSEQ)=NP                                                    PLOT·HV
C  READ IN TITLE                                                         PLOT·HV
      READ(5,1010) (TITLE(I),I=1,80)                                     PLOT·HV
 1010 FORMAT(80A1)                                                       PLOT·HV
C  SKIP THE THERMOPHYSICAL PROPERTY CARD                                 PLOT·HV
      READ(5,1010) IDUMMY                                                PLOT·HV
C  READ IN THE DATA ONE CARD AT A TIME                                   PLOT·HV
      DO 2 I=1,NP                                                        PLOT·HV
      READ(5,1020) SH(NSEQ),V,H                                          PLOT·HV
 1020 FORMAT(10X,F5.3,1X,F7.2,7X,F6.2)                                   PLOT·HV
      JX(I,NSEQ)=MAX0(1,MIN0(121,IFIX(1.+30.*ALOG10(V))))                PLOT·HV
    2 IY(I,NSEQ)=MAX0(1,MIN0(52,IFIX(82.-30.*ALOG10(H))))                PLOT·HV
      GO TO 1                                                            PLOT·HV
    3 CALL PLOT(JX,IY,SH,NSEQ,NPOINT,TITLE)                              PLOT·HV
      STOP                                                               PLOT·HV
      END                                                                PLOT·HV
      SUBROUTINE PLOT(JX,IY,SH,NSEQ,NPOINT)                              SUB PLOT
      INTEGER SYMBOL(10),V,H,BLANK,PLUS,TITLE(80),AT                     SUB PLOT
      DIMENSION JX(99,10),IY(99,10),NPOINT(10),LINE(121),                SUB PLOT
     >NAMEX(6,5),NAMEY(3,4),NAME(16)                                     SUB PLOT
      DATA V,H,BLANK,PLUS,AT/1HI,1H-,1H ,1H+,1H@/                        SUB PLOT
      DATA SYMBOL/1H0,1H1,1H2,1H3,1H4,1H5,1H6,1H7,1H8,1H9/               SUB PLOT
      DATA NAMEY/1HS,1HU,1HP,1HE,1HR,1HH,1H ,1HS,1HU,1H ,1H1,1H0/        SUB PLOT
      DATA NAMEX/1HH,1H ,1H ,1H ,1H ,1H ,1H ,1H ,1H ,1H ,1H1,1H0,        SUB PLOT
     > 1H ,1H ,1H ,1H1,1H0,1H0,1H ,1H ,1H1,1H0,1H0,1H0,                  SUB PLOT
     >1H1,1H0,1H,,1H0,1H0,1H0/                                           SUB PLOT
      DATA NAME/1HF,1HI,1HL,1HM,1H ,1HB,1HO,1HI,1HL,1HI,1HN,1HG,1H ,     SUB PLOT
     >1HO,1HF,1H /                                                       SUB PLOT
C  CENTER TITLE ABOVE PLOT                                               SUB PLOT
      DO 1 II=1,80                                                       SUB PLOT
      IF(TITLE(I1).NE.BLANK) GO TO 2                                     SUB PLOT
    1 CONTINUE                                                           SUB PLOT
      STOP 1111                                                          SUB PLOT
    2 DO 2 IN=2,80                                                       SUB PLOT
      I2=80-IN                                                           SUB PLOT
      IF(TITLE(I2+1).EQ.AT) GO TO 4                                      SUB PLOT
    3 CONTINUE                                                           SUB PLOT
      STOP 2222                                                          SUB PLOT
    4 N=I2-I1+1                                                          SUB PLOT
      M=(121-N-16)/2                                                     SUB PLOT
      IF(N.LT.1.OR.M.LT.1) STOP 3333                                     SUB PLOT
      DO 5 I=1,121                                                       SUB PLOT
    5 LINE(I)=BLANK                                                      SUB PLOT
      DO 6 I=1,16                                                        SUB PLOT
    6 LINE(M+I)=NAME(I)                                                  SUB PLOT
      DO 7 I=1,N                                                         SUB PLOT
    7 LINE(M+16+I)=TITLE(I1+I-1)                                         SUB PLOT
      WRITE(6,1000) (LINE(I),I=1,121)                                    SUB PLOT
 1000 FORMAT(1H1,10X,121A1,//)                                           SUB PLOT
C  WRITE SYMBOL TABLE                                                    SUB PLOT
      WRITE(6,1010) (SYMBOL(I),SH(I),I=1,NSEQ)                           SUB PLOT
 1010 FORMAT(14X,16HSYMBOL·SUPERHEAT,10(3X,A1,1H·,F5.3))                 SUB PLOT
      LY=0                                                               SUB PLOT
      DO 16 I=1,52                                                       SUB PLOT
      IF(I.NE.1.AND.I.NE.22.AND.I.NE.31.AND.I.NE.52) GO TO 10            SUB PLOT
C  WRITE NAMEY AND HORIZONTAL DIVISION                                   SUB PLOT
      LY=LY+1                                                            SUB PLOT
      DO 8 J=1,121                                                       SUB PLOT
    8 LINE(J)=H                                                          SUB PLOT
      DO 9 J=1,121,30                                                    SUB PLOT
    9 LINE(J)=PLUS                                                       SUB PLOT
      WRITE(6,1020) (NAMEY(L,LY),L=1,3),(LINE(J),J=1,121)                SUB PLOT
 1020 FORMAT(7X,3A1,1X,121A1)                                            SUB PLOT
      GO TO 13                                                           SUB PLOT
C  WRITE VERTICAL DIVISION                                               SUB PLOT
   10 DO 11 J=1,121                                                      SUB PLOT
   11 LINE(J)=BLANK                                                      SUB PLOT
```

```
      DO 12 J=1,121,30                                                  SUB PLOT
   12 LINE(J)=V                                                         SUB PLOT
      WRITE(6,1030) (LINE(J),J=1,121)                                   SUB PLOT
 1030 FORMAT(11X,121A1)                                                 SUB PLOT
C  SET-UP DATA POINTS AND WRITE ON TOP OF GRID                         SUB PLOT
   13 DO 19 ISEQ=1,NSEQ                                                 SUB PLOT
      DO 14 J=1,121                                                     SUB PLOT
   14 LINE(J)=BLANK                                                     SUB PLOT
      NP=NPOINT(ISEQ)                                                   SUB PLOT
      IPRT=0                                                            SUB PLOT
      DO 15 IPOINT=1,NP                                                 SUB PLOT
      IF(IY(IPOINT,ISEQ).NE.I) GO TO 15                                 SUB PLOT
      IPRT=1                                                            SUB PLOT
      LINE(JX(IPOINT,ISEQ))=SYMBOL(ISEQ)                                SUB PLOT
   15 CONTINUE                                                          SUB PLOT
   16 IF(IPRT.EQ.1) WRITE(6,1040) (LINE(J),J=1,121)                     SUB PLOT
 1040 FORMAT(1H+,10X,121A1)                                             SUB PLOT
C  WRITE NAMEX ALONG THE BOTTOM OF THE GRAPH                           SUB PLOT
      WRITE(6,1050) ((NAMEX(I,J),I=1,6),J=1,5)                          SUB PLOT
 1050 FORMAT(11X,6A1,19X,6A1,3(24X,6A1))                                SUB PLOT
C  WRITE SUBTITLE                                                      SUB PLOT
      WRITE(6,1060)                                                     SUB PLOT
 1060 FORMAT(/,60X,25HDIMENSIONLESS DROP VOLUME)                        SUB PLOT
      RETURN                                                            SUB PLOT
      END                                                               SUB PLOT
```

Program ROUGH

Program ROUGH was used to reduce the experimental heat transfer database (generated by program DATABASE) for the macro-roughened surfaces. Program ROUGH solved simultaneously Equations 3-30, 3-34 through 3-38, 3-40, 3-41, and 3-45 using the experimentally measured heat fluxes (which were provided in the database). The following quantities were computed and listed by program ROUGH: convective heat transfer coefficient, hp (Equation 3-35), contact heat transfer coefficient, he (Equation 3-37), radiative heat transfer coefficient, hR (Equation 3-36), computed vapor layer thickness, (Equation 3-30), dimensionless enthalpy flux, B (Equation 3-19), volumetric Nusselt number, Nuv (Equation 6-1), drop Nusselt number, Nun (Equation 6-4), convective Nusselt number, Nup (Equation 6-5), contact Nusselt number, Nuc (Equation 6-6), radiative Nusselt number, NuR (Equation 6-7), conduction parameter, n (Equation 6-8), and Biot number, Bic (Equation 6-9). A sample output of program ROUGH is given in Table 15. The following is a listing of program ROUGH. Comments are pro vided in the listing at various points to detail the specifics of program operation.

```
CREATE PROGRAM TO REDUCE ROUGH SURFACE DATA
C
      INTEGER TITLE(127),BLANK                                          ROUGH
      REAL LAMBDA,MUV,MUD,MUR,MUC,MUF,KG,KS,MUG,KF                      ROUGH
      DATA BLANK/1H /                                                   ROUGH
C  DEFINE PHYSICAL CONSTANTS                                            ROUGH
      DATA PI,G,SIGMA/3.14159,980.,.5.6688E-12/                         ROUGH
C  READ IN THE ROLL#, THE NUMBER OF POINTS IN THE SEQUENCE, AND THE     ROUGH
C  BULK SURFACE TEMPERATURE                                             ROUGH
    1 READ(5,1000) NROLL,NPOINT,TU                                      ROUGH
 1000 FORMAT(I2,5X,I2,5X,F4.0)                                          ROUGH
      IF(NROLL.LE.0) STOP                                               ROUGH
C  READ IN TITLE                                                        ROUGH
      READ(5,1010) (TITLE(I),I=1,80)                                    ROUGH
 1010 FORMAT(80A1)                                                      ROUGH
C  READ IN THERMOPHYSICAL PROPERTY DATA                                 ROUGH
      READ(5,1020) LAMBDA,CPG,KG,RHOF,RHOG,MUG,KS,EPS,TS,HFG,KF         ROUGH
 1020 FORMAT(F6.4,F5.3,E9.3,F6.4,F7.6,E9.3,F5.4,F7.5,F5.1,F6.1,E9.3)    ROUGH
C  CENTER TITLE AT TOP OF PAGE                                          ROUGH
      DO 2 I1=1,80                                                      ROUGH
      IF(TITLE(I1).NE.BLANK) GO TO 3                                    ROUGH
    2 CONTINUE                                                          ROUGH
      STOP 1111                                                         ROUGH
    3 DO 4 I=1,80                                                       ROUGH
      I2=81-I                                                           ROUGH
      IF(TITLE(I2).NE.BLANK) GO TO 5                                    ROUGH
    4 CONTINUE                                                          ROUGH
      STOP 2222                                                         ROUGH
    5 N=I2-I1+1                                                         ROUGH
      IF(N.LT.1) STOP 3333                                              ROUGH
      DO 6 I=1,N                                                        ROUGH
    6 TITLE(I)=TITLE(I1-1+I)                                            ROUGH
      DO 7 I=N,126                                                      ROUGH
    7 TITLE(I+1)=BLANK                                                  ROUGH
      M=(127-N)/2                                                       ROUGH
      IF(M.LT.1) STOP 4444                                              ROUGH
      DO 8 IN=1,N                                                       ROUGH
      I=N+1-IN                                                          ROUGH
    8 TITLE(I+M)=TITLE(I)                                               ROUGH
      DO 9 I=1,M                                                        ROUGH
    9 TITLE(I)=BLANK                                                    ROUGH
      WRITE(6,2000) (TITLE(I),I=1,127)                                  ROUGH
 2000 FORMAT(1H1,4X,127A1,/)                                            ROUGH
      WRITE(6,2010) LAMBDA,CPG,KG,RHOF,RHOG,MUG,KS,EPS,TS,HFG,KF        ROUGH
 2010 FORMAT(6X,6HLAMBDA,6X,3HCPG,10X,2HKG,8X,4HRHOF,7X,4HRHOG,10X,     ROUGH
     )3HMUG,9X,2HKS,7X,7HEPSILON,5X,4HTSAT,6X,3HHFG,10X,2HKF,/,         ROUGH
     )6X,F6.4,5X,F5.3,5X,E9.3,4X,F6.4,4X,F7.6,6X,E9.3,4X,F5.4,6X,F7.5,  ROUGH
     )5X,F5.1,4X,F6.1,5X,E9.3,/)                                        ROUGH
      WRITE(6,2020)                                                     ROUGH
 2020 FORMAT(5X,127H ROLL SEQ DATA    SH      U#      HD      HF      HC ROUGH
     )    HR      DELTA     B       NUV     NUD     NUF     NUC     NUR   OMEGAROUGH
     )    BIOT# )                                                      ROUGH
C  READ ROLL#, SEQUENCE#, DATA POINT#, DIMENSIONLESS SUPERHEAT,        ROUGH
C  DIMENSIONLESS DROP VOLUME, HEHB, AND DIMENSIONLESS HEAT FLUX         ROUGH
      DO 12 I=1,NPOINT                                                  ROUGH
      READ(5,3000) NROLL,NSEQ,NDATA,SH,VSTAR,HEHB,H                     ROUGH
 3000 FORMAT(I2,1X,I3,1X,I2,F6.3,F8.2,F6.3,F7.2)                        ROUGH
      IF(I.NE.1) GO TO 10                                               ROUGH
C  CALCULATE THE RADIATIVE HEAT TRANSFER COEFFICIENT                    ROUGH
      HR=SIGMA*((TU+273.)**4-(TS+273.)**4)/(TU-TS)                      ROUGH
C  CALCULATE DROP VOLUME                                                ROUGH
   10 V=VSTAR*LAMBDA**3                                                 ROUGH
C  CALCULATE DROP HEAT TRANSFER COEFFICIENT FROM DIMENSIONLESS HEAT FLUXROUGH
      HD=H*KG/SH/V**.333333                                             ROUGH
C  DETERMINE DIMENSIONLESS DROP AREA                                    ROUGH
      ASTAR=AOFV(VSTAR)                                                 ROUGH
C  CALCULATE DROP AREA                                                  ROUGH
      A=ASTAR*LAMBDA**2                                                 ROUGH
C  CALCULATE MASS FLUX                                                  ROUGH
      GG=HD*(TU-TS)/HFG                                                 ROUGH
C  CALCULATE VAPOR LAYER THICKNESS DELTA                                ROUGH
      DELTA=0.                                                          ROUGH
      DO 11 ITER=1,5                                                    ROUGH
   11 DELTA=(GG*MUG*A*A*(9.*GG*DELTA/20./MUG+3.)/                       ROUGH
     )(2.*PI*G*RHOG*(RHOF-RHOG)*V))**.333333                            ROUGH
C  CALCULATE DIMENSIONLESS PARAMETER B                                  ROUGH
      B=GG*CPG*DELTA/KG                                                 ROUGH
C  CALCULATE DROP NUSSELT NUMBER                                        ROUGH
      NUV=H/SH                                                          ROUGH
      NUD=HD*DELTA/KG                                                   ROUGH
C  CALCULATE THE NUSSELT NUMBER FOR THE CONVECTIVE TRANSPORT            ROUGH
      NUF=KF/KG/F(B,KG/KF)                                              ROUGH
```

```
C  CALCULATE THE CONVECTIVE HEAT TRANSFER COEFFICIENT                    ROUGH
      HF=NUF*KG/DELTA                                                    ROUGH
C  CALCULATE THE RADIATIVE NUSSELT NUMBER                                ROUGH
      NUR=HR*DELTA/KG                                                    ROUGH
C  CALCULATE THE CONTACT NUSSELT NUMBER                                  ROUGH
      NUC=NUD-NUF-NUR                                                    ROUGH
C  CALCULATE THE CONTACT HEAT TRANSFER COEFFICIENT                       ROUGH
      HC=HD-HF-HR                                                        ROUGH
C  CALCULATE THE CONTACT HEAT TRANSFER PARAMETR OMEGA                    ROUGH
      OMEGA=DELTA*KS/(EPS*KG)                                            ROUGH
C  CALCULATE BIOT NUMBER                                                 ROUGH
      BIOT=NUC/OMEGA                                                     ROUGH
C  WRITE SUMMARY DATA TO LINE PRINTER                                    ROUGH
   12 WRITE(6,3010) NROLL,NSEQ,NDATA,SH,VSTAR,HD,HF,HC,HR,DELTA,B,NUV,   ROUGH
     >NUD,NUF,NUC,NUR,OMEGA,BIOT                                         ROUGH
 3010 FORMAT(7X,I2,2X,I3,2X,I2,2X,F5.3,1X,F6.1,5(2X,F6.5),F7.3,F8.2,     ROUGH
     >F8.3,F7.3,F7.3,F7.3,F7.0,F9.6)                                     ROUGH
      GO TO 1                                                            ROUGH
      END                                                                ROUGH
      FUNCTION AOFV(V)                                                   A*(V*)
      DATA C1,C2,C3/-.3084,-.5556,.545/                                  A*(V*)
      VL=ALOG10(V)                                                       A*(V*)
      ALOGA=((2.5*VL+C1)+SQRT(.25*VL*VL+C2*VL+C3))/3.                    A*(V*)
      AOFV=10.**ALOGA                                                    A*(V*)
      RETURN                                                             A*(V*)
      END                                                                A*(V*)
      FUNCTION F(B)                                                      F(B)
      F=1.+EXP(.5*B)                                                     F(B)
      DO 1 I=1,99                                                        F(B)
      Z=.01*FLOAT(I)                                                     F(B)
    1 F=F+2.*EXP(.5*B*(1.-Z*Z*Z*(2.-Z)))                                 F(B)
      F=.005*F                                                           F(B)
      RETURN                                                             F(B)
      END                                                                F(B)
```

Program SMOOTH

Program SMOOTH was used to reduce the experimental heat transfer database (generated by program DATABASE) for the smooth surface. program SMOOTH solved simultaneously Equations 3-30, 3-34 through 3-36, 3-38, 3-40, 3-41, 3-43, and 3-45 using the experimentally measured heat fluxes (which were provided in the database). The following quantities were computed and listed by program SMOOTH: convective heat transfer coefficient, hF (Equation 3-35), radiative heat transfer coefficient, hR (Equation 3-36), computed vapor layer thickness, (Equation 3-30), dimensionless enthalpy flux, B (Equation 3-19), volumetric Nusselt number, Nuv (Equation 6-1), drop Nusselt number, Nun (Equation 6-4), convective Nusselt number, NuF (Equation 6-5), and radiative Nusselt number, NuR (Equation 6-7). A sample output of program SMOOTH is given in Table 14. The following is a listing of program SMOOTH. Comments are provided in the listing at various points to detail the specifics of program operation.

```
CREATE PROGRAM TO REDUCE SMOOTH SURFACE DATA                                    SMOOTH
C                                                                               SMOOTH
      INTEGER TITLE(95),BLANK                                                   SMOOTH
      REAL LAMBDA,NUV,NUD,NUR,NUF,KG,KS,MUG,KF                                  SMOOTH
      DATA BLANK/1H /                                                           SMOOTH
C  DEFINE PHYSICAL CONSTANTS                                                    SMOOTH
      DATA PI,G,SIGMA/3.14159,980.,5.6688E-12/                                  SMOOTH
C  READ IN ROLL#, NUMBER OF DATA POINTS IN THE SEQUENCE, AND THE                SMOOTH
C  BULK SURFACE TEMPERATURE                                                     SMOOTH
    1 READ(5,1000) NROLL,NPOINT,TU                                              SMOOTH
 1000 FORMAT(I2,5X,I2,5X,F4.0)                                                  SMOOTH
      IF(NROLL.LE.0) STOP                                                       SMOOTH
C  READ IN TITLE OF NEXT SEQUENCE                                               SMOOTH
      READ(5,1010) (TITLE(I),I=1,80)                                            SMOOTH
 1010 FORMAT(80A1)                                                              SMOOTH
C  READ IN THERMOPHYSICAL PROPERTY DATA                                         SMOOTH
      READ(5,1020) LAMBDA,CPG,KG,RHOF,RHOG,MUG,KS,EPS,TS,HFG,KF                 SMOOTH
 1020 FORMAT(F6.4,F5.3,E9.3,F6.4,F7.6,E9.3,F5.4,F7.5,F5.1,F6.1,E9.3)            SMOOTH
C  CENTER TITLE ON TOP OF NEW PAGE                                              SMOOTH
      DO 2 I1=1,80                                                              SMOOTH
      IF(TITLE(I1).NE.BLANK) GO TO 3                                            SMOOTH
    2 CONTINUE                                                                  SMOOTH
      STOP 1111                                                                 SMOOTH
    3 DO 4 I=1,80                                                               SMOOTH
      I2=81-I                                                                   SMOOTH
      IF(TITLE(I2).NE.BLANK) GO TO 5                                            SMOOTH
    4 CONTINUE                                                                  SMOOTH
      STOP 2222                                                                 SMOOTH
    5 N=I2-I1+1                                                                 SMOOTH
      IF(N.LT.1) STOP 3333                                                      SMOOTH
      DO 6 I=1,N                                                                SMOOTH
    6 TITLE(I)=TITLE(I1-1+I)                                                    SMOOTH
      DO 7 I=N,94                                                               SMOOTH
    7 TITLE(I+1)=BLANK                                                          SMOOTH
      M=(95-N)/2                                                                SMOOTH
      IF(M.LT.1) STOP 4444                                                      SMOOTH
      DO 8 IN=1,N                                                               SMOOTH
      I=N+1-IN                                                                  SMOOTH
    8 TITLE(I+M)=TITLE(I)                                                       SMOOTH
      DO 9 I=1,M                                                                SMOOTH
    9 TITLE(I)=BLANK                                                            SMOOTH
      WRITE(6,2000) (TITLE(I),I=1,95)                                           SMOOTH
 2000 FORMAT(1H1,4X,127A1,/)                                                    SMOOTH
      WRITE(6,2010) LAMBDA,CPG,KG,RHOF,RHOG,MUG,TS,HFG,KF                       SMOOTH
 2010 FORMAT(6X,6HLAMBDA,6X,3HCPG,10X,2HKG,8X,4HRHOF,7X,4HRHOG,10X,             SMOOTH
     )3HMUG,9X,4HTSAT,6X,3HHFG,10X,2HKF,/,                                      SMOOTH
     )6X,F6.4,5X,F5.3,5X,E9.3,4X,F6.4,4X,F7.6,6X,E9.3,                          SMOOTH
     )5X,F5.1,4X,F6.1,5X,E9.3,/)                                                SMOOTH
      WRITE(6,2020)                                                             SMOOTH
 2020 FORMAT(6X,95H ROLL SEQ DATA  SH      V%     HD      HF      HR            SMOOTH
     )DELTA    B       NUV     NUD     NUF     NUR )                          SMOOTH
C  READ IN ROLL#, SEQUENCE#, DATA POINT#, DIMENSIONLESS SUPERHEAT,             SMOOTH
C  DIMENSIONLESS VOLUME, HEHB, AND DIMENSIONLESS HEAT FLUX                      SMOOTH
      DO 12 I=1,NPOINT                                                          SMOOTH
      READ(5,3000) NROLL,NSEQ,NDATA,SH,USTAR,HEHB,H                             SMOOTH
 3000 FORMAT(I2,1X,I3,1X,I2,1X,F5.3,1X,F7.2,1X,F5.3,1X,F6.2)                    SMOOTH
      IF(I.NE.1) GO TO 10                                                       SMOOTH
C  CALCULATE RADIATION HEAT TRANSFER COEFFICIENT                                SMOOTH
      HR=SIGMA*((TU+273.)**4-(TS+273.)**4)/(TU-TS)                              SMOOTH
C  CALCULATE DROP VOLUME                                                        SMOOTH
   10 V=VSTAR*LAMBDA**3                                                         SMOOTH
C  CALCULATE DROP HEAT TRANSFER COEFFICIENT FROM DIMENSIONLESS HEAT FLUX        SMOOTH
      HD=H*KG/SH/V**.333333                                                     SMOOTH
C  DETERMINE DIMENSIONLESS DROP AREA                                            SMOOTH
      ASTAR=AOFV(VSTAR)                                                         SMOOTH
C  CALCULATE DROP AREA                                                          SMOOTH
      A=ASTAR*LAMBDA**2                                                         SMOOTH
C  CALCULATE MASS FLUX                                                          SMOOTH
      GG=HD*(TU-TS)/HFG                                                         SMOOTH
C  CALCULATE VAPOR LAYER THICKNESS DELTA                                        SMOOTH
      DELTA=0.                                                                  SMOOTH
      DO 11 ITER=1,5                                                            SMOOTH
   11 DELTA=(GG*MUG*A*A*(9.*GG*DELTA/20./MUG+3.)/                               SMOOTH
     )(2.*PI*G*RHOG*(RHOF-RHOG)*V))**.333333                                    SMOOTH
C  CALCULATE DIMENSIONLESS PARAMETER B                                          SMOOTH
      B=GG*CPG*DELTA/KG                                                         SMOOTH
C  CALCULATE DROP NUSSELT NUMBER                                                SMOOTH
      NUV=H/SH                                                                  SMOOTH
      NUD=HD*DELTA/KG                                                           SMOOTH
C  CALCULATE THE NUSSELT NUMBER FOR THE CONVECTIVE TRANSPORT                    SMOOTH
      NUF=KF/KG/F(B,KG/KF)                                                      SMOOTH
C  CALCULATE THE CONVECTIVE HEAT TRANSFER COEFFICIENT                           SMOOTH
```

```
      HF=NUF*KG/DELTA                                                   SMOOTH
C  CALCULATE THE RADIATIVE NUSSELT NUMBER                              SMOOTH
      NUR=HR*DELTA/KG                                                   SMOOTH
C  WRITE SUMMARY DATA TO LINE PRINTER                                  SMOOTH
   12 WRITE(6,3010) NROLL,NSEQ,NDATA,SH,VSTAR,HD,HF,HR,DELTA,B,NUV,     SMOOTH
     >NUD,NUF,NUR                                                       SMOOTH
 3010 FORMAT(7X,I2,2X,I3,2X,I2,2X,F5.3,1X,F6.1,4(2X,F6.5),2X,F5.3,      SMOOTH
     >2X,F6.2,2X,F6.3,2(2X,F5.3))                                       SMOOTH
      GO TO 1                                                           SMOOTH
      END                                                               SMOOTH
      FUNCTION AOFV(V)                                                  A*(V*)
      DATA C1,C2,C3/-.3084,-.5556,.545/                                 A*(V*)
      VL=ALOG10(V)                                                      A*(V*)
      ALOGA=((2.5*VL+C1)+SQRT(.25*VL*VL+C2*VL+C3))/3.                   A*(V*)
      AOFV=10.**ALOGA                                                   A*(V*)
      RETURN                                                            A*(V*)
      END                                                               A*(V*)
      FUNCTION F(B)                                                     F(B)
      F=1.+EXP(.5*B)                                                    F(B)
      DO 1 I=1,99                                                       F(B)
      Z=.01*FLOAT(I)                                                    F(B)
    1 F=F+2.*EXP(.5*B*(1.-Z*Z*Z*(2.-Z)))                               F(B)
      F=.005*F                                                          F(B)
      RETURN                                                            F(B)
      END                                                               F(B)
```

Program VOLUME

Program VOLUME uses fourth-order Runge-Kutta integration (Reference 64) to solve the Laplace capillary equation for the size and shape of an axisymmetric sessile drop (similar to that of Reference45). The present solution to the Laplace capillary equation is not a duplication of the effort of Reference 45. In Reference 45 Hartland and Hartley do not develop the solution in a form that is directly adaptable to the present application. The Laplace capillary equation as presented in Chapter 3 may be cast into the form of Equations C-2 through C-8 by algebraic manipulation.

$$\frac{dr^*}{d\theta} = \frac{\cos\theta}{\frac{2}{b^*} + z^* - \frac{\sin\theta}{r^*}} \tag{C-2}$$

$$\frac{dz^*}{d\theta} = \tan\theta \frac{dr^*}{d\theta} \tag{C-3}$$

$$\frac{dV^*}{d\theta} = \pi \cdot r^{*2} \frac{dz^*}{d\theta} \tag{C-4}$$

$$A^* = \pi \cdot r_{\max}^{*2} \tag{C-5}$$

$$r^* = \frac{r}{\lambda} \tag{C-6}$$

$$z^* = \frac{z}{\lambda} \tag{C-7}$$

$$b^* = \frac{1}{\lambda} \frac{dz^2}{d\theta^2}\bigg|_{\theta=0} \tag{C-8}$$

For illustration of the variables r, z, and e see Figure 81. For examples of computed drop shape see Figure 7. The following is a listing of program VOLUME. Comments are provided in the listing at various points to detail the specifics of program operation.

```
      CREATE PROGRAM TO DETERMINE THE SIZE AND SHAPE OF LEIDENFROST DROPS
C
C     DEFINITION OF VARIABLES USED IN THIS PROGRAM                          VOLUME
C                                                                           VOLUME
C       A      - THE VERTICALLY PROJECTED AREA OF THE DROP                  VOLUME
C       B      - THE CURVATURE OF THE DROP AT THE VERTEX                    VOLUME
C       L      - THE AVERAGE THICKNESS OF THE DROP (L=V/A)                  VOLUME
C       RMAX   - THE RADIUS OF THE DROP (AS SEEN FROM THE TOP)              VOLUME
C       V      - THE VOLUME OF THE DROP                                     VOLUME
C       X      - THE HORIZONTAL DISTANCE FROM THE VERTEX OF THE DROP        VOLUME
C                OUTWARD FROM THE CENTERLINE                                VOLUME
C       Z      - THE VERTICAL DISTANCE (DOWN) FROM THE VERTEX OF THE DROP   VOLUME
C                                                                           VOLUME
            DOUBLE PRECISION B,A,V                                          VOLUME
            WRITE(6,1000)                                                   VOLUME
 1000 FORMAT(1H1,19X,33HDROP VOLUME AS A FUNCTION OF AREA,//,               VOLUME
           )10X,9HALOG10(B),5X,9HALOG10(A),5X,9HALOG10(V),5X,9HALOG10(L))   VOLUME
            DO 1 I=10,70                                                    VOLUME
            B=1.D1**((DFLOAT(I)-3.D1)/1.D1)                                 VOLUME
            CALL DROP (B,A,V)                                               VOLUME
            ALOGB=SNGL(DLOG10(B))                                           VOLUME
            ALOGA=SNGL(DLOG10(A))                                           VOLUME
            ALOGV=SNGL(DLOG10(V))                                           VOLUME
            ALOGL=ALOGV-ALOGA                                               VOLUME
          1 WRITE(6,1010) ALOGB,ALOGA,ALOGV,ALOGL                           VOLUME
 1010 FORMAT(3X,4(8X,F6.3))                                                 VOLUME
            STOP                                                            VOLUME
            END                                                             VOLUME
            SUBROUTINE DROP(B,A,V)                                          DROP
C   DROP USES FOURTH ORDER RUNGE-KUTTA INTEGRATION TO DETERMINE             DROP
C   THE VOLUME AND VERTICALLY PROJECTED AREA OF A SESSILE DROP              DROP
C   AS A FUNCTION OF THE CURVATURE AT THE VERTEX                            DROP
            DOUBLE PRECISION B,A,V,X,Z,RMAX,TH,DTH,DX,DZ,DV,XDX,PI          DROP
            RMAX=0.D0                                                       DROP
            X=0.D0                                                          DROP
            Z=0.D0                                                          DROP
            V=0.D0                                                          DROP
            N=1000                                                          DROP
            PI=3.141592654D0                                                DROP
            DTH=PI/DFLOAT(N)                                                DROP
            DO 10 I=1,N                                                     DROP
            TH=DTH*(DFLOAT(I)-1.D0)                                         DROP
            CALL RKUTTA(B,X,Z,V,TH,DTH,DX,DZ,DV)                            DROP
            XDX=X+DX                                                        DROP
            RMAX=DMAX1(RMAX,XDX)                                            DROP
            X=X+DX                                                          DROP
            Z=Z+DZ                                                          DROP
            V=V+DV                                                          DROP
         10 CONTINUE                                                        DROP
            A=PI*RMAX*RMAX                                                  DROP
            RETURN                                                          DROP
            END                                                             DROP
            SUBROUTINE RKUTTA(B,X,Z,V,TH,DTH,DX,DZ,DV)                      RKUTTA
C   RKUTTA PERFORMS ONE STEP OF FOURTH ORDER RUNGE-KUTTA INTEGRATION        RKUTTA
            DOUBLE PRECISION B,X,Z,V,TH,DTH,DX,DZ,DV,XK0,XK1,XK2,XK3,       RKUTTA
           )ZK0,ZK1,ZK2,ZK3,VK0,VK1,VK2,VK3,XP,ZP,THP,FX,FV,FZ               RKUTTA
C   STEP#1  ---------------------------------------------------------------RKUTTA
            CALL DIFF(B,X,Z,TH,FX,FZ,FV)                                    RKUTTA
            XK0=DTH*FX                                                      RKUTTA
            ZK0=DTH*FZ                                                      RKUTTA
            VK0=DTH*FV                                                      RKUTTA
C   STEP#2  ---------------------------------------------------------------RKUTTA
            THP=TH+5.D-1*DTH                                                RKUTTA
            XP=X+5.D-1*XK0                                                  RKUTTA
            ZP=Z+5.D-1*ZK0                                                  RKUTTA
            CALL DIFF(B,XP,ZP,THP,FX,FZ,FV)                                 RKUTTA
            XK1=DTH*FX                                                      RKUTTA
            ZK1=DTH*FZ                                                      RKUTTA
            VK1=DTH*FV                                                      RKUTTA
C   STEP#3  ---------------------------------------------------------------RKUTTA
            XP=X+5.D-1*XK1                                                  RKUTTA
            ZP=Z+5.D-1*ZK1                                                  RKUTTA
            CALL DIFF(B,XP,ZP,THP,FX,FZ,FV)                                 RKUTTA
            XK2=DTH*FX                                                      RKUTTA
            ZK2=DTH*FZ                                                      RKUTTA
            VK2=DTH*FV                                                      RKUTTA
C   STEP#4  ---------------------------------------------------------------RKUTTA
            THP=TH+DTH                                                      RKUTTA
            XP=X+XK2                                                        RKUTTA
            ZP=Z+ZK2                                                        RKUTTA
            CALL DIFF(B,XP,ZP,THP,FX,FZ,FV)                                 RKUTTA
            XK3=DTH*FX                                                      RKUTTA
```

```
      ZK3=DTH*FZ                                                        RKUTTA
      VK3=DTH*FV                                                        RKUTTA
      DX=(XK0+2.D0*XK1+2.D0*XK2+XK3)/6.D0                               RKUTTA
      DZ=(ZK0+2.D0*ZK1+2.D0*ZK2+ZK3)/6.D0                               RKUTTA
      DV=(VK0+2.D0*VK1+2.D0*VK2+VK3)/6.D0                               RKUTTA
      RETURN                                                            RKUTTA
      END                                                               RKUTTA
      SUBROUTINE DIFF(B,X,Z,TH,FX,FZ,FV)                                DIFF
C  DIFF COMPUTES THE DIFFERENTIALS OF X, Z, & V W.R.T. THETA            DIFF
      DOUBLE PRECISION B,Z,X,TH,FX,FZ,FV,DS,DSX                         DIFF
      DS=1.D0/B+Z                                                       DIFF
      IF(DABS(X).LT.1.D-20) GO TO 1                                     DIFF
      DSX=DSIN(TH)/X                                                    DIFF
      IF(DSX.GT.0.D0.AND.DSX.LT.1.D0/B) DS=2.D0/B+Z-DSX                 DIFF
    1 FX=DCOS(TH)/DS                                                    DIFF
      FZ=DSIN(TH)/DS                                                    DIFF
      FV=3.14159265D0*X*X*DSIN(TH)/DS                                   DIFF
      RETURN                                                            DIFF
      END                                                               DIFF
```

Program 2-D PINT

Program 2-D PINT is a two-dimensional, transient, finite difference heat conduction model for a cylindrical pin. In program 2-D PINT the transient heat conduction equation (3-46) is solved using finite differences and fourth-order Runge-Kutta Integration [62,64]. The location of the nodal points as well as further information about the finite difference modeling is given in Figure 29. An example of the output of program 2-D PINT is given in Table 12. A plot of computed temperature of the thermocouple junction located in the top/center of the instrumented pin (nodal point 1, see Figure 29) as a function of time is given in Figure 82. The following is a listing of program 2-D PINT. Comments are provided at various locations to detail the specifics of program operation.

```
CREATE FINITE DIFFERENCE PROGRAM TO DETERMINE THE TRANSIENT
C     TEMPERATURE OF A CYLINDRICAL PIN SUBJECTED TO PULSE-LIKE
C     PERIODIC LIQUID-SOLID CONTACT
C
C-------------------------------------------------------------------------2-D PINT
C  VARIABLES USED IN THIS PROGRAM                                         2-D PINT
C                                                                         2-D PINT
C     CL     - SPECIFIC HEAT OF LIQUID (J/GM/C)                           2-D PINT
C     CPG    - CONSTANT PRESSURE SPECIFIC HEAT OF VAPOR (J/GM/C)          2-D PINT
C     D      - DIAMETER OF PROTRUSION (CM)                                2-D PINT
C     DA     - DIFFERENTIAL AREA (CM**2)                                  2-D PINT
C     DELTAT - TEMPERATURE DIFFERENCE (C)                                 2-D PINT
C     DT     - DERIVITIVE OF TEMPERATURE W.R.T. TIME (C/SEC)              2-D PINT
C     DTCHF  - TEMPERATURE DIFFERENCE AT THE CRITICAL HEAT FLUX (C)       2-D PINT
C     DTIME  - TIME STEP SIZE (SEC)                                       2-D PINT
C     DTMFB  - TEMPERATURE DIFFERENCE AT THE MINIMUM HEAT FLUX (C)        2-D PINT
C     E      - PROTRUSION HEIGHT (CM)                                     2-D PINT
C     E0     - THE DISTANCE BETWEEN THE TOP OF THE SURFACE (THE BOTTOM    2-D PINT
C              OF THE PIN) AND THE CENTER OF THE THERMOCOUPLE USED TO     2-D PINT
C              DETERMINE BULK SURFACE TEMPERATURE (CM)                    2-D PINT
C     G      - ACCELERATION OF GRAVITY (980. CM/SEC**2)                   2-D PINT
C     HAVE   - AVERAGE HEAT TRANSFER COEFFICIENT (W/CM**2/C)              2-D PINT
C     HFG    - LATENT HEAT OF VAPORIZATION (J/GM)                         2-D PINT
C     ICPROP - SWITCH TO CONSTANT PROPERTIES FOR ICPROP>0                 2-D PINT
C              (THIS IS TO CONSERVE RUN-TIME IF DESIRED)                  2-D PINT
C     ITIME  - INTEGER COUNTER (THE NUMBER OF TIME STEPS)                 2-D PINT
C     NSKIP  - THE NUMBER OF TIME STEPS 'SKIPPED' BETWEEN PRINTING        2-D PINT
C     NTIME  - THE NUMBER OF TIME STEPS BEFORE ENDING EXECUTION           2-D PINT
C     Q      - HEAT FLUX (W/CM**2)                                        2-D PINT
C     QCHF   - CRITICAL HEAT FLUX (W/CM**2)                               2-D PINT
C     QMFB   - MINIMUM FILM BOILING HEAT FLUX (W/CM**2)                   2-D PINT
C     RKL    - THERMAL CONDUCTIVITY OF LIQUID (W/CM/C)                    2-D PINT
C     RHOG   - DENSITY OF VAPOR (GM/CM**3)                                2-D PINT
C     RHOL   - DENSITY OF LIQUID (GM/CM**3)                               2-D PINT
C     RHOS   - DENSITY OF SOLID MATERIAL (GM/CM**3)                       2-D PINT
C     RLAM   - 'LAMBDA' CHARACTERISTIC LENGTH PARAMETER (CM)              2-D PINT
C     RMUG   - VISCOSITY OF VAPOR (POISE)                                 2-D PINT
C     RKG    - THERMAL CONDUCTIVITY OF VAPOR (W/CM/C)                     2-D PINT
C     S      - THE CENTER-TO-CENTER PIN SPACING (CM)                      2-D PINT
C     T      - TEMPERATURE (C)                                            2-D PINT
C     TAU    - CONTACT PERIOD (SEC)                                       2-D PINT
C     TAUC   - CONTACT DURATION (TAUC<TAU) (SEC)                          2-D PINT
C     TAUCHF - CONTACT PERIOD ASSOCIATED WITH THE CRITICAL HEAT FLUX (SEC)2-D PINT
C     TCHF   - TEMPERATURE CORRESPONDING TO CRITICAL HEAT FLUX (C)        2-D PINT
C     TIME   - TIME (SEC)                                                 2-D PINT
C     TL     - TEMPERATURE OF THE LIQUID (C)                              2-D PINT
C     TMFB   - MINIMUM FILM BOILING TEMPERATURE (C)                       2-D PINT
C     TMIN   - MINIMUM TIME SET TO PREVENT OVERFLOW IN SQRT (SEE          2-D PINT
C              SUBROUTINE HEATF)                                          2-D PINT
C     TW     - WALL TEMPERATURE (SUBSTRATA) (C)                           2-D PINT
C                                                                         2-D PINT
C-------------------------------------------------------------------------2-D PINT
      COMMON TL,RHOL,CL,RKL,RHOG,CPG,RMUG,RKG,HFG,RLAM,RHOS              2-D PINT
     ),QCHF,DTCHF,QMFB,DTMFB,NBOIL(20),E0,S,TMIN,ICPROP,INSP             2-D PINT
      DIMENSION T(20),Q(9),DA(9),IT(20),LIQUID(9)                        2-D PINT
      INTEGER BLANK                                                      2-D PINT
      DATA G,PI,SIGMA/980.,3.1415927,5.6688E-12/                         2-D PINT
      DATA BLANK/1H /                                                    2-D PINT
C  INPUT FILE                                                           2-D PINT
      OPEN(5,FILE='$TEMP',STATUS='OLD')                                  2-D PINT
C  PLOT FILE                                                            2-D PINT
      OPEN(7,FILE='$PLOT..DB.4',STATUS='UNKNOWN')                        2-D PINT
C  READ IN PIN DIMENSIONS AND CONTACT PARAMETERS                        2-D PINT
   10 READ(5,*,END=99) E,D,E0,S,TW,TAU,TAUC,TMIN,DTIME,NTIME,NSKIP,      2-D PINT
     >ICPROP                                                            2-D PINT
 1000 FORMAT(10F5.0,I5)                                                 2-D PINT
C  CHECK FOR END OF FILE                                                2-D PINT
      IF(E.LE.0.) GO TO 99                                              2-D PINT
C  READ IN LIQUID THERMOPHYSICAL PROPERTIES                             2-D PINT
      READ(5,1010) TL,RHOL,CL,RKL,RHOG,CPG,RMUG,RKG,HFG,RLAM,           2-D PINT
     >(LIQUID(I),I=1,9)                                                 2-D PINT
 1010 FORMAT(F4.0,F5.4,F4.2,E9.3,F7.6,F4.2,2E9.3,F5.0,F6.4,9A2)         2-D PINT
C-------------------------------------------------------------------------2-D PINT
C  CALCULATE MAXIMUM AND MINIMUM POINTS ON THE BOILING CURVE            2-D PINT
C  CRITICAL HEAT FLUX (ZUBER'S THEORY)                                  2-D PINT
      QCHF=.18*HFG*SQRT(G*RLAM*RHOG*RHOL*(RHOL-RHOG)/(RHOL+RHOG))       2-D PINT
C  LIQUID-SOLID CONTACT PERIOD CORRESPONDING TO THE CRITICAL HEAT FLUX  2-D PINT
C  (AFTER THE ZUBER-TRIBIUS THEORY)                                     2-D PINT
      TAUCHF=PI*SQRT(2.*PI*RLAM*RHOG/G/(RHOL-RHOG))/3.                  2-D PINT
C  THE TEMPERATURE DIFFERENCE CORRESPONDING TO THE CRITICAL HEAT        2-D PINT
C  FLUX (BANKOFF D MEHRA)                                               2-D PINT
```

```
      DTCHF=QCHF*SQRT(PI*TAUCHF/RHOL/CL/RKL)/2.                          2-D PINT
      TCHF=TL+DTCHF                                                      2-D PINT
C  MINIMUM HEAT FLUX - LEIDENFROST POINT (ZUBER'S THEORY)                2-D PINT
      QMFB=QCHF*SQRT(RHOG/(RHOL+RHOG))                                   2-D PINT
C  TEMPERATURE DIFFERENCE CORRESPONDING TO THE MINIMUM HEAT FLUX          2-D PINT
C  (BERENSON'S THEORY)                                                   2-D PINT
      DTMFB=3.13*(QMFB*RLAM/RKG)*(QMFB*RMUG/G/HFG/RHOG/                  2-D PINT
     >(RHOL-RHOG)/RLAM**2)**.333333                                      2-D PINT
      TMFB=TL+DTMFB                                                      2-D PINT
C-----------------------------------------------------------------------2-D PINT
C  CHECK FOR BULK SURFACE TEMPERATURE BELOW TMFB                         2-D PINT
      IF(TW.GE.TMFB) GO TO 20                                            2-D PINT
      WRITE(6,1020) TW,TMFB                                              2-D PINT
 1020 FORMAT(1H1,5X,42H****  WARNING BULK SURFACE TEMPERATURE IS,         2-D PINT
     >40H BELOW MINIMUM FILM BOILING POINT  ****,//,                     2-D PINT
     >5X,3HTW=,F4.0,5X,5HTMFB=,F4.0,//,                                  2-D PINT
     >5X,40HEXECUTION TERMINATED.....................)                   2-D PINT
      GO TO 10                                                           2-D PINT
C-----------------------------------------------------------------------2-D PINT
C  CALCULATE SMOOTH SURFACE FILM BOILING PARAMETERS (FOR THE AREA        2-D PINT
C  BETWEEN THE PINS)                                                     2-D PINT
   20 SH=CPG*(TW-TL)/HFG                                                 2-D PINT
      HFGSML=HFG/(1.+7.*SH/20.)**3                                       2-D PINT
      HFGMAX=HFG*(2.*ALOG(1.+SH/2.)/SH)**3                               2-D PINT
      HFGS=(HFGSML+HFGMAX)/2.                                            2-D PINT
      HFB=.41*(RKG**3*RHOG*(RHOL-RHOG)*G*HFGS/(RMUG*(TW-TL)*RLAM))**.25  2-D PINT
      HR=SIGMA*((TW+273.15)**4-(TL+273.15)**4)/(TW-TL)                   2-D PINT
C-----------------------------------------------------------------------2-D PINT
C  INITIALIZE VARIABLES                                                  2-D PINT
      RHOS=7.754                                                         2-D PINT
      HSUM=0.                                                            2-D PINT
      DR=D/6.                                                            2-D PINT
      DZ=E/5.                                                            2-D PINT
      TIME=0.                                                            2-D PINT
C  INITIALIZE DIFFERENTIAL AREAS                                         2-D PINT
      DA(1)=1./36.                                                       2-D PINT
      DA(2)=2./9.                                                        2-D PINT
      DA(3)=4./9.                                                        2-D PINT
      DA(4)=11./36.                                                      2-D PINT
      DA(5)=DZ/3./DR                                                     2-D PINT
      DA(6)=2.*DZ/3./DR                                                  2-D PINT
      DA(7)=DA(6)                                                        2-D PINT
      DA(8)=DA(6)                                                        2-D PINT
      DA(9)=DZ/DR                                                        2-D PINT
      DA10=PI*D**2/4./S**2                                               2-D PINT
      DA11=1.-DA10                                                       2-D PINT
C  INITIALIZE COUNTERS                                                   2-D PINT
      NPRT=1                                                             2-D PINT
      ISKIP=0                                                            2-D PINT
      INSP=0                                                             2-D PINT
C  SET-UP INITIAL CONDITIONS                                             2-D PINT
      DO 30 I=1,20                                                       2-D PINT
      T(I)=TW                                                            2-D PINT
      IT(I)=INT(TW+.5)                                                   2-D PINT
   30 NBOIL(I)=BLANK                                                     2-D PINT
      DO 40 I=1,9                                                        2-D PINT
   40 Q(I)=0.                                                            2-D PINT
C-----------------------------------------------------------------------2-D PINT
C  WRITE HEADING AND INITIAL CONDITIONS                                  2-D PINT
      WRITE(6,1030) E,D,S,E0,TAU,TAUC,DTIME,NSKIP,TW,(LIQUID(I),I=1,9)   2-D PINT
 1030 FORMAT(1H1,4X,11HPIN HEIGHT=,F6.4,3H CM,5X,13HPIN DIAMETER=,F6.4,  2-D PINT
     >5X,12HPIN SPACING=,F6.4,5X,3HE0=,F6.4,/,                           2-D PINT
     >5X,15HCONTACT PERIOD=,F8.5,4H SEC,5X,17HCONTACT DURATION=,F8.5,    2-D PINT
     >4H SEC,/,5X,10HTIME STEP=,F8.5,4H SEC,5X,                          2-D PINT
     >23HOUTPUT IS PRINTED EVERY,I4,11H TIME STEPS,/,                    2-D PINT
     >5X,25HBULK SURFACE TEMPERATURE=,F4.0,5X,                           2-D PINT
     >39HTHE SURFACE IS STEEL AND THE LIQUID IS ,9A2)                    2-D PINT
      IF(ICPROP.EQ.0) WRITE(6,1031)                                      2-D PINT
 1031 FORMAT(1H )                                                        2-D PINT
      IF(ICPROP.NE.0) WRITE(6,1032)                                      2-D PINT
 1032 FORMAT(7X,45H(CONSTANT THERMOPHYSICAL PROPERTIES ARE USED))        2-D PINT
      WRITE(6,1033) TCHF,QCHF,TMFB,QMFB                                  2-D PINT
 1033 FORMAT(5X,5HTCHF=,F5.1,1HC,5X,5HQCHF=,F6.2,9H(W CM**2),5X,         2-D PINT
     >5HTMFB=,F5.1,1HC,5X,5HQMFB=,F6.2,9H(W/CM**2),//,                   2-D PINT
     >132H     TIME     T1    T2    T3    T4    T5    T6    T7    T8    T9   T10  2-D PINT
     > T11  T12  T13  T14  T15  T16  T17  T18  T19  T20      HPIN      H2-D PINT
     >AVE )                                                              2-D PINT
      WRITE(6,1040) TIME,(IT(I),NBOIL(I),I=1,20)                         2-D PINT
 1040 FORMAT(1X,F9.5,2X,20(I4,A1),2F10.5)                                2-D PINT
      WRITE(7,7777) TIME,TW                                              2-D PINT
 7777 FORMAT(F7.6,2(1X,F7.6))                                            2-D PINT
C-----------------------------------------------------------------------2-D PINT
C  BEGIN TIME STEPS                                                      2-D PINT
      DO 90 ITIME=1,NTIME                                                2-D PINT
```

```
C  DETERMINE NEW TEMPERATURES BY FOURTH ORDER RUNGE-KUTTA METHOD          2-D PINT
      CALL RKUTTA(T,Q,TIME,DTIME,TAU,TAUC,DZ,DR,TW)                      2-D PINT
      TIME=SNGL(DBLE(DTIME)*DBLE(FLOAT(ITIME)))                          2-D PINT
      WRITE(7,7777) TIME,T(1),T(4)                                       2-D PINT
C  DETERMINE TOTAL HEAT FLUX AND CORRESPONDING HEAT TRANSFER COEFFICIENT2-D PINT
      H=0.                                                               2-D PINT
      DO 50 I=1,9                                                        2-D PINT
   50 H=H+Q(I)*DA(I)                                                     2-D PINT
      H=H/(TW-TL)                                                        2-D PINT
      HSUM=HSUM+H                                                        2-D PINT
      HPIN=HSUM*DTIME/TIME                                               2-D PINT
      ISKIP=ISKIP+1                                                      2-D PINT
C  WRITE HEADING ON NEW PAGE AFTER EVERY 50 LINES                        2-D PINT
      IF(NPRT.NE.50.OR.ITIME.EQ.NTIME) GO TO 60                          2-D PINT
      WRITE(6,1030) E,D,S,E0,TAU,TAUC,DTIME,NSKIP,TW,(LIQUID(I),I=1,9)   2-D PINT
      IF(ICPROP.EQ.0) WRITE(6,1031)                                      2-D PINT
      IF(ICPROP.NE.0) WRITE(6,1032)                                      2-D PINT
      WRITE(6,1033) TCHF,QCHF,TMFB,QMFB                                  2-D PINT
      NPRT=0                                                             2-D PINT
C  WRITE ONE LINE OF OUTPUT EVERY NSKIP TIME STEPS                       2-D PINT
   60 IF(ISKIP.NE.NSKIP) GO TO 90                                        2-D PINT
      DO 70 I=1,20                                                       2-D PINT
   70 IT(I)=INT(T(I)+.5)                                                 2-D PINT
      HAVE=DA10*HPIN+DA11*(.75*HFB+HR)                                   2-D PINT
      DO 80 ITER=1,5                                                     2-D PINT
   80 HAVE=DA10*HPIN+DA11*(HFB*(HFB/HAVE)**.333333+HR)                   2-D PINT
      WRITE(6,1040) TIME,(IT(I),NBOIL(I),I=1,20),HPIN,HAVE               2-D PINT
      NPRT=NPRT+1                                                        2-D PINT
      ISKIP=0                                                            2-D PINT
   90 CONTINUE                                                           2-D PINT
      GO TO 10                                                           2-D PINT
   99 CLOSE(5)                                                           2-D PINT
      CLOSE(7)                                                           2-D PINT
      STOP                                                               2-D PINT
      END                                                                2-D PINT
      SUBROUTINE TDERIV(T,Q,DZ,DR,TW,DT)                                 TDERIV
C  TDERIV DETERMINES THE TEMPERATURE DERIVITIVES W.R.T TIME FOR          TDERIV
C  THE 20 NODAL POINTS                                                   TDERIV
C--------------------------------------------------------------------------TDERIV
      COMMON TL,RHOL,CL,RKL,RHOG,CPG,RMUG,RKG,HFG,RLAM,RHOS              TDERIV
     >,QCHF,DTCHF,QMFB,DTMFB,NBOIL(20),E0,S,TMIN,ICPROP,INSP             TDERIV
      DIMENSION T(20),Q(9),DT(20),RHO(20),C(20),METAL(12),INSULA(8)      TDERIV
      REAL K(20),KI                                                      TDERIV
C  METAL NODES                                                           TDERIV
      DATA METAL/1,2,3,4,7,8,11,12,15,16,19,20/                          TDERIV
C  INSULATOR NODES                                                       TDERIV
      DATA INSULA/5,6,9,10,13,14,17,18/                                  TDERIV
      DATA RHOI,CI,KI/2.4,1.09,.0104/                                    TDERIV
C--------------------------------------------------------------------------TDERIV
      IF(ICPROP.LT.0) GO TO 30                                           TDERIV
C  SET-UP THERMOPHYSICAL PROPERTIES OF METAL                             TDERIV
      DO 10 I=1,12                                                       TDERIV
      RHO(METAL(I))=RHOS                                                 TDERIV
      C(METAL(I))=CS(T(METAL(I)))                                        TDERIV
   10 K(METAL(I))=RKS(T(METAL(I)))                                       TDERIV
      IF(INSP.NE.0) GO TO 30                                             TDERIV
C  SET-UP THE THERMOPHYSICAL PROPERTIES OF THE INSULATOR                 TDERIV
      DO 20 I=1,8                                                        TDERIV
      RHO(INSULA(I))=RHOI                                                TDERIV
      C(INSULA(I))=CI                                                    TDERIV
   20 K(INSULA(I))=KI                                                    TDERIV
      IF(ICPROP.GT.0) ICPROP=-1                                          TDERIV
      INSP=1                                                             TDERIV
   30 DRDR=DR*DR                                                         TDERIV
      DZDZ=DZ*DZ                                                         TDERIV
C--------------------------------------------------------------------------TDERIV
C  CALCULATE NET HEAT FLUXES AT EACH NODE                                TDERIV
C  NODE#1                                                                TDERIV
      DT(1)=4.*(T(5)-T(1))*K(5)*K(1)/(K(5)+K(1))/DZDZ                    TDERIV
     >+8.*(T(2)-T(1))*K(2)*K(1)/(K(2)+K(1))/DRDR                         TDERIV
     >-2.*Q(1)/DZ                                                        TDERIV
C  NODE#2                                                                TDERIV
      DT(2)=4.*(T(6)-T(2))*K(6)*K(2)/(K(6)+K(2))/DZDZ                    TDERIV
     >+(T(1)-T(2))*K(1)*K(2)/(K(1)+K(2))/DRDR                            TDERIV
     >+3.*(T(3)-T(2))*K(3)*K(2)/(K(3)+K(2))/DRDR                         TDERIV
     >-2.*Q(2)/DZ                                                        TDERIV
C  NODE#3                                                                TDERIV
      DT(3)=4.*(T(7)-T(3))*K(7)*K(3)/(K(7)+K(3))/DZDZ                    TDERIV
     >+1.5*(T(2)-T(3))*K(2)*K(3)/(K(2)+K(3))/DRDR                        TDERIV
     >+2.5*(T(4)-T(3))*K(4)*K(3)/(K(4)+K(3))/DRDR                        TDERIV
     >-2.*Q(3)/DZ                                                        TDERIV
C  NODE#4                                                                TDERIV
```

```
      DT(4)=4.*(T(8)-T(4))*K(8)*K(4)/(K(8)+K(4))/DZDZ                    TDERIV
     )+40.*(T(3)-T(4))*K(3)*K(4)/(K(3)+K(4))/11./DRDR                   TDERIV
     )-2.*Q(4)/DZ                                                       TDERIV
     )-24.*Q(5)/11./DR                                                  TDERIV
C  NODE#5                                                              TDERIV
      DT(5)=2.*(T(1)-T(5))*K(1)*K(5)/(K(1)+K(5))/DZDZ                   TDERIV
     )+2.*(T(9)-T(5))*K(9)*K(5)/(K(9)+K(5))/DZDZ                        TDERIV
     )+8.*(T(6)-T(5))*K(6)*K(5)/(K(6)+K(5))/DRDR                        TDERIV
C  NODE#6                                                              TDERIV
      DT(6)=2.*(T(2)-T(6))*K(2)*K(6)/(K(2)+K(6))/DZDZ                   TDERIV
     )+2.*(T(10)-T(6))*K(10)*K(6)/(K(10)+K(6))/DZDZ                     TDERIV
     )+3.*(T(7)-T(6))*K(7)*K(6)/(K(7)+K(6))/DRDR                        TDERIV
     )+(T(5)-T(6))*K(5)*K(6)/(K(5)+K(6))/DRDR                           TDERIV
C  NODE#7                                                              TDERIV
      DT(7)=2.*(T(3)-T(7))*K(3)*K(7)/(K(3)+K(7))/DZDZ                   TDERIV
     )+2.*(T(11)-T(7))*K(11)*K(7)/(K(11)+K(7))/DZDZ                     TDERIV
     )+2.5*(T(8)-T(7))*K(8)*K(7)/(K(8)+K(7))/DRDR                       TDERIV
     )+1.5*(T(6)-T(7))*K(6)*K(7)/(K(6)+K(7))/DRDR                       TDERIV
C  NODE#8                                                              TDERIV
      DT(8)=2.*(T(4)-T(8))*K(4)*K(8)/(K(4)+K(8))/DZDZ                   TDERIV
     )+2.*(T(12)-T(8))*K(12)*K(8)/(K(12)+K(8))/DZDZ                     TDERIV
     )+40.*(T(7)-T(8))*K(7)*K(8)/(K(7)+K(8))/11./DRDR                   TDERIV
     )-24.*Q(6)/11./DR                                                  TDERIV
C  NODE#9                                                              TDERIV
      DT(9)=2.*(T(5)-T(9))*K(5)*K(9)/(K(5)+K(9))/DZDZ                   TDERIV
     )+2.*(T(13)-T(9))*K(13)*K(9)/(K(13)+K(9))/DZDZ                     TDERIV
     )+8.*(T(10)-T(9))*K(10)*K(9)/(K(10)+K(9))/DRDR                     TDERIV
C  NODE#10                                                             TDERIV
      DT(10)=2.*(T(6)-T(10))*K(6)*K(10)/(K(6)+K(10))/DZDZ               TDERIV
     )+2.*(T(14)-T(10))*K(14)*K(10)/(K(14)+K(10))/DZDZ                  TDERIV
     )+1.5*(T(11)-T(10))*K(11)*K(10)/(K(11)+K(10))/DRDR                 TDERIV
     )+(T(9)-T(10))*K(9)*K(10)/(K(9)+K(10))/DRDR                        TDERIV
C  NODE#11                                                             TDERIV
      DT(11)=2.*(T(7)-T(11))*K(7)*K(11)/(K(7)+K(11))/DZDZ               TDERIV
     )+2.*(T(15)-T(11))*K(15)*K(11)/(K(15)+K(11))/DZDZ                  TDERIV
     )+2.5*(T(12)-T(11))*K(12)*K(11)/(K(12)+K(11))/DRDR                 TDERIV
     )+1.5*(T(10)-T(11))*K(10)*K(11)/(K(10)+K(11))/DRDR                 TDERIV
C  NODE#12                                                             TDERIV
      DT(12)=2.*(T(8)-T(12))*K(8)*K(12)/(K(8)+K(12))/DZDZ               TDERIV
     )+2.*(T(16)-T(12))*K(16)*K(12)/(K(16)+K(12))/DZDZ                  TDERIV
     )+40.*(T(11)-T(12))*K(11)*K(12)/(K(11)+K(12))/11./DRDR             TDERIV
     )-24.*Q(7)/11./DR                                                  TDERIV
C  NODE#13                                                             TDERIV
      DT(13)=2.*(T(9)-T(13))*K(9)*K(13)/(K(9)+K(13))/DZDZ               TDERIV
     )+1.6*(T(17)-T(13))*K(17)*K(13)/(K(17)+K(13))/DZDZ                 TDERIV
     )+8.*(T(14)-T(13))*K(14)*K(13)/(K(14)+K(13))/DRDR                  TDERIV
C  NODE#14                                                             TDERIV
      DT(14)=2.*(T(10)-T(14))*K(10)*K(14)/(K(10)+K(14))/DZDZ            TDERIV
     )+1.6*(T(18)-T(14))*K(18)*K(14)/(K(18)+K(14))/DZDZ                 TDERIV
     )+3.*(T(15)-T(14))*K(15)*K(14)/(K(15)+K(14))/DRDR                  TDERIV
     )+(T(13)-T(14))*K(13)*K(14)/(K(13)+K(14))/DRDR                     TDERIV
C  NODE#15                                                             TDERIV
      DT(15)=2.*(T(11)-T(15))*K(11)*K(15)/(K(11)+K(15))/DZDZ            TDERIV
     )+1.6*(T(19)-T(15))*K(19)*K(15)/(K(19)+K(15))/DZDZ                 TDERIV
     )+2.5*(T(16)-T(15))*K(16)*K(15)/(K(16)+K(15))/DRDR                 TDERIV
     )+1.5*(T(14)-T(15))*K(14)*K(15)/(K(14)+K(15))/DRDR                 TDERIV
C  NODE#16                                                             TDERIV
      DT(16)=2.*(T(12)-T(16))*K(12)*K(16)/(K(12)+K(16))/DZDZ            TDERIV
     )+40.*(T(15)-T(16))*K(15)*K(16)/(K(15)+K(16))/11./DRDR             TDERIV
     )+1.6*(T(20)-T(16))*K(20)*K(16)/(K(20)+K(16))/DZDZ                 TDERIV
     )-24.*Q(8)/11./DR                                                  TDERIV
C  NODE#17                                                             TDERIV
      DT(17)=16.*(T(13)-T(17))*K(13)*K(17)/(K(13)+K(17))/15./DZDZ       TDERIV
     )+8.*(T(18)-T(17))*K(18)*K(17)/(K(18)+K(17))/DRDR                  TDERIV
C  NODE#18                                                             TDERIV
      DT(18)=16.*(T(14)-T(18))*K(14)*K(18)/(K(14)+K(18))/15./DZDZ       TDERIV
     )+(T(17)-T(18))*K(17)*K(18)/(K(17)+K(18))/DRDR                     TDERIV
     )+3.*(T(19)-T(18))*K(19)*K(18)/(K(19)+K(18))/DRDR                  TDERIV
C  NODE#19                                                             TDERIV
      DT(19)=12.*(T(15)-T(19))*K(15)*K(19)/(K(15)+K(19))/5./DZDZ        TDERIV
     )+45.*(T(20)-T(19))*K(20)*K(19)/(K(20)+K(19))/8./DRDR              TDERIV
     )+27.*(T(18)-T(19))*K(18)*K(19)/(K(18)+K(19))/8./DRDR              TDERIV
C  NODE#20                                                             TDERIV
      DT(20)=16.*(T(16)-T(20))*K(16)*K(20)/(K(16)+K(20))/15./DZDZ       TDERIV
     )+40.*(T(19)-T(20))*K(19)*K(20)/(K(19)+K(20))/11./DRDR             TDERIV
     )+2.*K(20)*(TW-T(20))/DZ/(.75*DZ+E0)/3.                            TDERIV
     )-24.*Q(9)/11./DR                                                  TDERIV
C-------------------------------------------------------------------   TDERIV
C  DIVIDE BY RHO*C TO OBTAIN TEMPERATURE DERIVITIVES W.R.T. TIME        TDERIV
      DO 40 I=1,20                                                      TDERIV
   40 DT(I)=DT(I)/RHO(I)/C(I)                                           TDERIV
      RETURN                                                            TDERIV
      END                                                               TDERIV
```

```
      SUBROUTINE HEATF(TIME,TAU,TAUC,T,Q)                                HEATF
C  HEATF DETERMINES THE HEAT FLUXES FROM EACH EXTERIOR NODE              HEATF
      COMMON TL,RHOL,CL,RKL,RHOG,CPG,RMUG,RKG,HFG,RLAM,RHOS              HEATF
     >,QCHF,DTCHF,QMFB,DTMFB,NBOIL(20),E0,S,TMIN,ICPROP,INSP             HEATF
      DIMENSION T(20),Q(9),NODE(9)                                       HEATF
      INTEGER C,F,QNB                                                    HEATF
      DATA NODE/1,2,3,4,4,8,12,16,20/                                    HEATF
      DATA C,N,QNB,F/1HC,1HN,1HQ,1HF/                                    HEATF
      DATA SIGMA,G,PI/5.6688E-12,980.,3.141593/                          HEATF
C-------------------------------------------------------------------------HEATF
C  DETERMINE THE HEAT FLUX FOR EACH OF THE 9 EXTERNAL NODES              HEATF
      DO 5 IQ=1,9                                                        HEATF
      TS=T(NODE(IQ))                                                     HEATF
C  DETERMINE IF THE BOILING PROCESS IS CONTACT/FILM. NUCLEATE.           HEATF
C  OR TRANSITION (QUASI-NUCLEATE)                                        HEATF
      DELTAT=TS-TL                                                       HEATF
      IF(DELTAT.LE.DTCHF) GO TO 4                                        HEATF
      IF(DELTAT.LE.DTMFB) GO TO 3                                        HEATF
C-------------------------------------------------------------------------HEATF
C  BOILING PROCESS IS CONTACT/FILM                                       HEATF
C  DETERMINE IF THE NODE IS SUBJECTED TO LIQUID-SOLID CONTACT            HEATF
      IF(IQ.GT.6) GO TO 1                                                HEATF
C  DETERMINE IF THE CONTACT IS DURING THE "ON" OR "OFF" PERIOD           HEATF
      NTAU=INT(TIME/TAU)                                                 HEATF
      IF(TIME.GT.FLOAT(NTAU)*TAU+TAUC) GO TO 1                           HEATF
C-------------------------------------------------------------------------HEATF
C  IF LIQUID-SOLID CONTACT IS OCCURRING USE A CONTACT-TYPE HEAT FLUX     HEATF
      NBOIL(NODE(IQ))=C                                                  HEATF
C  SET A MINIMUM TIME TO AVOID THE SINGULATITY IN-CONTACT HEAT TRANSFER HEATF
      TI=AMAX1(TMIN,TIME-FLOAT(NTAU)*TAU)                                HEATF
      QI=(TS-TL)*SQRT(RHOL*CL*RKL/(PI*TI))+                              HEATF
     >SIGMA*((TS+273.15)**4-(TL+273.15)**4)                              HEATF
      GO TO 5                                                            HEATF
C-------------------------------------------------------------------------HEATF
C  IF LIQUID-SOLID CONTACT IS NOT OCCURRING USE A POOL FILM BOILING      HEATF
C  TYPE HEAT FLUX                                                        HEATF
    1 NBOIL(NODE(IQ))=F                                                  HEATF
C  USE BAUMEISTER'S EQUATION FOR LEIDENFROST BOILING OF EXTENDED         HEATF
C  LIQUID MASSES                                                         HEATF
      SH=CPG*(TS-TL)/HFG                                                 HEATF
      HFGSML=HFG/(1.+7.*SH/20.)**3                                       HEATF
      HFGMAX=HFG*(2.*ALOG(1.+SH/2.)/SH)**3                               HEATF
      HFGS=(HFGSML+HFGMAX)/2.                                            HEATF
      HFB=.41*(RKG**3*RHOG*(RHOL-RHOG)*G*HFGS/(RMUG*(TS-TL)*RLAM))       HEATF
     >**.25                                                              HEATF
      HR=SIGMA*((TS+273.15)**4-(TL+273.15)**4)/(TS-TL)                   HEATF
      H=.75*HFB+HR                                                       HEATF
      DO 2 ITER=1,5                                                      HEATF
    2 H=HFB*(HFB/H)**.333333+HR                                          HEATF
      QI=H*(TS-TL)                                                       HEATF
      GO TO 5                                                            HEATF
C-------------------------------------------------------------------------HEATF
C  BOILING PROCESS IS TRANSITION (QUASI-NUCLEATE)                        HEATF
    3 NBOIL(NODE(IQ))=QNB                                                HEATF
      QI=EXP(ALOG(QCHF)+(ALOG(QMFB)-ALOG(QCHF))*ALOG(DELTAT/DTCHF)/      HEATF
     >ALOG(DTMFB/DTCHF))                                                 HEATF
      GO TO 5                                                            HEATF
C-------------------------------------------------------------------------HEATF
C  BOILING PROCESS IS NUCLEATE                                           HEATF
    4 NBOIL(NODE(IQ))=N                                                  HEATF
C  POWER LAW RELATIONSHIP FOR NUCLEATE BOILING (MC NELLEY)               HEATF
      QI=QCHF*(DELTAT/DTCHF)**3.23                                       HEATF
C-------------------------------------------------------------------------HEATF
    5 Q(IQ)=QI                                                           HEATF
      RETURN                                                             HEATF
      END                                                                HEATF
      SUBROUTINE RKUTTA(T,Q,TIME,DTIME,TAU,TAUC,DZ,DR,TW)                RKUTTA
C  RKUTTA PERFORMS 1 STEP OF FOURTH ORDER RUNGE-KUTTA INTEGRATION        RKUTTA
      DIMENSION T(20),Q(9),DT(20),T1(20),T2(20),T3(20),DT1(20),          RKUTTA
     >DT2(20),DT3(20),DT4(20)                                            RKUTTA
C  USE PREVIOUS HEAT FLUXES AND TEMPERATURES                             RKUTTA
C  DETERMINE NEW TEMPERATURE DERIVITIVES                                 RKUTTA
      CALL TDERIV(T,Q,DZ,DR,TW,DT)                                       RKUTTA
C  SETP#1  ----------------------------------------------------------------RKUTTA
      DO 1 I=1,20                                                        RKUTTA
      DT1(I)=DT(I)*DTIME                                                 RKUTTA
    1 T1(I)=T(I)+.5*DT1(I)                                               RKUTTA
      TIME1=TIME+.5*DTIME                                                RKUTTA
C  DETERMINE NEW HEAT FLUXES                                             RKUTTA
      CALL HEATF(TIME1,TAU,TAUC,T1,Q)                                    RKUTTA
C  DETERMINE NEW TEMPERATURE DERIVITIVES                                 RKUTTA
      CALL TDERIV(T1,Q,DZ,DR,TW,DT)                                      RKUTTA
C  SETP#2  ----------------------------------------------------------------RKUTTA
```

```
      DO 2 I=1,20                                                       RKUTTA
      DT2(I)=DT(I)*DTIME                                                RKUTTA
    2 T2(I)=T(I)+ 5*DT2(I)                                              RKUTTA
      TIME2=TIME+ 5*DTIME                                               RKUTTA
C   DETERMINE NEW HEAT FLUXES                                           RKUTTA
      CALL HEATF(TIME2,TAU,TAUC,T2,Q)                                   RKUTTA
C   DETERMINE NEW TEMPERATURE DERIVITIVES                               RKUTTA
      CALL TDERIV(T2,Q,DZ,DR,TW,DT)                                     RKUTTA
C   SETP$3  ---------------------------------------------------------------RKUTTA
      DO 3 I=1,20                                                       RKUTTA
      DT3(I)=DT(I)*DTIME                                                RKUTTA
    3 T3(I)=T(I)+DT3(I)                                                 RKUTTA
      TIME3=TIME+DTIME                                                  RKUTTA
C   DETERMINE NEW HEAT FLUXES                                           RKUTTA
      CALL HEATF(TIME3,TAU,TAUC,T3,Q)                                   RKUTTA
C   DETERMINE NEW TEMPERATURE DERIVITIVES                               RKUTTA
      CALL TDERIV(T3,Q,DZ,DR,TW,DT)                                     RKUTTA
C   SETP$4  ---------------------------------------------------------------RKUTTA
      DO 4 I=1,20                                                       RKUTTA
      DT4(I)=DT(I)*DTIME                                                RKUTTA
      DT(I)=(DT1(I)+2.*DT2(I)+2.*DT3(I)+DT4(I))/6.                      RKUTTA
    4 T(I)=T(I)+DT(I)                                                   RKUTTA
C   DETERMINE NEW HEAT FLUXES                                           RKUTTA
      TIME4=TIME+DTIME                                                  RKUTTA
      CALL HEATF(TIME4,TAU,TAUC,T,Q)                                    RKUTTA
      RETURN                                                            RKUTTA
      END                                                               RKUTTA
      FUNCTION CS(T)                                                    CS(T)
C   CS INTERPOLATES TABULAR DATA FOR SPECIFIC HEAT                      CS(T)
C   DATA IS FOR CARBON STEEL                                            CS(T)
C   TEMPERATURE IS IN DEGREES C                                         CS(T)
C   SPECIFIC HEAT IS IN CAL/GM/C                                        CS(T)
      DIMENSION C(17)                                                   CS(T)
      DATA C/.1051,.1166,.1280,.1395,.1508,.1622,.1731,.1853,.1741,.1805CS(T)
     ),.1505,.1505,.1505,.1505,.1505,.1790,.1460/                       CS(T)
      I=MAX0(1,MIN0(16,INT(T/100.)+1))                                  CS(T)
      X=(T-100.*FLOAT(I-1))/100.                                        CS(T)
      CS=C(I)+X*(C(I+1)-C(I))                                           CS(T)
C   CONVERT TO J/GM/C                                                   CS(T)
      CS=CS*4.184                                                       CS(T)
      RETURN                                                            CS(T)
      END                                                               CS(T)
      FUNCTION RKS(T)                                                   RKS(T)
C   RKS INTERPOLATES TABULAR DATA FOR THERMAL CONDUCTIVITY              RKS(T)
C   DATA IS FOR CARBON STEEL                                            RKS(T)
C   TEMPERATURE IS IN DEGREES C                                         RKS(T)
C   THERMAL CONDUCTIVITY IS IN BTU/HR/FT/F                              RKS(T)
      DIMENSION RK(7)                                                   RKS(T)
      DATA RK/21.,21.,19.,18.,16.,16.,17./                              RKS(T)
      I=MAX0(1,MIN0(6,INT(T/200.)+1))                                   RKS(T)
      X=(T-200.*FLOAT(I-1))/200.                                        RKS(T)
      RKS=RK(I)+X*(RK(I+1)-RK(I))                                       RKS(T)
C   CONVERT TO W/CM/C                                                   RKS(T)
      RKS=RKS*.01730                                                    RKS(T)
      RETURN                                                            RKS(T)
      END
```

Vita

Dudley James Benton was born in Atlanta, Georgia on February 16, 1952. His family moved to Fort Lauderdale, Florida shortly thereafter where he lived until moving to Knoxville, Tennessee in 1977. He received the Bachelor and Master of Science degrees in Ocean Engineering from Florida Atlantic University, Boca Raton, Florida in 1976 and 1977 respectively and the Doctor of Philosophy degree from The University of Tennessee, Knoxville in August 1982. He is married to the former Patricia Newman, also of Fort Lauderdale, Florida. He was been employed by the Tennessee Valley Authority as an engineer from June 1980 through December 1992. Since then he has continued to work in the power and process industries as well as in the areas of environmental remediation and software development.